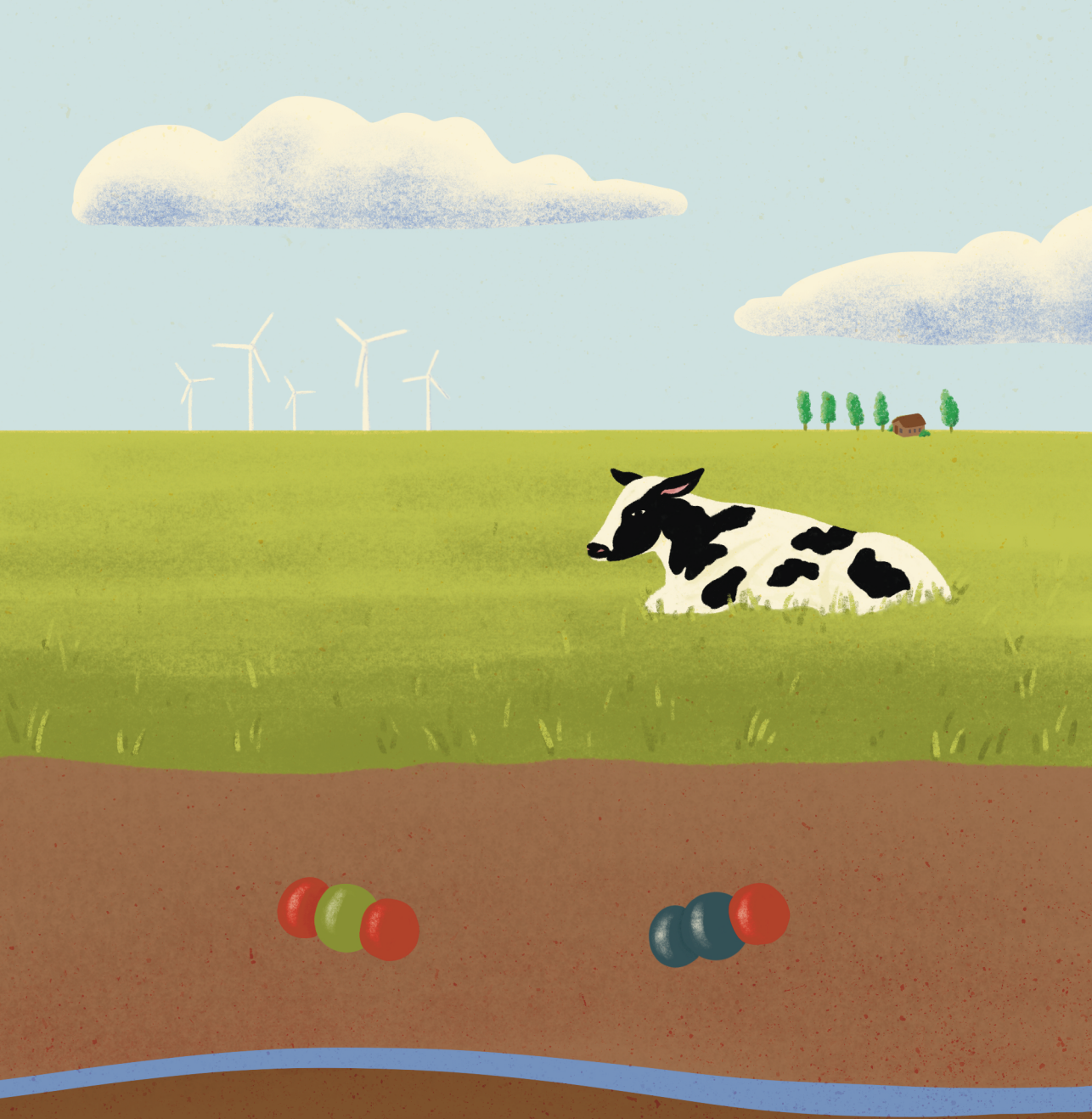


Greenhouse gas emissions from managed peat grasslands in the Netherlands

Erne Blondeau

Propositions

1. Measures to reduces CO_2 emissions from managed peat grasslands, create a risk for increased N_2O emission (this thesis)

2. Emission factors used by the Netherlands for peat soils overestimate N_2O emissions from grazing and underestimate emissions from mineral fertilizers (this thesis)

3. Vanity is a strong driver of scientific achievements.

4. Scenario studies are as much about wishful thinking as about rational thinking.

5. Contrasting the individual's responsibility with the government's in reducing greenhouse gas emissions creates a false dichotomy.

6. *Autobesity* is a demonstration of technology's inability to solve climate change.

Propositions belonging to the thesis, entitled

Greenhouse gas emissions from managed peat grasslands in the Netherlands

Erne Blondeau
Wageningen, 29 October 2026

Greenhouse gas emissions from managed peat grasslands in the Netherlands

Erne Blondeau

Thesis committee
Promotors
Prof. Dr J. W. Van Groenigen
Professor of Soil Biology
Wageningen University & Research

Prof. Dr G. Velthof
Special Professor in Soil Biology
Wageningen University & Research

Co-promotor
Dr M. Heinen
Scientific researcher Soil Physics and Agrohydrology
Wageningen University & Research

Other members
Prof. Dr M. van der Ploeg, Wageningen University & Research
Dr J. Leifeld, Agroscope, Zurich, Switzerland
Dr C. de Klein, Bioeconomy Science Institute, Mosgiel, New Zealand
Dr J. Pijlman, Louis Bolk Instituut, Bunnik, The Netherlands

This research was conducted under the auspices of the C.T. de Wit Graduate School for Production Ecology and Resource Conservation (PE&RC)

Greenhouse gas emissions from managed peat grasslands in the Netherlands

Erne Blondeau

Thesis
submitted in fulfilment of the requirements for the degree of doctor
at Wageningen University
by the authority of the Rector Magnificus,
Prof. Dr C. Kroeze,
in the presence of the
Thesis Committee appointed by the Academic Board
to be defended in public
on Thursday 29 October 2026
at 1 p.m. in the Omnia Auditorium.

Erne Blondeau
Greenhouse gas emissions from managed peat grasslands in the Netherlands,
227 pages.

PhD thesis, Wageningen University, Wageningen, the Netherlands (2026)
With references, with summary in English
DOI: 10.18174/681377

Table of contents

Chapter 1 - General introduction 7

Chapter 2 - Moisture and temperature effects on the heterotrophic respiration of peat soil 23

Chapter 3 - Groundwater level effects on greenhouse gas emissions from undisturbed peat cores 51

Chapter 4 - Drainage, cattle excreta and trampling effects on nitrous oxide emissions from a peat grassland 89

Chapter 5 - Drainage and fertilizer effects on nitrous oxide emissions from peat grasslands 133

Chapter 6 - General discussion 167

References 183

Summary 209

Samenvatting 213

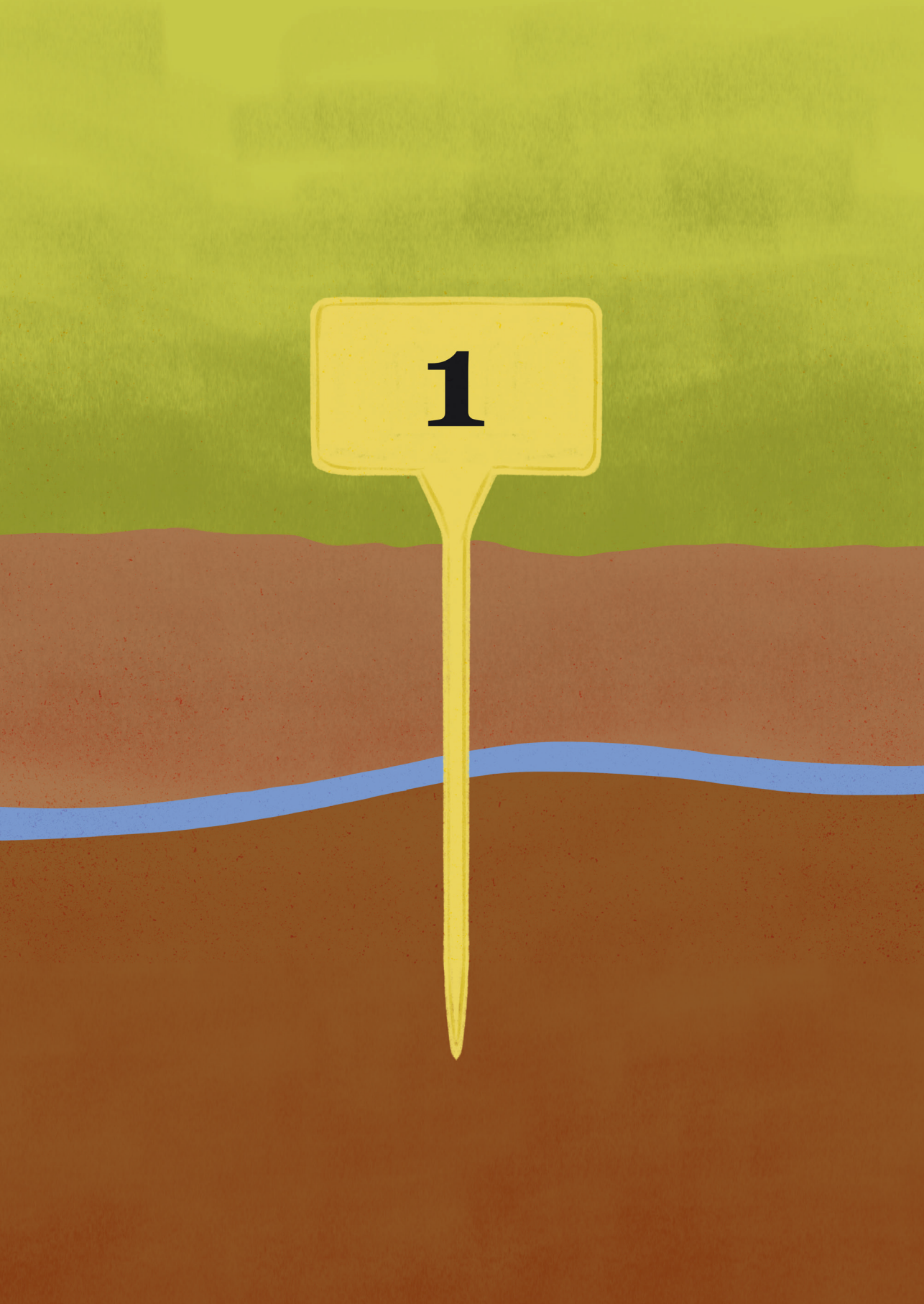
Acknowledgements 217

About the author 221

Affiliations of co-authors 222

PE&RC Training and Education Statement 224

List of publications 226


1

Chapter 1

General introduction

Erne Blondeau

1.1 Background

Soils provide important functions such as climate regulation, water regulation, biodiversity conservation, and crop production (Bunemann et al., 2018; Carter et al., 1997; Doran & Parkin, 1994). Maintaining those functions supports several sustainable development goals (SDGs), including Good Health and Wellbeing (SDG 3), Clean Water and Sanitation (SDG 6), Responsible Consumption and Production (SDG 12), Climate Action (SDG 13) and Life on Land (SDG 15, Lal et al., 2021). Peat soils are of special importance due to their high nutrient content, water storage capacity, and organic carbon content (Batjes, 1996; Deru et al., 2018; Parish et al., 2008). Peat is the common term used for the soil class histosol, as defined in the World Reference Base (WRB) for Soil Resources (IUSS Working Group WRB, 2015). This soil type is formed under wet, anaerobic conditions, which enable the accumulation of organic matter from dead plant material (Parish et al., 2008). The WRB classification of histosols dictates 40 cm or more of the upper 100 cm of the soil being organic matter, or the presence of a ≥10 cm organic horizon directly at the surface (IUSS Working Group WRB, 2015). The Intergovernmental Panel on Climate Change (IPCC) uses a slightly broader definition for *organic soils* to distinguish them from mineral soils, which better accommodates the several country-specific definitions of peat (Hiraishi et al., 2014). The Dutch classification system largely follows the WRB definition for peat, requiring an organic horizon (15% organic matter or more in dry weight) of 40 cm or more in the upper 80 cm (De Bakker & Schelling, 1989).

Globally, peat soils are estimated to have accumulated over 600 Pg carbon over their formation (Yu et al., 2010), making up about 25% of the estimated carbon stock stored in soils worldwide (Jobbagy & Jackson, 2000) on a relatively small part of the terrestrial surface area (UNEP, 2022). While natural peat lands are characterized by near-continuous waterlogging, many present-day peat areas are drained under human management (Parish et al., 2008). Artificial drainage drives the oxidation of soil organic matter (SOM) to carbon dioxide (CO_2), which is lost to the atmosphere and contributes to global warming (Hiraishi et al., 2014). By introducing oxygen in the soil matrix, oxidation of the organic matter is accelerated compared to the slower anaerobic oxidation reactions occurring in flooded soil (Hiraishi et al., 2014). The current carbon loss rate from Dutch peat lands is rapidly exceeding the estimated accumulation rates during the Holocene, when these soils were formed (Erkens et al., 2016; RIVM, 2026; Van den Akker et al., 2008).

Already 10% of the former extent of European peatlands has disappeared due to extraction or drainage, and active drainage for agriculture and forestry is still driving peat degradation to this day (UNEP, 2022). Agricultural land use of European drained peat soils is dominated by grasslands and to a lesser extent cultivation of crops such as cereals or potato (Oleszczuk et al., 2008). In the Netherlands, organic soils cover around 11% of the land area and are mainly used as grassland for dairy farming (RIVM, 2026). Where the artificial drainage of Dutch peat soils was previously powered by windmills, drainage intensity has increased over the past decades, due to advances in pumping technology and the use of heavier machinery, which requires higher load bearing capacity of the soil (Bakema et al., 2025; Erkens et al., 2016).

As carbon is transported to the atmosphere, the soil volume inevitably decreases, which results in subsidence of the surface level (Erkens et al., 2016; Ma et al., 2022; Schothorst, 1977). Concomitantly, the removal of water from soil pores drives reversible shrinkage and irreversible compaction of the soil matrix (Massop et al., 2024; Wösten et al., 1997). In a recent study on irreversible soil subsidence in several peat grasslands throughout the Netherlands between 1970 and 2020, a mean rate of 7 mm yr^{-1} was reported (Bakema et al., 2025). Subsidence and oxidation rates are even greater in tropical areas due to higher temperatures that promote faster decomposition (Hooijer et al., 2012; Wösten et al., 1997). Adverse effects of soil subsidence include damage to foundations and infrastructure, upwards seepage of salt water, disturbed groundwater regulation in adjacent areas and increased risk of flooding (Bucx et al., 2015; Herrera-García et al., 2021; Van den Born et al., 2016).

Besides CO_2, the strong greenhouse gas (GHG) nitrous oxide (N_2O) is produced and released from peat soils after mineralization of organic nitrogen (Martikainen et al., 1993; Pärn et al., 2018; Van Beek et al., 2004; Velthof & Oenema, 1995). The global warming potential of N_2O is 273 times greater than that of CO_2 over a 100-year horizon, attributable to its long residence time in the troposphere and high effective radiative forcing per molecule (Forster et al., 2021). Nitrous oxide remains relatively inert in the troposphere but typically undergoes photodissociation in the stratosphere, forming reactive nitrogen and thereby contributing to stratospheric ozone depletion (Portmann et al., 2012; Ravishankara et al., 2009). Atmospheric N_2O concentrations increased by 0.95 ppb per year over the previous decade as a result of human activities and reached 338 ppb by the end of 2025 (Canadell et

al., 2021; Lan et al., 2025). Agriculture is the largest anthropogenic source of N_2O emissions worldwide, mostly due to fertilizer applications (Canadell et al., 2021). In the European Union, 72% of the total N_2O emissions is derived from agriculture (European Environment Agency, 2024).

In addition to direct emissions to the atmosphere, degraded carbon is partly lost through leaching of dissolved carbon to the groundwater and eventually surface water, where it can again be lost as CO_2 (Evans et al., 2016; Freeman et al., 2022; Hiraishi et al., 2014). Similarly, nitrogen mineralization can lead to nitrate NO_3^- leaching, resulting in eutrophication of nearby environments and indirect N_2O emissions (Tian et al., 2019). On the other hand, the aeration of peat soils inhibits production of methane (CH_4), a strong GHG emitted from wetlands under the naturally occurring anaerobic conditions (Abdalla et al., 2016; Kayranli et al., 2010; Le Mer & Roger, 2001).

Grassland cultivation in the Netherlands is predominantly practiced for feed production in cattle farming (Jellema et al., 2025). Despite high nitrogen supply through peat oxidation, grassland management on peat soils is therefore frequently accompanied by additional N inputs via manure applications or excreta of grazing cattle (Deru et al., 2019; Leppelt et al., 2014; Pijlman et al., 2020; Vellinga & André, 1999). Additional mineral fertilizer applications on top of these organic fertilizers is not uncommon in the Netherlands (CBGV, 2026; Velthof & Mosquera, 2011b). These inputs increase herbage yields on the one hand, but can be lost as N_2O as well, introducing an additional challenge for climate change mitigation and the environment in peatland management (Velthof et al., 2024).

Peatland degradation caused by excavation and agriculture is estimated to account for 4% of global anthropogenic greenhouse gas emissions (UNEP, 2022). In the Netherlands, annual CO_2 and N_2O emissions due to oxidation of drained peat soils were calculated to be 4.4 and 0.6 Tg CO_2-eq, respectively, in 2024 (RIVM, 2026). Together, the CO_2 and N_2O emissions from oxidation of peat soils account for over 3% of the total national GHG emissions from the Netherlands (RIVM, 2026). Peat drainage exacerbates a range of issues, compromising the potential of peat grassland management to advance multiple Sustainable Development Goals and meet the Paris Agreement's global warming limits (Evans et al., 2021; Leifeld et al., 2019; Smith et al., 2019; UNEP, 2022). While the Dutch peat meadow area is an intensively studied region, understanding of the effect of agricultural mitigation measures on

greenhouse gas emissions is still limited. This thesis, therefore, focusses on the direct emissions of greenhouse gases (in particular CO_2 and N_2O, and to a lesser extent CH_4) related to drainage and fertilization of peat grasslands.

1.2 Release of CO_2 and N_2O from drained peat soils

1.2.1 CO_2 emissions resulting from peat oxidation

Activity of heterotrophic soil microorganisms (bacteria, archaea and fungi) requires the consumption of SOM and yields gaseous CO_2 (Fig. 1.1). Heterotrophic microorganisms obtain energy from organic compounds in the soil such as polysaccharides, lignins or proteins (Megonigal et al., 2004; Schlesinger & Bernhardt, 2013). In peat soils, organic matter is predominantly plant-derived, with the fibrous material remaining recognizable as plant tissue (Boelter, 1969; Klingenfuß et al., 2014). Additional sources of organic matter include both dead and living microbial biomass (Chapin et al., 2002a). Through microbially synthesized extracellular enzymes - either oxidative (requiring oxygen) or hydrolytic (not requiring oxygen) - these larger organic compounds undergo initial decomposition into smaller monomeric components (Panis & Rompel, 2022; Schimel & Weintraub, 2003; Sinsabaugh et al., 1991). These are subsequently oxidized in the presence of oxygen, or undergo a fermentation reaction under anaerobic conditions (Megonigal et al., 2004; Schlesinger & Bernhardt, 2013). Coupling with electron accepting compounds is required for the oxidation of the organic monomers or fermentation products to take place. Electrons are preferentially transferred to oxygen molecules, as this results in the highest energy yield for microbe metabolism (Burgin et al., 2011; Megonigal et al., 2004). In wet, anaerobic environments, however, the availability of electron acceptors is often limited to species associated with lower energy yields, resulting in low microbial activity and carbon mineralization, and enabling the accretion of peat material (Clymo, 1984; McLatchey & Reddy, 1998).

The relevant alternative electron acceptors in wetlands or peat soils are, in order of decreasing energy yield of the coupled reduction-oxidation reactions: NO_3^-, oxidized iron and sulphate (Bethke et al., 2011; Schlesinger & Bernhardt, 2013). In the absence or after depletion of these electron acceptors, CH_4 can be produced by methanogenic archaea through CO_2 reduction or the splitting of acetate molecules (Le Mer & Roger, 2001; Schlesinger & Bernhardt, 2013) (Fig. 1.1). The actual release of CH_4 to the atmosphere strongly depends on the oxygen levels throughout the soil profile. During upward diffusion through aerated

topsoil, CH_4 can be oxidized by methanotrophic bacteria, either to form microbial biomass or CO_2 (Bridgham et al., 2013).

By introducing the thermodynamically favored oxygen into the soil pores, drainage of peat soils strongly enhances microbial activity and organic matter oxidation (Schlesinger & Bernhardt, 2013; Tolunay et al., 2024). The first step of decay, the cleavage of complex organic compounds, may itself be directly and indirectly dependent on oxygen presence. It is hypothesized that even the activity of hydrolytic (non-oxygen requiring) extracellular enzymes is inhibited in wetland soils, by the presence of phenolic compounds (e.g. humic acids) (Freeman et al., 2001). The recalcitrant phenolic compounds are allowed to steadily accumulate in wetland soils, but after drainage of the soil pores oxygen activates the specific enzymes (phenol oxidases) able to degrade these recalcitrant molecules (Freeman et al., 2004; McLatchey & Reddy, 1998; Panis & Rompel, 2022).

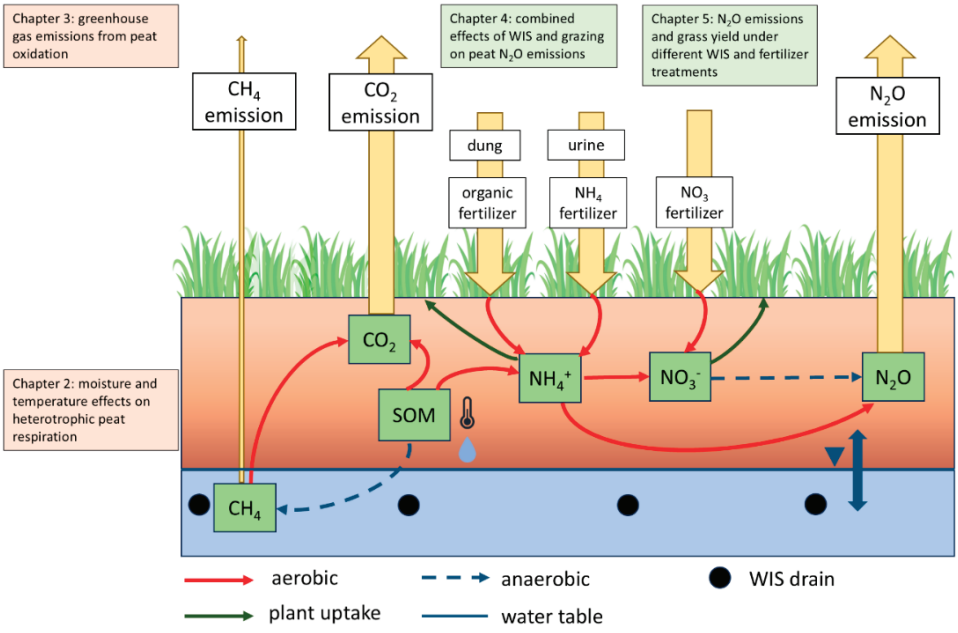


Figure 1.1*: Carbon and nitrogen transformations in drained peat grassland soil, through aerobic and anaerobic processes and plant uptake, which are affected by groundwater level control through WIS drainage, soil moisture content, temperature and external nitrogen inputs. Chapters 2 and 3 describe lab experiments on soil samples of two different scales; chapters 4 and 5 describe field experiments on peat grasslands. CH_4, methane; CO_2, carbon dioxide; SOM, soil organic matter; NH_4, ammonium; NO_3, nitrate; N_2O, nitrous oxide; WIS, water infiltration system.*

Soil moisture content, commonly expressed as relative saturation, or water filled pore space (WFPS), is often used as a proxy for oxygen availability. A high WFPS implies a low air filled pore volume and thereby low soil oxygen content. While oxygen is necessary for aerobic respiration, a deficit in moisture may hamper microbial activity by limiting transport of soluble nutrients, substrates and exoenzymes (Linn & Doran, 1984; Schjønning et al., 2003; Skopp et al., 1990). The result is a non-linear, unimodal relationship between soil respiration and moisture content, with an optimum around 60% WFPS under most soil conditions (Linn & Doran, 1984; Moyano et al., 2013). In peat soils, maximum respiration rates generally occur under higher WFPS values, between 60 and 90% due to high porosity, and organic matter availability (Byun et al., 2021; Saurich et al., 2019a; Van Lent et al., 2019; Wickland & Neff, 2008). Other factors, such as the high water retention and biological oxygen demand (due to high microbial activity) may affect the relationship between soil moisture content and peat respiration (Moyano et al., 2013).

Additionally, respiratory activity is understood to be positively related to temperature (Lloyd & Taylor, 1994; Sierra et al., 2015). Soil respiration can be empirically related to soil temperature and is quantified by the fractional increase in respiration rate with a temperature increase of 10°C (Lloyd & Taylor, 1994). The underlying theory, supported by ample observations, shows that this coefficient (Q_{10}) itself depends on temperature: sensitivity to a temperature increase is stronger under cold conditions than under warm conditions (Davidson et al., 2006; Liu et al., 2024; Moinet et al., 2025). The ongoing global warming may thus stimulate peat oxidation further (Vicca et al., 2009). Since the temperature sensitivity of organic matter decomposition is dependent on the availability of carbon and oxygen to decomposing microbes, it will interact with the effect of the soil moisture content (Clark & Gilmour, 1983; Davidson et al., 2006; Liu et al., 2024). Soil properties, such as nutrient content, degree of humification, clay content, bulk density and plant litter composition are determining factors for soil respiration and may affect the correlation with temperature and moisture content further (Moyano et al., 2013; Saurich et al., 2019b; Van Lent et al., 2019; Verhoeven & Toth, 1995).

1.2.2 N_2O emissions from peat soils

Nitrous oxide is produced during microbial conversion processes in the soil, most importantly through auto- or heterotrophic nitrification and heterotrophic denitrification (Baggs & Philippot, 2010; Butterbach-Bahl et al., 2013). Over half of the anthropogenic N_2O emissions are produced in agricultural soils, mainly linked to N inputs via soil amendments (Reay et al., 2012; Tian et al., 2020). Nitrification is the oxidation of ammonium (NH_4^+) to hydroxylamine and subsequently to nitrite (NO_2^-) and NO_3^- by autotrophic bacteria and archaea (Fig. 1.1). Plants take up NH_4^+ and NO_3^- for biomass production, yet N losses to the environment occur (Chapin et al., 2002b). Nitrous oxide can be formed during nitrification as a by-product during the chemical decomposition of hydroxylamine, or its reaction with NO_2^- (Bremner et al., 1980). During the anaerobic oxidation of an organic compound, NO_3^- can serve as an electron acceptor. In a sequence of denitrification reactions, NO_3^- is completely reduced via NO_2^-, NO and N_2O to N_2. Incomplete denitrification can result in N_2O as end product. Since the reduction of NO_3^- has a higher energy yield than N_2O reduction, a high NO_3^- availability increases the ratio of N_2O to N_2 in gaseous emissions (Senbayram et al., 2019; Weier et al., 1993).

Following the above, the availability of NH_4^+ and NO_3^- are controlling factors for N_2O production. The mineralization of organic matter, abundant in drained peat soil, provides a source for NH_4^+. This is often followed by nitrification in aerobic soil pores, with intermediate N_2O release, or resulting in NO_3^- production. After a rise in soil moisture, the dominant conditions for denitrification (anaerobicity and the availability of NO_3^- and organic carbon) are subsequently met (Pärn et al., 2018; Van Beek et al., 2004). Denitrification is often identified as the dominant N_2O producing process in drained peat soils (subject to variable moisture conditions) (Anthony & Silver, 2021; Baggs & Philippot, 2010; Butterbach-Bahl et al., 2013; Van Lent et al., 2019). Since N_2O is an intermediate in the denitrification reduction sequence, denitrification in the top soil particularly may form a risk of N_2O; nitrous oxide produced near the soil surface has a shorter residence time than at greater depths, limiting its reduction to N_2 before atmospheric release (Chapuis-Lardy et al., 2007; Clough et al., 2005), while high NO_3^- levels in topsoil - e.g. due to fertilization - may further inhibit this reduction (Senbayram et al., 2019; Zhang et al., 2023). This stresses the importance of N inputs to the soil surface through application of organic and mineral fertilizers and excreta by grazing cattle. Mineral fertilizers commonly contain NH_4^+ or NO_3^- which is directly available for microbial metabolism, while N in manure fertilizers

is partly present in organic matter, which requires mineralization before further transformation (Fig. 1.1). Cattle urine has a high concentration of urea, which is relatively quickly converted to NH_4^+, while in dung most N is present in organic matter and consequently takes longer to become available for plant uptake and nitrification (Bolan et al., 2004; Oenema et al., 1997). Fertilizer or grazing induced N_2O emissions are therefore affected by the composition of the N compound, the soil type and the method, rate and timing of the application (Bell et al., 2016; Chadwick et al., 2011; De Klein et al., 2006; Velthof et al., 2024).

1.3 Effects of peat rewetting

1.3.1 Carbon mineralization and emissions of CO_2 and CH_4

In order to limit the oxidation of peat and thereby reduce subsidence and CO_2 emissions, permanently raising the groundwater level (GWL) of peat grasslands is proposed as a potential solution (Freeman et al., 2022; Wils et al., 2025). In the absence of drainage, peat oxidation and associated CO_2 emissions are significantly reduced (Evans et al., 2021; Wilson et al., 2016a). Full rewetting of peat grasslands would hinder the current land use, however, implying a transition towards either a wet cropping system (paludiculture) or nature restoration (Jongbloed et al., 2026; Tanneberger et al., 2022; Temmink et al., 2026; Temmink et al., 2024). Such a transition would likely generate a reduction in the intensity of dairy farming in the Netherlands, with associated benefits related to GHG emission reduction, NH_3 volatilization and animal welfare (Leip et al., 2015; Van Grinsven et al., 2015). Nevertheless, efforts to address these challenges have primarily targeted scenarios that reduce GHG emissions and soil subsidence, while enabling continued grassland production and grazing (Freeman et al., 2022). A substantial reduction in carbon emissions may already be achieved with partial rewetting (Aben et al., 2024; Evans et al., 2021). In line with this, intentions have been expressed by the Dutch government to raise the GWL in some areas to 40 to 20 cm below the soil surface (Harbers & Heijnen, 2022). By implementing approaches tailored to regional conditions, a national reduction of 1 Tg CO_2-equivalent per year should be achieved in the Netherlands by 2030 (Ministry of Agriculture Nature and Food Quality, 2019).

Existing research has evaluated interventions designed to minimize temporal GWL fluctuations in peat grasslands, thereby mitigating extreme drainage in dry conditions and flooding in wet conditions (Harpenslager et al., 2024; Kechavarzi et al., 2007; Van

Asselen et al., 2023; van de Craats et al., 2025). Dry and warm periods were shown to constitute a large part of the annual CO_2 emission from peat grasslands (Hoving et al., 2022). A substantial reduction in peat oxidation could therefore potentially be achieved by reducing the aerated volume of peat during warm periods (Boonman et al., 2022). One of the proposed measures is the water infiltration system (WIS), consisting of artificial drain tubes, which connect the ditches on both sides of a field (Van Asselen et al., 2023). The hydraulic conductivity of peat soils can be relatively low, with large variability between peat types and generally decreasing with degradation (Kechavarzi et al., 2010b; Kechavarzi et al., 2007; Liu et al., 2016). A low conductivity limits the effectiveness of ditches to drain or infiltrate the entire field (van de Craats et al., 2025). A WIS ensures faster and more homogeneous water transport through the soil. Several studies have reported positive results about a mitigating effect of WIS on CO_2 emissions from peat grasslands (Aben et al., 2024; Boonman et al., 2022).

Under flooded conditions, the risk of CH_4 production also increases. Increased CH_4 emissions have been observed in studies on peat restoration or rewetting (Abdalla et al., 2016). However, reducing drainage intensity from deep to shallow levels still leaves an aerated top soil layer. Most CH_4 produced in the deeper anaerobic soil is therefore oxidized to CO_2 and H_2O during diffusive transport through the aerobic top soil (Fig. 1.1). Consequently, CH_4 emissions are generally negligible under deep or even shallow groundwater levels (Van den Pol-van Dasselaar et al., 1997).

1.3.2 Rewetting effects on N_2O emissions

The effect of a raised GWL through water infiltration systems on N_2O emissions in grassland production systems is still unclear. While the mineralization of organic nitrogen will be restricted under wet conditions, anaerobic soil pores may constitute suitable environments to denitrification (Baggs & Philippot, 2010). Additionally, the application of fertilizers or cattle excreta during grazing provides a source of mineral N, which may be denitrified under the partially anaerobic conditions created by a high GWL (Cai & Akiyama, 2016; De Klein & Vanlogtestijn, 1994; Kandel et al., 2019; Van Groenigen et al., 2005a). Thus, mineralization of organic N and application of N amendments constitute separate sources of N_2O that respond differently to drainage management.

Under the United Nations Framework Convention on Climate Change, countries are required to quantify and report their annual GHG

emissions from specific activities within all sectors, including agriculture (IPCC, 2019). The IPCC provides guidelines to estimate emissions using default emission factors for specific activities, which can be replaced by country-specific values, when available (Hergoualc'h et al., 2019). The Netherlands has specific emission factors for cattle grazing on organic soils, as well as application of mineral fertilizers or animal manure (Van der Zee et al., 2025), based on a limited number of studies (Velthof et al., 1996; Velthof & Mosquera, 2010).

On grazed grasslands, cattle excreta constitute an important N input, characterized by patchy "hot spots" for N_2O production (Cai & Akiyama, 2016; Selbie et al., 2015). About 80-95% of the N intake by grazing cattle is excreted, primarily as urea in urine, while in dung patches most N is present in organic form (Bolan et al., 2004; Cai et al., 2017; Oenema et al., 1997). Slurry is a mixture of urine and faeces collected in livestock housing, which is typically stored in a tank below or near the stable before dilution and land application (Chadwick et al., 2011; Kupper et al., 2020). Cattle slurry is the dominant organic N source applied to EU agricultural land, in particular in northwestern European countries, such as the Netherlands (Velthof et al., 2024). Through mechanical separation, the relatively concentrated solid slurry fraction - characterized by high organic N content - can be isolated from the liquid fraction, where N predominantly occurs as NH_4^+ or within small suspended particles (Fangueiro et al., 2008). The application of liquid slurry may improve the grass N uptake compared to unseparated slurry, due to fast infiltration in the soil and directly available NH_4^+, yet may simultaneously increase the risk of N_2O losses (Bittman et al., 2011; Velthof et al., 2024; Wang et al., 2024a). Mineral fertilizers containing ammonium or nitrate are similarly associated with high yields as well as N_2O losses (Velthof & Rietra, 2018). The granular calcium ammonium nitrate (CAN) fertilizer is commonly used on Dutch grassland, often complementing the maximum rate of allowed slurry application, while frequently resulting in highest (denitrification derived) N_2O emissions, in particular under wet conditions (Velthof & Mosquera, 2011b). Thus, the N composition and moisture content of the different N sources determine the transformations, mobility and plant uptake, in interaction with the soil conditions. In particular a combination of high NO_3^- availability and variable soil moisture, could create conditions beneficial for (incomplete) denitrification in peat soils (Fig. 1.1). These conditions can generate peak emission events, which take up a large portion of the total annual N_2O emissions (Anthony & Silver, 2024).

Additional experimental observations are required to update the N_2O emission factors for managed organic soils and to incorporate a disaggregation of different manure separation products, which differ in organic matter and mineral and organic N contents (Fangueiro et al., 2008; Velthof et al., 2024). These include processed manure products that resemble mineral fertilizers due to a low carbon to nitrogen ratio (≤ 3 kg kg^{-1}) and a high relative mineral N content (≥ 90% of total N), referred to as RENURE (REcovered Nitrogen from maNURE, Huygens et al., 2020). In February 2026, the European Commission adopted an amendment to the Nitrates Directive that allows for the use of RENURE products, providing a way to circumvent the prescribed limit for manure application in nitrate vulnerable zones of 170 kg N ha^{-1} (European Commission, 2026). While this may improve the recycling of manure nutrients, little research has been conducted yet on the N_2O emissions resulting from these fertilizers under different soil conditions.

In addition to the N inputs, cattle grazing causes soil compaction due to trampling, which increases the soil bulk density, WFPS and anaerobicity, restricts plant growth and subsequently may stimulate denitrification (Beare et al., 2009; Bhandral et al., 2007; Rivera & Chara, 2021). This can increase the N_2O-N losses following urine application, in particular at high soil moisture content (Thomas et al., 2008; Van Groenigen et al., 2005a). While these mechanisms have been studied on mineral soils, the effects of trampling on N_2O emissions from peat soils are still relatively unknown.

1.4 Objectives and thesis outline

To achieve global or national climate and environmental targets, amongst other measures, a reduction of greenhouse gas emissions from drained peat soils is required. While various mitigation measures - such as rewetting or water infiltration systems - have been proposed, their effects remain insufficiently understood. This PhD-study focuses on organic matter oxidation and resulting greenhouse gas emissions from peat grasslands in the Netherlands, considering the underlying mechanisms, and the mitigation options through groundwater and fertilization or grazing management. This is specified in four main objectives.

The **first objective** is to explore the effects of soil moisture, temperature and peat properties on peat oxidation. These are key factors affecting heterotrophic respiration in soils, and form intricate interactions with each other and other conditions. **Chapter 2** focuses on objective 1,

by exploring the temperature and moisture effects on heterotrophic respiration in a lab incubation experiment. Respiration rates are measured along a temperature and a water filled pore space gradient on soil sampled from three depths at three peat grasslands of different soil compositions in the Netherlands. Temperature sensitivity functions are described and related to WFPS, sampling site and depth. While temperature is expected to stimulate respiration exponentially, I expect soil moisture to be a constraint as well as a prerequisite. I hypothesize that this results in a non-linear relationship between the temperature sensitivity of respiration, expressed as Q_{10}, and soil WFPS. Additionally, since the peat organic matter is expected to become less humified and therefore less recalcitrant with increasing depth, respiration is expected to become less sensitive to temperature with depth.

Despite contributions of anaerobic oxidation, CO_2 emissions in a peat grassland are predominantly the result of organic matter oxidation above the GWL. While a shallow GWL is a promising measure to reduce CO_2 emissions, the effects on N_2O and CH_4 emissions are less clear. The **second objective** is, therefore, to study the potential of water management to reduce CO_2, N_2O and CH_4 emissions associated with peat oxidation and the possibility of a trade-off between these gases. This is addressed in **Chapter 3**, through a mesocosm experiment on undisturbed peat soil cores from the three grassland sites studied in Chapter 2. Over the course of a year, the cores are subjected to stepwise GWL changes in two cycles of drying-rewetting. Greenhouse gas emissions (CO_2, N_2O and CH_4) are measured, along with other biogeochemical and soil physical parameters, and related to the GWL. As a result of the respiration-WFPS relationship hypothesized in chapter 2, I hypothesized that CO_2 emissions show an optimum at a moderate GWL, due to an oxygen limitation in the soil at shallow GWL and the onset of moisture limitation in the top soil under a deep GWL. Nitrous oxide emissions on the other hand, are hypothesized to peak at a shallow GWL, while CH_4 emissions are expected to occur only under flooded conditions.

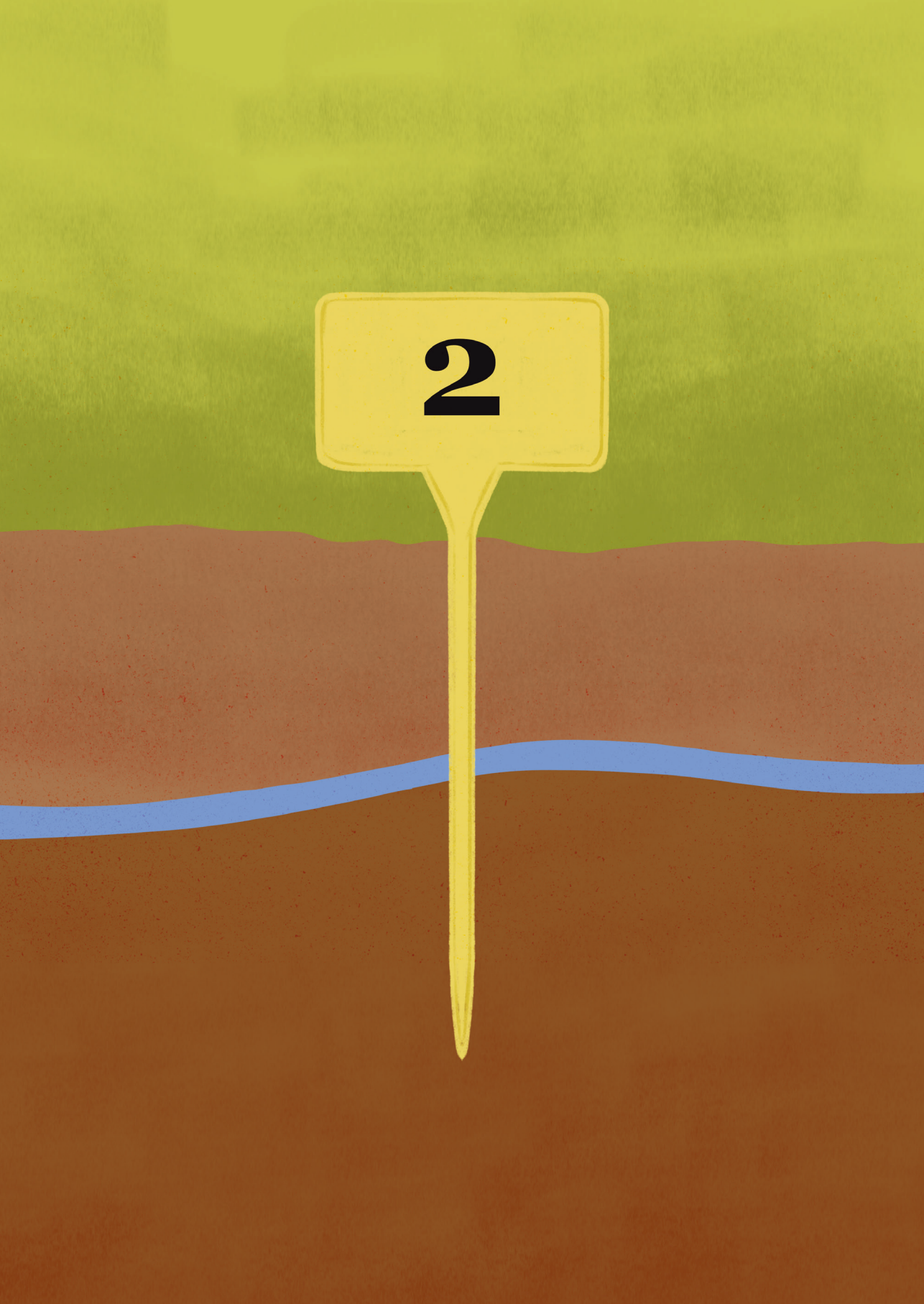
In the controlled environments of the first two experiments, GHG emissions are the results of soil processes, while in reality net outgoing emissions are the product of all the interactions between soil, plants and external inputs of nitrogen and carbon. Nitrous oxide emissions are particularly affected by inputs through fertilization or cattle grazing. These effects may interact with those of water level dynamics, the extent of which has not been studied yet. This brings forth the **third objective** of this PhD**:** to study the effect of raised water levels, achieved by water

infiltration systems, on N_2O emissions in fertilized or grazed peat grasslands. The concomitant emission factors are a necessary supplement to those currently used in the Dutch greenhouse gas inventory. Therefore our **fourth objective** is to quantify N_2O emissions and emission factors for different mineral fertilizers, manure and grazing.

Objectives 3 and 4 are studied in chapters 4 and 5. **Chapter 4** describes the findings of a field experiment on the combined effects of simulated cattle grazing and a raised GWL on N_2O emissions. Three measurement campaigns are performed on two fields, one drained conventionally through ditch levels, and the other using an active water infiltration system targeting a GWL around -40 cm. Nitrous oxide emissions are linked to the application of urine, dung and trampling, the drainage method, soil biological and meteorological parameters. I hypothesize that the higher summer GWL caused by a water infiltration system decreases N_2O emissions resulting from peat oxidation, but that WIS increases the N_2O emissions originating from cattle urine and dung. Compaction due to cattle trampling is expected to further increase these emissions.

Chapter 5 discusses our study on the effect of a raised GWL in combination with different fertilizers on N_2O emissions. Over the course of two years, emissions are measured in a field experiment including six different fertilizers and three drainage methods. The conventional ditch drainage method and the water infiltration system from chapter 4 are complemented with a second WIS, targeting a shallower GWL around -20 cm. Herbage (N) yields are measured and related to the amounts of fertilizer- N applications and N_2O losses. While the first WIS, targeting a GWL of -40 cm, is expected to decrease N_2O emissions, relative to conventional ditch drainage, I hypothesized for the shallow drainage measure to increase emissions due to increased denitrification. The application of nitrate-containing, mineral fertilizers is expected to result in both higher N_2O emissions, and higher grass yield, than ammonium-holding (manure) fertilizers. Consequently, highest N_2O emissions are hypothesized for WIS drainage aiming for a GWL of -20 cm in combination with nitrate-fertilizers as both factors enable denitrification.

Finally, in **Chapter 6** I synthesize the results from the previous chapters, discuss the limitations to this study and its implications.


2

Chapter 2

Moisture and temperature effects on the heterotrophic respiration of peat soil

Erne Blondeau, Marius Heinen, Eva Lammerts, Gerard Velthof, Jan Willem Van Groenigen

Abstract

Peat soils store a large part of worldwide soil carbon stocks, but drainage in agriculture results in peat oxidation and high CO_2 losses to the atmosphere. The oxidation of peat during microbial heterotrophic respiration is strongly affected by moisture and temperature conditions, but the interaction between these effects is not fully clear. We incubated soil samples from three different peat types and three depths (within 0 to 50 cm) at temperatures of 4.6, 13.9, 23.2 or 34 °C (±1.5 °C) and water filled pore spaces (WFPS) of 50, 60, 80 or 95%, in a full factorial design. Heterotrophic respiration was measured through changes in CO_2 concentration in the headspace of an incubation vial. The Q_{10} (the relative respiration increase for a 10 °C temperature increase) was calculated for each treatment combination (WFPS, location and depth) over the whole studied temperature interval. Additionally, an Arrhenius function was fitted for each combination of WFPS, sampling depth and location for the calculation of temperature-specific Q_{10} values.

Respiration ranged between 0 and 79 μg CO_2-C g^{-1} C h^{-1} and increased both with temperature and with WFPS (up to 80% WFPS, after which respiration remained constant). Temperature and WFPS did not have a significant interaction effect on respiration rates. However, an interaction between temperature and moisture became apparent from the significant negative WFPS effect on Q_{10}, which indicates a potential O_2 limitation on the temperature impact. The temperature-specific Q_{10} strongly decreased with temperature. Our results suggest that heterotrophic respiration of peat soil is most susceptible to warming under both dry and cold conditions.

2.1 Introduction

Peat soils store over 30% of the world's soil carbon (C) pool, while occupying only 3% of the global land area (Loisel et al., 2017; Yu et al., 2010). In Europe, peat soils are often drained for agriculture, causing soil subsidence and turning these soils in a net source of C to the atmosphere, due to peat decomposition during microbial respiration (Canadell et al., 2021; Erkens et al., 2016). Peat soil C stocks in the Netherlands are currently estimated to decrease by 1.2 Tg C yr^{-1}, corresponding with a carbon dioxide (CO_2) emission of 4.25 Tg CO_2 yr^{-1} (Van Baren et al., 2024). In order to adhere to the goals of the 2015 Paris Climate agreement, the Dutch government aims to reduce yearly greenhouse gas emissions from peat grasslands with 1 Tg CO_2-eq by 2030 (Ministry of Agriculture Nature and Food Quality, 2019). The moisture content, temperature and pH of the soil, as well as the peat type and composition, have been identified as the main physical drivers of microbial respiration rates in unsaturated peat soils (Bader et al., 2018; Bergman et al., 1999; Kechavarzi et al., 2010a; Mäkiranta et al., 2009; Moyano et al., 2013). A strong understanding of soil moisture and temperature effects on peat oxidation (heterotrophic respiration), and variation across peat types, may help to predict CO_2 emissions and carbon stock changes from managed peat soils in the Netherlands and the mitigation potentials of management measures.

The effect of moisture content on soil heterotrophic respiration is not linear; on the one hand it is limited by a high moisture content as it reduces O_2 diffusion and availability to aerobic respiration (Linn & Doran, 1984; Skopp et al., 1990). On the other hand, a low moisture availability limits oxidation by decreasing the solubility and mobility of enzymes and dissolved organic substrate and its availability to decomposing microbes (Schjønning et al., 2003; Skopp et al., 1990). The moisture-respiration relationship resulting from these mechanisms is a function with minima at both moisture extremes and an optimum range for moisture values that is dependent on the soil properties (Fig. 2.1a) (Moyano et al., 2013). In an incubation study on a silty clay loam soil, Linn and Doran (1984) found maximum respiration rates at a relative water saturation, or water filled pore space (WFPS), of 60%. Under saturated conditions, anaerobic oxidation pathways may still result in CO_2 emissions. Fairbairn et al. (2023) proposed an updated moisture-respiration model including a separate term for anaerobic processes. The extent of anaerobic oxidation is inhibited by O_2 and stimulated by moisture content. Such a model agrees with the non-zero CO_2 fluxes observed under saturated or

anaerobic conditions in several studies (Fairbairn et al., 2023; Moyano et al., 2018; Tolunay et al., 2024; Van Lent et al., 2019). The limiting effect of solute diffusion on respiration may be smaller in organic soils than mineral soils, due to a relatively high water retention and an abundance in C substrate (Moyano et al., 2013). On the other hand, the large pore volume decreases the oxygen limitation and may shift the optimum moisture content for respiration towards higher WFPS levels (Moyano et al., 2013). In peat respiration studies, unimodal WFPS-respiration relationships have been observed with maximum rates generally occurring at WFPS levels between 50 and 90% (Byun et al., 2021; Saurich et al., 2019a; Van Lent et al., 2019; Wickland & Neff, 2008).

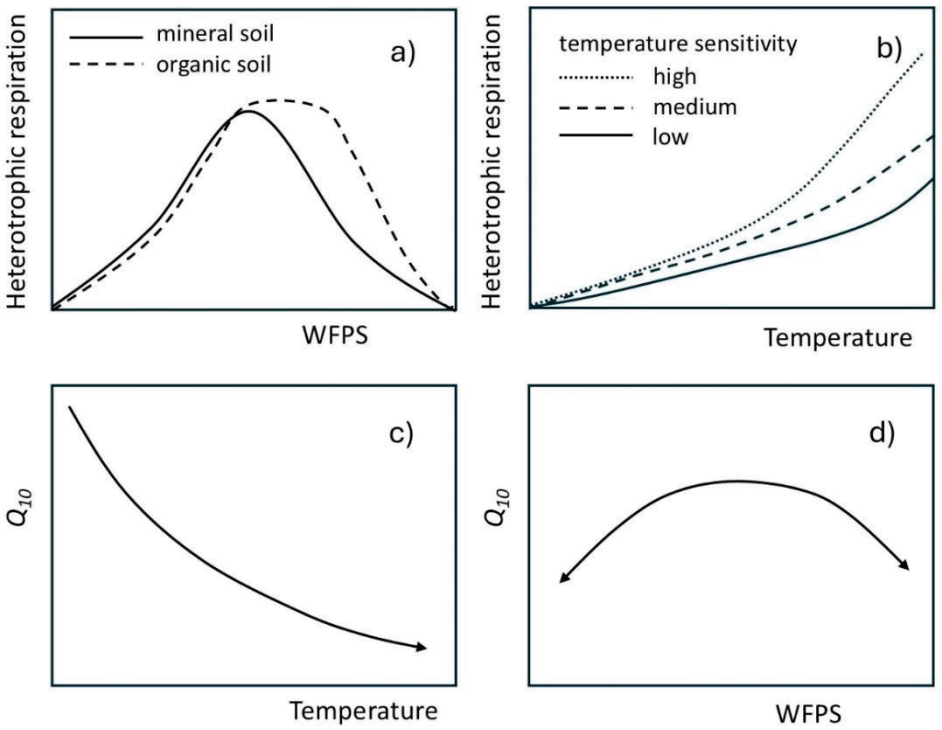


Figure 2.1*: Schematic illustrations of the response of heterotrophic respiration to water filled pore space (a), and temperature (b), the downwards response of Q_{10} to temperature (c) and the proposed temperature sensitivity optimum for WFPS conditions (d). Note that the axis scales are arbitrary, as the aim of these figures is to illustrate the direction of relationships and differences related to soil types.*

The response of soil respiration to temperature is generally described as an exponential relationship, modified by physical, chemical or environmental mechanisms in the soil matrix as well as the chemical composition of the organic material (Fig. 2.1b) (Davidson et al., 2006). Higher activation energies are required for the breakdown of relatively recalcitrant carbon compounds, making them more sensitive to temperature change than easily decomposable compounds (Davidson et al., 2006). Thus, the Q_{10}-value, the relative increase in reaction rate associated with a ten degrees temperature increase, is significantly higher for a recalcitrant and complex C compound, than for a more labile compound such as a carbohydrate (Fierer et al., 2005). This can be reflected in a positive relationship between Q_{10} and the C/N ratio of the substrate (Chen et al., 2018). On the other hand, external factors which reduce substrate availability to microbes, such as adsorption to minerals, soil aggregation, or drought decrease the relative sensitivity of respiration to temperature (Davidson et al., 2006). Additionally, while temperature increases reaction rates, its relative impact on respiration decreases with increasing temperatures (Fig. 2.1c) (Davidson et al., 2006). Global warming is therefore likely to have a larger impact on heterotrophic soil respiration in boreal than in tropical climates (Koven et al., 2017; Liu et al., 2024).

In peat soils, the temperature sensitivity of heterotrophic respiration is sometimes related to the degree of degradation. In samples from three depths in a blanket bog, Hardie et al. (2011) observed increasing Q_{10} with depth, where depth was considered analogue to degree of degradation and consequently the relative proportion of recalcitrant C molecules as part of all SOC. A similar pattern was observed by Li et al. (2021). In drained peat soils, this gradient in degree of degradation is reversed compared to undisturbed fens and bogs (apart from the labile litter and root C in the top soil) and therefore an opposite Q_{10} pattern may be expected, of decreasing Q_{10} with depth (Bader et al., 2018).

Soil moisture interacts with the temperature-respiration relationship mostly through substrate and O_2 availability, both constraining rates and temperature sensitivity of respiration (Clark & Gilmour, 1983; Davidson et al., 2006). This may imply that a measure of temperature sensitivity, such as the Q_{10}, follows a non-linear response curve to WFPS, with minima at both extremes (Fig. 2.1d). In a boreal forest peat soil, Wickland and Neff (2008) observed positive temperature effects on respiration under 50 or 75% WFPS, but not under drier (2 or

25%) or wetter (100%) treatments. Additionally, temperature increases O_2 consumption and thereby may exacerbate the O_2 limitation imposed by a high WFPS. This creates an indirect and time-lagged effect of temperature on respiration, which could become visible in increasing steepness of the moisture response under higher temperatures (Moyano et al., 2013). In peat soils, this may be enforced by the relatively high biological O_2 demand resulting from the high substrate availability. On the other hand, as relative pore volumes are larger than in mineral soils, O_2 diffusion may remain relatively high even at high WFPS, making such an effect of temperature less strong than in mineral soils (Moyano et al., 2013). Several studies have indicated that a deep water table or low WFPS intensifies the temperature sensitivity of peat respiration compared to conditions with higher soil moisture (Kechavarzi et al., 2010a; Swails et al., 2022). The study by Chen et al. (2018) demonstrated that temperature sensitivity is directly affected by oxygen availability, leading to higher Q_{10} values under aerobic conditions and a positive relationship between Q_{10} and the soil redox potential. Other studies on the other hand, demonstrate that particularly drought, rather than lack of oxygen, will inhibit the positive effect of temperature on respiration (Mäkiranta et al., 2009; Tiemeyer et al., 2024; Wickland & Neff, 2008). The interaction between soil moisture and temperature effects on peat soil respiration is therefore still unclear (Fig. 2.1d).

Ultimately, the actual maximum respiration rate and WFPS under which it occurs often varies between different peat types or stages of degradation. Generally, stronger respiration rates are observed in humified peat compared to relatively intact peat (Saurich et al., 2019b; Van Lent et al., 2019; Wickland & Neff, 2008), sometimes resulting in a decrease in respiration rates with depth (Saurich et al., 2019a). Additionally, different decomposition rates can be explained by differences in plant litter chemistry. Peat composed of Sphagnum moss litter generally decomposes at lower rates than the remains of sedge (*Carex* spp.) species (Verhoeven & Toth, 1995). This is often attributed to the lower pH and, under anaerobic conditions, the inhibiting effect of sphagnum acid on enzymatic activity (Bergman et al., 1999; Freeman et al., 2001; Verhoeven & Toth, 1995).

A high porosity, as can be found in peat soils, increases oxygen availability, even at high saturation. This raises the optimum moisture level for microbial activity (Moyano et al., 2013). On the other hand, a high C substrate availability may alleviate the limitation of moisture on respiration, as transport distance between the substrate and decomposer

is low. The combination of these two mechanisms could result in a wider plateau of optimal conditions for heterotrophic respiration (Moyano et al., 2013). Clay particles, by increasing the capillary force relative to sand, limit the amount of water available for substrate diffusion. As a result of this physical mechanism, optimal moisture levels for heterotrophic respiration are suggested to be higher in soils with a high clay content (Moyano et al., 2013). Oxidation changes the physical properties of peat soil, such as the pore space, hydraulic conductivity and water retention capacity (Kechavarzi et al., 2010b), thereby potentially affecting the moisture-respiration relationship and causing variation between soil layers in different stages of humification.

An accurate understanding of the impacts on peat oxidation is essential for reliable modelling and prediction of management effects. In this experiment we aim to improve our understanding of the interaction of the steady-state temperature and moisture impacts on heterotrophic respiration in peat soils. We studied this in an incubation experiment of disturbed soil samples from three peat sites and three depth increments (within the upper 50 cm), under four moisture and four temperature levels. Sieving and homogenizing the soil allowed us to remove roots that could interfere with the determination of peat oxidation rates. On the other hand, the soil structure and, thereby, the connections between pores are changed drastically by mixing a peat soil sample. Therefore, a parallel incubation of undisturbed cores from one site and depth was included to compare respiration rates between disturbed and undisturbed soil samples.

We hypothesized to find (1) a unimodal response curve of respiration to WFPS; (2) a positive exponential response of respiration to temperature; (3) interacting effects of soil moisture and temperature, resulting in a non-linear response of the Q_{10} to soil WFPS; (4) decreasing temperature sensitivities with depth, due to decreasing recalcitrance with depth.

2.2 Methods and materials

2.2.1 Sampling sites

Soil samples were collected in December 2023 from three sites with grassland on peat soil in the Netherlands: Aldeboarn (53°03' N, 5°54' E), Vlist (51°58' N, 4°49' E) and Zegveld (52°08' N, 4°50' E) (Fig. 2.2). The mean annual temperature at a weather station near Aldeboarn was 10.9 °C in 2023, and near Vlist and Zegveld it was 11.8 °C (www.knmi.nl). All fields are used for grass production and cattle grazing, and are normally fertilized with a combination of slurry and artificial fertilizer, at a rate of 200-250 kg N ha^{-1} yr^{-1} (Vlist and Zegveld) or slurry at 170 kg ha^{-1} yr^{-1} (Aldeboarn). The soil profile in Aldeboarn is composed of oligotrophic peat, consisting of Sphagnum, Eriphorium and heather remains, covered by a thick peaty clay top layer. On the Vlist location a peaty clay top layer is found above mesotrophic wood peat with peat and clay layers reaching as deep as ten meters. The soil in Zegveld, consists of a clayey peat top layer, containing some anthropogenic debris, covering a thick mesotrophic wood peat layer, and eutrophic sedge peat underneath, which reaches down to six meters below the soil surface (Van Asselen et al., 2023).

At each site, several gauge auger cores (50 cm long, 2 cm diameter) were taken within a 0.5 m^2 area nearby (within 50 m) the sampling locations of Blondeau et al. (2024). Bulk samples from three depths (below the soil surface) were collected and stored in separate bags: 5-10 cm, 20-25 cm, and 45-50 cm from the Aldeboarn and Vlist sites, and 5-10 cm, 20-25 and 35-40 from the Zegveld site. Previous observations of the soil horizons were used as a basis for the chosen sampling depths. In addition, 27 undisturbed soil cores were sampled in 100 cm^3 steel rings from 5-10 cm depth at the Zegveld site.

The disturbed soil samples from the three sites and three depths were air dried for three days at 20°C. Soil clumps were broken up, roots and debris were removed by hand, and the soil was mixed homogeneously and stored in a cool (4 °C), dark place until the start of the experiment. A subsample was taken from each sample and dried at 105 °C, for determination of the moisture content of the air-dried soil.



***Figure 2.2**: Locations of the three sampling sites, Aldeboarn, Zegveld and Vlist.*

2.2.2 Temperature gradient block: setup and measurements

We conducted a respiration experiment under four soil moisture treatments: 50, 60, 80 and 95% WFPS. These were combined in a full factorial design with a gradient of temperature treatments (3.1 to 35.5 °C), which were grouped in four treatment ranges: 4.6 (±1.5), 13.9 (±1.5), 23.2 (±1.5) and 34 (±1.5) °C. This resulted in 144 unique combinations of soil type and categorical treatments, each replicated three times. The Vlist sample at 45-50 cm had a WFPS of 61% after air drying. Therefore moisture treatments of 61% and 70% WFPS instead of 50 and 60% were applied for this soil.

Three grams of air-dried soil were weighed into a 60 ml vial and water was added to reach the desired WFPS treatment, while considering the moisture content of the air-dried soil. Porosity of each soil type was

determined after calculating the bulk density of the soil sample inside the vial and using the horizons' particle densities calculated using the data from Blondeau et al. (2024). After the WFPS adjustment, the vials were covered with cotton to prevent evaporation while allowing for gas exchange and they were pre-incubated for seven days at 20 °C. After seven days, the water content was adjusted to the original treatment after weighing, and the vials were placed inside the temperature incubator.

The temperature treatments were applied in a custom temperature gradient block, for measuring short term temperature effects on soil organic matter decomposition (Morán-Rivera et al., 2026). The temperature block is an insulated box, fitting four rows of 22 sample vials, along which a linear temperature gradient is applied (Fig. 2.3). A temperature gradient is established by a heater on one end and a cooler on the other end, with eight temperature sensors spaced evenly along the gradient to measure and check the actual temperature. Four temperature intervals of 3 °C were selected, within which vials with different soil-moisture combinations were distributed randomly. Nine block-runs were performed in total to measure all treatment combinations in threefold.

Vials were placed inside the temperature block and incubated overnight for approximately 17 hours. Moisture content of the vials was checked again and adjusted if necessary in the morning. The vials were closed air-tight with stoppers and headspace CO_2 concentrations were measured after four hours using Optical Feedback Cavity Enhanced Absorption Spectroscopy (LI-7815, LI-COR Inc., USA) for 20 seconds, while checking for a linear concentration increase. Fluxes of CO_2 were calculated from the linear slope over the headspace concentration at $t = 4$ hours and the ambient concentration at $t = 0$.

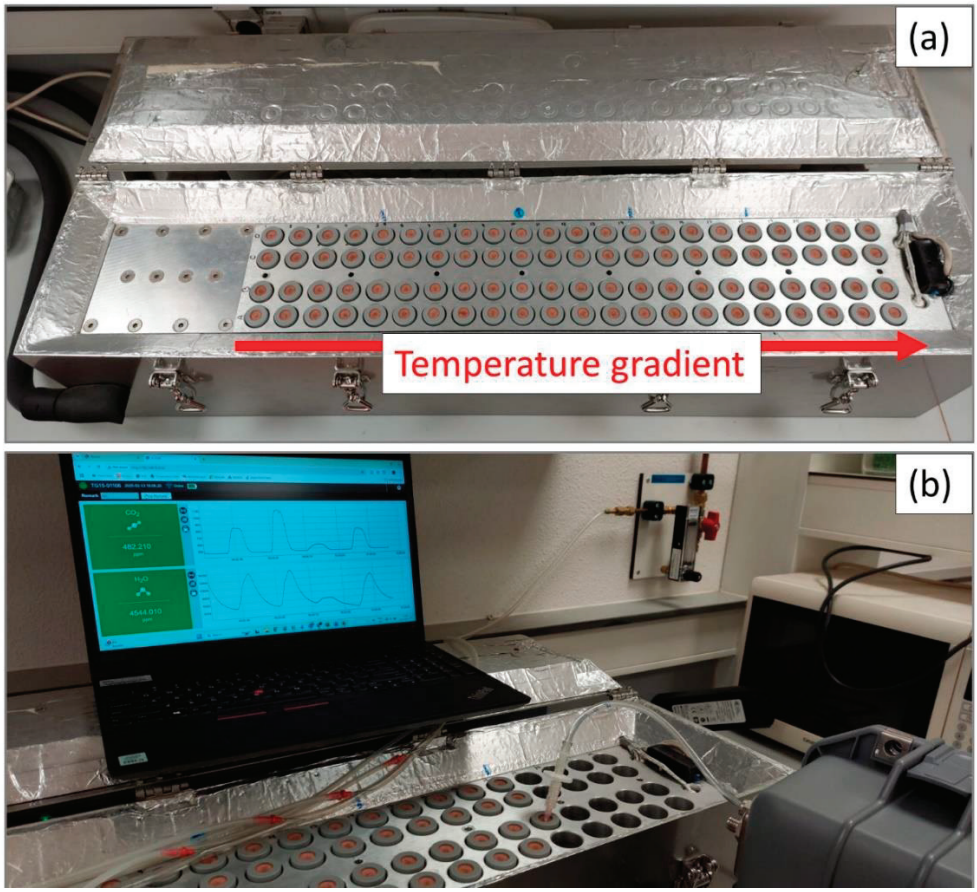


***Figure 2.3**: The temperature gradient block seen from above with the lid opened, with incubation vials in each slot (a) and a gas flux measurement taking place in one of the soil vials, using the LI-7815 analyzer (b). The red arrow in (a) indicates the direction of increasing temperature along the length of the block.*

2.2.3 Undisturbed samples: setup and measurements

The 27 undisturbed soil cores from Zegveld (5-10 cm) were stored air-tight at 4 °C until the start of the experiment. During a seven day pre-incubation at 16 °C, the cores were first saturated (three days) and subsequently subjected to a pressure head in the middle of the soil core of either -3 cm, -50 cm or -100 cm on a sandbox (four days). This resulted in nine cores per moisture treatment. Over this period, the samples were weighed twice a day, to check for equilibrium in the water tension. After pre-incubation, all cores were placed inside polypropylene jars (open at the top) and three cores per moisture treatment were moved to either a cabinet incubator at 6°C, a climate controlled room at 16 °C or at 20 °C. Soil CO_2 emissions were measured after 4, 28 and 52 hours. The jars were

closed and headspace concentrations measured after a minimum closure time of 22 minutes, using a photoacoustic gas analyzer (Gasera One, Gasera Ltd., Finland). Fluxes were calculated from the linear slope between the headspace concentration at the end of the chamber closure and the ambient concentration at t=0 and expressed as μg CO_2-C g^{-1}C h^{-1}. The cores were weighed before each flux measurement and after drying at 105 °C, to calculate the actual WFPS at the time of measurement. Due to a technical error, the actual pressure heads under the -100 cm treatment showed little difference with the -50 cm treatment. Therefore, statistical analyses were performed using the numeric WFPS values, rather than the discrete pressure head treatment levels.

2.2.4 Soil chemical parameters

Batches of the air dried, homogenized soil from all sites and depths were oven-dried at 40°C for subsequent analysis of chemical soil parameters. Readily available concentrations of P, NH_4^+ and NO_3^- + NO_2^-, as well as soil pH were measured using segmented flow analysis (Skalar SAN++, Skalar Analytical B.V., The Netherlands) after extracting three grams of oven dried soil in a 0.01 M $CaCl_2$ solution. Total concentrations of carbon and nitrogen were determined on colloid grinded samples, using dry combustion at 1050°C (LECO CN 828, LECO Corporation, USA). The soil organic matter (SOM) content was determined on oven-dried soil at 105°C, as the relative loss on ignition at 550°C for three hours.

2.2.5 Data analysis

All data analyses were performed using R (v4.3.1; R Core Team, 2023) and were interpreted using a significance threshold level p = 0.05. The effects of the discrete WFPS (50, 60, 80, 95%) and temperature (4.6±1.5, 13.9±1.5, 23.2±1.5 and 34±1.5 °C) treatments on the respiration rates (μg C g^{-1}C h^{-1}) of the disturbed samples were tested using a linear mixed effects model (LMEM) from the 'nlme' R package (Pinheiro et al., 2023), with the sampling depth and site incorporated as nested random factors. To meet the assumptions of normal and homogeneous distribution of the residuals, a Box Cox transformation of the respiration rates was performed using the 'MASS' R package (Venables & Ripley, 2002). Pair-wise comparisons were performed based on the estimated marginal means of each treatment level.

For each combination of sampling location, depth and WFPS treatment, the relationship between the CO_2 production rate

(R; µg C g^{-1} C h^{-1}) and temperature was fitted using an empirical exponential function after Van ‘t Hoff (Van 't Hoff, 1898):

$$R = \alpha * e^{\beta T} \quad (1)$$

Where α (µg C g^{-1} C h^{-1}) and β (°C^{-1}) are fitted parameters and T is the *actual* temperature (°C) of each separate sample (instead of the grouped, discrete treatment ranges which were used in the LMEM above).
Following Eq. 1, a Q_{10} value over the temperature range 3.1-35.5 °C was calculated for each combination of location, depth and WFPS treatment:

$$Q_{10} = e^{10\beta} \quad (2)$$

where the factor 10 refers to a change in temperature of 10 °C (or 10 K). The effect of the WFPS treatment on Q_{10} was tested in an LMEM with depth nested in site as random factors.

Additionally we calculated temperature-specific Q_{10} values following a function derived from the Arrhenius equation, introduced by Lloyd and Taylor (1994) and described in Moinet et al. (2025). First, the respiration-temperature relationship was fitted using:

$$R = R_{10} * e^{E_0\left(\frac{1}{56.02} - \frac{1}{T - T_0}\right)} \quad (3)$$

where R_{10} is a fitted parameter representing the respiration at 10 °C (µg C g^{-1} C h^{-1}), E_0 is a fitted parameter originally representing the activation energy divided by the ideal gas constant (K), T_0 is a constant with a value of 227.13 K, and T is the sample temperature (K). The Q_{10} for a given reference temperature (tQ_{10}) can then be derived following:

$$tQ_{10} = e^{\frac{10\,E_0}{(T-T_0)(T-T_0+10)}} \quad (4)$$

Effects of the WFPS treatment on the R_{10} and E_0 parameters were tested in an LMEM with depth nested in site as random factors.

We performed a two-way analysis of variance (ANOVA) to test whether respiration rates from the different locations and depths varied significantly. The same was done to test variation of Q_{10} values between sites and depths.

Pearson correlations were calculated between the chemical sample properties and the mean heterotrophic respiration rates and Q_{10} values, respectively, using the *cor.test* function in R (R Core Team, 2023).

2.3. Results

2.3.1 WFPS and temperature effects on respiration and Q_{10}

Respiration rates ranged between 0 and 79 µg CO_2-C g^{-1} C h^{-1} and were significantly affected by the WFPS (LMEM, F = 45.8, p < 0.0001). The respiration rates under 50, 60 and 80% WFPS levels showed significant pair-wise differences amongst each other, increasing with WFPS. Respiration rates for the 80% and 95% WFPS levels did not differ significantly, indicating arrival at an optimum (Fig. 2.4). All soils in this experiment showed the above pattern (Fig. S2.1), except for the Aldeboarn samples from 45-50 cm depth which showed unimodal responses to WFPS under 23.2 and 34 °C (Fig. S1.c).

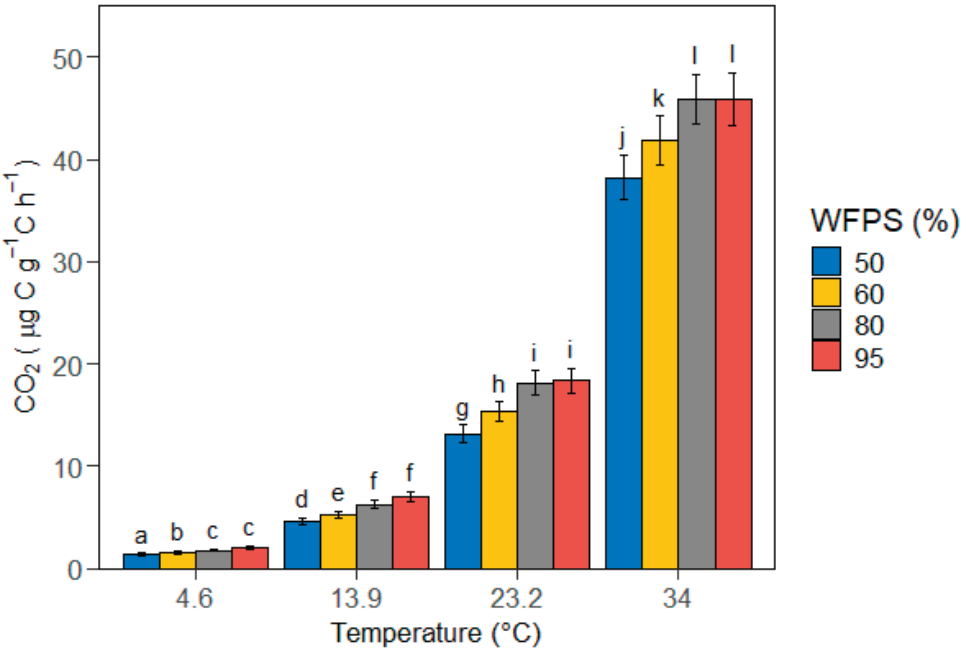


***Figure 2.4**: Mean respiration rates (µg C g^{-1} C h^{-1}) and standard errors of the mean (n = 3) for each discrete temperature and WFPS treatment level. The letters above the bars indicate significant pairwise differences between factor levels, determined in the LMEM's post-hoc test (p < 0.05).*

The discrete temperature treatment levels had a significant positive effect (LMEM, F = 4340.9, p < 0.0001) on respiration rates, with

significant differences between all paired combinations of temperature levels (Fig. 2.4). Respiration rates showed an exponential increase with temperature for each location, depth and WFPS treatment combination (Fig. 2.5). There was no significant interaction effect between WFPS and temperature on soil respiration (LMEM, $p > 0.05$).

The Q_{10} values calculated over the 3.1-35.5 °C interval ranged between 2.0 and 3.3 (Table 2.1) and were significantly affected by WFPS (LMEM, $F = 17.0$, $p < 0.001$), showing a decreasing Q_{10} with increasing WFPS (Fig. 2.6a). A significant difference was observed between Q_{10} values at 50% (mean 2.9) and 95% WFPS (mean 2.5), a difference of 17%.

The WFPS treatment significantly affected the fitting parameters in Eq. 3, R_{10} ($F = 16.2$, $p < 0.0001$) and E_0 ($F = 16.2$, $p < 0.0001$). Under 50 ($n = 8$), 60, 80 and 95% WFPS ($n = 9$) the E_0 parameter had mean values of 564, 524, 492 and 466, respectively. The temperature-specific tQ_{10} strongly decreased with temperature, from 4.5-6.2 under 5 °C to 2.0-2.4 under 30 °C (Fig. 2.6.b).

2.3.2 Sampling location and -depth effects

Heterotrophic respiration grouped per sampling location and depth showed high variation within the factor levels, and high heterogeneity between levels (Fig. 2.7a, 2.7b). Q_{10} values of the different locations differed significantly (ANOVA, $F = 8.8$, $p = 0.001$) while depth had no effect ($F = 0.61$, $p = 0.5$). At each sampling depth, the Aldeboarn soil showed the lowest Q_{10}, with slightly lower values than for the Vlist and Zegveld soils. The only significant pair-wise difference was found between Aldeboarn and Zegveld samples at the third sampling depth (45-50 and 35-40 cm, respectively; Fig. 2.7.c).

Soil organic matter content, total C and N content and the readily available N and P concentrations differed between sampling locations and depths, reflecting the vegetation composition and the locations of clay layers (Table 2.2). A strong, positive and significant Pearson correlation was observed between heterotrophic respiration and (plant-)available P ($r = 0.88$, $p < 0.01$), but not with other soil parameters (Table 2.3). Mineral nitrogen concentration (the sum of $CaCl_2$ extracted NH_4 and $NO_3 + NO_2$) showed a positive, significant correlation with Q_{10} ($r = 0.69$, $p < 0.05$).

2.3.3 Respiration rates of the undisturbed soil cores

Respiration rates from the undisturbed core samples ranged between 3.7 and 31.0 µg CO_2-C g^{-1} C h^{-1} (0.6 to 4.2 µg CO_2-C g^{-1} dry soil h^{-1}) and slightly increased over days one to three from an average value (n = 27) of 12.9 to 15.0 µg CO_2-C g^{-1} C h^{-1} (Fig. S2.2). These values are slightly higher, but of the same magnitude as respiration rates from the disturbed samples in this experiment. The three matric potential applications resulted in WFPS values between 77 and 98%, which slightly decreased over the three measurement days.

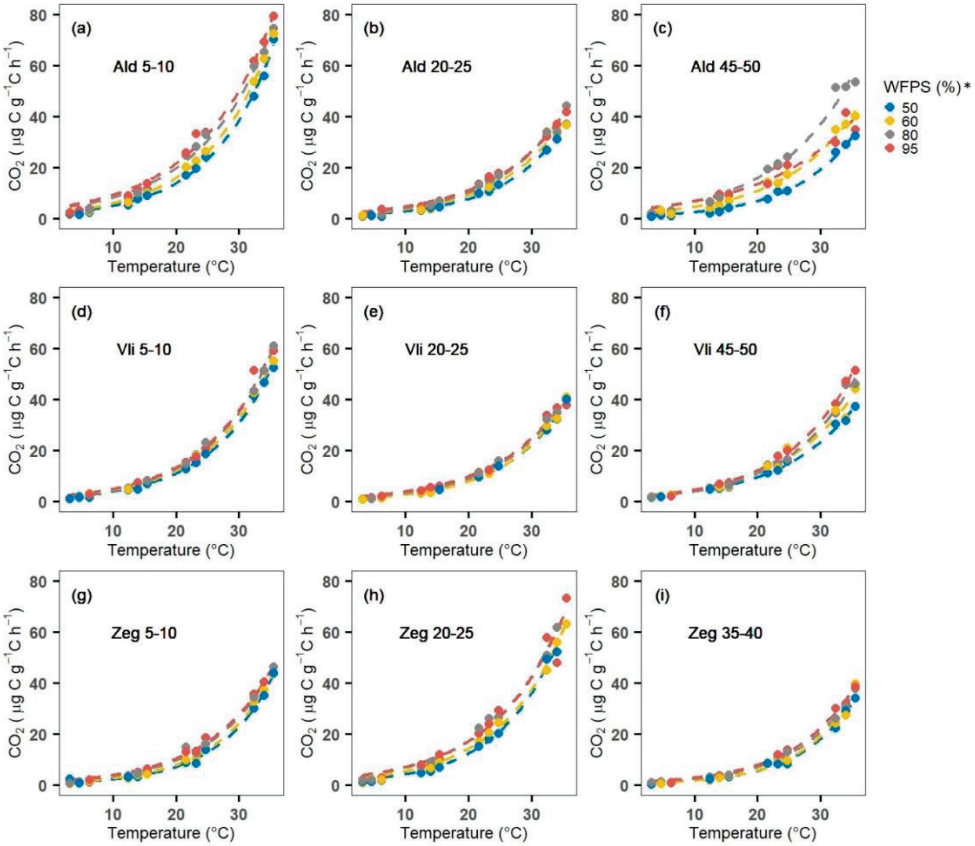


***Figure 2.5**: Respiration rates (µg C g^{-1} C h^{-1}) against temperature under the four WFPS treatments in samples from Aldeboarn at 5-10 cm (a), 20-25 cm (b) and 45-50 (c), from Vlist at 5-10 cm (d), 20-25 cm (e) and 45-50 cm (f) or from Zegveld at 5-10 cm (g), 20-25 cm (h) and 35-40 cm (i). Points show the measured respiration rates and dashed lines the fitted Eq. 1. * The Vlist sample at 45-50 cm (f) had a WFPS of 61% after air drying. Therefore moisture treatments of 61% and 70% WFPS instead of 50 and 60% were applied to this soil.*

***Table 2.1**: Q_{10} values (3.1-35.5°C interval) for each sampling location and depth.*

Location	Depth (cm)	50%*	60%*	80%	95%
Aldeboarn	5-10	2.79	2.66	2.39	2.33
	20-25	2.74	2.55	2.53	2.37
	45-50	2.80	2.41	2.32	2.00
Vlist	5-10	2.78	2.66	2.69	2.67
	20-25	2.80	2.85	2.65	2.48
	45-50	2.40	2.37	2.60	2.57
Zegveld	5-10	3.16	3.02	2.75	2.64
	20-25	2.90	2.62	2.49	2.43
	35-40	3.21	3.32	2.89	2.79

*The Vlist sample at 45-50 cm had a WFPS of 61% after air drying. Therefore moisture treatments of 61% and 70% WFPS were applied instead of 50 and 60%.

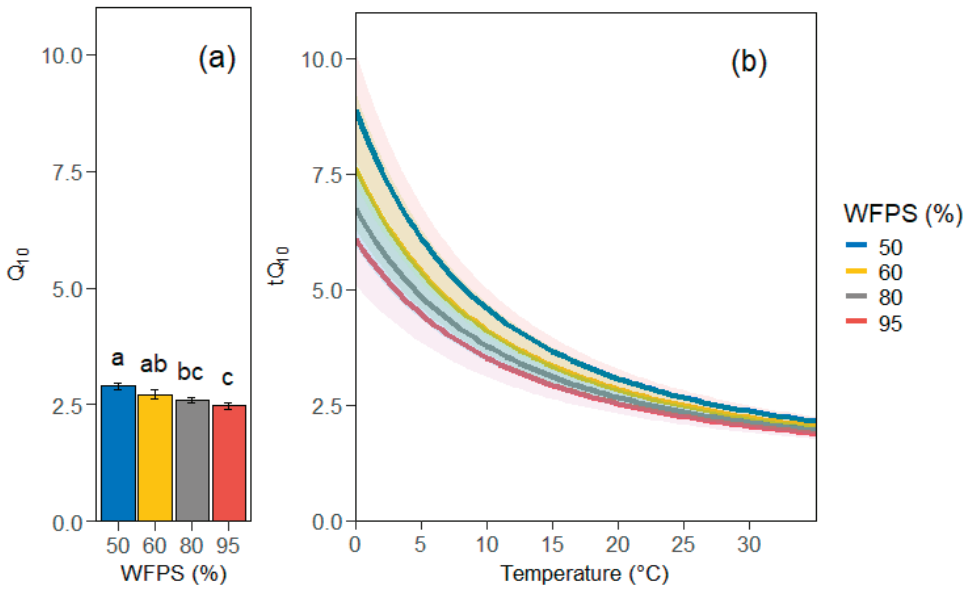


***Figure 2.6**: Mean Q_{10} values calculated over the 3.1-35.5 °C temperature interval using Eq. 2, and grouped per WFPS level (a) and the temperature-specific tQ_{10}, fitted using the mean E_0 parameter for each WFPS level in Eq. 4 (b). Error bars in (a) show the standard error of the mean, with n = 8 for 50% and n = 9 for the other WFPS levels. The letters above each bar in (a) indicate significant pairwise differences between factor levels, determined in an LMEM using a significance level of $p < 0.05$. The shaded areas in (b) show the 95% confidence interval of the estimated tQ_{10}.*

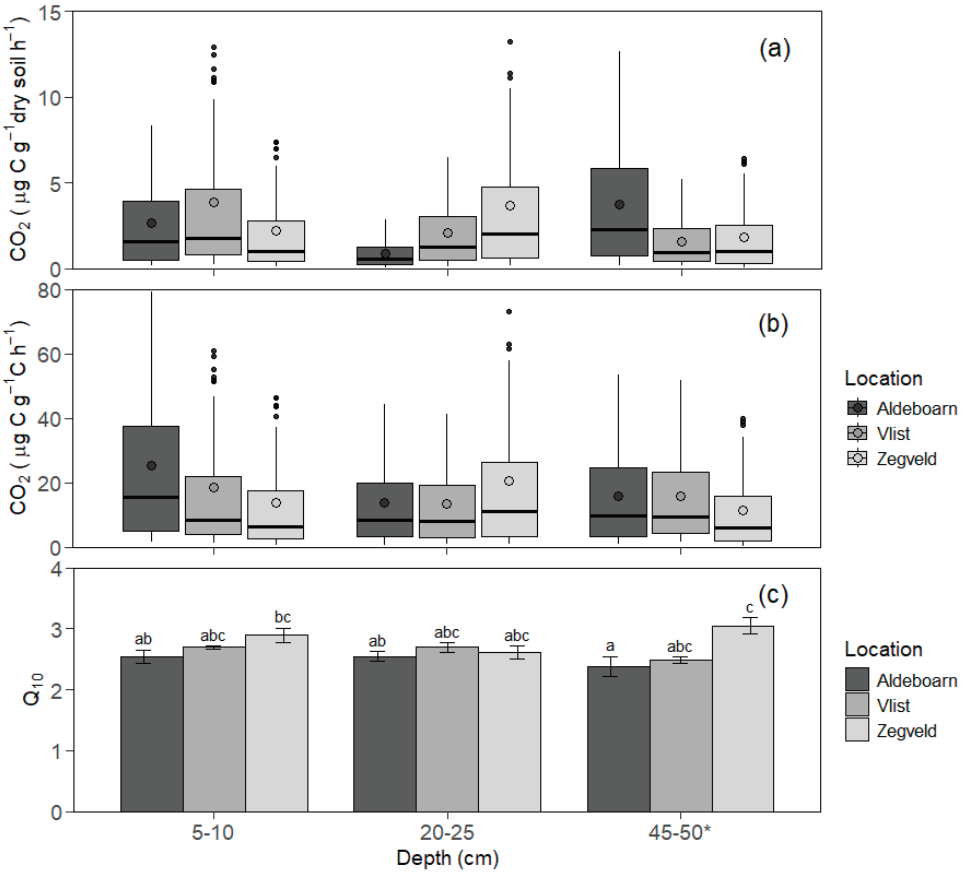


***Figure 2.7**: Boxplots of the respiration rates, expressed as µg C g^{-1} dry soil h^{-1} (a) or µg C g^{-1} C h^{-1} (b), and mean Q_{10} values (c) for each location and depth. The gray-scale colored symbols in (a) and (b) represent the mean respiration value (n = 48), whiskers show the distance of 1.5 times the interquartile range (IQR), and black dots are outliers falling outside 1.5*IQR. Error bars in (c) indicate the standard error of the mean (n = 48). * The third sample in Zegveld was taken at a depth of 35-40 cm.*

***Table 2.2**: Soil properties in the three sites and depths.*

Location	Depth (cm)	SOM (weight %)	C/N (kg C kg^{-1} N)	C-tot (g C kg^{-1})	N-tot (g N kg^{-1})	N-min (mg N kg^{-1})	P_{CaCl2} (mg P kg^{-1})	pH-$CaCl_2$
Ald.	0 - 5	22.2	12.1	104.9	8.70	27.68	0.64	5.3
	20 - 25	15.2	14.6	64.9	4.46	13.69	0.10	5.1
	45 - 50	41.7	29.4	236.0	8.02	16.38	0.27	4.6
Vli.	0 – 5	42.9	11.0	211.1	19.17	30.17	0.50	4.8
	20 - 25	32.8	12.4	158.0	12.76	40.20	0.03	5.3
	45 - 50	24.7	9.94	100.9	10.15	23.22	0.07	4.8
Zeg.	0 - 5	33.4	10.5	159.3	15.12	37.77	0.13	5.3
	20 - 25	40.1	10.7	180.5	16.85	27.77	0.27	5.1
	35 - 40	35.5	11.2	160.5	14.30	32.17	0.07	5.2

***Table 2.3**: Pearson correlation coefficients between the mean heterotrophic respiration (µg C $g^{-1}C$ h^{-1}), or Q_{10} values (n = 9), and the measured chemical properties of the nine soils. Significance levels are indicated by asterisks.*

	Respiration	Q_{10}
SOM	-0.04	0.21
C-tot	-0.03	0.08
N-min	-0.11	0.69*
N-tot	0.04	0.56
pH	0.09	0.53
C/N ratio	-0.08	-0.52
P ($CaCl_2$)	0.88**	-0.28

*p < 0.05, ** p < 0.01

2.4. Discussion

2.4.1 Soil water filled pore space effects on respiration

We hypothesized to find a unimodal response of soil heterotrophic respiration to WFPS, with maximum respiration rates around 80% WFPS and rates decreasing under lower or higher WFPS values. The heterotrophic respiration measured in our disturbed soil samples did arrive at an optimum at the 80% WFPS treatment, but did not decrease under the higher level of 95% WPFS (Fig. 2.4).

While we could not point out a precise optimum WFPS for heterotrophic respiration in our experiment with only four treatment levels, these data suggest that the substrate supply required for heterotrophic respiration, become limited by low moisture availability at a WFPS of 60% or lower.

Several other studies on peat soils have reported wide moisture ranges, under which conditions for heterotrophic respiration are optimal. Unimodal WFPS-respiration relationships have been observed with maximum rates occurring at WFPS levels between 50 and 75% in boreal black spruce forest peat (Wickland & Neff, 2008), 56 and 92% in temperate agricultural peat soil (Saurich et al., 2019a), 60 to 70% in tropical swamp forest peat (Van Lent et al., 2019), or between 60 and 90% in boreal peat (Byun et al., 2021).

The optimum WFPS level of 80-95% observed here, falls towards the higher end of previously reported observations. Under the relative O_2 limitation associated with a 95% WFPS, respiration appeared to level off, but not yet decrease. This pattern suggests that a substantial reduction in peat oxidation will only be achieved under (near) saturated conditions. Berglund and Berglund (2011) derived from their observations on incubated (10 cm) peat cores that a small suction level of -5 cm, corresponding to 1-8% air filled pore space, was sufficient to induce high rates of respiration – in some cases higher than or similar to the respiration under stronger suction levels. This proposed the existence of a unimodal moisture response curve due to even higher respiration rates under moisture conditions between 80 and 95% WFPS, a range not studied in this experiment. A unimodal response of respiration to soil WFPS was observed only in the Aldeboarn samples from 45-50 cm depth, with an optimum at 80% WFPS (Fig. S2.1). Under 80% WFPS and the 23.2 and 34 °C treatments, mean maximum rates of 21.8 and 52.2 μg CO_2-C g^{-1} C h^{-1} were measured, respectively; 18 and 48% higher than the respective rates at 95% WFPS. This soil horizon was composed of Sphagnum peat, characterized by a relatively low N content and pH

compared to the other soils in our study, which may have imposed limitations on decomposition. Although we did not measure bulk densities in our study, previous research on this location reported lower bulk densities for the Aldeboarn 45-50 cm soil than the other samples in this experiment (e.g., Blondeau et al., 2024). Kechavarzi et al. (2010a) observed stronger sensitivity to moisture changes, with optimum respiration at lower soil moisture levels, in (semi-) fibrous peat than humified peat samples. On the other hand, Saurich et al. (2019a) observed clear unimodal WFPS dependencies with similar optima around 84% WFPS for both decomposed, nutrient rich top-soil samples and fibrous sub-soil samples.

A second interpretation of our results is that they indicate a non-negligible contribution of anaerobic oxidation to CO_2 emissions at high WFPS (Fairbairn et al., 2023). In an aerobic incubation experiment on mineral soil, Fairbairn et al. (2023) observed significant respiration under near saturated conditions (WFPS > 80%). While O_2 diffusion can still occur at a low rate in (near) saturated soils, the authors measured similar respiration rates under saturation combined with an anaerobic headspace. After a period of drought or water table drawdown, peat soils are typically abundant in nitrate, sulphate and oxidized iron (Fe^{3+}) compounds, which can subsequently function as electron acceptors in the oxidation of organic matter after flooding of the soil (Harpenslager et al., 2024; Reiche et al., 2009). These anaerobic metabolisms have a lower energy yield and consequently proceed more slowly and constrained than aerobic peat oxidation (Keiluweit et al., 2017). When both occur simultaneously, however, anaerobic oxidation in saturated pores may partly compensate for the decline in aerobic oxidation (Fairbairn et al., 2023). The question remains, however, whether fully anaerobic conditions can be established, even in microsites, in such small samples. The volume of these samples may have been so small relative to the surface area that diffusion of O_2 was possible into most soil pores.

In a third explanation, the increasing respiration rate with WFPS may have been part of a bimodal response pattern caused by the different pore sizes present in peat. Arnold et al. (2015) observed peak respiration rates from incubated peat samples under the minimum *and* maximum drainage treatments included in their experiment, which they attribute to high availability and mobility of labile SOM in the macropores and micropores, respectively. They explain the lower C turnover rates under the intermediate water potential treatments (-10 to -250 kPa), by a

simultaneous water limitation in the macropores and O_2 limitation in the micropores. A similar pattern was observed by Kechavarzi et al. (2010a).

2.4.2 Temperature effect and interaction with soil moisture

In accordance with our hypothesis, heterotrophic respiration showed an exponential increase with temperature. We also hypothesized to find an interaction effect between moisture and temperature on soil respiration. The response to temperature was expected to be limited by O_2 as well as by moisture, resulting in a unimodal response of Q_{10} or tQ_{10} to WFPS. While the moisture and temperature treatments did not have a significant interaction effect on respiration, Q_{10} and tQ_{10} values decreased with increasing WFPS, and differed significantly between 50 and 95% (Fig. 2.6a).

This indicates a limitation posed by O_2 availability, rather than moisture availability on the temperature effect. This may be attributed to the WFPS interval included in this experiment, which did not include drier levels than 50% WFPS and may not have resulted in sufficient moisture deficit to limit substrate mobility. However, the importance of O_2 availability for the impact of temperature on peat respiration was also stressed by Chen et al. (2018), who reported increasing Q_{10} values along a gradient from extreme anaerobic to aerobic conditions. Similarly, in a meta-analysis on 31 paired Q_{10} observations under wet and dry conditions, temperature sensitivity was found to be stronger under dry conditions (Liu et al., 2024). This was particularly significant in samples from temperate and boreal climates. Other trends have been reported in the field, however, of increasing temperature sensitivity with higher mean (summer) water levels (Mäkiranta et al., 2009; Taggart et al., 2012; Tiemeyer et al., 2024).

The WFPS had a significant effect on the temperature-independent Q_{10}, as well as the fitting parameters R_{10} and E_0 for the temperature dependent tQ_{10}. This is not surprising, since the β and E_0 parameters from Eqs. 2 and 4, respectively, are closely related to each other (Moinet et al., 2025) and the exponential parameter E_0 and Q_{10} following van 't Hoff can be directly related to each other (Heinen, 2006), indicating the temperature dependence of Q_{10}. This is due to the activation energy requirements of oxidation reactions, which, with increasing temperature, are met for an increasing fraction of the organic molecules (Davidson & Janssens, 2006).

Despite the importance of this characteristic, temperature-independent Q_{10} values (following exponential Eqs. 1 and 2, or by

calculating the respiration rate difference for one specific temperature interval) are more commonly reported for peat soils (e.g., Chen et al., 2018; Kechavarzi et al., 2010a; Liu et al., 2024). Many soil process models use a temperature reduction function with a fixed Q_{10} for the description of SOC mineralization (Bakema et al., 2022; Heinen, 2006). Ranging between 2.0 and 3.3, our Q_{10} values across the 3.1-35.5°C temperature range were comparable to other observations in peat soils or litter incubations (Bader et al., 2018; Byun et al., 2021; Fierer et al., 2005; Li et al., 2021; Liu et al., 2024).

The importance of reporting temperature-specific Q_{10} values becomes clear from Fig. 2.6b, however, which shows a negative relationship between tQ_{10} and temperature. Along a temperature gradient from 0 to 35 °C the values of individual treatment combinations ranged between a maximum tQ_{10} of 12.3 (Zegveld 35-40 cm, fitted to 0 °C) and a minimum tQ_{10} of 1.7 (Aldeboarn 45-50 cm, fitted to 35 °C).

Moinet et al. (2025) set out to explain the significance of reporting temperature-specific, rather than temperature-independent Q_{10} values. By plotting the constant Q_{10} derived from Eq. 2, together with a temperature dependent tQ_{10} (from Eq. 4) against temperature, they clearly visualize how a constant Q_{10} can under- and overestimate the temperature dependency of heterotrophic respiration under low and high temperatures, respectively. We can interpret Fig. 2.6 in the same way: mean Q_{10} values in Fig. 2.6a fall largely below the lines in Fig. 2.6b, suggesting an underestimation of the actual temperature sensitivity below a temperature of approximately 20 °C. This is an important consideration when estimating warming effects on soil respiration in a climate with a mean annual temperature around 11 °C.

The effect of WFPS (as well as the effect confidence interval) appeared to decrease with temperature. Our results indicate that the heterotrophic respiration was most affected by temperature under low soil moisture content and low temperatures. This suggests strongest sensitivity to temperature increase under dry conditions in a relatively cold environment, which is in agreement with previous findings (e.g., Li et al., 2021; Liu et al., 2024). These dynamics should be explored further on larger, undisturbed soil samples, which better represent the soil structure in the field. While we confirmed that respiration rates of the disturbed samples were of similar size as those in the 100 cm^3 cores, the temperature and moisture patterns were less pronounced and showed a time dependence (Fig. S2).

2.4.3 Soil properties effects

We hypothesized to measure decreasing Q_{10} values with depth, in accordance with relative enrichment in recalcitrant organic matter in more degraded peat. We did not find a gradient with depth however, nor any differences between the three sampling depths (Fig. 2.7).

This is surprising, given strong differences in soil texture between some of the layers. Even in the second sampling depths at Aldeboarn and Vlist, which were located in horizons previously determined to have a high clay content (Blondeau et al., 2024), the respiration-moisture response did not diverge from the other soils (Fig. S1). Clay content affects SOM decomposition directly through mineral association as well as indirectly through water availability. A high clay content may raise the optimal moisture content for soil respiration (Moyano et al., 2013; Moyano et al., 2012), but it did not seem to affect the relationship in our observations.

Respiration rate did not correlate significantly with N-min or N-tot, but did with available P (Table 2.3, $p < 0.05$). This may indicate a P limitation rather than an N limitation to the decomposing microbial communities (Saurich et al., 2019b). The Q_{10} showed a significant relation (Table 2.3, $p < 0.05$) with mineral nitrogen concentration (NH_4^+ and NO_3/NO_2) and relatively strong correlation coefficients with N-tot and C/N ratio (negative correlation). Decomposing peat becomes progressively enriched in nitrogen, relative to carbon, due to preferential oxidation of C (Leifeld et al., 2020; Malmer & Holm, 1984). These results on the correlation between mineral N content and Q_{10} may therefore be related to the degree of decomposition, which in turn is generally positively related with Q_{10} (Bader et al., 2018; Hardie et al., 2011; Li et al., 2021).

2.5 Conclusion

Heterotrophic respiration of incubated peat samples showed an exponential increase with soil temperature treatments ranging between 3.1 and 35.5 °C, and an increase with soil moisture between 50 and 95% WFPS. The respiration temperature sensitivity tQ_{10} decreased with WFPS, indicating a limitation of O_2 availability on the temperature effect. The temperature dependent tQ_{10} decreased exponentially with soil temperature, stressing the importance of taking this dependency into account. There was no effect of sampling location or depth on the respiration rates or Q_{10}. Our results suggest that heterotrophic respiration of peat soil is most susceptible to warming under dry and cold conditions.

Acknowledgements
We would like to thank Karen Morán-Rivera and Gabriel Moinet for the use of, and assistance with the Eunice temperature incubation block. The research presented in this chapter is part of the project Living on soft soils: subsidence and society (grantnr.: NWA.1160.18.259). This project is funded by the Dutch Research Council (NWO-NWA-ORC), Utrecht University, Wageningen University, Delft University of Technology, Ministry of Infrastructure & Water Management, Ministry of the Interior & Kingdom Relations, Deltares, Wageningen Environmental Research, TNO-Geological Survey of The Netherlands, STOWA, Water Authority: Hoogheemraadschap de Stichtse Rijnlanden, Water Authority: Drents Overijsselse Delta, Province of Utrecht, Province of Zuid-Holland, Municipality of Gouda, Platform Soft Soil, Sweco, Tauw BV, NAM. This study was a collaboration with the project "Nationaal Onderzoeksprogramma Broeikasgassen Veenweiden" (NOBV).

Chapter 2 Supplementary material

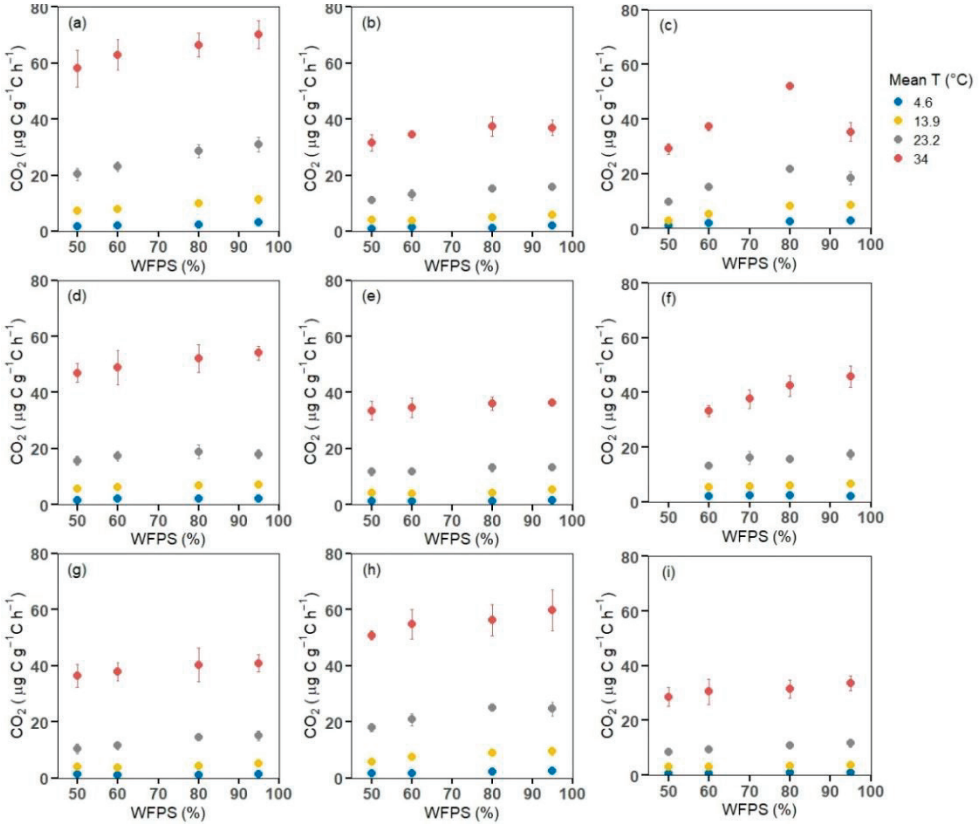


***Figure S2.1**: Mean respiration rates (µg C g^{-1} C h^{-1}) plotted against the WFPS treatment under the four temperature treatment levels (mean of three values within a 3°C interval) in samples from Aldeboarn at 5-10 cm (a), 20-25 cm (b) and 45-50 (c), from Vlist at 5-10 cm (d), 20-25 cm (e) and 45-50 cm (f) or from Zegveld at 5-10 cm (g), 20-25 cm (h) and 35-40 cm (i). Error bars show the standard error of the mean (n = 3).*

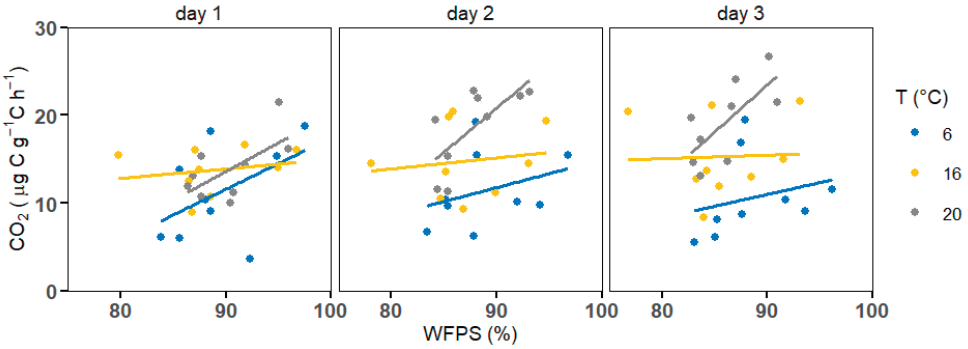


Figure S2.2: Respiration rates of the undisturbed soil cores from 5-10 cm depth in Zegveld, plotted against the WFPS on days 1 to 3 of the temperature incubation.


3

Chapter 3

Groundwater level effects on greenhouse gas emissions from undisturbed peat cores

Erne Blondeau, Gerard L. Velthof, Marius Heinen, Rob F. A. Hendriks, Anneke Stam, Jan J. H. van den Akker, Monne Weghorst, Jan Willem van Groenigen

Published as: Blondeau, E., Velthof, G. L., Heinen, M., Hendriks, R. F. A., Stam, A., van den Akker, J. J. H., Weghorst, M., van Groenigen, J. W. (2024). Groundwater level effects on greenhouse gas emissions from undisturbed peat cores. *Geoderma, 450*.
https://doi.org/10.1016/j.geoderma.2024.117043

Abstract

Peat soils store a large part of the global soil carbon stock, which can potentially be lost when they are drained and taken into cultivation, resulting in CO_2 emission and land subsidence. Groundwater level (GWL) management has been proposed to mitigate peat oxidation, but may lead to increased emissions of nitrous oxide (N_2O) and methane (CH_4).

The aim of this experiment was to study trade-offs between greenhouse gas emissions from peat soils as a function of GWL. We incubated 1 m deep, 24 cm diameter undisturbed bare soil cores, after removal of the grass layer, from three contrasting Dutch grassland peat sites for 370 days at 16°C. The cores were subjected to drying-wetting cycles, with the GWL varying between near the soil surface to 160 cm below the surface. We measured gas fluxes of CO_2, N_2O and CH_4 from the soil surface, extracted pore water for DOC and mineral nitrogen analysis, and measured soil hydraulic and shrinkage characteristics.

Emissions of CO_2 increased after lowering the GWL, but showed different GWL-response curves during rewetting of the soil. On average, highest CO_2 emissions of 1.5 g C m^{-2} day^{-1} were found at a GWL of 80 cm below the surface. However, the 0 cm GWL was the only treatment with significantly lower CO_2 emissions than other GWLs. Cumulative CO_2 emissions differed significantly between sampling sites. Emissions of N_2O showed a different response, peaking at GWL heights above -20 cm, particularly after a recent GWL rise. Though not significantly different, the highest N_2O emissions were measured at the 0 cm GWL treatment. We confirmed this pattern for N_2O in un-replicated soil cores with grass sward, although emission values were lower in these cores due to the root uptake of mineral nitrogen. CH_4 emissions or -uptake remained low under any GWL. We conclude that raising the GWL is a successful strategy to reduce CO_2 emissions from peat oxidation. However, raising the GWL close to the soil surface could lead to N_2O emissions that negate any gains in terms of global warming potential. Our results suggest that raising the GWL in peat grasslands to -20 cm creates such a risk. A constant GWL at the surface (0 cm) would be preferential for mitigating both CO_2 and N_2O emissions, although such conditions don't allow for agricultural grass production (mowing or grazing).

3.1 Introduction

Peatlands are formed under wet, anaerobic conditions and are characterized by a high soil organic matter (SOM) content resulting from the accumulation of dead plant material. Globally, peat soils are estimated to have accumulated over 600 Gt carbon (C) during their formation (Yu et al., 2010), making up about 25% of the current estimated C pool stored in soils worldwide (Jobbagy & Jackson, 2000). Across the world, many peat soils experience C loss due to oxidation of their SOM, resulting in emissions of carbon dioxide (CO_2). This can be the result of active drainage for agricultural practices or groundwater extraction resulting in aeration of the soil and accelerating oxidation reactions (Hiraishi et al., 2014). Greenhouse gas (GHG) emissions from peat soils (of which by definition at least 40 of the upper 80 cm of the soil profile is organic soil) are especially important in the Netherlands, as many peat soils are drained for dairy farming (RIVM, 2022). Drainage of organic soils (peat and peaty soils, of which the latter contain an organic layer making up less than 40 cm in the upper 80 cm) is the largest source of CO_2 emissions from land use and land use change in the Netherlands, accounting for a substantial part of the Dutch national GHG emissions (RIVM, 2022). In addition to increasing GHG emissions, drainage causes subsidence of peat soils at rates ranging from 2 to 25 mm yr^{-1}, through SOM oxidation as well as shrinkage and consolidation processes (Erkens et al., 2016; Van den Akker et al., 2008). Van den Akker et al. (2008) estimated that a subsidence of 1 mm yr^{-1} is associated with an emission of 2.2 Mg CO_2 ha^{-1} yr^{-1}. Soil subsidence can cause damage to buildings and infrastructure, affects the water regulation in adjacent nature reserves, reduces the water storage capacity of an area and can cause upwards seepage of salt water (Van den Born et al., 2016). Moreover, it increases the flood risk of the Dutch low coastal peat land, an area already situated below the mean sea level.

In order to reduce CO_2 emissions from these soils, as well as to prevent further subsidence, it has been suggested to raise the groundwater level (GWL) through the raising of ditchwater levels and improving infiltration via drains or trenches. Particularly the prevention of relatively deep GWLs during dry summer periods may be effective in reducing CO_2 emissions and subsidence (Hoving et al., 2022). Based on several past and ongoing studies to explore the potential of subsoil irrigation systems for better GWL manipulation (Boonman et al., 2022; Van Asselen et al., 2023), the Dutch government has expressed its intent to raise the GWL in the low lying peat meadow areas to -40 or even -20 cm

with respect to the soil surface (z-coordinate positive upwards). This should eventually result in an emission reduction from peat soils of 1 Tg CO_2-eq yr^{-1} (Ministerie van Landbouw Natuur en Voedselkwaliteit, 2019).

However, raising the GWL might create conditions beneficial to the production of nitrous oxide (N_2O) and methane (CH_4), two GHGs with a strong warming potential that possibly could negate positive effects of CO_2 reduction. Production of N_2O in soils mainly occurs through microbial nitrification and denitrification (Butterbach-Bahl et al., 2013; Canadell et al., 2021). The rate of emission is the result of several processes, each affected by soil parameters, soil-plant interactions and external conditions such as nitrogen (N) input through fertilizer application or precipitation and temperature (Butterbach-Bahl et al., 2013; Firestone & Davidson, 1989). In cultivated peat soils, denitrification is the dominant N_2O producing process, due to the high SOM content, frequent anaerobic conditions, and high mineral-N availability, resulting from organic N mineralization and fertilizer input (Van Beek et al., 2004). Annual N_2O emissions due to mineralization of organic N in organic soils (grasslands and croplands) were estimated at 0.7 Tg CO_2-eq in 2020, about 14% of total N_2O emissions from agricultural soils in the Netherlands (RIVM, 2022). Although raising the GWL in peat soils may reduce N_2O resulting from peat mineralization (Van Beek et al., 2010), it may also introduce a risk of high N_2O production (Velthof et al., 1996). The attempt to create a fixed high GWL close to (but below) the soil surface, may lead to strong fluctuations in moisture conditions in the topsoil during rainfall events. This could give rise to a combination of nitrate (NO_3^-) production during SOM oxidation and nitrification under aerobic conditions, followed by incomplete denitrification and N_2O diffusion to the atmosphere under anaerobic conditions (Goldberg et al., 2010). The presence of the anaerobic-aerobic interface close to the surface, may decrease the diffusion time to the atmosphere. Given the relative delayed activation response of N_2O reductase to anaerobic conditions (Baggs & Philippot, 2010), a higher N_2O/N_2 ratio may be expected for denitrification at shallow depth compared to deeper soil. Mineral N applied as fertilizer (particularly as NO_3^-) and manure to the soil surface, may also be denitrified under the partially anaerobic conditions created by a high GWL (Velthof et al., 1997). The greenhouse gas CH_4, with a warming potential 27 times higher than CO_2 (global warming potential over 100 years, Forster et al., 2021), is commonly only produced under the strongly anaerobic conditions of

wetland soils, and less so in managed peat soils (Van den Pol-van Dasselaar et al., 1997).

The mitigating effect on CO_2 emissions of reducing drainage levels in peat grasslands has been widely confirmed (Evans et al., 2021), although some have suggested an optimum in the relation between water table depth and CO_2 (Laiho, 2006; Tiemeyer et al., 2016). Optima have also been observed for the relationship with soil suction levels (Berglund & Berglund, 2011; Kechavarzi et al., 2010a; Saurich et al., 2019a). N_2O emissions are known to prevail during variable moisture conditions, often translated into hot moments and hotspots (Berendt et al., 2023). Emissions of CH_4, on the other hand, are highest under wet conditions in a restored peat grassland (Hendriks et al., 2007) or in inundated mesocosms (Van de Riet et al., 2013). Soil inundation did not always result in CH_4 emissions, however, potentially due to an insufficient duration of the treatments (Saurich et al., 2019a; Taft et al., 2018). Field experiments are useful for their high degree of realism, incorporating not only the field scale, but also the soil depth dimension. While lab experiments have the benefit of a controlled environment, the size of experimental objects is often reduced to a representation of a single soil horizon, and the soil structure may be disturbed during sieving or drying. Potential reactions during upwards gas transport in the soil column are therefore not fully represented in such studies (Koops et al., 1997b). Neither are the hydrological processes creating the environmental conditions in the soil matrix. Experiments on soil mesocosms (with lengths ranging between 25 and 80 cm) in field or lab settings have confirmed the mitigating effect of GWL rise on CO_2 emissions, in combination with a (slightly) increasing CH_4 flux (e.g., Karki et al., 2016; Moore & Dalva, 1993; Nielsen et al., 2023; Van de Riet et al., 2013). Constraints to these studies involved the use of disturbed soil in repacked columns (Moore & Dalva, 1993), a limited number of static GWL treatments (Karki et al., 2016; Nielsen et al., 2023; Van de Riet et al., 2013), or a relatively small column depth, limited to the topsoil (Van de Riet et al., 2013). The hysteresis in CH_4 emissions observed by Moore and Dalva (1993) after drying and rewetting to 50 cm indicates the importance of GWL dynamics. Emissions were strong during drying and near absent during rewetting, indicating production and storage along the depth gradient. A similar importance of dynamic water levels can be expected for N_2O emissions. Unlike CH_4 however, N_2O production may be most pronounced during rewetting of previously aerated layers (Goldberg et al., 2010). Regina et al. (2015) observed an increase in N_2O during wetting from 70 to 30 cm

GWL depth, although shallower GWLs were not included. A mesocosm incubation treated with dynamic drainage levels (drying and rewetting) and including detailed monitoring of moisture content, matric potential and GHG emissions could provide better insight into the oxidation processes occurring in drained grassland peat soils. To our knowledge, no such an experiment has been conducted yet.

Therefore our aim in this experiment was to study the trade-offs between CO_2, N_2O and CH_4 emissions associated with peat oxidation, from incubated, non-disturbed soil cores from Dutch peat meadows as a function of a dynamically changing GWL. To be able to measure the effects of heterotrophic respiration, an experiment using bare soil cores was required. We hypothesized that (1) CO_2 emissions are negatively related to the GWL, i.e., higher emissions at a deeper GWL, but reach a maximum when the shallower soil layers have moved from oxygen limitation to moisture limitation; (2) N_2O emissions are highest at a shallow groundwater level, 30 to 10 cm below the soil surface, and occur strongest during rewetting of the soil; (3) CH_4 emissions are low or absent except during inundated conditions; and (4) CO_2 will be the main contributor to the total global warming potential (GWP).

3.2 Materials and methods

3.2.1 Locations and sampling

Three dairy farms in the Netherlands, cultivating grassland on peat soils, were selected as sampling locations: Zegveld (52°08' N, 4°50' E) and Vlist (51°58' N, 4°49' E) in the "Groene Hart" area in central-western Netherlands and Aldeboarn (53°03' N, 5°54' E) in the northern Friesland province (Fig. 3.1). In Zegveld, a clayey peat top layer, containing some anthropogenic debris, is found above a thick mesotrophic wood peat layer, with eutrophic sedge peat underneath, which reaches down to six meters. The soil on the Vlist location has a peaty clay top layer above mesotrophic wood peat with peat and clay layers reaching as deep as ten meters. In Aldeboarn, two meter deep oligotrophic peat, composed of Sphagnum, Eriophorum and heather, is covered by a thick peaty clay top layer (Van Asselen et al., 2023). Physical and chemical properties of the soil horizons included in this experiment are provided in Table 3.1. On all three farms the effects of subsoil irrigation systems compared to regular ditch drainage are studied as part of a Dutch research program on reducing greenhouse gas emissions from peat meadows (NOBV, 2021). The fields in Zegveld and Vlist are fertilized with a combination of slurry and artificial fertilizer, at a rate of 200-250 kg N ha^{-1} yr^{-1}. In Aldeboarn, the fields

receive only slurry at 170 kg ha^{-1} yr^{-1}. In the summer of 2021, four undisturbed soil cores were sampled close to each other on the experimental field with subsoil irrigation of each location. The sampling plot was kept free from fertilizer application for at least three months before sampling. Three replicates were sampled after removing the upper 5 cm soil including the grass sward, while one replicate was taken without removal of the grass sward. Acrylate tubes with a length of 120 cm and inner diameter of 24 cm were pushed carefully 113 or 118 cm into the soil for the bare and grass cores respectively. To prevent the soil inside the tube from compressing, the tube was closed off on top and connected to a pump to establish a negative air pressure inside the tube while pushing it down.



***Figure 3.1**: Locations of the three sampling sites in the Netherlands.*

***Table 3.1**: Properties of the soil horizons, at the time of sampling in Aldeboarn (Ald.), Vlist (Vli.) and Zegveld (Zeg.). SOM content is given as the percentage of the total dry mass. Clay particles (< 2 µm) content is given as fraction of the remaining (mineral) mass. SOM, total carbon and nitrogen and C/N ratio were measured in the five cm interval in the middle of a horizon. Dry bulk density values are the mean of four replicate 100 cm^3 ring samples. The peat humification status is based on the soil classification performed in the field.*

Location	Horizon depth (cm)	SOM (% of dry soil)	Clay (% mineral mass)	Tot-C (g kg^{-1} dry soil)	Tot-N (g kg^{-1} dry soil)	C/N	Dry BD (g cm^{-3})	Peat humification status
Ald.	0 - 12	28.9	40	128	11.4	11.2	0.6	-
	12 - 28	18.1	45	78.7	5.5	14.3	0.927	-
	28 - 45	70.5	20	367	10.6	34.5	0.233	Humified
	45 - 80	93.6	15	472	9.4	50	0.138	Lightly humified
	80-180	95.4	15	476	10.9	43.5	0.128	Reduced
Vli.	0 - 15	45	50	203	19.4	10.5	0.595	-
	15 - 37	17.5	60	60.2	7	8.6	0.835	-
	37 - 55	60.9	45	322	24.2	13.3	0.256	Humified
	55 - 75	77.8	40	383	27.6	13.9	0.204	Lightly humified
	75-130	71.4	40	350	23.3	15	0.166	Reduced
Zeg.	0 - 30	36.5	35	174	16.8	10.4	0.62	Humified
	30 - 45	69.7	55	334	24.2	13.8	0.248	Humified
	45 - 65	74.7	35	367	22.9	16	0.204	Lightly humified
	65-150	79.8	45	383	22.6	16.9	0.158	Reduced

3.2.2 Setup experiment

The cores were transported to the laboratory where they were stored in a climate controlled room at 16°C and 70% relative humidity. The lower 10 cm of each peat core was removed and replaced with fine grained sand, chosen for its strong capillary suction, after which the tube was closed at the bottom with a watertight PVC cap. Tap water was used for all groundwater level manipulation in the climate room. The cores were kept saturated until the start of the experiment, except during the installation of drains and sensors, for which the cores were drained temporarily. All cores had been saturated for at least two weeks before day 1 of the experiment. Two drainage pipes were installed; one inside the sand layer and the second at the bottom of the peat core. A hanging water column was connected to the upper drain to regulate the water levels down to -100 cm or to the sand drain for suction levels down to -160 cm. To be able to apply suction levels lower than the soil cores bottoms, all cores were mounted on top of a 50 cm high bench (Fig. S3.1, see Supplemental Information). We used the horizon borders identified during sampling in the field (Table 3.1), to distinguish layers with different properties in the columns. In the middle of each horizon, a porous cup for pore water extraction, a volumetric water content (VWC) sensor and a tensiometer were installed horizontally into the soil. The thicker top horizon of the Zegveld cores received two rows of probes at equal distances from the horizon borders. To allow for the three highest rows of probes to move along with the vertical shrinkage movement of the soil matrix, they entered the column tube through vertical slots that were sealed water tight (Fig. S3.2). The cores received no fertilizer throughout the experiment.

3.2.3 Groundwater level treatments

Between January 2022 and February 2023, all cores were subjected simultaneously to two drying-wetting cycles. The first cycle was aimed at testing the drainage system down to a water table of 100 cm below the soil surface, in eleven one-week steps. These treatment steps included 0, -20, -40, -60, -80 and -100 cm with respect to the soil surface (z-coordinate positive upwards) and vice-versa. The second cycle included the same treatment steps as above, as well as suction induced steps of -140 and -160 cm with respect to the soil surface. All levels in cycle two were maintained for two (sometimes three) weeks, resulting in a duration of 33 weeks for this cycle.

3.2.4 Biochemical analyses

Gas emissions of CO_2, N_2O and CH_4 were measured using the static chamber method, at the start and the end of each GWL step. Opaque PVC chambers were closed over the cylinders for a period of 30 minutes, during which the concentration inside was measured four times with a Gasera One photoacoustic gas monitor (Gasera, Finland). Concentration change slopes were determined using linear regression between sampling points, after which flux values were calculated using the ideal gas law. Cumulative emissions over the period of the experiment were subsequently calculated using the 'gasfluxes' package in R (Fuss, 2023). N_2O and CH_4 emissions were converted to CO_2 equivalents using the global warming potential (GWP) values for a 100 years horizon reported in the sixth IPCC assessment report: 273 and 27 for N_2O and CH_4, respectively (Forster et al., 2021).

Water samples were extracted at the end of each GWL step from those rhizon suction cups (Rhizosphere Research Products, the Netherlands) that were located above and below the prevailing water table. At water tables below -100 cm, no water samples were extracted. The samples were analyzed for NO_3^-, NH_4^+ and inorganic and total carbon using segmented flow analysis. Dissolved organic carbon (DOC) was calculated as the difference between total and inorganic carbon.

3.2.5 Physical analyses

Volumetric water content and matric potential were monitored using EC-5 capacitance sensors (Metergroup, USA) and tensiometers (Rhizo Instruments, the Netherlands) respectively. All sensors were connected to dataloggers; the recording frequency was every ten minutes. Calibration curves for the relationship between VWC and the EC-5 signal were composed experimentally for each soil horizon present in the soil cores (the Vlist horizons 4 and 5 were merged in one calibration function as well as Aldeboarn horizons 1 and 2).

Vertical displacement of the soil surface was monitored during each gas flux measurement, to account for changing headspace volumes. To monitor vertical as well as horizontal shrinkage of the different soil horizons, small cylindrical markers (20 mm long, 6 mm diameter) were pushed horizontally into the soil through small holes, drilled for this purpose, such that the marker intersection was visible either through the transparent acrylate or through the hole. Four markers were placed at equal distances around the core perimeter, at the middle of each horizon as well as the horizon boundaries and at 2 cm below the core top. This

resulted in 36 markers in the Zegveld columns and 40 markers in the Aldeboarn and Vlist columns. At the end of each GWL step, vertical displacements of the markers were determined with a ruler and horizontal displacements by pointing a caliper through the hole in front of the marker. When the marker had moved vertically beyond the level of the hole, the horizontal distance to the soil in front of the hole was measured instead.

3.2.6 Statistical analyses

Data analyses were performed using the R statistical software (v4.3.1; R Core Team, 2023). We used linear regression to study the relationship between GWL during the two drying and two rewetting tracks and CO_2 emissions for each sampling location and the three locations combined. The intermediate period between cycle 1 and 2 was excluded from these relationships. Cycle 1 ended on 29-03-2022, one week after raising the GWL to 0 cm. Cycle 2 started on 30-05-2022; this was three weeks after raising the GWL from the intermediate -20 cm level to 0 cm, at which point we assume a stable situation of saturation was prevalent again (rather than the response to rewetting). The best fit model was selected based on the models' adjusted R^2 value, Akaike information criterion, and p-values of the coefficients. The CO_2 fluxes and log-transformed N_2O and CH_4 fluxes at different GWL conditions (averaged over the soil types and cycles) were compared in linear mixed effects models using the *lme* function in the R package 'nlme' (Pinheiro et al., 2023). The individual objects- i.e., the soil cores – were added as random factor and the groundwater level treatment, sampling location or both (according to the best fit based on the Akaike information criterion) were added as fixed factors. The model was validated by checking the residuals for normality, homogeneity and independence graphically. Pairwise comparison was performed in case of a significant GWL effect, using a Tukey's honest significant difference test (alpha = 0.05). The same was done for the sum of CO_2 and N_2O, expressed as CO_2-equivalent emissions. CH_4 was excluded from the summed analysis, due to missing values in the CH_4 timeseries. An analysis of variance (ANOVA) was used to compare cumulative emissions of CO_2, N_2O and CH_4 from the three soil types.

3.3. Results

3.3.1 Soil moisture and GHG dynamics during drying-wetting cycles

Matric potential values moved along with GWL changes (Fig. S3.3). The pressure of the water column, recorded by the lowest tensiometer, installed at depths between 80 and 87.5 cm below the surface, generally corresponded with the imposed GWL. At these depths, VWC observations rarely deviated from the saturated VWC levels identified in the sensor calibrations (Fig. S3.4). In the shallow soil layers (-3.5 to -21 cm depth), tensiometer readings were often obscured by air intrusion into the ceramic cups. The VWC in the top horizon decreased steeply after lowering of the GWL in Aldeboarn and Vlist soils, while it showed a more gradual and less strong decrease in the Zegveld soils.

Cumulative CO_2 emissions, standardized as the yearly rate, ranged between 0.33and 0.64 kg C m^{-2} yr^{-1}, with stronger emissions occurring in the first drying-wetting cycle (Table 3.2). Over the course of the whole experiment, cumulative emission was highest in the Zegveld and lowest in the Vlist soil. Lowering of the GWL resulted in CO_2 emission increases for all three soil types (Fig. 3.2a, 3.3a, 3.4a). On average the highest CO_2 emissions were measured at a GWL of -80 cm, but only a 0 cm GWL resulted in significantly lower emissions than other treatments (Fig. 3.5a). The response of CO_2 to GWL change differed according to the direction of the change (Fig. 3.6a, 3.6c, 3.6e). Lowering the GWL in cycle 1 resulted in bell-shaped CO_2 responses (Fig. 3.6a, 3.6c, 3.6e), best described by second or third order polynomial functions (Table 3.3). In the second drying track, this pattern was only observed in the Zegveld cores (Fig. 3.6e). No clear relationship was found in the Aldeboarn cores, while in the Vlist cores, CO_2 emissions even decreased in response to drying (Fig. 3.6a, 3.6c, Table 3.3). Rewetting, on the other hand, resulted in decreasing CO_2 emissions. Contrary to the drying tracks, highest emissions in the rewetting tracks were found at the deepest GWLs (Fig. 3.6a, 3.6c, 3.6e). The response of CO_2 emissions to a rising GWL was best described by linear equations for the three locations together. Separating the locations, however, resulted in quadratic or third order polynomial functions for Zegveld and the second rewetting track of the Aldeboarn columns (Table 3.3). In cycle 1, rewetting started by raising the GWL to -80 cm, at which point mean emissions of 1.8 g C m^{-2} day^{-1} were observed. In cycle 2, the deepest rewetting level was associated with CO_2-C emissions of 1.2 g C m^{-2} day^{-1} on average.

Cumulative N_2O emissions ranged between 1.27 and 4.22 g N m^{-2} yr^{-1} (Table 3.2). Over the whole experiment, the cumulative emissions were highest in the Zegveld and lowest in the Vlist soil cores. Peak emissions occurred particularly after a recent raise of the GWL to 0 cm for all of the locations (Fig. 3.2b, 3.3b, 3.4b). Averaged over all locations and both tracks and cycles, the highest emissions were measured at a GWL of 0 cm, though not significant (Fig. 3.5b). Strongest emission peaks occurred in response to raising the GWL to 0 cm after the intermediate period at -20 cm (up to 67 mg N m^{-2} day^{-1}). With the exception of the Aldeboarn soils during cycle 1, N_2O emissions were relatively low- below 2 mg N m^{-2} day^{-1} - at GWLs deeper than -20 cm. Mean cumulative emissions were very high in all soils, particularly for Zegveld (2.78 g N $m^{-2}yr^{-1}$) and Aldeboarn (2.97 g N $m^{-2}yr^{-1}$). The cumulative emissions in the Vlist soils were almost two times smaller than the other sites, on average 1.54 g N $m^{-2}yr^{-1}$ (Table 3.2). Tests with (un-replicated) vegetated soil cores resulted in much lower emissions (Fig. S3.5), because mineral N was used for crop uptake and thus less N was left for N_2O production. The highest observed N_2O emission in the vegetated cores was 29.3 mg N m^{-2} day^{-1}, which occurred in the Aldeboarn grass core, after a GWL rise to 0 cm.

Emission or uptake of CH_4 was generally low (Fig. 3.2c, 3.3c, 3.4c), with a few strong peaks, resulting in emission values ranging between -4.7 and 67.2 mg C m^{-2} day^{-1}. Similarly to the N_2O emissions, there was a period of strong CH_4 increase during the first drying track in the Aldeboarn cores (Fig. 3.2c). Although this pattern occurred in all three replicates, variation was very high. CH_4 emissions showed no relation with GWL conditions (Fig. 3.5c). Cumulative fluxes showed strong variation between drying-wetting cycles and ranged between -0.68 and 4.47 g C m^{-2} yr^{-1} (Table 3.2).

Over the course of both drying-wetting cycles, the highest GWP (composed of the cumulative emissions of the three GHG's together) was found in the Zegveld soil cores- 3.18 versus 2.84 and 1.98 kg CO_2-eq m^{-2} yr^{-1} for Aldeboarn and Vlist, respectively (Table 3.2). High mean N_2O and CH_4 cumulative emissions (with large standard errors) raised the total GWP of the Aldeboarn cores in cycle 1. Both in cycles 1 and 2 and for all locations, mean cumulative CO_2 emissions had a larger GWP than the sum of cumulative N_2O and cumulative CH_4 emissions together (Table 3.2). However, N_2O was the main contributor at shallow GWL depths, resulting in the highest CO_2 equivalent emissions occurring at the 0 cm GWL treatment (Fig. 3.5d).

***Table 3.2**: Mean cumulative emissions from bare soil columns (n=3, ±SE) of CO_2 (kg C m^{-2} y^{-1}), N_2O (g N m^{-2} yr^{-1}) and CH_4 (g C $m^{-2}yr^{-1}$) and the corresponding CO_2 equivalent values over a 100 year horizon (kg CO_2 $m^{-2}yr^{-1}$). The cumulative emission values were calculated for cycle 1 and 2 separately, as well as together, using linear interpolation between individual measurements and converted to yearly values. Superscript letters indicate significant differences between sampling locations for cycle 1 and 2 separately, tested with an ANOVA ($p < 0.05$).*

Cycle	Location	CO_2 emission		N_2O emission		CH_4 emission	
		kg C $m^{-2}yr^{-1}$	kg CO_2 $m^{-2}yr^{-1}$	g N $m^{-2}yr^{-1}$	kg CO_2-eq $m^{-2}yr^{-1}$	g C $m^{-2}yr^{-1}$	kg CO_2-eq $m^{-2}yr^{-1}$
1	Aldeboarn	0.640±0.06 ^{a}	2.35±0.21	4.22±1.66^{a}	1.81±0.71	4.47±3.51^{a}	0.16±0.13
1	Vlist	0.501±0.03^{a}	1.84±0.12	1.89±0.10^{a}	0.81±0.04	-0.40±0.09^{a}	-0.01±0.003
1	Zegveld	0.614±0.03^{a}	2.25±0.10	1.35±0.25^{a}	0.58±0.11	0.30±0.17^{a}	0.01±0.006
2	Aldeboarn	0.390±0.05^{ab}	1.43±0.17	2.14±0.24^{ab}	0.92±0.10	-0.31±0.22^{a}	-0.01±0.008
2	Vlist	0.327±0.03^{a}	1.20±0.10	1.27±0.30^{a}	0.54±0.13	-0.68±0.07^{a}	-0.02±0.002
2	Zegveld	0.516±0.04^{b}	1.89±0.14	2.98±0.31^{b}	1.28±0.13	-0.57±0.05^{a}	-0.02±0.002
1+2	Aldeboarn	0.44 ± 0.04^{ab}	1.61 ± 0.13	2.78±0.43^{a}	1.19±0.18	1.02±0.76^{a}	0.04±0.03
1+2	Vlist	0.36 ± 0.02^{a}	1.33 ± 0.09	1.54±0.30^{a}	0.66±0.13	-0.59±0.07^{a}	-0.02±0.003
1+2	Zegveld	0.52 ± 0.04^{b}	1.91 ± 0.15	2.97±0.41^{a}	1.28±0.18	-0.32±0.01^{a}	-0.01±0.000

***Table 3.3**: Least squares coefficient estimates describing the relationships between the CO_2 emission rates (g CO_2-C $m^{-2}d^{-1}$) and the GWL (m) at the time of measuring, for GWL levels within the ranges of -1.0 to 0 m for cycle 1 and -1.6 to 0 m for cycle 2.*

Location	Cycle	Direction	Model	Adjusted R^2
Aldeboarn	1	Drying	$CO_2 = 1.3 - 6.0GWL - 11GWL^2 - 5.6GWL^3$	0.44
	1	Wetting	$CO_2 = 0.84 - 1.4GWL$	0.57
	2	Drying	n.s.	-
	2	Wetting	$CO_2 = 0.57 + 1.6GWL + 3.1GWL^2 + 1.2GWL^3$	0.48
Vlist	1	Drying	$CO_2 = 1.6 - 2.0GWL - 5.4GWL^2 - 3.1GWL^3$	0.57
	1	Wetting	$CO_2 = 0.59 - 1.2GWL$	0.77
	2	Drying	$CO_2 = 1.4 + 0.66GWL + 0.28GWL^2$	0.31
	2	Wetting	$CO_2 = 0.35 - 0.45GWL$	0.54
Zegveld	1	Drying	$CO_2 = 0.63 - 4.7GWL - 3.3GWL^2$	0.83
	1	Wetting	$CO_2 = 0.52 - 4.2GWL - 2.8GWL^2$	0.93
	2	Drying	$CO_2 = 0.94 - 3.6GWL - 4.2GWL^2 - 1.4GWL^3$	0.61
	2	Wetting	$CO_2 = 0.60 - 7*10^{-4}GWL + 2.3GWL^2 + 1.3GWL^3$	0.78
All locations	1	Drying	$CO_2 = 1.17 - 5.04GWL - 8.77GWL^2 - 4.38GWL^3$	0.33
	1	Wetting	$CO_2 = 0.72 - 1.50GWL$	0.61
	2	Drying	n.s.	-
	2	Wetting	$CO_2 = 0.43 - 0.60GWL$	0.36

3.3.2 Pore water chemistry

Dissolved organic carbon concentrations in the pore solution ranged between 39 and 645 mg C l^{-1} in cycle 1 and 22 and 712 mg C l^{-1} in cycle 2 (Fig. S3.7a). At any GWL condition, DOC concentrations were higher when the experiment was in a drying phase, than during the corresponding rewetting phase observation (Fig. S3.8a). There was no apparent effect of sampling depth or GWL on DOC concentrations. Mean NO_3^- concentrations in the ranges 0-123 mg NO_3-N l^{-1} and 0-220 mg NO_3-N l^{-1} were observed during cycles 1 and 2, respectively. The highest peaks were measured in pore water extracted from the upper 10 cm of the soil. More NO_3^- was available during the rewetting tracks than the drying tracks (Fig. S3.7b, S3.8b). Concentrations of NH_4^+ on the other hand, appeared to be higher under waterlogged conditions, although a strong relationship was not detected (Fig. S3.7c, S3.8c). Mean values

ranged between 0 and 12 or 0 and 4.8 mg NH_4^+-N l^{-1} during cycles 1 and 2 respectively. Mean pH values in the pore water samples ranged between 4.9 and 6.4 in cycle 1 and 4.6 and 6.2 in cycle 2. The pH was higher during drying than during rewetting (Fig. S3.8d).

3.3.3 Carbon and soil volume losses

Location markers showed vertical as well as horizontal displacement in response to GWL lowering. This was most pronounced at the soil surface. At the end of drying-wetting cycle two, the columns had not risen back to their original volume again (Fig. 3.7, Table 3.4). Instead, the soil surface was located at a height of 0.87 to 1.32 cm below the original elevation 62 days after the final GWL rise up to the surface.

Table 3.4*: Mean surface subsidence in the bare soil cores and the volume loss of the top horizon in vertical and horizontal direction. The potential carbon loss is calculated as the amount of carbon in the lost volume and compared to the carbon loss derived through interpolation of flux observations (cumulative CO_2-C emission). The proportion of volume loss that can be attributed to oxidation is the ratio of the actual and the potential C loss.*

	Aldeboarn	Vlist	Zegveld
Top horizon depth in field (cm)	0 to 12	0 to 15	0 to 30
Subsidence (cm)	0.917	0.873	1.32
Horizontal shrinkage (cm, change in surface radius)	1.87	1.25	2.30
Subsidence induced volume loss (m^3m^{-2} yr^{-1})*	0.00917	0.00873	0.0132
Subsidence induced potential C loss (kg m^{-2} yr^{-1})	0.560	0.555	0.795
Measured C loss (kg m^{-2} yr^{-1})	0.440	0.364	0.522
Oxidation component subsidence (%)	78.6	65.6	65.6

*Volume loss of top horizon is expressed as m^3 per m^2 of initial soil surface (before horizontal shrinkage).

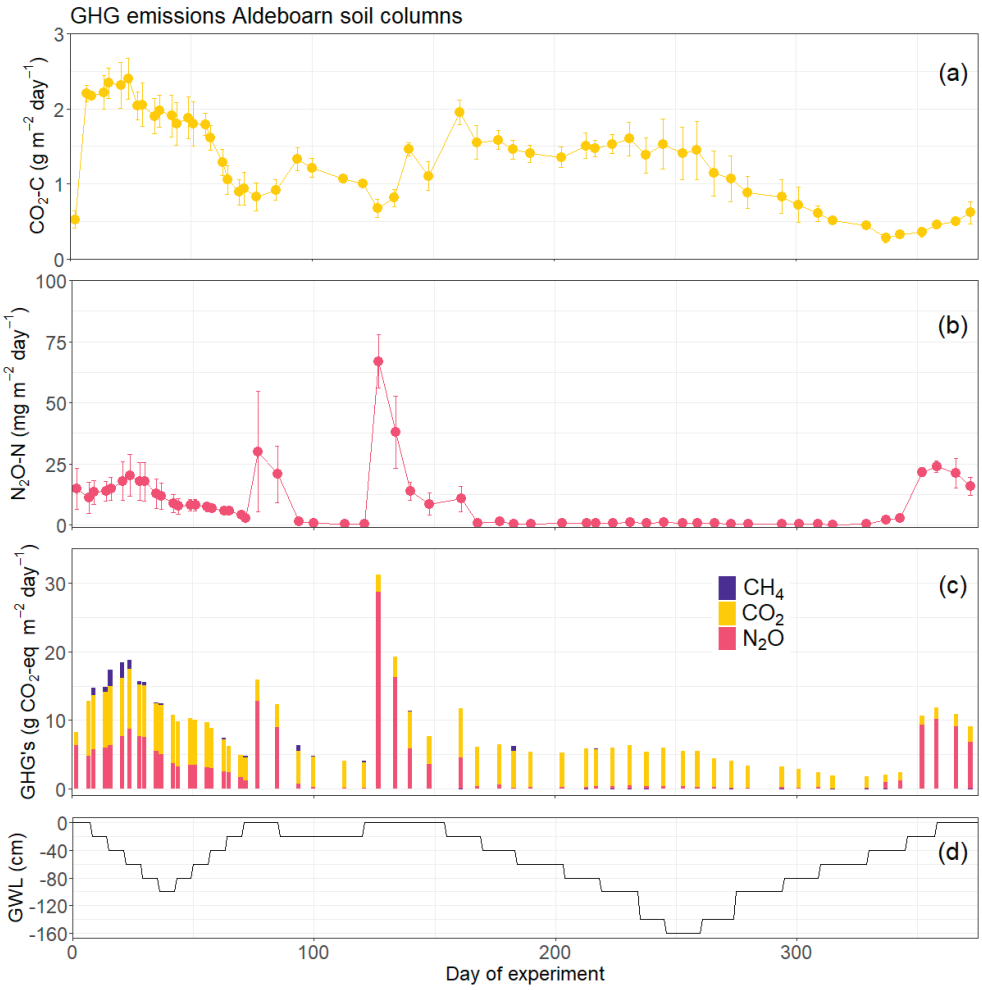


***Figure 3.2**: Average CO_2 (a) and N_2O (b) emissions from Aldeboarn bare soil columns (n=3), as well as the contributions of CO_2, N_2O and CH_4 to the total CO_2-equivalent emissions (c) during the corresponding GWL treatments (d). Error bars in (a) and (b) indicate the standard error of the mean.*

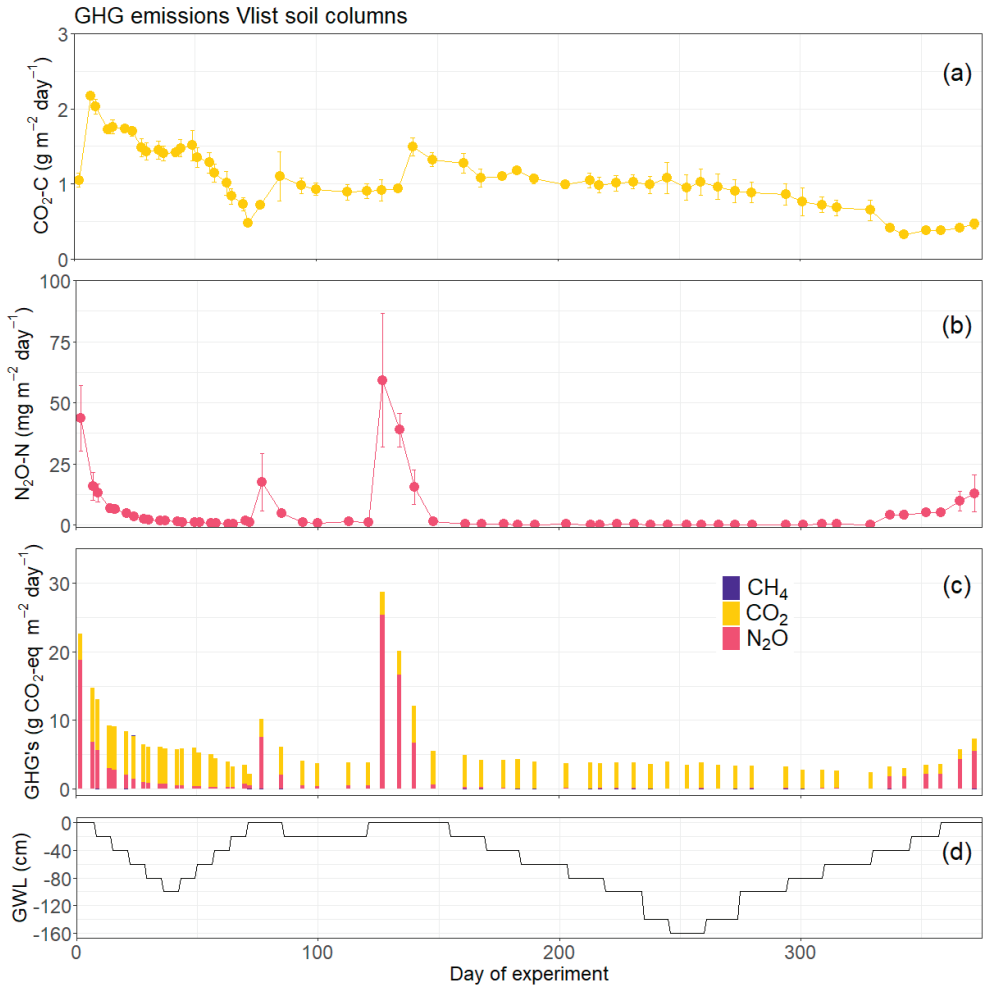


***Figure 3.3**: Average CO_2 (a), N_2O (b) and total CO_2-equivalent emissions (c) from Vlist bare soil columns (n=3) during the corresponding GWL treatments (d). Error bars in (a) and (b) indicate the standard error of the mean.*

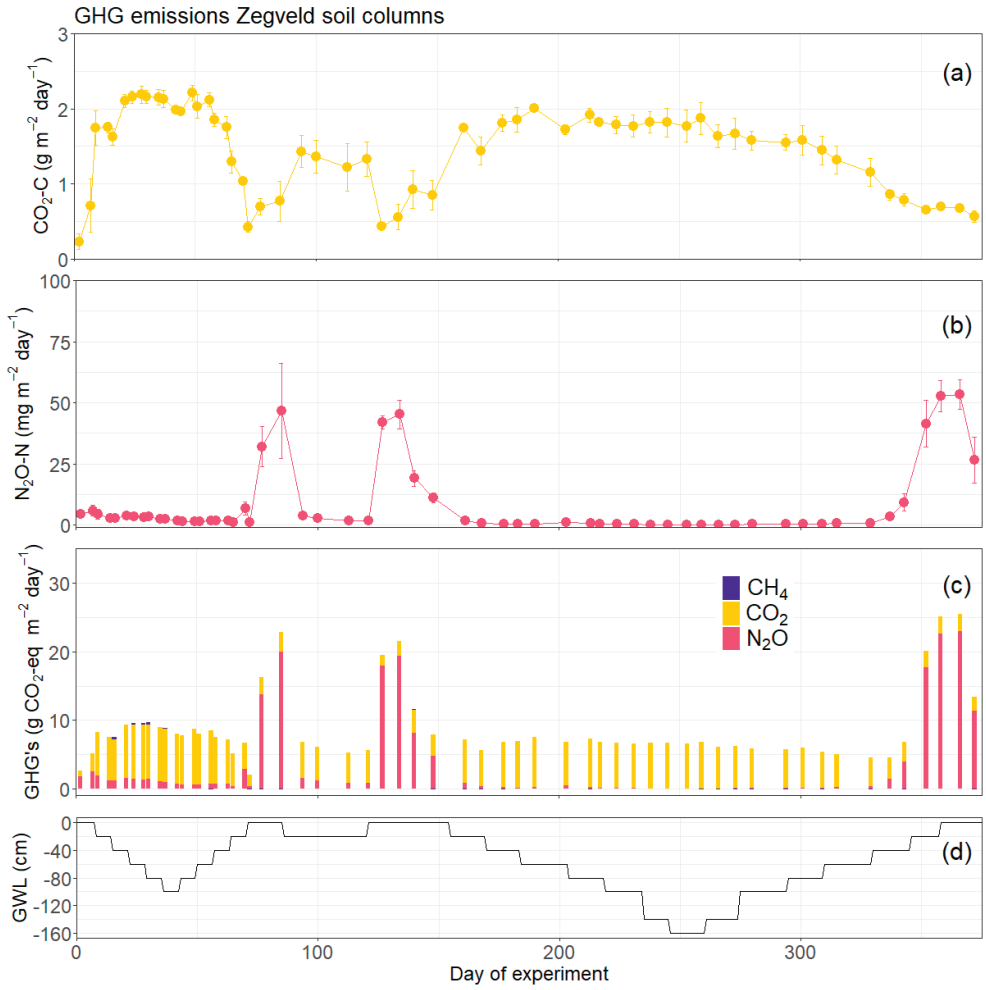


***Figure 3.4**: Average CO_2 (a), N_2O (b) and total CO_2-equivalent emissions (c) from Zegveld bare soil columns (n=3) during the corresponding GWL treatments (d). Error bars in (a) and (b) indicate the standard error of the mean.*

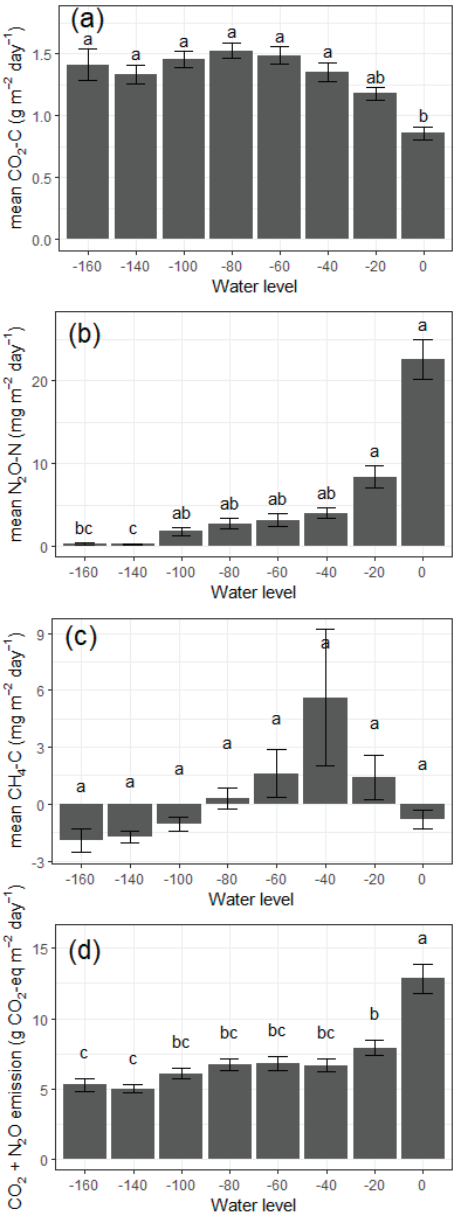


***Figure 3.5**: Mean emissions grouped per GWL treatment, and averaged over locations, drying-wetting cycles and tracks. Letters indicate significant differences using a significance level of alpha=0.05, following from linear mixed effects models using the experimental objects as random factor and GWL and/or location as fixed factors. Note that the y-axis of (a) uses units of g C m^{-2} day^{-1}, while fluxes in (d) are expressed in g CO_2-eq. m^{-2} day^{-1}.*

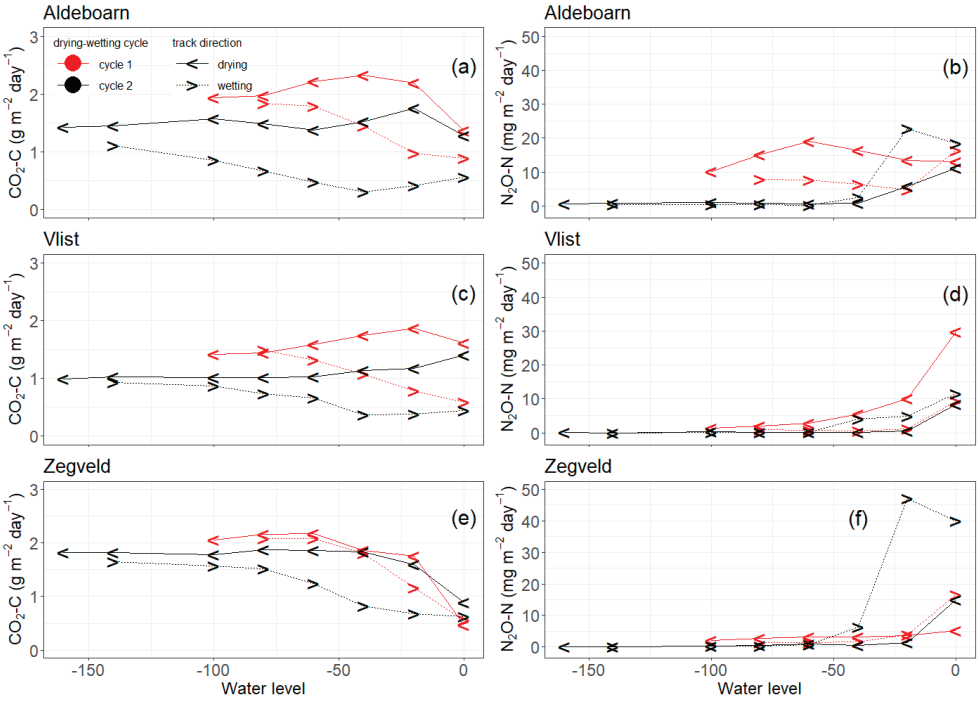


***Figure 3.6**: Mean CO_2 (left) and N_2O (right) emissions released from bare soil columns from Aldeboarn (a, b), Vlist (c, d) and Zegveld (e, f) against the applied GWL. Each point is the mean of three replicates that were measured twice, each, during a GWL step (n = 6). The intermediate period between the two drying wetting cycles is not included here. The two drying-wetting cycles are indicated in different colours and the direction of the GWL change (drying or wetting) by shape and line-type.*

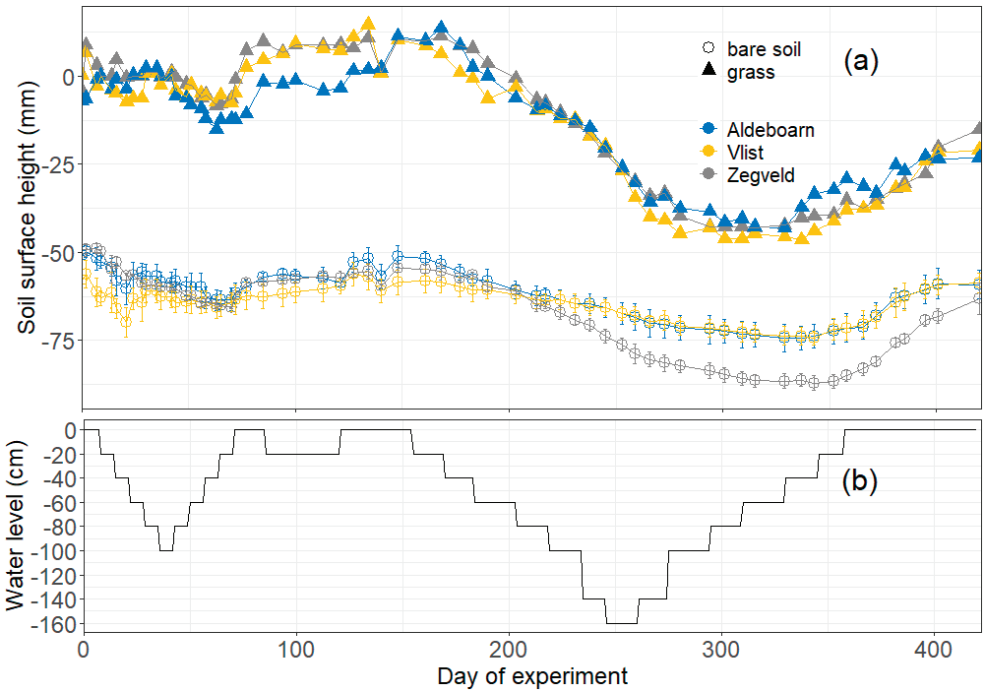


***Figure 3.7**: Soil surface movement of bare (n = 3) and vegetated (grass) soil cores (n = 1) over the course of two drying wetting cycles. The reference heights, 0 mm for grass cores and -50 mm for bare cores, are chosen relative to the soil surface in the field: the top 5 cm of the soil was removed before sampling the bare cores.*

3.4 Discussion

3.4.1 Effect of GWL on CO_2 emissions

We hypothesized to find a negative relationship between GWL and CO_2 emissions, meaning higher emissions for deeper groundwater tables. Soil moisture content controls C mineralization by affecting oxygen content as well as substrate mobility and availability (Linn & Doran, 1984; Moyano et al., 2013). Therefore, we had hypothesized to find an optimum GWL for CO_2 emissions, with lower emissions both for deeper and shallower GWL conditions. Our measurement series consisted of two drying tracks and two wetting tracks. While drainage always led to an increase in CO_2 emissions, in accordance with our hypothesis, different response patterns were observed in the four tracks (Fig. 3.6a, 3.6c, 3.6e, Table 3.3). Other studies that measured CO_2 emissions in the lab under a range of suction treatments have found maximum emissions at a water potential of -50 cm (Kechavarzi et al., 2010a), -40 cm (Berglund & Berglund, 2011) or between -20 and -60 cm (Saurich et al., 2019a), with

emissions decreasing at dryer and wetter conditions. Our expectation was to find a similar parabolic relationship with GWL. We only found this characteristic response in the first drying track, however. There, CO_2 emissions increased with drainage up to a peak at -60 cm on average, after which emission rates decreased with lower GWLs. In this experiment, only a GWL treatment of 0 cm was associated with lower average CO_2 emissions than the other GWL steps (Fig. 3.5a).

Rewetting of the soil did not result in a CO_2 response resembling the path during GWL lowering. Instead of rising back to their drying-track optima, emission rates decreased further during rewetting (Fig. 3.6a, 3.6c, 3.6e). It was on average associated with a steady, linear decrease in emissions, although individual differences between soil types were found (Table 3.3). From the drying trajectory we conclude that, on average, GWL lowering increased decomposition rates by enlarging the volume of aerated soil, up to a GWL of 60 cm below the surface. Further drainage, while increasing the volume of aerated soil, increased the volume potentially under drought stress. This may have intensified moisture limitation in the shallow soil to such an extent that the total CO_2 flux was negatively affected by deeper GWLs than -60 cm (Mäkiranta et al., 2009). Raising the GWL, and thereby potentially mediating the moisture limitation on respiration within soil zones subject to capillary rise, did not result in higher CO_2 emission rates. This may be an indication that the top soil layer was the main contributor to the total flux, which is in accordance with findings in other studies that reported stronger respiration rates in top soil than in sub soil samples (Berglund & Berglund, 2011; Saurich et al., 2019a). In support of this, the VWC observations suggested that the moisture content of the shallow soil layers was not directly affected by an initial GWL rise, particularly after a prolonged dry period, as seen in cycle 2 (Fig. S3.4). Above a soil depth of 20 cm, the VWC would often continue to decrease, even during rewetting, until the soil layer was overtaken by the water table again. It is generally known that in peat soils the VWC is subject to hysteresis, which can be substantial (e.g., Dasilva et al., 1993; Schwärzel et al., 2002). Schwärzel et al. (2002) showed that, at the same soil water potentials, the VWC can differ up to 30 volume percentages, with lower VWC during the wetting track. Alternatively, the prolonged drought throughout the drained profile has imposed such a stress on the microbial community, that the recovery of activity and therefore respiration is delayed.

High DOC concentrations were mainly found at the start of the experiment, before drying had commenced, and during subsequent drying

(Fig. S3.8a). This pattern indicates increased DOC consumption in response to drying, rather than increased production. The latter would have been reflected in higher DOC concentrations during the rewetting track. However, we can't rule out the possibility that a large portion of the dissolved C left the soil with the outflowing water during drainage. In this study, we did not quantify outgoing fluxes of DOC.

CO_2 emissions were on average lower in the second drying-rewetting cycle, which we attribute to the fast decomposition of labile C compounds in cycle 1. Although the grass sward including the upper 5 cm of the soil had been removed before the start of the experiment, some root material may still have been present.

3.4.2 Effect of GWL on N_2O emissions

Our observations agreed with the hypothesis that N_2O emissions would be strongest under GWLs close to the soil surface, and in particular during soil rewetting (Fig. 3.2b, 3.3b, 3.4c). Lowest cumulative N_2O emissions were measured in the Vlist soil (Table 3.2), which is surprising, as it had the highest N content in all soil horizons, with the exception of horizon 2, a clay deposit layer (Table 3.1). During the course of the experiment, strong pulses of N_2O emissions solely occurred after a GWL rise from -20 to 0 cm, or from -40 to -20 cm. These peaks coincided with sudden increases in the top horizons' VWC values (Fig. S3.4), which suggests that they can mainly be attributed to denitrification in the top soil layers. Denitrification sharply increases when the soil moisture content rises above a certain threshold degree of saturation (Heinen, 2006). Due to the relatively high organic matter content, originating from inputs of plant material and root exudates, the top soil generally provides advantageous conditions for denitrification (Berglund & Berglund, 2011; Van Beek et al., 2004; Velthof & Oenema, 1995). In peat soils, however, organic matter is abundant throughout the vertical profile, making all layers potentially suitable for denitrification (particularly those below the water table) (Van Beek et al., 2004). Still, similarly to mineral soils, in cultivated peat soils a relative abundance of easily degradable C compounds is found in the top soil compared to the sub soil, serving as a limiting factor to denitrification (Bader et al., 2018; Koops et al., 1996). Additionally, N_2O produced at greater depth will face a longer travel time and distance to diffuse up towards the surface, during which it may be reduced to N_2 (Koops et al., 1997b). Therefore, the large peaks of N_2O in our experiment may be best explained by incomplete denitrification in the top soil.

In finding higher emissions under wet conditions, our observations differ from some studies, where a mitigation in N_2O emissions was found in rewetted peat meadows or undrained peatlands, compared to drained fields (Martikainen et al., 1993; Regina et al., 1996; Regina et al., 2015; Van Beek et al., 2010). This is not surprising, since our experiment looked at GWL dynamics, while some of the above studies involved permanent pristine peatland (Martikainen et al., 1993; Regina et al., 1996). Regina et al. (2015) included only drainage levels in their study that would still allow for grass cultivation and identified their most shallow drainage treatment of 30 cm depth as the best in terms of GHG mitigation. In other cases, both in field and lab experiments, N_2O emissions were quite low in general, or even negative (Dinsmore et al., 2009; Hendriks et al., 2007; Nielsen et al., 2023; Van de Riet et al., 2013; Wilson et al., 2016b). In bare peat cores in an outdoor setup, Nielsen et al. (2023) found 72% lower emissions at a -5 cm GWL than at -40 cm, but emissions were low in general. Peak emissions measured in their bare soil cores were a factor 1000 lower than our peaks, despite their soils having comparable N contents and being subject to precipitation. In a drought experiment on a minerotrophic fen, Goldberg et al. (2010) did observe strong N_2O emission pulses during the weeks after rewetting. Dinsmore et al. (2009) observed N_2O peaks in response to both drainage and rewetting of their soil cores. Some other cases have been reported of increased N_2O emissions under higher GWL conditions (Berglund & Berglund, 2011; Norberg et al., 2021).

A positive relationship between drainage and N_2O emissions is generally attributed to mineralization of organic nitrogen in the peat SOM. Since our experiment involved unvegetated, unfertilized soil cores, mineralization will have been the main N source to N_2O production as well. Indeed, NH_4^+ concentrations in pore water samples had decreased and NO_3^- concentrations had increased by the time of rewetting, compared to the drying track concentrations (Fig. S3.8b, S3.8c), indicating subsequent mineralization and nitrification under the preceding aerobic conditions. The main contrast with other studies is the magnitude of the N_2O pulses which we measured after a GWL rise to -20 or 0 cm, which could be as high as 67 mg N m^{-2} day^{-1}. In the vegetated cores, of which we had sampled one replicate per location, N_2O peaks were generally lower, which is due to plant N uptake (Schimel & Bennett, 2004). Here, N_2O peaks occurred up to 29.3 mg N m^{-2} day^{-1}, and followed similar patterns as the bare core fluxes (Fig. S3.5).

Our flux rates showed more resemblance with N_2O responses to precipitation events in field experiments on peat meadows (Berendt et al.,

2023; Van Beek et al., 2010; Velthof et al., 1996; Velthof & Oenema, 1995). Velthof et al. (1996) have illustrated the effect that a GWL rise due to precipitation can have on N_2O production in the soil layers above. This was particularly the case in the top layer, during a shallow GWL. In our experiment, we have consistently seen strong N_2O emissions after a GWL increase from -20 to 0 cm. A GWL rise to 0 cm did not completely saturate the top layer yet, as was evident from the VWC (Fig. S3.4). Air pockets may remain in the peat soil due to hysteresis (Schwärzel et al., 2002), resulting in a lower degree of saturation and intermittent aerobic and anaerobic conditions, which are optimal for N_2O production during incomplete denitrification (Wagner-Riddle et al., 2020). In the field, maintaining a GWL at -20 cm may pose a risk of such hot spot events, where the previously aerated top layer is rapidly overtaken by the water table due to a heavy rainfall event. Although these events may be temporary and infrequent, the large N_2O peaks brought forth by a sudden shift in the GWL can contribute significantly to the total GHG emissions (Anthony & Silver, 2021). Such a risk will be much smaller at a permanent GWL above 0 cm, where mineralization and nitrification are limited (Taft et al., 2018). In practice a peat meadow is rarely a homogeneous level surface however, complicating the achievement of a stable GWL and prevention of N_2O peaks.

This experiment did not take the effect of N input through fertilizers into account, while fertilizer application is a common practice on peat meadows cultivated for dairy farming. Fertilizer events are potential key moments for N_2O emissions and the fertilizer type and soil moisture content are determining factors in the emission size (Velthof et al., 1997). Therefore, the interaction with fertilizer amendment should be taken into account in the consideration of a GWL rise in peat meadow soils.

3.4.3 GHG balance

In accordance with our hypothesis, CO_2 was, with 56.8 to 67.6%, the main contributor to the net cumulative GWP over the entire measurement series (Table 3.2). This result can be attributed to GWL treatments deeper than 0 cm (Fig. 3.5a). At a GWL of 0 cm, however, N_2O was the main contributor to total GHG emissions (Fig. 3.2c, 3.3c, 3.4c, 3.5). The cumulative N_2O emissions contributed 33.5 to 41.9 % to the net cumulative GWP. Cumulative emissions of CH_4 contributed only 1.3% to total CO_2-equivalent emissions from the Aldeboarn soils, while cumulative CH_4 uptake led to a net 1.1% or 0.4% abatement of the summed CO_2 and N_2O emissions in the Vlist and Zegveld soils, respectively. The relatively

low contribution of CH_4 agreed with our hypothesis. However, this study did not include the effect of long term inundation on CH_4 emissions.

Although the relation between oxidation and soil moisture content or groundwater conditions has been studied often using static treatments in a factorial design or in stepwise drying schemes, studies on the response to rewetting are lacking. In this experiment, we observe an effect of the direction of GWL change on oxidation dynamics. Our results suggest that the moisture conditions in the top 40 cm, rather than those in the subsoil, are a major factor for the total CO_2 and N_2O emission. In a field situation, top soil conditions are largely affected by fertilization, grazing and rainfall events, factors that were not included in this experiment. To understand the dynamics contributing to total peat oxidation and subsequent GHG emissions in a peat meadow soil, we would recommend to study grass growth, fertilization, grazing and/or weather effects in interaction with shallow (-20 to 0 cm) GWL treatments.

3.4.4 Volume loss due to oxidation

A vertical displacement of 0.87 to 1.32 cm was observed after two drying-rewetting cycles (Fig. 3.7, Table 3.4). While we used the surface level elevation measured 427 days after the start of the experiment (we continued volume measurements for two more months after the end of cycle 2, to allow the soil to swell at a constant GWL of 0 cm), we consider the subsidence as a yearly rate, as the time span encompassed one period resembling summer drought conditions. We tried to estimate the relative contribution of oxidation to the total volume loss, using a function relating volume loss to C loss, and comparing the result to our measured C losses (cumulative CO_2-C emissions per year). A conventional way to estimate the C loss (kg C $ha^{-1}yr^{-1}$) in the absence of (sufficient) emission observations is to use yearly subsidence observations (Hiraishi et al., 2014). Carbon emissions can be calculated based on subsidence and peat properties, according to (e.g., Van den Akker et al., 2008):

$$C_{loss} = S \cdot F_{ox} \cdot \rho_{peat} \cdot SOC \cdot 10^4 \quad (1)$$

where C_{loss} is the carbon loss (kg C ha^{-1} yr^{-1}), S is subsidence rate (m yr^{-1}), F_{ox} is the fraction of subsidence caused by oxidation of organic matter (-), ρ_{peat} is bulk density (kg m^{-3}), SOC is soil organic carbon content of the peat (kg C kg^{-1} soil), and 10^4 is a unit conversion factor (m^2 ha^{-1}). Van den Akker et al. (2008) proposed that a constant F_{ox} value of 1 could be taken, when using the ρ_{peat} and SOC values of the reduced, fibric peat

below the groundwater table. The reasoning behind this approach is that, in peat grasslands with controlled GWLs, a steady state situation is created where the periodically lowering GWL exposes new layers of fibric peat to permanent aerobic conditions. This approach has been applied in the Dutch national Greenhouse gas inventory, to estimate annual C losses from drained peat soils (Arets et al., 2022). Following this relationship, by using the ρ_{peat} and *SOC* values of the deepest horizons in our soil cores, the subsidence values should correspond with a C_{loss} of 0.56 to 0.80 kg C $m^{-2}yr^{-1}$ (Table 3.4). These potential C-losses are higher than the actual measured CO_2-C emission, and the actual fraction of volume loss that could be attributed to oxidation (F_{ox}) was, therefore, estimated to range between 66 and 79% (Table 3.4). Other studies have reported similar relative contributions of oxidation to volume loss (Ishikura et al., 2018; Leifeld et al., 2011; Schothorst, 1977; Wösten et al., 1997). Our mean subsidence observations approximate typical subsidence rates, which are reported to range between 1 and 15 mm per year in temperate peat meadows (Hoogland et al., 2012; Koster et al., 2018; Leifeld et al., 2011; Schothorst, 1977; Van den Akker et al., 2008; Van der Meulen et al., 2007). The surface of the Zegveld cores subsided stronger than those in the Vlist and Aldeboarn cores, which both contained a 16 to 22 cm clay layer just below the top soil (Table 3.1). This observation agrees with the suggestion by Van den Akker et al. (2008) of an inhibiting effect by a clay cover on subsidence.

The estimates did not include the horizontal volume losses, which occurred in particular in the highest soil layers. At the last recording, three weeks after the last GWL rise, the radiuses of the surface areas were still 1.25 to 2.30 cm smaller than at the start of the experiment (Table 3.4). Considering this, we can assume that the reported volume losses are actually underestimations, and the oxidation components to volume loss are overestimations.

3.5 Conclusion

In this study, we manipulated GWL conditions in incubated, undisturbed bare peat cores from three peat areas in the Netherlands. Over a period of 370 days, we applied two drying-rewetting cycles on the cores and measured surface emissions of CO_2, N_2O and CH_4, as well as solute pore water concentrations, VWC and matric potential throughout the vertical profile and volume change at the surface. In accordance with our hypothesis, cumulative total greenhouse gas emissions over the course of the experiment were dominated by CO_2. Raising the GWL

to -20 or 0 cm, however, resulted in strong N_2O emissions. Due to these peaks, the 0 cm GWL step was associated with highest N_2O emissions and the highest CO_2-eq sum of CO_2 and N_2O. A small number of peak N_2O emission events provided a substantial contribution to total CO_2-equivalent emissions. CH_4 emissions or uptake was small and showed no relation with the GWL, contrary to our hypothesis. We confirmed our hypothesis that CO_2 emissions increase with drainage, and observed on average the highest emissions at a GWL of -80 cm. Relationships between the GWL and CO_2 emissions were different for drying and rewetting pathways, however, indicating hysteresis in the WFPS and the oxidation process, and suggesting that the upper 40 cm of the soil was the largest contributor to CO_2 emissions. Similarly, the high N_2O peaks after a GWL rise to -20 or 0 cm, may indicate that the conditions in the top 40 cm are most important to N_2O production. In accordance with our hypothesis, the results suggest that a GWL of 20 cm constitutes the risk for large N_2O pulse emissions during rewetting of the soil. This is a potential risk in the field, were soil moisture in the top soil can be highly variable due to precipitation events. A GWL of 0 cm would be preferential in terms of mitigation of both CO_2 and N_2O emissions, but the continuation of current dairy farming practices would demand less conditions. Further research is therefore needed to study the interactions between the potential GWL scenario's and nitrogen input through fertilizers and grazing.

Acknowledgements
The research presented in this paper is part of the project Living on soft soils: subsidence and society (grantnr.: NWA.1160.18.259). This project is funded by the Dutch Research Council (NWO-NWA-ORC), Utrecht University, Wageningen University, Delft University of Technology, Ministry of Infrastructure & Water Management, Ministry of the Interior & Kingdom Relations, Deltares, Wageningen Environmental Research, TNO-Geological Survey of The Netherlands, STOWA, Water Authority: Hoogheemraadschap de Stichtse Rijnlanden, Water Authority: Drents Overijsselse Delta, Province of Utrecht, Province of Zuid-Holland, Municipality of Gouda, Platform Soft Soil, Sweco, Tauw BV, NAM. This study was a collaboration with the project "Nationaal Onderzoeksprogramma Broeikasgassen Veenweiden" (NOBV). We would like to thank all researchers, technicians, laboratory staff and farmers who have facilitated or contributed to this project. In particular, we would like to thank Frank Gerritsen, Paul Gerritsen, Harm Gooren, Rudi Hessel and Jos van Dam of Wageningen University & Research.

Chapter 3 Supplementary material



Figure S3.1*: Soil columns in the experimental setup, standing on a 50 cm high platform.*

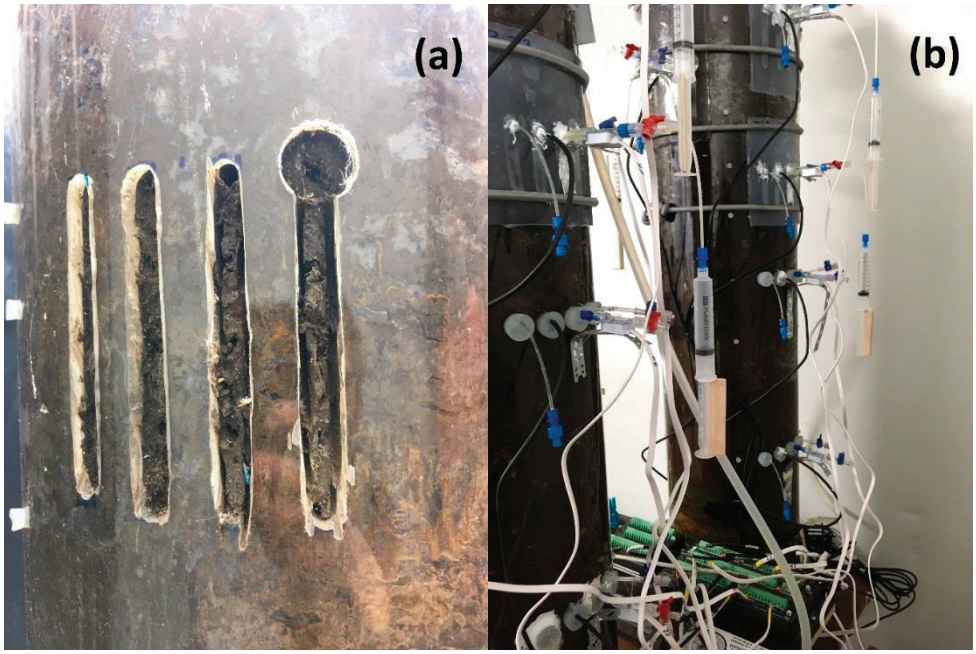


***Figure S3.2**: Vertical slot openings in the tube wall, before placement of probes (a), and rows of probes installed in the soil columns (b). The upper three rows of probes were inserted in the vertical slots, covered by a sheet of curved acrylate and silicone gel for watertight closure. The lower two rows of probes were inserted through holes closed off with silicon corks.*

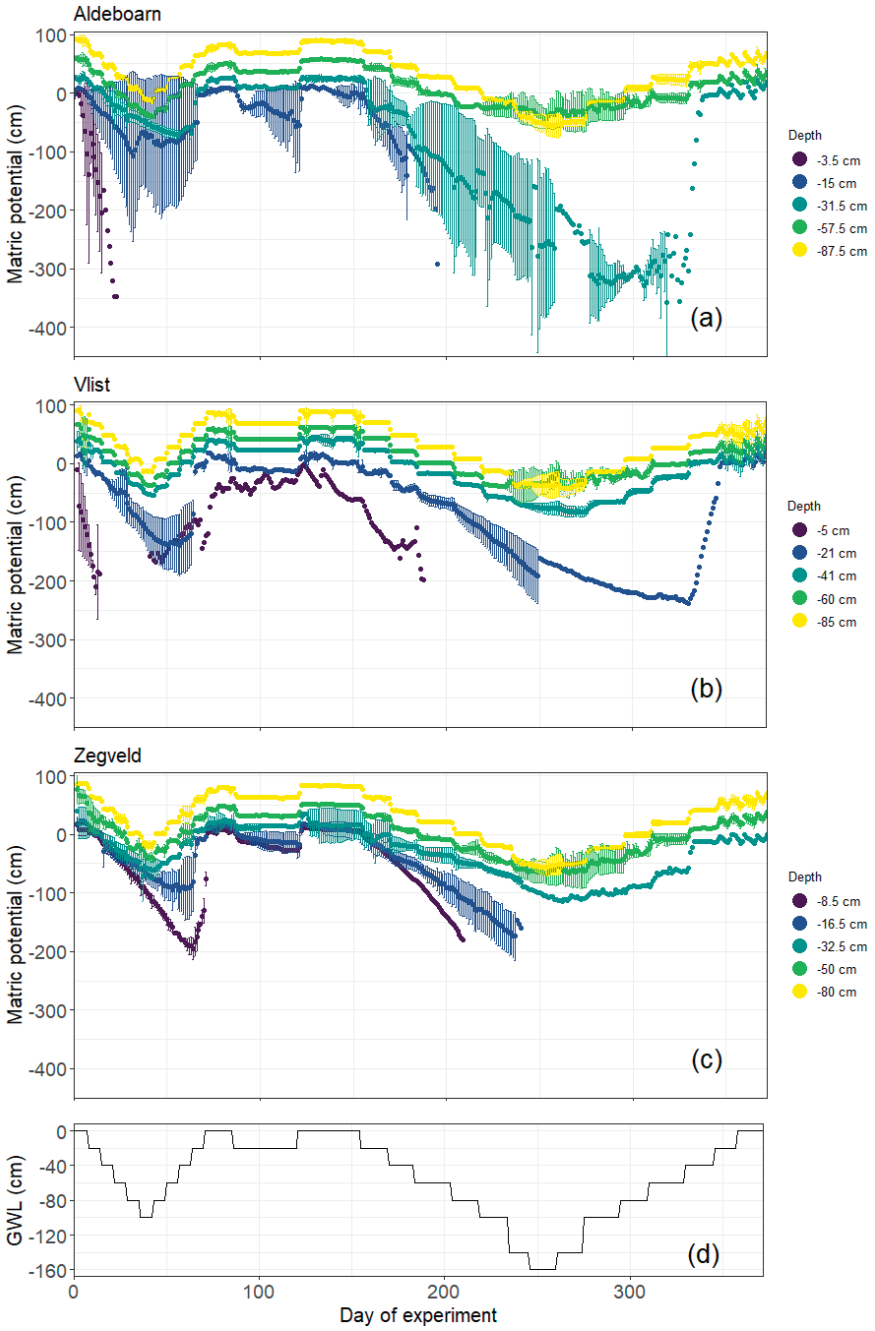


***Figure S3.3**: Mean matric potential observations in the three soils and standard deviations (n = 3, unless observations were omitted due to erroneous sensor readings).*

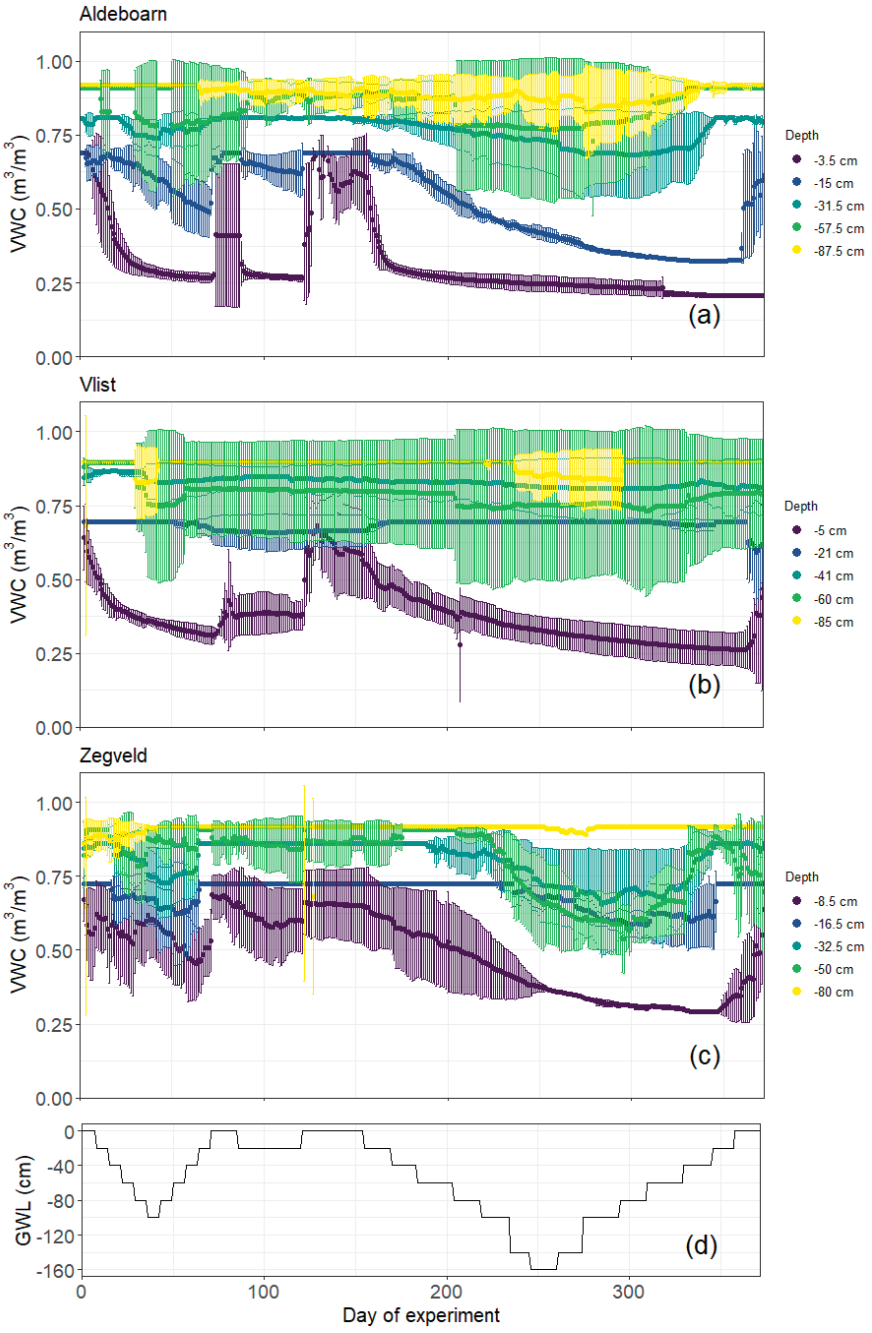


***Figure S3.4**: Mean volumetric water content observations in the three soils and standard deviations (n = 3, unless observations were omitted due to erroneous sensor readings).*

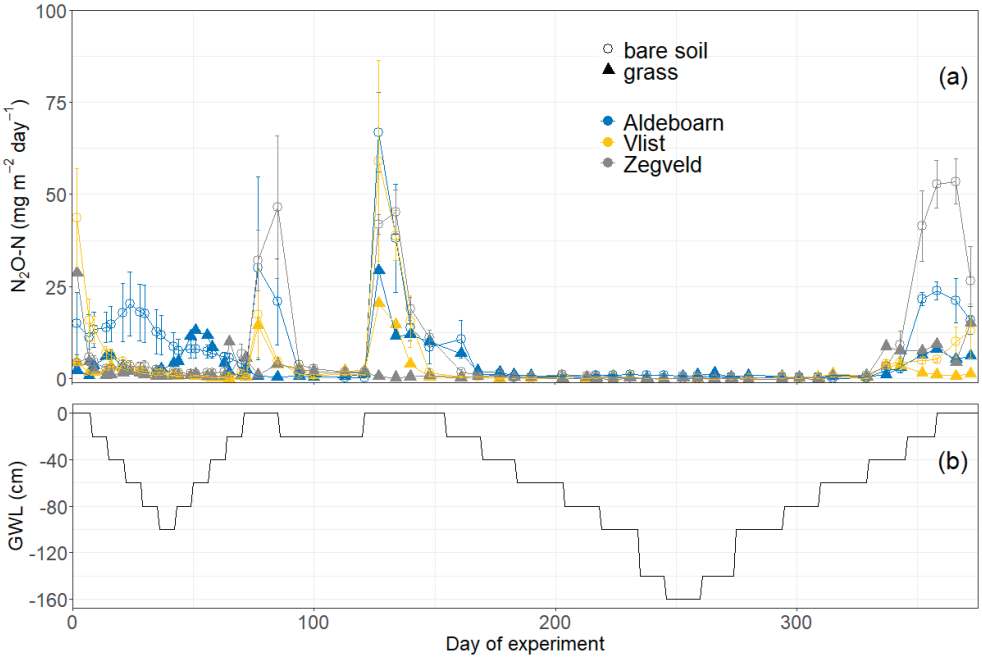


***Figure S3.5**: N_2O emissions (a) from bare (n = 3) and vegetated (n = 1) soil columns from the three sampling locations during the corresponding GWL treatments (b).*

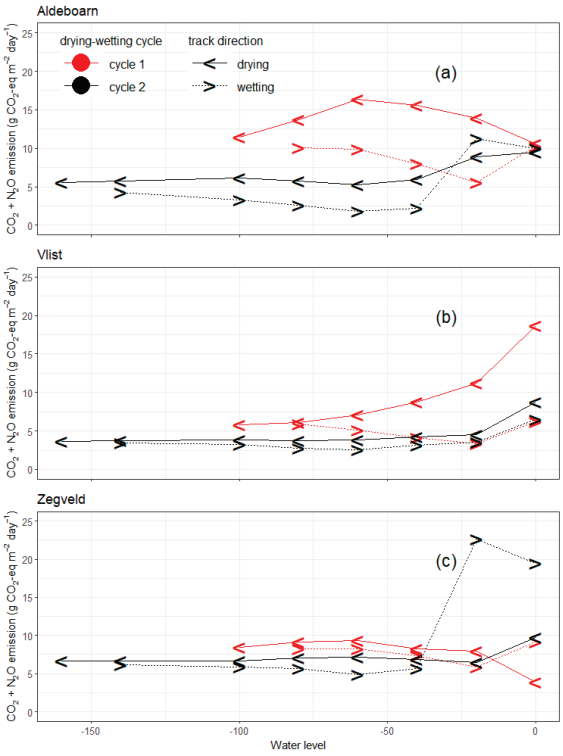


***Figure S3.6**: CO_2 and N_2O emissions together expressed in CO_2-equivalents (g m^{-2} day^{-1}) released from bare soil columns from Aldeboarn (a), Vlist (b) and Zegveld (c) plotted against the applied GWL.*

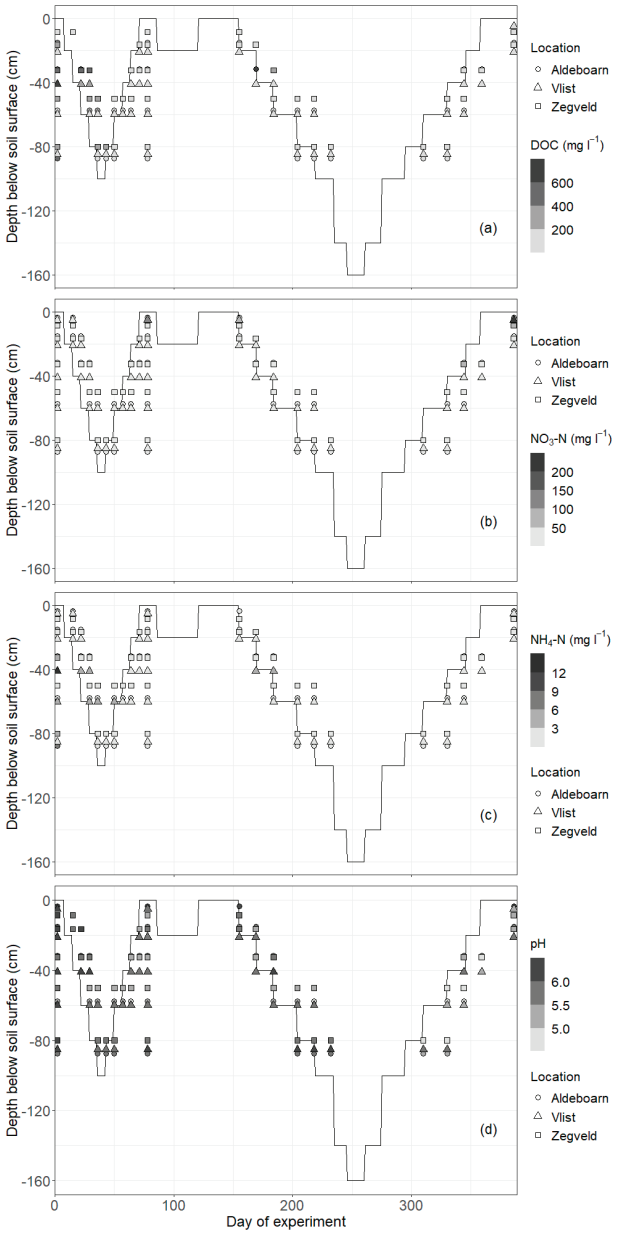


***Figure S3.7**: DOC (a), NO_3-N (b), NH_4-N (c) concentrations (mg l^{-1}) and pH (d) in extracted pore water samples from bare soil columns over the course of the two drying-wetting cycles. The y-coordinates of the points indicate the depths (cm below the soil surface) from which the samples were extracted. The GWL change is indicated by the black line. Each pore water extraction was performed at the end of a GWL step, shortly before changing the GWL.*

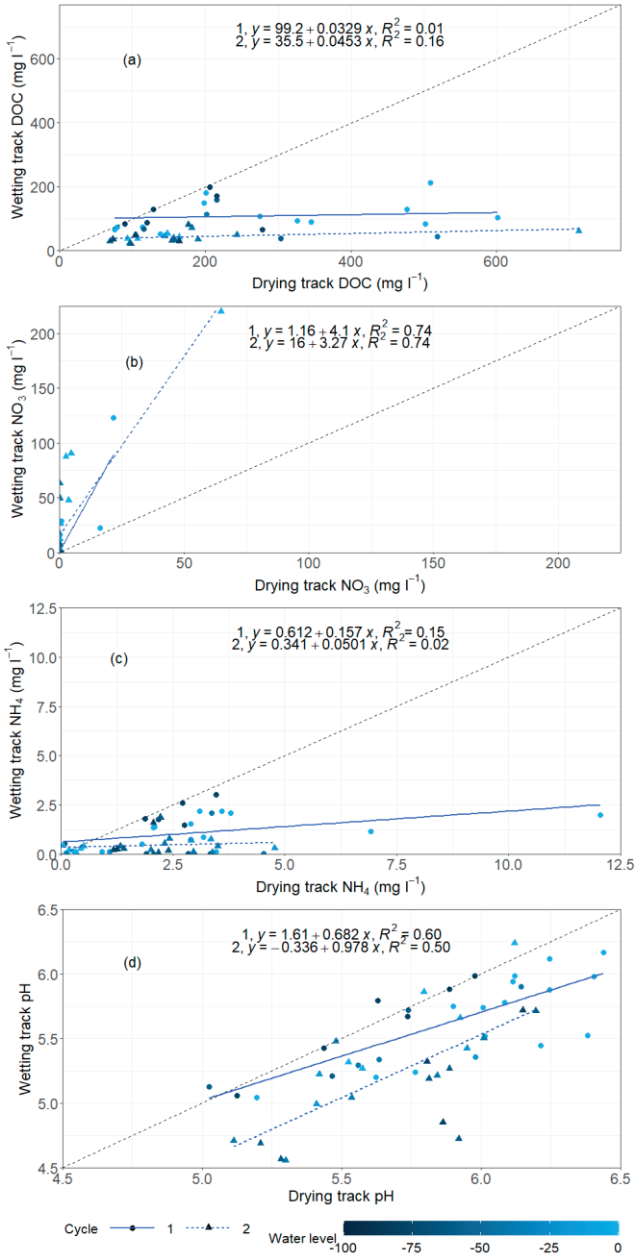


***Figure S3.8**: DOC (a), NO_3-N (b), NH_4-N (c) concentrations (mg l^{-1}) and pH (d) in pore water extracted from all soil cores from all locations during the drying trajectory of the soil GWL, plotted against concentration in pore water extracted from the same depth and at the same GWL condition during the wetting track.*


4

Chapter 4

Drainage, cattle excreta and trampling effects on nitrous oxide emissions from a peat grassland

Erne Blondeau, Dorien Westerik, Thomas Gremmen, Sarah Faye Harpenslager, Marius Heinen, Gijs van Dijk, Jan Willem Van Groenigen, Gerard Velthof

Published as: Blondeau, E., Westerik, D., Gremmen, T., Harpenslager, S. F., Heinen, M., van Dijk, G., van Groenigen, J. W., Velthof, G. (2026). Drainage, cattle excreta and trampling effects on nitrous oxide emissions from a peat grassland. *Agriculture, Ecosystems and Environment, 397*. https://doi.org/10.1016/j.agee.2025.110093

Abstract

To mitigate the effects of drainage on carbon dioxide emissions and soil subsidence from grasslands on peat soils, measures are explored to raise groundwater levels or reduce groundwater level fluctuations, such as the implementation of a water infiltration system. The effect of water infiltration systems on nitrous oxide emissions from peat grasslands has not received much attention yet. On peat grasslands, nitrous oxide emissions can be intensified by cattle grazing through the input of nitrogen in urine and dung, as well as soil compaction caused by trampling. Therefore, the combined effects of a water infiltration system and simulated grazing on nitrous oxide emissions from a peat grassland were studied in a two-year field experiment.

Without nitrogen inputs, cumulative nitrous oxide emissions from peat oxidation were lower, but not significantly, under a water infiltration system compared to conventional drainage (1.2 ± 0.25 kg N ha^{-1} vs 8.8 ± 3.7 kg N ha^{-1}). Urine, dung and trampling application all significantly increased cumulative nitrous oxide emissions in both drainage systems. There was a significant interaction effect between drainage type and urine application, indicating different effects of water infiltration systems in the absence or presence of urine application. Urine and dung emission factors were higher under a water infiltration system than conventional ditch drainage.

These results suggest that water infiltration system effects on nitrous oxide emissions from peat grasslands are not consistent, and interact with external nitrogen inputs through cattle grazing.

4.1 Introduction

Peat soils store over 30% of the world soil organic carbon (C) pool, while occupying only 3% of the global land area (Loisel et al., 2017; Yu et al., 2010). In Europe, peat soils are often drained for agriculture. Drainage improves the bearing capacity of the field, which enables access with machinery and cattle grazing, but also leads to peat oxidation resulting in carbon dioxide (CO_2) emissions and soil subsidence (Canadell et al., 2021; Erkens et al., 2016). Additionally, drained peat soils emit nitrous oxide (N_2O) (Liu et al., 2020; Minkkinen et al., 2020), a GHG with a global warming potential 273 times stronger than CO_2 over a 100-year horizon (Forster et al., 2021). In the Netherlands, the oxidation of drained organic soils resulted in an N_2O emission of 0.6 Tg CO_2-eq in 2022 (RIVM, 2024). Permanent rewetting is an effective measure to reduce peat oxidation (Evans et al., 2021; Wilson et al., 2016a), but implies adopting an alternative agricultural system, such as paludiculture (the production of crops on rewetted peat) (Tanneberger et al., 2022), or a transition towards nature restoration (Temmink et al., 2023; Temmink et al., 2024).

Alternatively, the implementation of a water infiltration system (WIS) is increasingly studied as a measure to mitigate emissions while maintaining the current land use (Aben et al., 2024; Boonman et al., 2022; Kechavarzi et al., 2007; Offermanns et al., 2023). A WIS consists of evenly spaced drainage pipes installed in agricultural parcels at 15-20 cm below the ditch water level and connected to ditches either directly or via a collector drain and/or managed reservoir. Through WIS, infiltration of ditch water can prevent strong drops in the groundwater level (GWL) during drought, while also providing more effective drainage in wet periods (Harpenslager et al., 2024; Van Asselen et al., 2023). While several studies have observed reduced CO_2 emissions and altered redox processes and nutrient availability after WIS implementation (Aben et al., 2024; Boonman et al., 2024; Boonman et al., 2022; Harpenslager et al., 2024), the effects of WIS on N_2O emissions are still poorly studied. Weideveld et al. (2021) observed no significant differences between N_2O emissions from WIS drained and conventionally drained fields in the north of the Netherlands but may have missed key flux moments due to the low measurement frequency. Offermanns et al. (2023) measured increased N_2O emissions after a combination of WIS and grassland renewal, but not for WIS alone. The increasing interest in the implementation of WIS in peat grasslands stresses the importance of understanding its effect on N_2O emissions.

Soils are the main source of N_2O emissions worldwide, with direct emissions from agricultural soils estimated to be 1.8 Tg N yr^{-1} and from natural soils 6-7 Tg N yr^{-1} (Syakila & Kroeze, 2011). Total agricultural emissions, including manure management and indirect emissions, were estimated to reach 5.3 Tg N yr^{-1} in 2006, about 60% of the total anthropogenic N_2O emissions (Syakila & Kroeze, 2011). Within soils, N_2O is produced during microbial and abiotic conversion processes, most importantly microbial aerobic nitrification and anaerobic denitrification (Butterbach-Bahl et al., 2013). Considering the high nitrogen (N) availability due to peat mineralization, high organic carbon content and frequent anaerobic conditions, peat soils can (potentially) be important sources of N_2O (Van Beek et al., 2004). Emissions of N_2O typically show a temporal pattern with predominantly low emissions and occasional strong peak events (Anthony & Silver, 2021; Berendt et al., 2023). Similarly, emission patterns can show a heterogeneous pattern on a spatial scale, e.g. within a single field (Charteris et al., 2020).

A primary controlling factor for N_2O emissions is the soil moisture content: by restraining oxygen diffusion, soil moisture regulates N mineralization, nitrification, and thereby nitrate (NO_3^-) availability, as well as denitrification (Pärn et al., 2018). Since nitrification and denitrification are the dominant processes that produce N_2O, conditions enabling these processes can indirectly promote N_2O emissions (Abbasi & Adams, 2000; Taghizadeh-Toosi et al., 2019). The capillary fringe, the soil region just above the water table, has been identified as a hot-spot for N_2O production (Taghizadeh-Toosi et al., 2019), while sudden shifts from aerobic to anaerobic conditions, caused by precipitation events or a sudden rise in the GWL can form hot-moments (Norberg et al., 2021; Taft et al., 2018). A raised GWL, while mitigating N-mineralization (Baggs, 2011; Martikainen et al., 1993; Regina et al., 2015), will temporarily favour conditions for denitrification and move the capillary fringe closer to the surface compared to drained conditions, thereby increasing the upwards diffusion rate of N_2O and potentially the N_2O:N_2 ratio of denitrification end products (Baggs & Philippot, 2010; Butterbach-Bahl et al., 2013).

Alternatively, N_2O peak events can be driven by external N inputs, mainly through fertilizer applications or cattle excretion (Kandel et al., 2019). Cows assimilate only up to 20% of the consumed N into their tissue and milk, while 80-95% is excreted in the urine and faeces (Oenema et al., 1997). About 60-65% of the excreted N ends up in the urine, of which 50-90% is present as urea ($(NH_2)_2CO$) and the rest as amino acids and

peptides (Bolan et al., 2004; Oenema et al., 1997). Nitrification has been identified as an important source of N_2O from urine and dung patches (Carter, 2007), while under anaerobic conditions, caused by a high moisture content or low porosity, denitrification may increase in importance (Bhandral et al., 2007). After deposition onto the soil, urine will distribute through the pore spaces within the upper soil. Within days, most of the urea is hydrolysed to NH_4^+, which is subsequently nitrified (Haynes & Williams, 1992) and denitrified under aerobic and anaerobic conditions (Bolan et al., 2004). Urine deposition frequently causes an increase in ammonia oxidizing bacteria (Cai et al., 2017). Conversely, the rise in pH following urea hydrolysis (temporarily) inhibits nitrification due to the inhibitory effects of high pH and gaseous ammonia (formed during the reaction of ammonium with hydroxyl ions) on ammonia oxidizing bacteria as well as nitrite oxidizing bacteria (Heil et al., 2016; Monaghan & Barraclough, 1992). Increased pH may also affect (N_2O losses from) denitrification by stimulating most reductase enzymes, while decreasing the relative proportion of N_2O as the intermediate denitrification end-product (Cuhel et al., 2010). Moreover, an alkaline environment indirectly enhances denitrification through increased solubilization of organic matter (Lambie et al., 2013; Monaghan & Barraclough, 1993; Scott et al., 2015). In dung, nitrogen is mostly present in organic compounds, and becomes available less rapidly, first requiring mineralization of organic matter to form NH_4^+, after which nitrogen undergoes similar transformations as in urine patches (Bolan et al., 2004).

The abundance of labile carbon in dung may stimulate denitrification below a dung patch, both by providing a C substrate and by increasing oxygen consumption (Cai et al., 2017). Within days after dung application, easily degradable carbon may drive the reduction of soil NO_3^-, even before mineralization of dung N (Van Groenigen et al., 2005a; Velthof et al., 2003). Nitrous oxide emissions associated with urine or dung excretion may show seasonal variation, due to differences in grass nitrogen uptake, nitrogen lost as NH_3 and soil moisture content (De Klein et al., 2006; Krol et al., 2016; Lockyer & Whitehead, 1990 ; Selbie et al., 2015; Van Groenigen et al., 2005b).

Cattle grazing is also associated with compaction due to trampling, which may stimulate denitrification by increasing anaerobic microsites (Bhandral et al., 2007; Van Groenigen et al., 2005b). The proportion of the N applied onto the soil in the form of urine or dung that is lost as N_2O (the emission factor) may thus be increased by trampling (Van Groenigen et al., 2005a). Beare et al. (2009) observed that compaction has a strong

positive effect on N_2O emissions by raising the water filled pore space (WFPS) above 60% and thereby stimulating denitrification. The effect of trampling on N_2O emissions from peat soils, where the WFPS often is relatively high in the first place, is not well studied, however.

Thus, urine and dung patches as well as trampling during cattle grazing may increase N_2O emissions, particularly in organic soils (Velthof et al., 1996). Raising the GWL in a drained peat grassland under grazing may increase the risk of denitrification-associated N_2O emissions. This is reflected in high N_2O emissions under urine application in lab incubations of mineral soils with relatively high moisture contents (Cai & Akiyama, 2016; Van Groenigen et al., 2005a). On the other hand, rewetting projects of drained peatlands under unfertilized conditions have frequently been reported to reduce N_2O emissions from peat oxidation (Minkkinen et al., 2020; Ojanen & Minkkinen, 2020; Wilson et al., 2016a). The interaction effects of increased anaerobic conditions under a WIS measure and grazing effects is, however, not well understood.

The aim of this study was to determine the effects of WIS in a peat grassland soil in combination with cattle excretion (simulated by applying synthetic urine and cattle dung) and trampling (simulated by compacting the soil) on N_2O emissions. It was hypothesized that (1) WIS decreases N mineralization from peat and N_2O emissions originating from mineralized N compared to a conventionally drained peat soil, (2) urine or dung application increases N_2O emissions, especially in combination with WIS due to higher mineral N availability and enhanced denitrification, and (3) trampling increases N_2O emissions from denitrification.

4.2 Methods and materials

4.2.1 Field location

The field experiment took place between July 2022 and February 2024, at a farm near Zegveld in the Netherlands (52°08' N, 4°50' E, Fig. 4.1a) on drained peat soil in intensive agricultural use with dairy farming. The soil is characterized as mesotrophic wood peat, above a eutrophic sedge peat layer, which can be as thick as six meters in some places. The field experiment was carried out on two adjacent fields with similar soil properties (Table 4.1 and Table 4.2), which were both subjected to the same management, with vegetation dominated by rye grass (*Lolium perenne*), fertilizer application of about 230 kg N ha^{-1} yr^{-1}, mowing and cattle grazing. Three months before the first treatment application (February 2022), WIS drains were installed lengthwise in one field at a depth of 60-70 cm below the surface (10-20 cm below the ditch water

level) and with an average spacing of 4 m. The WIS, which was designed to reduce GWL fluctuations (i.e. to lower levels in winter and raise them in summer, in comparison to conventional ditch-controlled drainage), had a target GWL set at 40 cm below the soil surface (Van Asselen et al., 2023). The second field served as a reference situation with conventional ditch drainage (CDD). The abbreviations WIS and CDD are used to refer to the two treatment fields in this paper.

Table 4.1*: Soil characteristics measured in the control plots on 07-10-2022, two days after the 2022 treatment applications. Samples were taken in 50x50 cm squares in the C subplots from a depth of 0-15 cm and averaged per field (n = 3). Moisture content, dry bulk density and soil organic matter (SOM) content were determined after drying at 105°C. Soil pH and bioavailable NO_3^- and NH_4^+ were determined in NaCl extracts. The complete overview of soil characteristics can be found in Table S4.4.*

Parameter	CDD field	WIS field
Moisture (% of fresh weight)	39.0 ± 2.1*	48.0 ± 2.0
Dry bulk density (g cm^{-3})	0.46 ± 0.01	0.44 ± 0.006
SOM (% of dry weight)	47.9 ± 0.24	50.7 ± 1.3
pH	4.5 ± 0.062	4.7 ± 0.06
NO_3-N (mg l^{-1})	27.7 ± 5.4	12.3 ± 3.0
NH_4-N (mg l^{-1})	7.70 ± 1.2	3.194 ± 0.087

* Mean values of the two fields differ significantly (t-test, $p < 0.05$).

***Table 4.2**: Soil characteristics measured at 0-10 and 10-20 cm depth on 27-09-2023, one day before the 2023 treatment applications. Samples were taken in 50x50 cm squares in the C, U and D subplots and averaged per field and depth (n = 12). Moisture content, dry bulk density and soil organic matter (SOM) content were determined after drying at 105°C. Soil pH and bioavailable NO_3^-, NH_4^+, DOC-C and total dissolved N (organic plus inorganic) were determined in water extracts. The complete overview of soil characteristics can be found in Table S4.5.*

Parameter	0-10 cm		10-20 cm	
	CDD field	WIS field	CDD field	WIS field
Moisture (% of fresh weight)	40.3 ± 1.73*	48.2 ± 0.71	46.0 ± 1.39*	49.4 ± 0.56
Dry bulk density (g cm^{-3})	0.42 ± 0.01	0.43 ± 0.02	0.47 ± 0.01	0.49 ± 0.02
SOM (% of dry weight)	49.7 ± 0.47*	54.9 ± 0.45	45.3 ± 0.45*	46.3 ± 0.61
pH	5.13 ± 0.07	5.24 ± 0.09	5.08 ± 0.11	5.32 ± 0.06
NO_3-N (mg l^{-1})	7.68 ± 1.40	5.07 ± 0.42	7.57 ± 0.84	6.02 ± 0.90
NH_4-N (mg l^{-1})	1.57 ± 0.50*	0.44 ± 0.08	0.11 ± 0.02	0.22 ± 0.06
DOC-C (mg l^{-1})	139.7 ± 8.09	141.1 ± 6.08	139.5 ± 4.21	148.5 ± 5.84
Total dissolved N (mg l^{-1})	21.0 ± 2.65	15.2 ± 0.51	17.8 ± 0.77	16.4 ± 0.76

* Mean values of the two fields (at the same depth) differ significantly (t-test, $p < 0.05$).

4.2.2 Experimental design

The experiment consisted of three treatment applications: one in the summer of 2022, and two in the autumns of 2022 and 2023. The fields were mowed approximately one week before each experimental treatment application. In the middle of each field, a main plot of approximately 0 by 20 meters was fenced off. Inside, a randomized block experiment was set up containing the three simulated effects of grazing in subplots: (1) urine, (2) dung and (3) trampling, in a full factorial design including a control treatment (Fig. 4.1b). This resulted in eight treatment levels: control (C), urine (U), dung (D), trampling (T), urine + dung (UD), urine + trampling (UT), dung + trampling (DT) and urine + dung + trampling (UDT). The experiment included three treatment replicates in 2022 and four replicates in 2023, due to the high variability within treatments (Fig. 4.1b). The subplots of 1 by 2 m were positioned directly adjacent to each other in three rows (four in 2023) of eight subplots. To account for potential spatial variability, each row was considered a block, with treatments randomly assigned to subplots within each block. A PVC collar with a height of 10 cm and an outer diameter of 20 cm was inserted approximately 5 cm deep into the soil of each subplot for static chamber measurements of N_2O fluxes (Fig. 4.1c,d). The dung, urine and trampling treatments were applied inside the PVC collars. A 50 x 50 cm square was demarcated on all replicates of the C, D and U subplots, on which the respective treatments were also applied at the same application rates as inside the flux chamber collars (Fig. 4.1c,d). These squares were used for sampling of porewater (in autumn 2022) or soil samples (in autumn 2023) for biochemical analysis (see paragraph 2.4). The treatment applications of the 2022 summer, 2022 autumn and 2023 autumn campaigns took place on 21-07-2022, 05-10-2022 and 28-09-2023, respectively. The three applications were each applied on new and untreated parts of the field, with the intention for each application to represent one urination event, dung patch or trampling event (Fig. 4.1c, 1d).

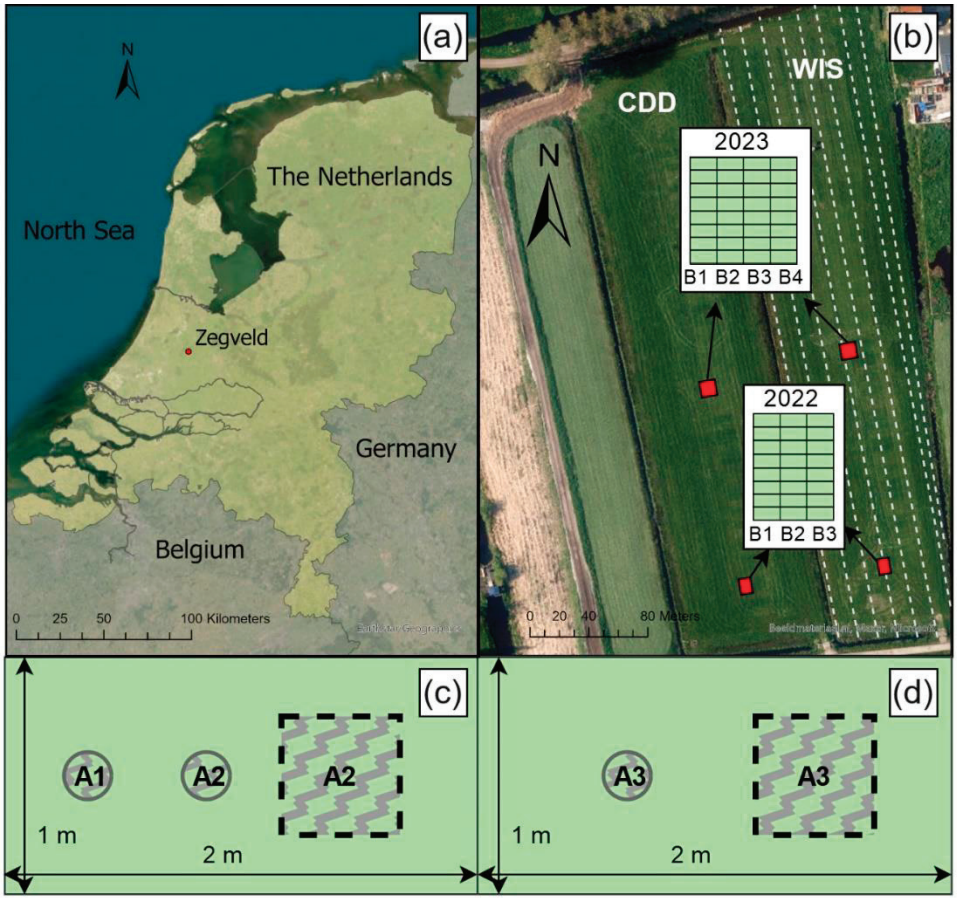


***Figure 4.1**: Location and set-up of the experiment. Geographical location of the field site (a); set-up of the conventional ditch drainage (CDD) and water infiltration system (WIS) fields, with in red the positions of the fenced-off plots in the summer and autumn of 2022, and autumn 2023, respectively, and schematic representations of the block designs (B1 to B4) (b); set-up of a subplot in 2022 (c) and in 2023 (d). The circles and squares in (c) and (d) represent the treated soil areas for flux measurements and porewater/soil sampling, respectively. Squares for porewater/soil sampling were present only in the C, U and D subplots. Numbers within the treated areas indicate the application round: summer 2022 (A1), autumn 2022 (A2) or autumn 2023 (A3). Note that the dotted lines representing WIS drains in (b) are schematic and not to scale.*

Cattle urine was simulated by a synthetic solution, which resembles the composition of real cattle urine in terms of nitrogenous compounds and salts based on two urine solutions in a study by Kool et al. (2006). The solution contained demineralized water and the main nitrogenous components of cattle urine: urea, allantoin, hippuric acid,

creatinine and uric acid. Salts were added to better approximate the pH of cattle urine at 14 g L^{-1} $KHCO_3$, 10.5 g L^{-1} KCl, 0.4 g L^{-1} $CaCl_2$ •$2H_2O$, 1.2 g L^{-1} $MgCl_2$ • $6H_2O$ and 3.7 g L^{-1} Na_2SO_4. Due to a miscommunication, the urine composition in fall was different from the summer, and the total amount of N applied was lower. All urine N application rates fell within a realistic range, however. Cattle urine is reported to be deposited at rates between 20 and 200 g N m^{-2} (Selbie et al., 2015). During the summer application, the synthetic urine (22 g N L^{-1}) was applied at a rate of 89 g N m^{-2} and its N content consisted of 71.7% of urea, 21.5 % allantoin, 2.1% hippuric acid, 3.9% creatinine and 0.9% uric acid. During the two autumn applications, the solution (10 g N L^{-1}) was applied at a rate of 40 g N m^{-2}. The N content of this solution consisted of 80% urea, 12% allantoin, 4.6% hippuric acid, 2.9% creatinine and 0.5% uric acid. Fresh cattle dung was collected in the cattle housing (without getting in contact with cattle urine) within 24 hours before treatment application, and mixed into one homogeneous batch. Due to natural variation in N content which could only be measured later, N application rates varied slightly, between approximately 26 g N m^{-2} (summer 2022), 29 g N m^{-2} (autumn 2022) and 27 g N m^{-2} (autumn 2023). Subsamples were collected from the batches for organic matter and nutrient analysis (Table S4.1). Trampling simulated by compaction was created using an 8 kg, cylindrical weight, described by Janssen et al. (2023). A consistent procedure was followed, by dropping the cylinder from a fixed height of 0.6 m, six times onto the treated soil area inside the flux chamber collar in a fixed pattern. When subplots received more than one grazing effect, the treatments were applied following the order trampling, urine, dung.

4.2.3 N_2O flux measurements

N_2O concentrations were measured using cavity ring-down spectroscopy (Picarro G2508; Picarro Inc., USA) during the 2022 applications. During the 2023 application, a gas analyser with photoacoustic infrared spectroscopy (INNOVA 1512; LumaSense Technologies Inc., USA) was used due to unavailability of the former analyser. Gas fluxes were measured using the static chamber method, with a closure time of 10 to 15 minutes. When necessary – in particular the days after treatment application – the closure time was shortened to prevent interference of high NH_3 concentrations with the N_2O observations. The headspace concentration was measured once after closing the chamber for 10 to 15 minutes and gas fluxes were calculated assuming a linear slope between the head space concentration and the

ambient air N_2O concentration at the time of chamber closure (Abalos et al., 2014; Oram et al., 2020; Van 't Hull et al., 2025). To check the assumption that the headspace concentration was increasing linearly during the full course of chamber closure, at least one extra flux observation was performed per measurement day, for at least 20 minutes with continuous concentration measurements in a closed loop.

4.2.4 Biochemical analyses

At the start of the 2022 autumn campaign, ceramic cups (pore size 2.5 µm) were installed inside the 50x50 cm squares within the U, D and C subplots to collect porewater at 15-20 cm depth (Fig. 4.1c). In some plots, porewater extraction was not possible due to dry conditions. Therefore, in the second year, soil samples were collected at 0-10 cm and 10-20 cm instead of the porewater extraction.

To check the conditions before treatment applications, soil samples (0-15 cm depth) were collected in the autumn of 2022 and 2023, from each 50x50 cm square on both fields before the application of the U and D treatments. Soil samples were wrapped in plastic and stored at 4 °C until analyses at the laboratory. Fresh and dry weight fractions were determined by filling two aluminium cups with a known volume (40.5 ml) of homogenized soil and weighing these before and after drying (>48 hours at 60 °C). The organic matter fraction was approximated by loss on ignition (4 hours at 550 °C). Total elemental content was determined by digesting 200 mg of homogenized dried soil with 5 ml 65% HNO_3 and 2 ml H_2O_2 in a microwave (Ethos Easy Rotor Maxi-44, Milestone, Sorisole, Italy). Samples were filled up to 100 ml with demineralized water and analysed for total Al, Ca, Cl, Fe, K, Mg, Mn, Na, P, S, Si and Zn on an inductively coupled spectrometer (ICP-OES ARCOS MV with horizontal plasma and axial plasma observation and a Seaspray nebulizer, Spectro Analytical Instruments, Kleve, Germany).

In 2022, porewater was collected on days 2, 6, 13, 20, 28, 34, 43, 48 and 56 after treatment application, by attaching a vacuum syringe to the ceramic cups. Porewater was frozen on site and returned to room temperature before analysis at the laboratory. Porewater concentrations of NO_3^-, NO_2^- and NH_4^+ were determined on a segmented flow auto-analyser (AA500, SEAL Analytic Norderstedt, Germany) using hydrazine sulphate and salicylate reagent, respectively. Total concentrations of Al, Ca, Cl, Fe, K, Mg, Mn, Na, P, S, Si and Zn were determined in acidified samples (10 ml with 0.1 ml 65% HNO_3) on an ICP-OES, as described above.

In 2023, soil samples were collected from 0-10 cm and 10-20 cm depth on days 0, 4, 7, 14, 21 and 34 after the autumn treatment application. At the laboratory, 17.5 g of fresh soil was shaken with 50 ml demineralized water for 2 hours (at 105 rpm on an orbital shaker), after which a water sample was extracted using porewater samplers (pore size 0.15 µm, Rhizons, Rhizosphere research products, Wageningen, the Netherlands). In the extracted sample, pH was measured using an HQD pH electrode (Hach, Loveland, USA), after which samples were analysed for concentrations of NO_3^- and NH_4^+ using an auto-analyser (described above) and concentrations of Al, Ca, Cl, Fe, K, Mg, Mn, Na, P, S, Si and Zn using an ICP-OES (described above). Concentrations of dissolved organic carbon (DOC) were measured on a TOC-L CPH/CPN analyser (Shimadzu, Kyoto, Japan) after acidification with HCl (2 M,0.15 mL per 10 mL) to remove dissolved inorganic carbon. Bioavailable phosphorus (P) (Olsen-P extraction; Olsen et al., 1954) was determined by shaking 3 g of dried soil in 60 ml 0.5 M sodium carbonate ($NaHCO_3$) for 30 min (at 105 rpm on an orbital shaker). Bio-available NH_4^+ and NO_3^- were determined by shaking 17.5 g of fresh soil in 50 ml of 0.2 M sodium chloride (NaCl) for 120 min (at 105 rpm on an orbital shaker). Next, the supernatant was collected under vacuum conditions with Teflon porewater samplers, after which NH_4^+ and NO_3^- were determined using an auto-analyser (described above).

4.2.5 Groundwater level and soil moisture

Volumetric water content (VWC) was measured in 2023 in the top 10 cm of the soil, using time domain transmission. In each field, two sensors (TMS-4, TOMST s.r.o., Czech Republic) were inserted vertically into the soil at the start of the experiment to a depth of 12 cm. A calibration curve was created by incubating undisturbed cores in the lab and recording the gravimetric moisture content over a twelve-week drying campaign. The GWL was monitored at four points in each field, and logged every hour (ElliTrack, Leiderdorp Instruments, The Netherlands). The daily averages for each field were used for the analyses in this paper.

4.2.6 Data analysis

All data analyses were performed using the R software (v4.3.1; R Core Team, 2023). The soil characteristics of the two fields before treatment application were compared using Welch's independent *t*-tests. Cumulative emissions were calculated per treatment campaign separately, using the *agg.fluxes* function in the 'gasfluxes' package in R

(Fuss, 2023). This function uses linear interpolation between data points, to calculate the area under the curve for emissions over time. Cumulative emissions were calculated over measurement periods of approximately 125 days. The effects of the treatment applications on the flux rates were tested for each individual measurement day, using an analysis of variance (*anova* function in R), after checking the distribution of the data points and residuals for normality and homogeneity. By day 125, no effects of the treatments remained ($p > 0.05$).

The emission factor (EF) of the treated objects was calculated as:

$$EF = (N_2O\text{-}N_{treatment} - N_2O\text{-}N_{control})/N_{applied} \quad (1)$$

Where $N_2O\text{-}N_{treatment}$ and $N_2O\text{-}N_{control}$ are the cumulative emissions from the treated and the control treatment within the same block (kg N ha^{-1}) and $N_{applied}$ is the amount of N applied to the treated object as urine and/or dung (kg N ha^{-1}).

The effects of treatment factors (urine, dung and trampling, each with two levels) and drainage type on cumulative N_2O emissions in the two autumn campaigns were tested using a linear mixed effects model using restricted maximum likelihood (*lme* function in the 'nlme' package), with the random factors block nested within main plot, nested within year (N_2O ~ urine * dung * trampling * drainage + (1| year/main plot/block)). When the datapoints and residuals showed a skewed distribution, the response variable was transformed using a Yeo-Johnson transformation, which, similarly to the Box-Cox method, estimates the most suitable transformation to achieve a normal distribution of the response variable and has the additional advantage of accepting negative values (Yeo & Johnson, 2000). The cumulative emissions from the summer campaign were tested in a linear mixed effects model with fixed factors urine, dung and trampling (no replicates exist for the factor drainage type) and random factors block nested within main plot (N_2O ~ urine * dung * trampling + (1| main plot/block)).

Treatment and WIS effects on autumn campaign EFs were analysed in a linear mixed effects with the treatment application variable (with the six levels in which N was applied) and drainage type as fixed factors and block, nested within main plot, nested within year as random factors (EF ~ treatment * drainage + (1| year/ main plot/block)). Pairwise comparisons for all combinations of the fixed factors in the above models for cumulative N_2O or EF were performed using the Tukey method for multiple comparisons.

A linear mixed effects model was used to explore the effects of NO_2^-, NO_3^- or NH_4^+ concentration in pore water (measured in 2022) or pH, NO_3^-, NH_4^+, DOC, or gravimetric water content in (water extracts from) soil samples (measured in 2023) as well as GWL, temperature, precipitation, volumetric water content (in 2023, from sensor measurements) and the day since treatment application on N_2O emission rates. The precipitation on the day of the flux measurement was considered as a variable as well as the two days prior to measuring. Collinearity between the covariables was checked based on correlation coefficients and variance inflation factors (VIF). Parameters with a VIF > 3 were not included in the initial model and the final model was reached by dropping variables if they were not significant. Soil samples in 2023 were taken from two depths; for each concentration variable, the depth with the highest correlation coefficient with N_2O was used. Data of the two autumn campaigns and two fields were analysed in four separate models. The random effects were structured as subplot nested within block (random = 1|block/subplot) to account for repeated measurements within the same subplots.

Additionally, the relationship between N_2O emission rate and GWL was explored. After checking for a linear relationship, a generalized additive mixed model was fitted to the data points, using the 'mgcv' package in R, to visually explore the pattern of the relationship. A constant was added to the dependent variable (N_2O flux) to make all values positive, GWL and treatment were added as fixed effects, and date and plot as random effects.

Effects were considered significant for p-values < 0.05.

4.3. Results

4.3.1 GWL depth and soil properties

During the summer of 2022, the mean GWL depth was over 40 cm lower in the CDD field than the WIS field, indicating successful infiltration by the WIS (Fig. 4.2, Table S4.2). During the summer of 2023, a similar WIS effect was found, although this was less strong with on average a 15.5 cm higher GWL on the WIS field than the CDD field (Fig. 4.3, Table S4.2). During the two autumn seasons, the mean groundwater levels were 15.8 and 5.6 cm higher on the WIS field than the CDD field. The winter and spring periods showed smaller differences in GWL depth, with slightly higher levels in the WIS field (Table S4.2). At the start of the 2022 autumn campaign, the soil in the WIS field showed higher moisture content than the CDD field (t-test, $p < 0.05$, Table 4.1). Bulk density, SOM content, pH,

NO_3^- and NH_4^+ concentrations at 0-15 cm depth differed slightly but not significantly ($p > 0.05$, Table 4.1). Similarly, the moisture and SOM contents at 0-10 and 10-20 cm were higher in the WIS field before treatment application in 2023 (Table 4.2). Ammonium content was significantly higher at 0-10 cm in the CDD field than the WIS field (Table 4.2). There were no significant differences between the two fields in bulk density, pH, and concentrations of NO_3^-, DOC and dissolved N (Table 4.2).

4.3.2 N_2O emissions

Cumulative N_2O emissions from all treatments measured in the 2022 summer campaign ranged between 3 and 25 kg N ha^{-1} over 125 days (Fig. 4.4). In the two autumn campaigns, cumulative N_2O emissions ranged between 0 and 55 kg N ha^{-1} over 125 days (Fig. 4.4). Overall, the cumulative emissions were highest in the autumn of 2022, while they were 20% and 64% lower in the summer 2022 and autumn 2023 experiments, respectively (Fig. 4.4).

There was a significant interaction effect of urine and drainage on cumulative N_2O emissions in the autumn ($F = 13.4$, $p < 0.001$). Urine ($F = 109.6$, $p < 0.001$), dung ($F = 6.0$, $p = 0.02$) and trampling ($F = 7.1$, $p = 0.01$) applications significantly increased cumulative N_2O emissions in both autumn campaigns. The emissions of N_2O were on average higher under CDD than WIS (11.7 ± 8.8 versus 9.1 ± 9.3), but this difference was not significant ($F = 0.9$, $p = 0.52$). The significant interaction between urine and drainage indicates that the difference between WIS and CDD is larger in the absence than in the presence of urine application. High cumulative N_2O emissions were observed in particular in the urine treatments: U, UT, UD and UDT on the WIS field showed significantly higher cumulative N_2O than the WIS C, T and D treatments (Fig. 4.4a). No significant pair-wise differences existed between WIS and CDD objects. In the summer campaign, the application of urine had a significant positive effect on cumulative N_2O ($F = 9.9$, $p = 0.003$). This was not reflected in significant pairwise differences between treatment means (Fig. 4.4b).

In the generalized additive mixed model, GWL explained only 6% of the variation in the N_2O emission rates ($R^2 = 0.061$, Fig. 4.8). This indicates that the GWL and grazing treatment alone did not suffice to predict N_2O emissions in this experiment. Peaks in N_2O emissions occurred mostly under groundwater levels between -5 and -50 cm.

4.3.3 Effects of soil and environmental parameters autumn 2022

Concentrations of NO_3^- on the CDD field exceeded those in the WIS field for the C, D and U treatments (Fig. 4.2b). Mean NH_4^+ concentrations in U plots on the CDD field exceeded concentrations in all other plots, although they also showed high variation between replicates and over time (Fig. 4.2c). Emissions of N_2O were usually highest on the CDD field, except on 09-11-2022, where N_2O peaked in the WIS urine plots, following a rise in GWL (Fig. 4.2a, 2d). Between 07-10-2022 and 30-11-2022, N_2O emissions on the WIS field correlated positively with the NO_3^- (t = 4.1, p < 0.001) and NH_4^+ (t = 2.9, p = 0.005) concentrations in porewater samples from 15-20 cm depth and precipitation (t = 2.1, p = 0.044) (Fig. 4.5, Table S4.3). None of the variables included in the initial model for N_2O emissions from the CDD field (NO_2^-, NO_3^- and NH_4^+ concentrations at 15-20 cm, precipitation, GWL and the day since treatment application) had a significant effect in autumn 2022. Concentrations of other components from the urine solution (Ca, Cl, K, Mg) increased shortly after treatment application in the U plots (Fig. S4.1). Iron (Fe) and manganese (Mn) concentrations at 15-20 cm depth were generally higher in the WIS field than the CDD field (Fig. S4.1).

4.3.4 Effects of soil and environmental parameters autumn 2023

Seven days after treatment application on 28-09-2023, the soil NH_4^+ concentration peaked in the urine plots, followed by an increase in the NO_3^- concentration in subsequent weeks (Fig. 4.3c, 3b). A peak in N_2O emissions from the urine treated plots appeared as NO_3^- concentrations in the soil decreased again (Fig. 4.3a). Between 28-09-2023 and 01-11-2023, soil NH_4^+ concentrations at 10-20 cm depth were positively correlated with N_2O emissions from the CDD field (t = 3.2, p = 0.002, Fig. 4.6, Table S4.3). The N_2O emissions from the WIS field were positively correlated with soil NH_4^+ (t = 3.3, p = 0.002) and negatively with DOC (t = -4.2, p < 0.001) concentrations at 0-10 cm depth. Emissions decreased with increasing VWC (t = -2.1, p = 0.04) and increased with temperature (t = 2.4, p = 0.02, Fig. 4.7, Table S4.3). The components of the urine application (N, Ca, Cl, K, and Mg) were detected at higher concentrations at 0-10 cm depth than in the 10-20 cm layer (Fig. S4.2, Fig. S4.3), indicating limited downwards leaching of the urine solution.

4.3.5 Emission factors

Mean summer emission factors ranged between 0.7 and 1.2% on the WIS field and were often slightly negative on the CDD field (-1.0 to 0.6%, Table 4.3). Mean autumn emission factors on the WIS field ranged between 1.2 and 3.8%, generally exceeding those on the CDD field (-0.1 to 1.6%) (Table 4.3). There was no significant interaction effect of treatment and drainage on emission factors (F = 0.9, p = 0.47). The treatment main effect was significant (F = 4.5, p = 0.002), but not the drainage effect (F = 3.1, p = 0.33). On both fields, the emission factors were highest in the UT plots and a significant pairwise difference was observed between the WIS UT and D plots (Table 4.3).

On 22 of the 120 subplots, a negative EF was observed, mostly occurring on the CDD field in the summer or autumn of 2022 (Table 4.3). This was the result of high emissions on the CDD control plots in 2022, which often exceeded the treatment emissions (Fig. 4.4).

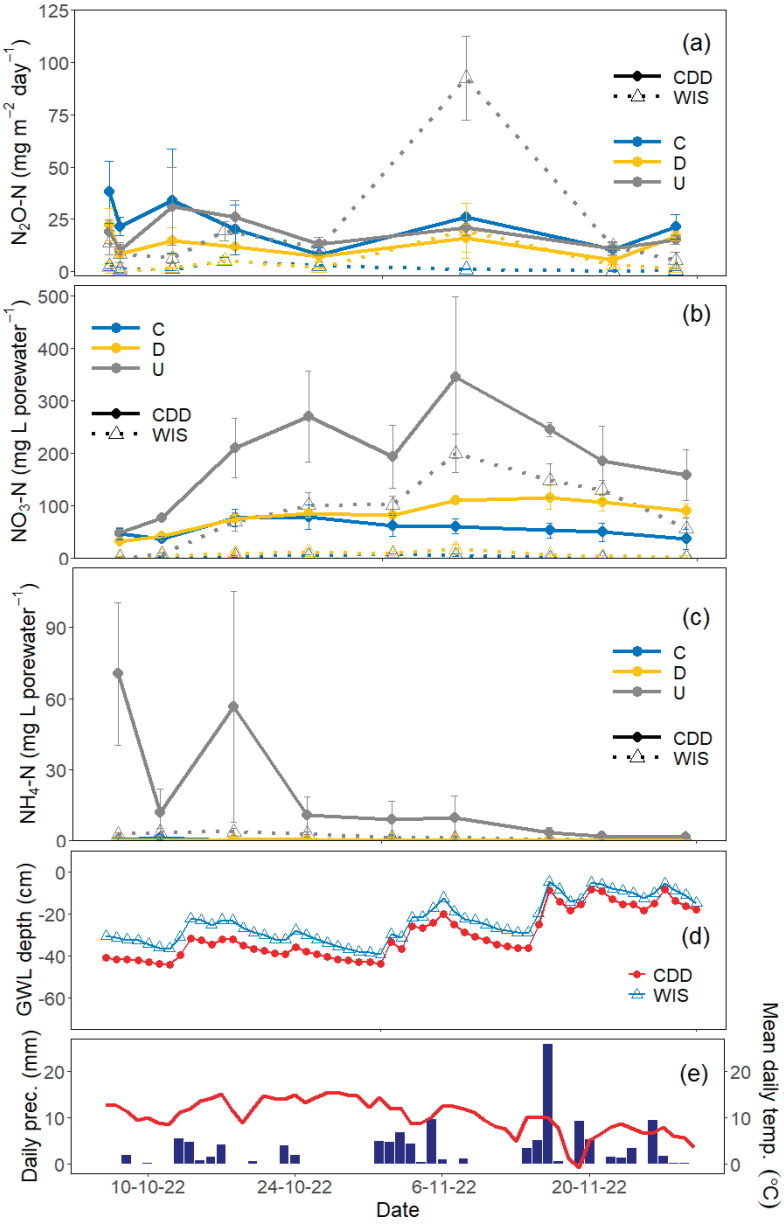


***Figure 4.2**: Soil and weather observations after treatment application on 05-10-2022. N2O emissions from 06-10-2022 till 29-11-2022 (a) and concentrations of NO3- (b) and NH4+ (c) expressed per volume of pore water extracted at 15-20 cm depth between 07-10-2022 and 30-11-2022, together with groundwater level depth (d), mean daily temperature (red line) and total daily precipitation (blue bars) (e).*

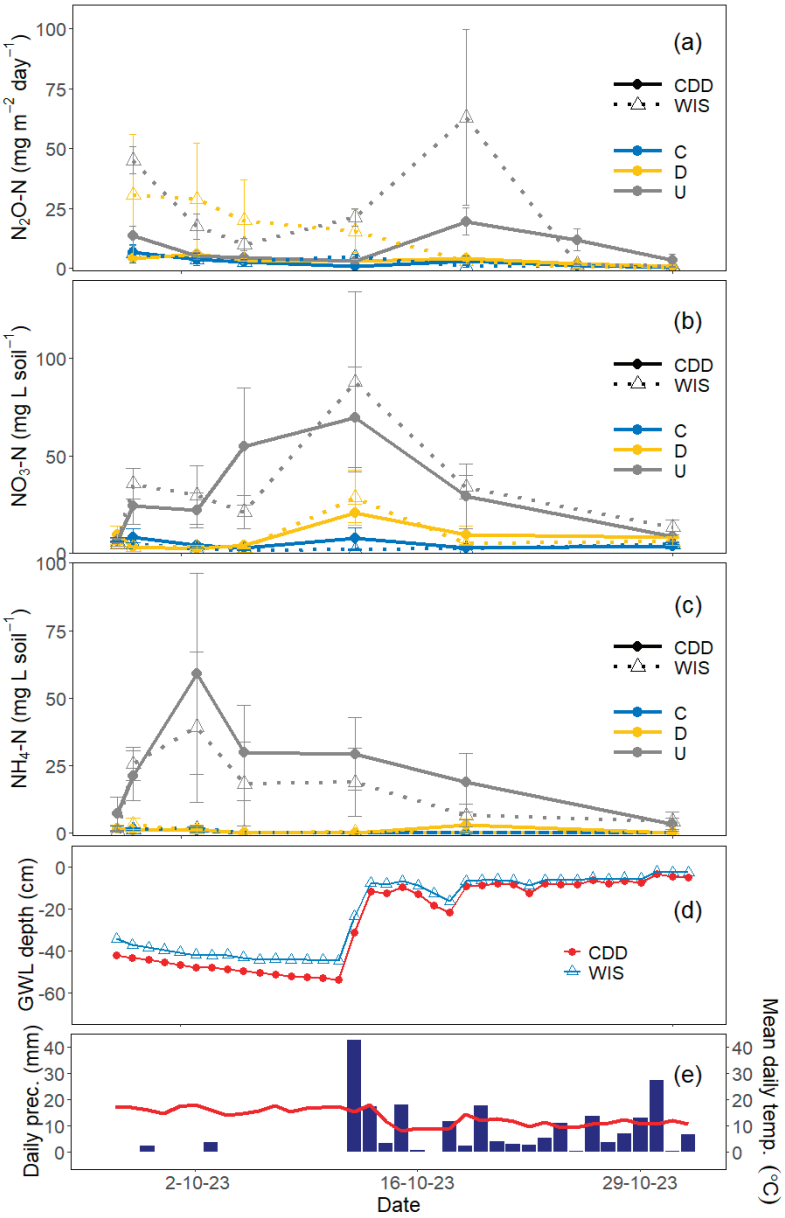


***Figure 4.3**: Soil and weather observations after treatment application on 28-09-2023. N_2O emissions from 28-09-2023 till 01-11-2023 (a) and concentrations of NO_3^- (b) and NH_4^+ (c) expressed per volume of soil, sampled at 0-10 cm depth between 27-09-2023 and 01-11-2023, together with groundwater level depth (d), mean daily temperature (red line) and total daily precipitation (blue bars) (e).*

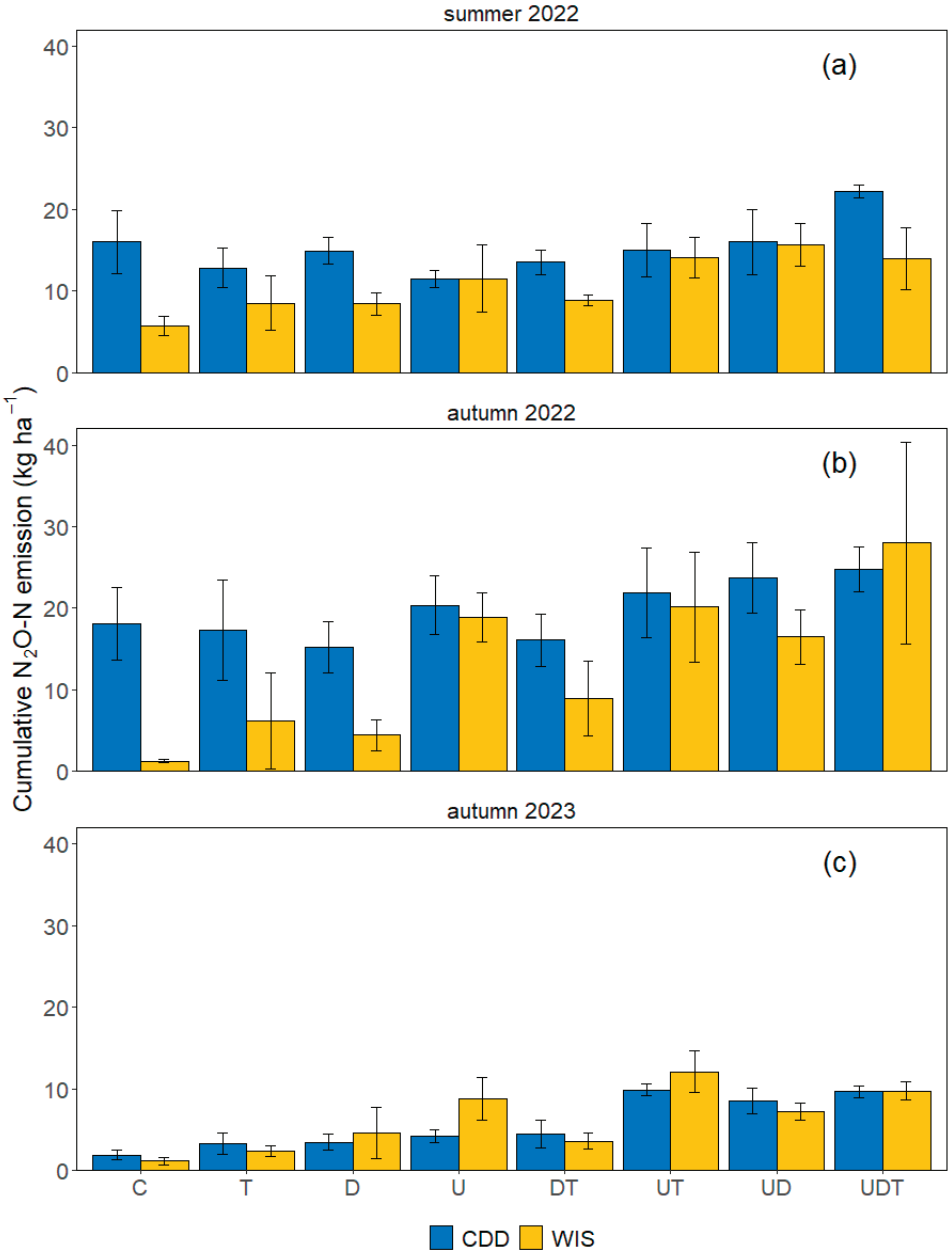


***Figure 4.4**: Mean cumulative N_2O emissions and standard errors over a 125-day period in summer 2022 (a), autumn 2022, or autumn 2023 (c).*

***Table 4.3**: Mean N_2O emission factors and standard errors calculated over the 125 day autumn-winter periods of 2022 and 2023. Superscript letters in the last column report the results of the linear mixed effects model for EF on both fields together (EF = treatment * drainage + (1| year/main plot/block)): objects sharing the same letter (a, b) were not shown to differ significantly ($p < 0.05$).*

Field	Treatment	Summer 2022 EF (%) ± SE (*n* = 3)	Autumn 2022 EF (%) ± SE (*n* = 3)	Autumn 2023 EF (%) ± SE (*n* = 4)	Autumns 2022-2023 average EF (%) ± SE (*n* = 7)
CDD	D	-0.42 ± 1.42	-1.0 ± 0.58	0.60 ± 0.50	-0.09 ± 0.47^{ab}
	DT	-0.95 ± 1.11	-0.71 ± 1.43	0.96 ± 0.52	0.25 ± 0.70^{ab}
	U	-0.54 ± 0.34	0.59 ± 1.29	0.62 ± 0.23	0.60 ± 0.50^{ab}
	UT	-0.12 ± 0.26	0.99 ± 2.37	2.10 ± 0.13	1.63 ± 0.93^{ab}
	UD	-0.001 ± 0.19	0.84 ± 0.99	1.03 ± 0.17	0.95 ± 0.39^{ab}
	UDT	0.56 ± 0.31	0.99 ± 0.88	1.20 ± 0.21	1.11 ± 0.35^{ab}
WIS	D	1.02 ± 0.17	1.09 ± 0.61	1.28 ± 1.08	1.20 ± 0.63^{a}
	DT	1.18 ± 0.71	2.63 ± 1.55	0.90 ± 0.49	1.64± 0.73^{ab}
	U	0.69 ± 0.44	4.65 ± 0.79	2.00 ± 0.80	3.14 ± 0.75^{ab}
	UT	0.99 ± 0.17	4.98 ± 1.82	2.88 ± 0.77	3.78 ± 0.91^{b}
	UD	0.89 ± 0.20	2.28 ± 0.48	0.93 ± 0.23	1.51 ± 0.35^{ab}
	UDT	0.74 ± 0.45	4.00 ± 1.84	1.33 ± 0.24	2.47 ± 0.89^{ab}

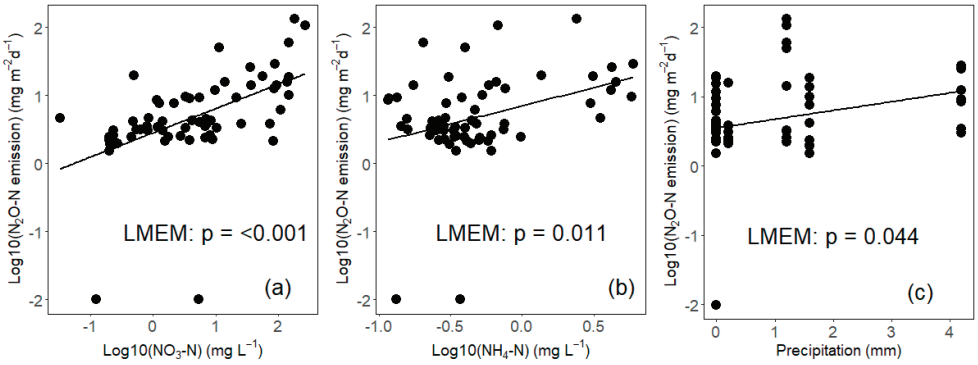


***Figure 4.5**: Responses of N_2O emissions on the WIS field to pore water NO_3^- (a) and NH_4^+ (b) concentrations at 15-20 cm depth, and precipitation (c) during the period 06-10-2022 to 29-11-2022. NO_3-N and NH_4-N concentrations were determined in pore water extracts and expressed per volume of pore water. Precipitation values represented the sum of precipitation on the measurement day. The black lines show a linear regression fit of log10(N_2O-N) against the explanatory x-axis variable. The p-values are given of the effects determined in the linear mixed effects model (LMEM).*

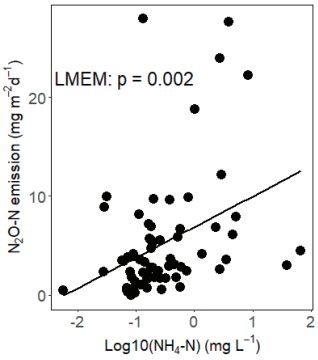


***Figure 4.6**: Response of N_2O emissions on the CDD field to soil NH_4^+ concentrations (in water-extracts) at 10-20 cm depth during the period 27-09-2023 to 01-11-2023. NH_4-N concentrations were determined in soil water extracts and expressed per volume of soil. The black line shows a linear* regression fit of *N_2O-N against log10(NH_4-N). The p-value is given of the effect determined in the linear mixed effects model (LMEM).*

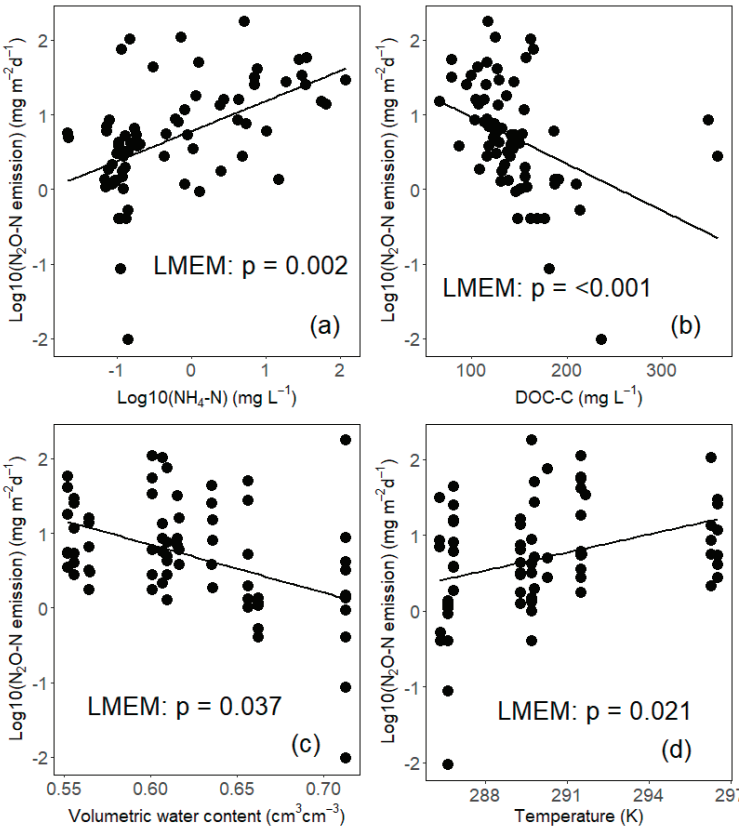


***Figure 4.7**: Responses of N_2O emissions on the WIS field to soil log10(NH_4-N) (a) and DOC-C (b) concentrations at 0-10 cm depth, volumetric water content (c) and ambient temperature (d) during the period 27-09-2023 to 01-11-2023. NH_4-N and DOC-C concentrations were determined in soil water extracts and expressed per volume of soil. The volumetric water content was measured every 10 minutes at 0-12 cm depth and temperature every hour at a height of approximately 2 m. The black lines show a linear regression fit of log10(N_2O-N) against the explanatory x-axis variable. The p-values are given of the effects determined in the LMEM model (LMEM).*

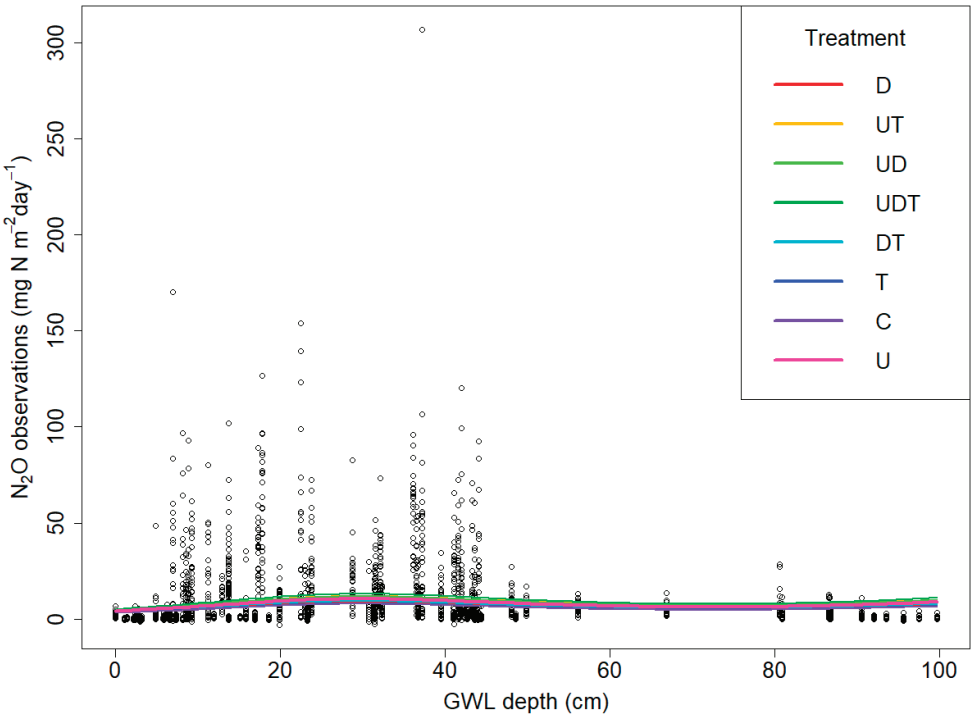


***Figure 4.8**: N_2O emission rates plotted against the groundwater level depth (positive numbers indicate depth of the GWL below the soil) and the generalized additive mixed model regression lines for each of the grazing treatment levels.*

4.4. Discussion

4.4.1 Water infiltration system effects on N_2O emissions

Water infiltration systems were hypothesized to reduce N_2O emissions by reducing N mineralization of organic N in the peat material, and potential subsequent nitrification and denitrification. Indeed, mean cumulative N_2O emissions were higher on the unfertilized (C and T) plots of the CDD field than the WIS field (Fig. 4.4). The drainage effect was not significant, however, and the null hypothesis of equal emissions under both drainage treatment levels can't be rejected.

In other studies, long term drainage was shown to increase N_2O emissions from minerotrophic peat soils, compared to undrained peat soils (Martikainen et al., 1993; Regina et al., 1996). Rewetting of previously drained peat soils has similarly led to a decrease in N_2O emissions (Minkkinen et al., 2020). At other times, drainage effects were obscured by generally low fluxes due to drought (Berendt et al., 2023), or low soil and fertilizer N-availability (Wilson et al., 2016b). On the other hand, N_2O production is often enhanced by variable soil moisture conditions over time (Anthony & Silver, 2024; Blondeau et al., 2024; Pärn et al., 2018) and can occur more frequently in formerly drained and rewetted than undrained peatlands (Kreyling et al., 2021). Particularly precipitation (Berendt et al., 2023; Velthof et al., 1996) or flooding events (Anthony & Silver, 2021; Goldberg et al., 2010) have frequently been identified as drivers of N_2O peaks in peat soils, with denitrification as the main N_2O producing process (Anthony & Silver, 2021).

Continued flooding or permanent inundation on the other hand, may decrease N_2O emission, since mineralization and nitrification are hampered under permanently anaerobic conditions, thereby depleting the NO_3^- supply for denitrification and stimulating the full reduction of N_2O to N_2 in complete denitrification (Butterbach-Bahl et al., 2013). By reducing the fluctuation in GWL and redox potential, WIS may help to limit NO_3^- formation and reduction (Boonman et al., 2024; Harpenslager et al., 2024). While peat mineralization may be particularly pronounced in the summer, the subsequent effects on N_2O emissions could continue throughout the autumn season, where precipitation stimulates denitrification. This is reflected in higher ammonium and nitrate concentrations in the top soil under CDD than WIS at the start of the 2022 and 2023 autumn campaigns (Table 4.1, Table 4.2), which likely results from higher peat mineralization and in turn affects N_2O emissions during the following period. Additionally, porewater and soil ammonium concentrations continued to be higher under CDD than WIS throughout

the sampling periods in (Fig. 4.2, Fig. 4.3). Mean cumulative N_2O emissions in the summer (13.1 ± 5.4 kg N ha^{-1}) and autumn (16.4 ± 10.4 kg N ha^{-1}) of 2022 far exceeded those in the autumn of 2023 (5.9 ± 4.3 kg N ha^{-1}, Fig. 4.4). Meteorological variability can strongly increase variability in N_2O emissions between different measurement years (Fig. 4.4), emphasizing the importance of multi-year experiments in order to get a robust estimate of drainage treatment effects. High N_2O emissions on the CCD control plots in 2022 may have been due to high mineralization under the dry conditions of that year. Overall, 2023 was a much wetter year than 2022. During the autumn of 2023, 200 mm more precipitation was recorded than in the autumn of 2022, and it was preceded by 88 mm more summer rainfall (Table S4.2). In autumn 2022, mean cumulative N_2O emissions from the unfertilized C and T plots on the CDD field far exceeded those of the WIS field (14 and 2.8 times higher, respectively), while differences were smaller in 2023 (1.6 and 1.4 times higher, respectively). These emission differences coincided with a substantially deeper mean summer and autumn GWL in 2022 (Table S4.2). High mineralization-related N_2O emissions in the control plots on the CDD field also occurred during the summer campaign, seemingly overshadowing effects of nitrogen application on emissions and emission factors (Fig. 4.4, Table 4.3).

The linear mixed effects models which described the effects of multiple soil and meteorological variables during the first few weeks after treatment application, indicated no significant linear relationship between GWL and the N_2O emissions (Table S4.3). Given the GWL variability within both fields, we proceeded to explore the N_2O-GWL relationship for both fields together in a generalized additive mixed model (Fig. 4.8). While the non-linear model, containing the GWL and treatment variables, did not perform well at explaining variability, Fig. 4.8 demonstrates that high N_2O emissions occurred mainly within a GWL range between approximately 5 and 50 cm below the surface. This resembles relationships with the mean annual GWL from other studies (Eickenscheidt et al., 2014; Leppelt et al., 2014). There is indication for a parabolic relationship of N_2O production with the soil WFPS, which typically shows an optimum around 60% WFPS (Davidson et al., 2000) although for peat soils the optimum is frequently found above 80% (Saurich et al., 2019a; Van Lent et al., 2019). The relationship between GWL and N_2O flux, which is the net outcome of production and consumption during upwards transport through the soil profile, is not as well understood, and may depend on many other variables that affect microbial N transformation in soil, such as

temperature, rainfall, pH (Weslien et al., 2009) and C:N ratio (Klemedtsson et al., 2005; Minkkinen et al., 2020).

4.4.2 Grazing effects on N_2O and interaction with WIS

Although WIS was expected to reduce N_2O emissions resulting from peat oxidation, the second hypothesis stated that urine and dung application enhance N_2O emissions and that WIS fields show higher N_2O emissions than CDD fields under N application through dung or urine, because mineral N input and anaerobic conditions together form a strong stimulation of denitrification. Indeed, there was a significant interaction effect between urine application and drainage treatment during the autumn experiments. While average cumulative emissions were 5.1 kg N ha^{-1} lower under WIS than CDD in the absence of urine (3.9 versus 9.0 kg N ha^{-1}), there was no difference between the drainage types under urine application (both 14.3 kg N ha^{-1}, Fig. 4.4). This suggests that the input of urine-N has more impact on N_2O emissions from a field with WIS than with CDD. This effect is also apparent from the significant pair-wise differences that were observed between objects with and without urine application under WIS, but not under CDD (Fig. 4.4).

Increased N_2O emissions under urine application and WIS were likely the result of incomplete denitrification. The pore water concentration of NO_3^- at 15-20 cm depth correlated positively with log-transformed N_2O emission rates on the WIS field in autumn 2022 (Fig. 4.5, Table S4.3). Figure 2 shows that particularly in the urine plots the N_2O and NO_3^- peaks coincide. In the soil samples from 0-10 depth in 2023 (Fig. 4.3) even a clear sequence could be distinguished of an initial peak in NH_4^+ due to hydrolysis of urea, followed by a rise in NO_3^- due to nitrification and a peak in N_2O emission, likely resulting from denitrification, given the shallow GWL depth at that point. Dung application also significantly increased cumulative N_2O emissions during the autumn campaigns, but there was no interaction with drainage: dung application did not change the relationship between drainage and N_2O. While the application of urine decreased the observed difference between CDD and WIS emissions, this difference (CDD > WIS) remained under dung application. A possible explanation is that, similarly to soil organic matter, the mineralization of dung organic matter may benefit from aerobic conditions.

Koops et al. (1997a) identified nitrification as the dominant N_2O source, with ammonium and organic nitrogen content as the main explaining factors, after urine application in a field and incubation

experiment at the same experimental farm as this study. Contrastingly, Boon et al. (2014) attributed N_2O emissions from urine excretion on peat grassland to denitrification. In their study, high N_2O emissions similarly coincided with high ammonium concentrations, but these were attributed to accumulation under shallow groundwater levels. The results from the present study indicate significant correlations between N_2O emissions and ammonium concentrations on the WIS field in autumn 2022 (Fig. 4.5b) and autumn 2023 (Fig. 4.7a), and on the CDD field in autumn 2023 (Fig. 4.6), as well as nitrate concentrations on the WIS field in 2022 (Fig. 4.5a). Quantification of microbial functional groups can help to further disentangle the sources and biotic processes involved in N_2O production (Cai et al., 2017). To our knowledge, no studies have quantified microbial activity involved in nitrogen transformations, following the application of urine or dung on peat soils, however. Future studies on grazing effects on peat soils could include measurements of the diverse genes involved in N_2O producing processes.

The significant interaction between urine and drainage treatment supports the second hypothesis that WIS does not have a reducing effect on N_2O emissions from urine application. This effect was not found for dung application.

Trampling was hypothesized to increase N_2O emissions from peat soil, and to enhance the effects of CDD and urine or dung application. In accordance with the hypothesis, trampling significantly increased cumulative N_2O emissions. Similarly, the EF of subplots treated with trampling was always higher than the corresponding subplots (under the same drainage, dung and urine treatment) without trampling application, with the exception of UDT in the summer 2022 campaign (Table 4.3). While these pair-wise differences were not significant, the patterns do correspond with previous observations. Compaction from trampling can increase denitrification-associated N_2O emissions by raising the bulk density and consequently the water filled pore space (Van Groenigen et al., 2005b). It can thus further enhance the effects of N inputs (Bhandral et al., 2007; Van Groenigen et al., 2005a).

4.4.3 N_2O emission factors

A larger part of the applied urine-N and dung-N was lost via N_2O on the WIS field than on the CDD field. While not significant, emission factors were consistently higher on the WIS field than the CDD field (Table 4.3). The drier summer conditions under CDD were hypothesized to lead to higher N_2O emissions due to higher N availability originating from peat

mineralization. N_2O production originating from N applied as urine or dung, on the other hand, was expected to be stronger under WIS, which would result in a higher EF under WIS than under CDD.

Within the Dutch national inventory report for annual greenhouse gas emissions, an aggregated emission factor of 6% is used for N_2O-N emissions for cattle urine and dung together, deposited on organic soils (Van der Zee et al., 2024; Velthof & Mosquera, 2011a), based on field measurements by Velthof et al. (1996) in the same peat area as this experiment. The aggregated mean emission factors over both fields for the UD and UDT treatments were 1.2% and 1.8% in the autumn campaigns and 0.4% and 0.7% in the summer campaign, respectively (Table 4.3). These values are substantially lower than the currently used EF, despite higher N-application rates than Velthof et al. (1996) (670-1160 kg N ha^{-1} versus 450-617 kg N ha^{-1}). This may be explained by several fundamental differences between the two experiments. First, Velthof et al. (1996) estimated the N excretion by the grazing cattle using standard calculation rules, which decreased the accuracy of the emission factor calculation in comparison to an experiment in which urine and dung are applied under controlled conditions. Secondly, in the experiment by Velthof et al. (1996), the grazing treatment involved actual cattle grazing on the plots for a duration of two days, as opposed to artificial urine in this experiment. In a lab experiment, no different N_2O emissions were observed after application of real cattle urine or an artificial urine with identical nitrogenous composition, but dissimilar organic compositions may have been the cause of differences in soil NH_4^+, NO_3^- and pH after application (Kool et al., 2006). Higher organic carbon content of real urine may have led to some N-immobilization after application and thus lower soil NH_4^+ than with artificial urine. This effect may be less relevant in the carbon-rich peat soil on which this experiment and that of Velthof et al. (1996) took place. Lastly, the grazing treatment in Velthof et al. (1996) was applied several times between spring and autumn and the EF was calculated using the annual N_2O-N losses, over a period almost three times longer than in this experiment. The highest N_2O losses occurred in the spring, summer and autumn of their two-year experiment. After treatment application in the autumn, N_2O emission peaks in this experiment had returned to background levels by the end of January or early February and, therefore, seemed to continue for a shorter duration than the emissions in Velthof et al. (1996). Yet autumn urine or dung applications, often associated with lower grass N-uptake, stronger soil compaction and higher WFPS, frequently lead to higher emission factors

than spring or summer applications (De Klein et al., 2006; Krol et al., 2016; Selbie et al., 2015). Similar to Velthof et al. (1996), emissions from the summer application were high, but still lower than the autumn 2022 emissions (Fig. 4.4). Unlike that study, little difference was observed here between grazed objects and the controls, resulting in low summer emission factors. It appears that a high mineralization of organic N caused by the deep GWL and high temperature (Table S4.2) had a stronger effect on N_2O emissions than applied N, despite the higher urine-N application rate in the summer 2022 campaign. Low N_2O losses from the summer urine treatments may have been the result of a relatively high NH_3 volatilization stimulated by the high temperature (Lockyer & Whitehead, 1990). Emission factors for dung were lower than those of urine, which is in accordance with other studies (Chadwick et al., 2018; Krol et al., 2016).

4.4.4 WIS N_2O climate impact

Autumn cumulative N_2O emissions in this experiment ranged between a small uptake of -0.2 and an emission of 55.3 kg ha^{-1}. Using a global warming potential (GWP) of 273 over a 100-year horizon (Forster et al., 2021), these N_2O emissions ranged between -0.1 and 23.7 tonne CO_2-eq ha^{-1}. The autumn control plot emissions were on average 7.6 kg N ha^{-1} lower under WIS than CDD. Similarly, the N_2O EFs defined by the IPCC for drainage of shallow-drained and deep-drained (nutrient-rich, temperate) organic grassland soils are 1.6 and 8.2 kg N_2O-N ha^{-1} yr^{-1}, respectively (Hiraishi et al., 2014). Assuming that the conditions over a whole year are similar to those during the autumn experiments, the potential of WIS to reduce N_2O emissions by 3.3 ton CO_2-eq ha^{-1} (7.6 kg N ha^{-1}) over 125 days would be extrapolated to 9.5 tonne CO_2-eq ha^{-1} yr^{-1}. A reduction of 9.5 tonne CO_2-eq ha^{-1} yr^{-1} under WIS is substantial given the default CO_2 EFs of (13.2 or 22.4 tonne CO_2 ha^{-1} yr^{-1}) for shallow- or deep-drained soils, respectively (Hiraishi et al., 2014). The results, therefore, suggest agreement with the IPCC default EFs, implying that the potential of reducing N_2O emissions through reduced oxidation of organic-N is substantial, and might also be achieved through WIS implementation. However, since the results in this experiment could not confirm a significant effect of WIS, the real potential of this measure should be explored further in future experiments. Additionally, the application of urine patches under grazing, which occurs on most Dutch peat grasslands, appears to undermine the mitigating effect of WIS.

4.5. Conclusion

During two measurement campaigns in the autumn and one in the summer, N_2O emissions from grassland on drained peat soils were lower under WIS than CDD. A significant effect of WIS on N_2O emission was not confirmed, however. Significant, positive effects on cumulative N_2O were observed of urine application in the autumn and summer campaigns as well as dung and trampling application in the autumn campaigns. There was an interaction effect between drainage treatment and urine application, indicating that the mitigating effect of WIS is reduced when urine-N is applied. In addition, N_2O emission factors for urine and dung were usually higher under WIS than under CDD and higher when trampling was applied, suggesting the stimulation of denitrification-derived N_2O emissions through increased WFPS.

Acknowledgements

This project is funded by the Dutch Ministry of Agriculture, Fisheries, Food Security and Nature. The research presented in this paper is part of the project Living on soft soils: subsidence and society (grantnr.: NWA.1160.18.259). This project is funded by the Dutch Research Council (NWO-NWA-ORC), Utrecht University, Wageningen University, Delft University of Technology, Ministry of Infrastructure & Water Management, Ministry of the Interior & Kingdom Relations, Deltares, Wageningen Environmental Research, TNO-Geological Survey of The Netherlands, STOWA, Water Authority: Hoogheemraadschap de Stichtse Rijnlanden, Water Authority: Drents Overijsselse Delta, Province of Utrecht, Province of Zuid-Holland, Municipality of Gouda, Platform Soft Soil, Sweco, Tauw BV, NAM. We would like to thank all researchers, technicians, laboratory staff and field staff who have facilitated or contributed to this project. In particular, we are grateful to Karel van Houwelingen for his contribution to the realization of the experiment.

Chapter 4 Supplementary material

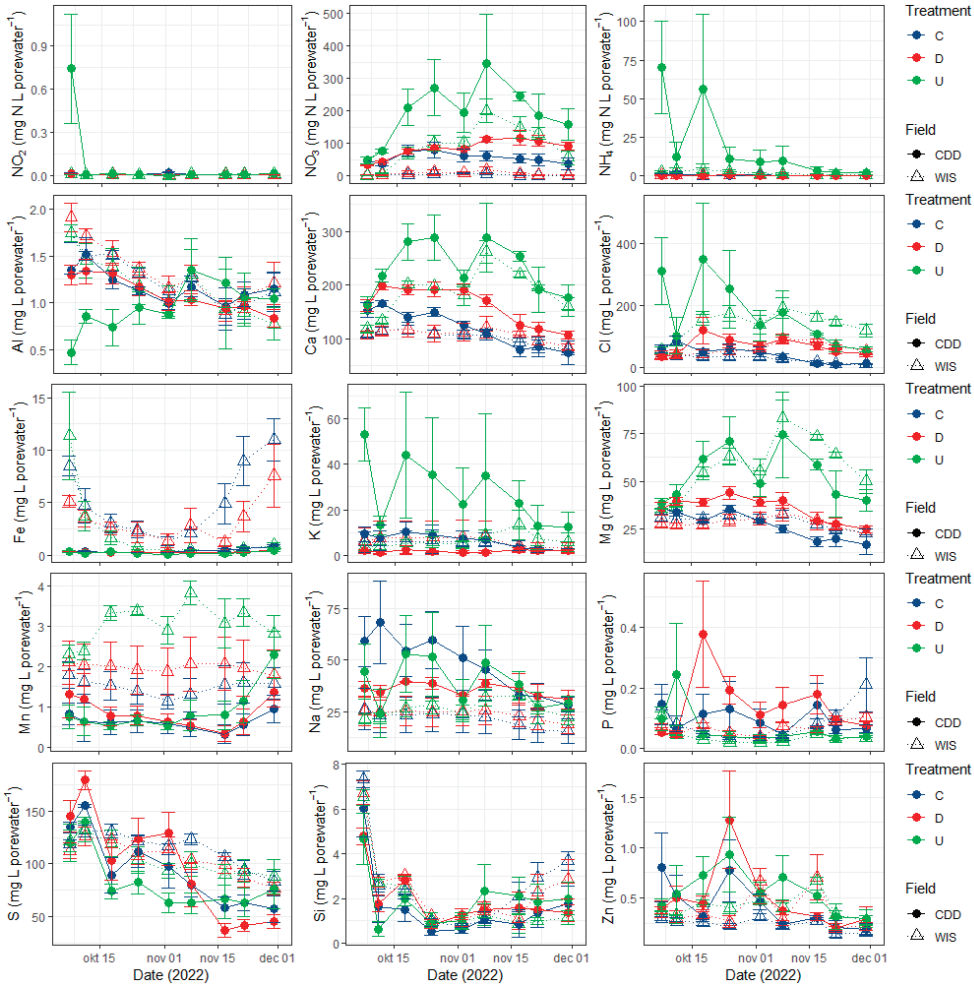


***Figure S4.1**: Concentrations in porewater samples from 15-20 cm depth (expressed per litre of porewater) measured from 07-10-2022 to 30-11-2022. Error bars show the standard errors per field and treatment (n = 3).*

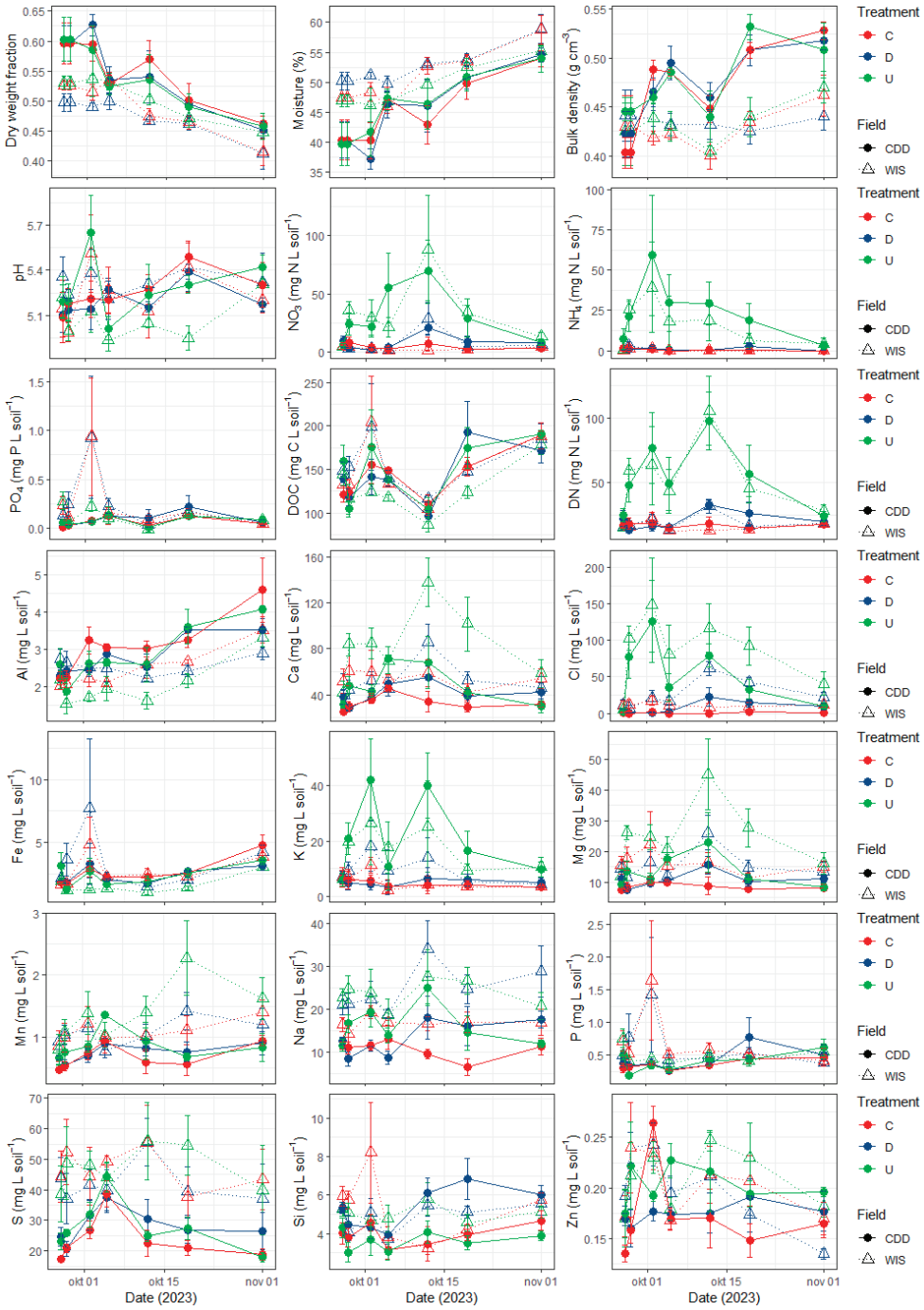


***Figure S4.2**: Water extracted concentrations in soil samples from 0-10 cm depth. Error bars show the standard errors per field and treatment (n = 4).*

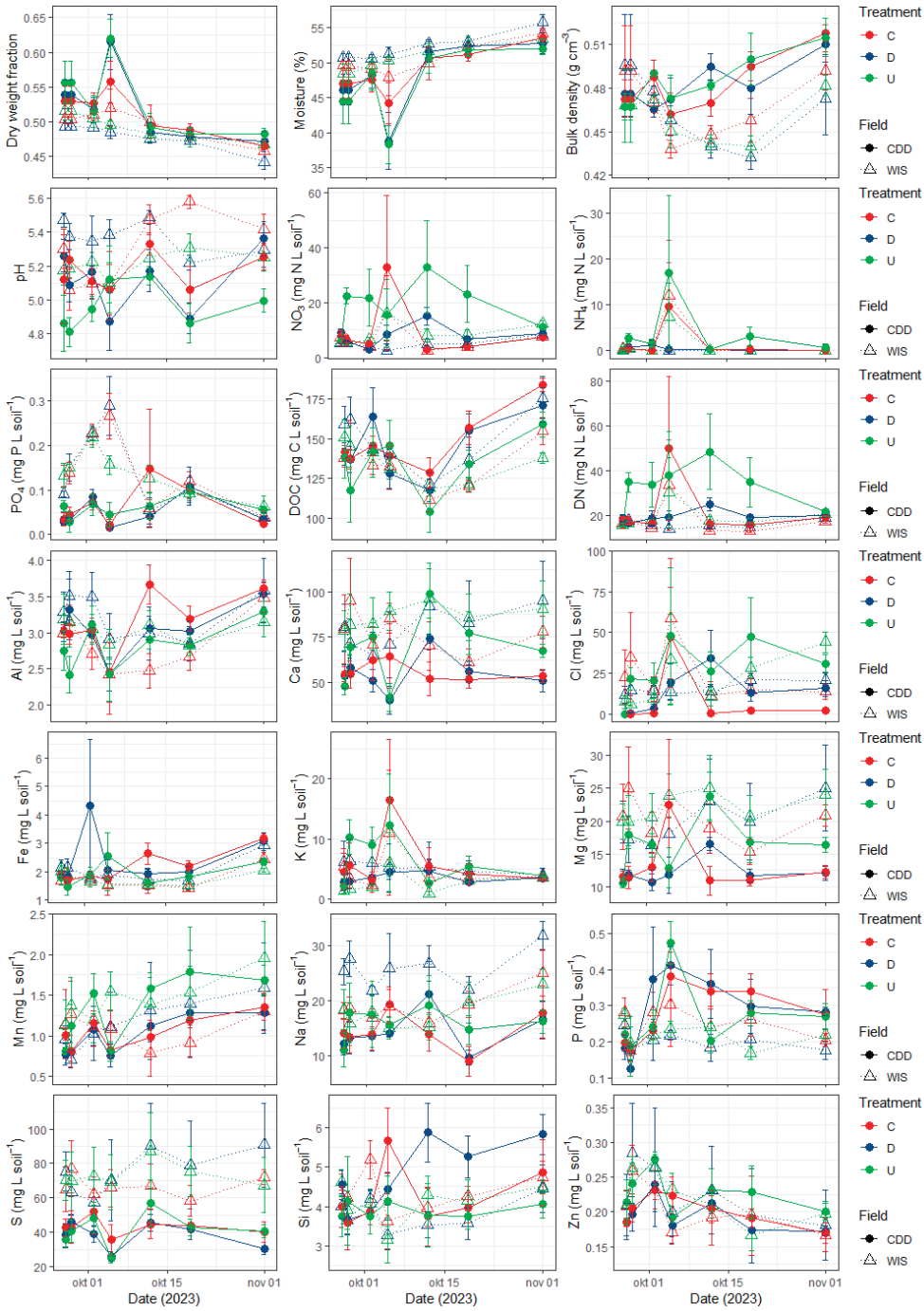


***Figure S4.3**: Water extracted concentrations in soil samples from 10-20 cm depth. Error bars show the standard errors per field and treatment (n = 4).*

***Table S4.1**: Composition of the cattle dung in the two application years. All concentrations are expressed as g kg fresh material^{-1}.*

	Summer 2022	Autumn 2022	Autumn 2023
Dry weight (g kg^{-1})	88	87	108
Ash content (g kg^{-1})	11	9	15
SOM (g kg^{-1})	77	78	93
N-tot. (g kg^{-1})	2.79	3.05	2.8
C/N	12	12	15
N-NH_3 (g kg^{-1})	0.4	0.1	0.1
N-organic (g kg^{-1})	2.4	NA	2.8
P_2O_5 (g kg^{-1})	1.26	1.35	1.49
K_2O (g kg^{-1})	0.7	1	1
MgO (g kg^{-1})	2.2	1.8	1.7
Na_2O (g kg^{-1})	0.6	0.6	0.5

***Table S4.2**: Summary statistics (mean, median, minimum value, maximum value and standard deviation (sd)) of the daily GWL depths measured in summer (June 1st till September 1st), autumn (September 1st till December 1st), winter (December 1st till March 1st) and spring (March 1st till June 1st) in each field. Groundwater table depths were measured at four points per field and summarized as one daily value. The values here summarize daily values and are expressed in cm relative to the soil surface level. Volumetric water content (VWC) data were only available during the autumn of 2023.*

		2022 summer	2022 autumn	2022 winter	2023 spring	2023 summer	2023 autumn	2023 winter
GWL CDD (cm)	mean	-80.4	-42.7	-11.6	-22.1	-63.0	-26.6	-6.8
	sd	12.5	22.9	9.2	16.7	13.8	22.0	4.5
	min	-100.0	-98.4	-31.0	-55.0	-83.6	-64.7	-19.9
	max	-57.0	-8.3	0.0	-3.0	-29.8	-2.4	2.9
	median	-82.1	-38.3	-9.7	-11.4	-64.8	-13.0	-5.7
GWL WIS (cm)	mean	-39.0	-26.9	-10.6	-19.8	-47.5	-21.0	-4.3
	sd	5.5	11.6	9.7	14.3	10.8	18.7	4.9
	min	-49.3	-52.9	-29.8	-44.5	-63.6	-53.2	-23.3
	max	-29.5	-4.9	0.0	-1.3	-14.2	0.2	6.4
	median	-40.2	-28.0	-7.5	-13.2	-48.7	-10.2	-2.8
Daily precipitation (mm)	mean	1.8	2.9	2.6	2.0	2.7	5.1	3.2
	sd	6.8	4.8	4.6	3.7	6.1	7.4	4.1
	min	0.0	0.0	0.0	0.0	0.0	0.0	0.0
	max	44.6	25.8	25.6	16.4	34.4	42.6	16.0
	median	0.0	0.6	0.7	0.0	0.0	2.2	1.0
	sum	162.6	267.4	235.8	188.4	251.0	467.4	291.0
Daily temperature (°C)	mean	18.3	12.0	5.0	9.5	18.0	12.8	6.1
	sd	2.6	4.0	3.9	3.9	2.4	4.9	3.9
	min	12.4	-0.8	-4.2	0.6	12.9	0.1	-3.2

		2022 summer	2022 autumn	2022 winter	2023 spring	2023 summer	2023 autumn	2023 winter
	max	25.8	20.8	13.2	16.6	24.1	23.6	12.6
	median	17.8	12.0	5.6	9.8	17.9	12.6	7.4
VWC CDD (cm^3/cm^3)	mean	-	-	-	-	-	0.62	-
	sd	-	-	-	-	-	0.07	-
	min	-	-	-	-	-	0.37	-
	max	-	-	-	-	-	0.70	-
	median	-	-	-	-	-	0.62	-
VWC WIS (cm^3/cm^3)	mean	-	-	-	-	-	0.67	-
	sd	-	-	-	-	-	0.05	-
	min	-	-	-	-	-	0.52	-
	max	-	-	-	-	-	0.71	-
	median	-	-	-	-	-	0.67	-

***Table S4.3**: Outputs of the best fit linear mixed effects models to describe environmental and soil parameter correlations with N_2O emissions during the periods 07-10-2022 to 30-11-2022 and 28-09-2023 to 01-11-2023. The fixed effects estimates are provided, along with their standard errors, the degrees of freedom (df), the t-statistic and its p-value, and the variances of the random effects and residual variance.*

Factor	Estimate	St. error	df	*t*-value	*p*-value	Variance
2022 CDD (log-N_2O)						
Block						0.00
Subplot						0.02
Residual						0.07
2022 WIS (log-N_2O)						
Log-NO_3[a]	0.29	0.07	51	4.09	<0.001 *	
Log-NH_4[a]	0.46	0.16	51	2.94	0.005*	
Precipitation	0.10	0.087	51	2.06	0.044*	
Block						0.01
Subplot						0.00
Residual						0.27
2023 CDD (N_2O)						
Log-NH_4[b]	3.04	0.94	58	3.22	0.002*	
Block						0.00
Subplot						1.0
Residual						30.7
2023 WIS (log-N_2O)						
Log-NH_4[c]	0.26	0.077	55	3.3	0.002*	
DOC-C[c]	-0.01	0.001	55	-4.2	<0.001 *	
VWC	-2.91	1.36	55	-2.1	0.04*	
Temperature	0.05	0.022	55	2.4	0.02*	
Block						0.00
Subplot						0.07
Residual						0.22

[a] Parameter measured in soil porewater, extracted at 15-20 cm depth.
[b] Parameter measured in (water extracted) soil sample, cored at 10-20 cm depth.
[c] Parameter measured in (water extracted) soil sample, cored at 0-10 cm depth.
* *P*-values fall within the 5% significance interval.

***Table S4.4**: Extended table of the soil characteristics measured at 0-15 cm depth in the control plots on 07-10-2022, two days after the 2022 treatment applications. Samples were taken in 50x50 cm squares in the C subplots from a depth of 0-15 cm and averaged per field (n = 3). The fresh weight density was determined as the mass of fresh soil per litre. Moisture content, dry bulk density and soil organic matter (SOM) content were determined after drying at 105°C. Soil pH and bioavailable NO_3^- and NH_4^+ were determined in NaCl extracts. Bioavailable P was determined using the Olsen method. Further element concentrations show the total concentrations, derived using digestions.*

Parameter	CDD field	WIS field
Fresh weight density (g l^{-1})	738.4 ± 15*	863.5 ± 25
Moisture (% of fresh weight)	39.0 ± 2.1*	48.0 ± 2.0
Dry bulk density (g cm^{-3})	0.46 ± 0.01	0.44 ± 0.006
SOM (% of dry weight)	47.9 ± 0.24	50.7 ± 1.3
pH	4.5 ± 0.062	4.7 ± 0.06
NO_3-N (mg l^{-1})	27.7 ± 5.4	12.3 ± 3.0
NH_4-N (mg l^{-1})	7.70 ± 1.2	3.194 ± 0.087
P-Olsen (mg l^{-1})	39.5 ± 2.0	46.0 ± 1.9
Al (g l^{-1})	10.5 ± 0.23	9.69 ± 0.45
Ca(g l^{-1})	4.18 ± 0.084*	4.53 ± 0.049
Cl(g l^{-1})	0.57 ± 0.062	0.18 ± 0.12
Fe (g l^{-1})	8.68 ± 0.26	8.06 ± 0.30
K (g l^{-1})	1.12 ± 0.095	0.844 ± 0.053
Mg (g l^{-1})	1.36 ± 0.041	1.38 ± 0.045
Mn (g l^{-1})	0.15 ± 0.0083	0.17 ± 0.0098
Na (mg l^{-1})	89.3 ± 12.9	39.4 ± 19.9
P (g l^{-1})	0.937 ± 0.080	0.984 ± 0.037
S (g l^{-1})	2.31 ± 0.070	2.44 ± 0.049
Si (mg l^{-1})	100 ± 9.1	91.1 ± 12
Zn (mg l^{-1})	52.8 ± 1.6	60.1 ± 2.4

* Mean values of the two fields differ significantly ($p < 0.05$).

***Table S4.5**: Extended table of the soil characteristics measured before the 2023 treatment applications in the control, urine and dung subplots, averaged per field and depth (n = 12). Soil characteristics measured at 0-10 and 10-20 cm depth on 27-09-2023, one day before the 2023 treatment applications. Samples were taken in 50x50 cm squares in the C, U and D subplots and averaged per field and depth (n = 12). Moisture content, dry bulk density and soil organic matter (SOM) content were determined after drying at 105°C. Soil pH, bioavailable NO_3^-, NH_4^+, PO_4-P, DOC-C and total dissolved N (organic plus inorganic) were determined in water extracts. Bioavailable P was determined using the Olsen method. Further elemental concentrations were measured either as bio-available pool using water-extracts or as total concentrations using digestions.*

Parameter	0-10 cm		10-20 cm	
	CDD field	WIS field	CDD field	WIS field
Fresh weight density (g l^{-1})	714.5 ± 20.6*	841.4 ±38.0	876.5 ±25.0	970.7 ±38.5
Moisture (% of fresh weight)	40.3 ± 1.73*	48.2 ± 0.71	46.0 ± 1.39*	49.4 ± 0.56
Dry bulk density (g cm^{-3})	0.42 ± 0.01	0.43 ± 0.02	0.47 ± 0.01	0.49 ± 0.02
SOM (% of dry weight)	49.7 ± 0.47*	54.9 ± 0.45	45.3 ± 0.45*	46.3 ± 0.61
Olsen-P (mg l^{-1})	38.2 ± 1.7*	43.6 ± 1.3	40. 7 ± 2.0	42.5 ± 2.1
Water extract				
pH	5.13 ± 0.07	5.24 ± 0.09	5.08 ± 0.11	5.32 ± 0.06
NO_3-N (mg l^{-1})	7.68 ± 1.40	5.07 ± 0.42	7.57 ± 0.84	6.02 ± 0.90
NH_4-N (mg l^{-1})	1.57 ± 0.50*	0.44 ± 0.08	0.11 ± 0.02	0.22 ± 0.06
PO_4-P (mg l^{-1})	0.03 ± 0.01*	0.04 ± 0.01	0.21 ± 0.04*	0.12 ± 0.01
DOC-C (mg l^{-1})	139.7 ± 8.09	141.1 ± 6.08	139.5 ± 4.21	148.5 ± 5.84
Dissolved N (mg l^{-1})	21.0 ± 2.65	15.2 ± 0.51	17.8 ± 0.77	16.4 ± 0.76
Al (mg l^{-1})	2.38 ± 0.17	2.93 ±0.10	2.31 ±0.15	3.14 ±0.14
Ca (mg l^{-1})	31.5 ± 2.7	51.97 ±2.70	48.2 ±5.02	79.2 ±7.75
Cl (mg l^{-1})	0.98 ± 0.56	0.00 ±0.00	8.98 ±3.20	13.8 ±5.63
Fe (mg l^{-1})	2.26 ± 0.35	1.86 ±0.09	1.91 ±0.11	1.94 ±0.13
K (mg l^{-1})	6.12 ± 1.19	3.20 ±1.13	6.84 ±1.31	4.33 ±1.52
Mg (mg l^{-1})	9.28 ± 0.92	11.3 ±0.46	13.7 ±1.35	20.1 ±1.98
Mn (mg l^{-1})	0.60 ± 0.05	0.86 ±0.06	0.85 ±0.11	1.07 ±0.17
Na (mg l^{-1})	11.9 ±0.56	12.5 ±1.43	19.9 ±1.37	20.6 ±1.70
P (mg l^{-1})	0.39 ±0.04	0.20 ±0.01	0.65 ±0.07	0.27 ±0.02
S (mg l^{-1})	21.6 ± 1.58	38.9 ±2.98	42.0 ±4.28	69.9 ±6.55
Si (mg l^{-1})	4.52 ± 0.27	4.10 ±0.27	5.48 ±0.23	4.39 ±0.17
Zn (mg l^{-1})	0.16 ± 0.01	0.20 ±0.01	0.18 ±0.01	0.21 ±0.02
Digestion				
Al (g l^{-1})	10.2 ± 0.59	9.63 ± 0.40	13.2 ± 0.76	13.1 ± 0.80
Ca (g l^{-1})	3.21 ± 0.10*	4.16 ± 0.14	3.65 ± 0.080*	4.39 ± 0.16
Cl (g l^{-1})	0.213 ± 0.04*	0.593 ± 0.04	0.201 ± 0.03*	0.730 ± 0.13
Fe (g l^{-1})	7.84 ± 0.29	7.64 ± 0.39	9.83 ± 0.29	10.94 ± 0.51
K (g l^{-1})	1.02 ± 0.073	0.922 ± 0.035	1.25 ± 0.095	1.10 ± 0.073
Mg (g l^{-1})	1.52 ± 0.076	1.55 ± 0.052	1.77 ± 0.079	1.84 ± 0.10
Mn (g l^{-1})	0.13 ± 0.004*	0.160 ± 0.006	0.124 ± 0.004	0.139 ± 0.007
Na (mg l^{-1})	23.3 ± 5.9	32.3 ±4.2	30.2 ±5.4	43.8 ±5.7

Parameter	0-10 cm		10-20 cm	
	CDD field	WIS field	CDD field	WIS field
P (g l^{-1})	0.848±0.028 *	1.11 ± 0.037	0.922 ± 0.028	1.15 ± 0.032
S (g l^{-1})	1.81 ± 0.057*	2.28 ± 0.090	1.97 ± 0.044*	2.17 ± 0.068
Si (mg l^{-1})	131 ± 5.5*	171 ±10.1	141 ±5.6*	194 ±11.1
Zn (mg l^{-1})	45.1 ±1.3*	55.6 ±2.1	52.3 ±1.6*	69.5 ±6.5

* Mean values of the two fields differ significantly (t-test, $p < 0.05$).


5

Chapter 5

Drainage and fertilizer effects on nitrous oxide emissions from peat grasslands

Erne Blondeau, Dorien Westerik, Marius Heinen, Rima Porre, Mart Ros, Jan Willem Van Groenigen, Gerard Velthof

Manuscript under review for publication

Abstract

Peat grassland drainage causes organic matter oxidation and emissions of greenhouse gases carbon dioxide (CO_2) and nitrous oxide (N_2O). Installation of a water infiltration system (WIS) may reduce peat oxidation while enabling grass production and cattle grazing. However, their effects on N_2O emissions and interaction with fertilizer applications have not been studied yet.

A two-year field experiment was conducted, including three drainage treatments: conventional ditch drainage (CDD) and water infiltration systems aimed for water levels of 20 cm (WIS20) and 40 cm (WIS40) below the surface. Plots were fertilized with mineral (calcium ammonium nitrate and ammonium sulphate) or organic (cattle slurry, the liquid and solid fractions of cattle slurry, and farmyard manure) fertilizers, differing in N and C content. Nitrous oxide emissions were measured weekly, and the grass yield and N uptake were measured over multiple cuts per year.

Cumulative N_2O emissions were lower under WIS40 than under CDD, while highest emissions were observed for the most shallow drainage treatment (WIS20). Application of mineral fertilizers resulted in significantly higher emissions (14.8 to 16.7 kg N ha^{-1}) than organic fertilizers (3.5 to 8.3 kg N ha^{-1}), particularly under WIS20. These differences remained when expressed as yield-scaled emissions, despite a greater apparent N recovery for mineral than for organic fertilizers.

Our results suggest that maintaining a shallow groundwater level increases the risk for N_2O emissions from peat grasslands, likely due to increased denitrification rates in the topsoil. This is exacerbated when combined with mineral fertilizer application.

5.1 Introduction

Peat soils are drained for agricultural use, such as grasslands for dairy farming. Draining the wet soil is necessary to allow for field operations and increase yields, but generally leads to enhanced peat oxidation, resulting in carbon dioxide (CO_2) emissions, and soil subsidence (Erkens et al., 2016). This may furthermore lead to emissions of nitrous oxide (N_2O) (Van 't Hull et al., 2026), a greenhouse gas with a global warming potential 273 times higher than CO_2 on a 100-year time scale (Forster et al., 2021).

Nitrous oxide is formed as an intermediate or by-product in several N conversion processes in the soil, most importantly during anaerobic denitrification, the reduction of nitrate (NO_3^-) to N_2, or aerobic nitrification, the oxidation of ammonia (NH_4^+) (Butterbach-Bahl et al., 2013). Soil N_2O emissions are primarily emitted in agricultural production systems, where the size and timing of emissions are strongly affected by the type of fertilizer, application method as well as the soil type and moisture content (Canadell et al., 2021; Velthof et al., 2024; Velthof et al., 1997). Additionally, the mineralization of soil organic matter can provide substrates and soil conditions optimal for nitrification (by the formation of NH_4^+) or denitrification (by consuming O_2 and providing labile C) (Chapin et al., 2002b).

Drainage of peat soils thus significantly contributes to greenhouse gas emissions (CO_2 and N_2O) associated with land use in several countries in Europe, including the Netherlands (European Environment Agency, 2024; Winiwarter et al., 2018). An alternative to conventional drainage (regulated through the ditch water levels) is the implementation of a water infiltration system (WIS), which enables fast equilibration of the groundwater level with the water level inside the ditches ("passive" system) or regulating reservoir ("active" system) and improves the homogenous distribution of water through the field (van de Craats et al., 2025). This results in improved infiltration and drainage of the field during dry and wet periods, respectively, compared to conventional ditch drainage (Harpenslager et al., 2024; Van Asselen et al., 2023).

Several studies have reported decreased CO_2 emissions as a result of WIS, compared to conventional ditch drainage (Aben et al., 2024; Boonman et al., 2022; Van 't Hull et al., 2026), but the effect on N_2O emissions remains less clear (Offermanns et al., 2023; Van 't Hull et al., 2026; Weideveld et al., 2021). Water infiltration systems may affect N_2O emissions in contrasting ways. They may have a mitigating effect by decreasing GWL fluctuations, as shifts from aerobic to anaerobic

conditions can create a sequence of nitrogen (N) mineralization, nitrification and denitrification (e.g., Goldberg et al., 2010; Taft et al., 2018). A higher summer GWL can decrease N_2O losses originating from peat mineralization, compared to conventionally drained soils (Blondeau et al., 2026; Tiemeyer et al., 2024). In a previous study, we quantified the combined effects of WIS drainage at a GWL of -40 cm with grazing effects (urine, dung and trampling application) (Blondeau et al., 2026). WIS drainage had no significant effect on cumulative N_2O emissions compared to conventional drainage, but was generally associated with lower emissions originating from organic N mineralization (without urine or dung application). However, a shallow groundwater level may have the opposite effect if it drives N_2O production during incomplete denitrification in the topsoil, from where the trace gas can diffuse to the atmosphere before reduction to N_2 (Clough et al., 2005). The anaerobic top soil conditions may particularly amplify N_2O losses driven by other management practices. Offermanns et al. (2023) observed this effect of WIS in combination with the organic matter mineralization caused by grassland renewal. Nitrogen input through fertilization may have a similar interaction with WIS drainage since more N is introduced in a system that is already suitable for denitrification.

The type and rate of applied mineral or organic fertilizers are important factors determining N_2O emissions from peat soils (Velthof et al., 2003; Velthof et al., 1997). Nitrate is directly available to plants but may be reduced to N_2O under carbon-rich and moist soil conditions. Ammonium- on the other hand, may stimulate N_2O release from nitrification under aerobic soil conditions (Butterbach-Bahl et al., 2013). Manures, and manure-derived products, typically contain N in ammoniacal or organic form, in varying ratios, depending on the type of manure processing (Velthof et al., 2024). Physical fractionation of manure produces a solid fraction with high dry OM content and relatively high N content, which is mostly present in organic form. The remaining liquid fraction holds a lower amount of N, present as NH_4^+ and in small suspended organic particles (Fangueiro et al., 2008).

There is an increasing interest in fertilizer materials derived from processed animal manure, which resemble inorganic fertilizers in their chemical properties (European Commission, 2026). These biobased materials are often collectively labelled RENURE (REcovered Nitrogen from manURE). Requirements for the label RENURE prescribe that mineral N (usually NH_4^+) takes up 90% or more of the total nitrogen content or when the total organic carbon to total N ratio does not exceed 3 kg kg^{-1}

(Huygens et al., 2020). The intention is for RENURE fertilizers to (partly) replace synthetic fertilizers in terms of agronomic efficiency and the N leaching risk (compared to manure), while improving the utilization of nutrients in manure (Huygens et al., 2020). Insight in potential differences in N_2O emission between (RENURE) fertilizers and manures, and the interaction with drainage management, can be used to derive mitigation options.

The aim of this study was, therefore, to quantify N_2O emissions after application of different fertilizer products to peat soil under three drainage systems. We hypothesized that (1) by decreasing the groundwater fluctuation in the summer around a stable level of 40 cm below the surface, a water infiltration system results in lower N_2O emissions originating from peat N mineralization than conventional ditch drainage; (2) WIS controlled drainage aiming for a shallow GWL around 20 cm below the surface results in increased N_2O emissions due to increased denitrification in the top soil; (3) application of nitrate-containing, mineral fertilizers leads to higher N_2O emissions, as well as higher grass yield, than ammonium-holding (manure) fertilizers; (4) WIS drainage aiming for a GWL of -20 cm enhances the N_2O increase under nitrate-fertilizers further, as both factors enable denitrification.

5.2 Methods and materials

5.2.1 Field location and WIS setup

We set up a field experiment between April 2023 and January 2025 at a dairy farm on drained peat soil near Zegveld in the Netherlands (around 52°08'20” N, 4°50'12” E, Fig. 5.1a). At this site, mesotrophic wood peat is found down to a depth around 3 m, followed by eutrophic sedge peat until approximately 6 m.

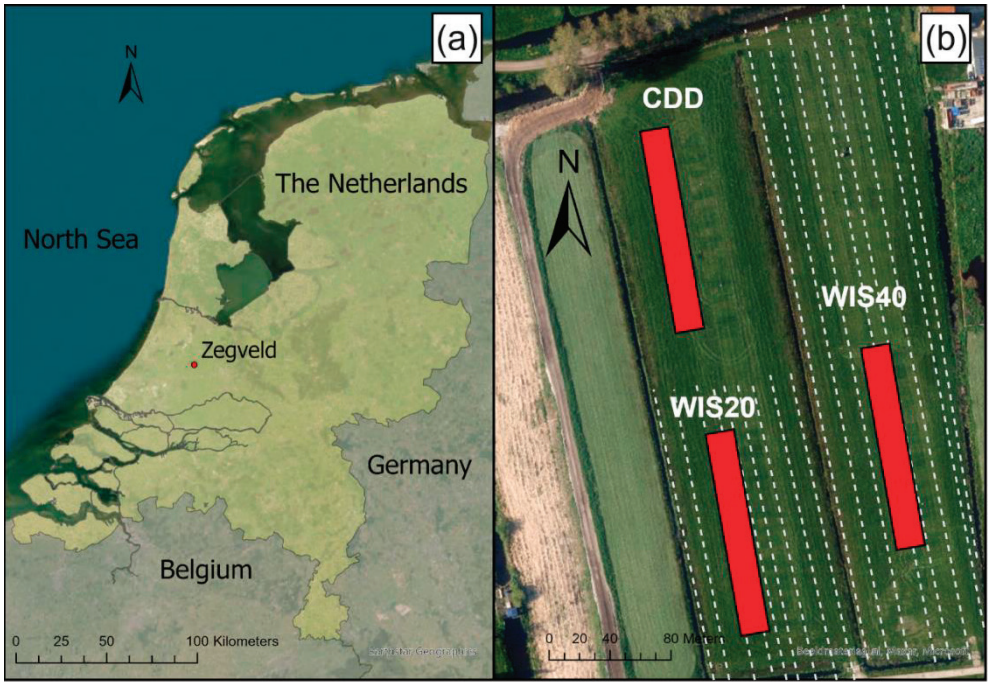


***Figure 5.1**: Geographical location of the field site at Zegveld (a) and overview of the three experimental fields (in red) under conventional ditch drainage (CDD), water infiltration system at -20 cm (WIS20) and water infiltration system at -40 cm (WIS40) (b).*

Two adjacent parcels with similar soil properties (Table 5.1) and similar past management were selected. The topsoil was sampled (0-20 cm) from each experimental block and mixed to make one representative sample per drainage field (CDD, WIS20, and WIS40; see Fig. 5.1). Soil samples were analysed in a commercial lab (Eurofins Scientific, The Netherlands) for total N content (similar to Dumas: thermal conductivity after high temperature combustion under an excess of O_2), total sulphur (drying and grinding; near infrared spectrometry), potentially available phosphorus (ammonium lactate extraction; discrete analysis spectrophotometry), plant available sulphur, potassium, magnesium, and sodium (0.01 M $CaCl_2$ extraction; ICP-MS), readily available phosphorus (0.01 M $CaCl_2$ extraction; discrete analysis spectrophotometry), pH ($CaCl_2$ extraction; potentiometry), soil organic matter content (loss on ignition at 550°C), sand, silt and clay fractions (sieving or density measurements after removing organic material and salts), microbial biomass, microbial activity, fungal and bacterial biomass

(drying and grinding; near infrared spectrometry). Soil properties of the three fields are provided in Table 5.1.

Prior to the experiment, both parcels had been in use as ryegrass-based production grassland (*Lolium perenne*) for more than 50 years with a combination of mowing and grazing and fertilizer application of around 230 kg N ha^{-1} yr^{-1}. In February 2022, WIS drains were installed along the length of one of the parcels and connected to a pump-controlled reservoir. Drainage tubes were installed at a depth of 60-70 cm below the surface (10-20 cm below the ditch water level) and spaced 4 m from each other. This WIS treatment (WIS40) aimed for a GWL of 40 cm below the surface through active infiltration and drainage, while the GWL of the second parcel was established through conventional ditch drainage (CDD) with summer ditch water levels around 40-50 cm. In February 2023, additional WIS drains were placed along the length of half of the second parcel at 60-70 cm depth, in which pump-infiltration aimed for a GWL of 20 cm below the surface (WIS20, Fig. 5.1b). The GWL relative to the soil surface level was monitored and logged hourly at four points in each drainage treatment (ElliTrack, Leiderdorp Instruments, The Netherlands). The daily averages for each drainage treatment were used in this paper. Some gaps were present in the GWL data series, due to instrument failure, which were filled using linear interpolation.

The study took place over two growing seasons, with emission measurements being conducted between 5-04-2023 and 21-03-2024 (352 days) and between 24-04-2024 and 29-01-2025 (280 days). Mean daily temperature and precipitation measured at this site were 11.9 °C and 3.2 mm respectively over the first period and 12.4 °C and 2.8 mm over the second period. Monthly values of the mean temperature and total precipitation are provided in the supplementary information (Table S5.1).

***Table 5.1**: Soil properties (0-20 cm) on the three fields before treatment application in spring 2023. The methods are provided in paragraph 2.1.*

	CDD[a]	WIS40	WIS20
Total N (g N kg^{-1})	22.4	25.2	22.5
Plant available S (mg S kg^{-1})	28.1	47.7	32
Total S (g S kg^{-1})	4.7	5.7	4.5
Readily available P ($CaCl_2$ extr., mg P kg^{-1})	0.4	1.2	0.7
Potentially available P (ammonium lactate extr., mg P kg^{-1})	87.2	139.5	100.3
Plant available K (mg K kg^{-1})	168	194	229
Plant available Mg (mg Mg kg^{-1})	437	577	505
Plant available Na (mg Na kg^{-1})	80	94	82
pH-$CaCl_2$	4.5	4.9	4.7
SOM (% of total dry mass)	43.9	51.4	43.7
clay (% of total mineral mass)	55	60	52
silt (% of total mineral mass)	21	27	23
sand (% of total mineral mass)	23	14	25
Microbial biomass (mg C kg^{-1})	4288	4263	4309
Microbial acitvity (mg N kg^{-1})	444	554	450
Fungal biomass (mg C kg^{-1})	960	862	903
Bacterial biomass (mg C kg^{-1})	1700	1753	1726
Fungal/bacterial	0.6	0.5	0.5

[a]CDD, conventional ditch drainage; WIS40, water infiltration system at -40 cm; WIS20, water infiltration system at -20 cm.

5.2.2 Experimental design and fertilization

Twenty-eight plots of 3 by 8 m were delineated on each of the CDD, WIS40 and WIS20 fields at the start of both measuring years, in April of 2023 and 2024. The plots were situated on different parts of the field each year, in order to prevent multi-year or carry-over effects. Each plot was treated with one of six fertilizer treatments: calcium ammonium nitrate (CAN), cattle slurry (CS), the liquid or the solid fraction of cattle slurry separation (CS_liq and CS_sol, respectively), ammonium sulphate (AS), and farm yard manure (FYM). All treatments and an unfertilized control were replicated four times per field in a randomized block design.

Total yearly fertilizer rates targeted at 220 kg N ha^{-1} yr^{-1} were split over three to four applications per year, between late April and late August (Table 5.2), except for the FYM treatment, which was applied only twice to resemble common farming practice. The N contents of most of the fertilizers (all fertilizers except CAN and FYM) were estimated before

application to determine the first application rate. At every fertilization event, samples of the fertilizers were taken and analyzed for total N (following Dumas, as described above) to calculate the actual N application and to adjust following applications if necessary. Application rates for FYM were based on a target volume of 10 ton ha^{-1} yr^{-1}. In 2023, the fertilizers were applied at a total rate approaching 220 kg total N ha^{-1} (Table 5.2). In 2024, a total rate of approximately 170 kg ha^{-1} was applied, as wet conditions during late summer prevented the last fertilizer application. Farmyard manure application rates differed from those of other fertilizers, with a rate of 160 kg N ha^{-1} in 2023 and 256 kg N ha^{-1} in 2024 (Table 5.2). The 2024 rate was higher than intended due to a much higher N content of the FYM in the second application (on 19-08-2024) than anticipated.

***Table 5.2**: Application dates and rates (kg N ha^{-1}) of the fertilizer treatments. Inside the brackets the initially planned application rates are shown.*

Year	Date application	CAN[a]	AS	CS_liq	CS	CS_sol	FYM
2023	21-4-2023	80 (80)	80 (80)	80 (80)	80 (80)	79 (80)	64 (80)
	2-6-2023	60 (60)	60 (60)	60 (60)	60 (60)	58 (60)	0 (0)
	13-7-2023	40 (40)	40 (40)	40 (40)	40 (40)	31 (40)	0 (0)
	25-8-2023	40 (40)	40 (40)	33 (40)	33 (40)	38 (40)	98 (80)
	Total	220 (220)	220 (220)	213 (220)	213 (220)	207 (220)	161 (160)
2024	22-4-2024	80 (80)	80 (80)	80 (80)	80 (80)	80 (80)	80 (80)
	25-6-2024	50 (50)	50 (50)	50 (50)	50 (50)	50 (50)	0 (0)
	19-8-2024	40 (40)	37 (40)	37 (40)	38 (40)	46 (40)	176[b] (60)
	Total	170 (170)	167 (170)	167 (170)	168 (170)	176 (170)	256 (140)

[a]FYM, farmyard manure; CS_sol, solid fraction of cattle slurry; CS, cattle slurry; CS_liq, liquid fraction of cattle slurry; AS, ammonium sulphate; CAN, calcium ammonium nitrate.

[b]The N content of this FYM application was almost 3 times higher than expected.

All fertilizers were applied to the plots manually. Granular CAN was broadcast by hand. Ammonium sulphate, a strongly concentrated product of ammonia scrubbed from the air of a dairy barn, was diluted and applied using band spreading with a watering can, simulating a trailing shoe or trailing hose technique. Cattle slurry was similarly diluted and applied via

band spreading with trailing hose after a 1:2 dilution with water, in line with Dutch regulations. The liquid and solid fractions of cattle slurry were obtained through mechanical separation and were applied via band spreading with trailing hose (after dilution) and broadcast surface spreading, respectively. Farmyard manure, a mixture of cattle feces, urine and straw from stable bedding, was applied via broadcast surface spreading. Detailed compositions of the ammonium sulphate and manure fertilizers are provided in the supplementary information (Table S5.2).

5.2.3 Yield and apparent nitrogen recovery

The plots were mown before each fertilizer application (Table 5.2) and at the end of the growing season. Subsamples were collected from a 1.5 m strip in the middle of each plot using a Haldrup plot harvester and dry matter yield was determined after drying at 70°C. The grass N content was determined (following Dumas, as described above) and the N uptake was calculated. The apparent nitrogen recovery (ANR) of the fertilized objects was calculated as the percentage of the applied N that was taken up by the grass:

$$ANR = (N\ uptake_{treatment} - N\ uptake_{control})/N_{applied} * 100 \quad (1)$$

Where $N\ uptake_{treatment}$ and $N\ uptake_{control}$ are the N uptakes (kg N ha^{-1}) of the treated plot and the control plot within the same block, and $N_{applied}$ is the total fertilizer application rate of the treatment over a growing season (kg N ha^{-1}, Table 5.2).

5.2.4 N_2O emissions

5.2.4.1 Flux measurements

In the two measurement years, N_2O emissions were measured weekly to biweekly between 5-04-2023 and 21-03-2024 and between 24-04-2024 and 29-01-2025. At the end of both years, N_2O emissions from the treated objects had returned to background levels (i.e. levels measured in control objects). Measurements were continued throughout the winter, until negligible emissions had been consistently observed for four weeks. N_2O concentrations were measured using cavity ring-down spectroscopy (Picarro G2508; Picarro Inc., USA) until 28-08-2023. Thereafter (the rest of 2023, and all of 2024-2025), for logistic reasons a gas analyzer with photoacoustic infrared spectroscopy technology was used (INNOVA 1512; LumaSense Technologies Inc., USA). The change in gas analyser did not affect continuity of the flux measurements (Fig.

S5.1). The static chamber method was used for gas flux measurements, with a closure time of 10 to 15 minutes. Gas fluxes were calculated assuming a linear slope between the headspace concentration at the end of the closure time and the ambient N_2O concentration at the start (Abalos et al., 2014; Oram et al., 2020; Van 't Hull et al., 2025). A check was included for the assumption of a linear headspace concentration slope, by performing at least one continuous flux measurement for a duration of 20 minutes on each measuring day.

5.2.4.2 Gap filling, derivation of emission factors and yield scaled emissions

A non-linear gap filling method was used to estimate N_2O emission values on the days without measurements, following the process described in Van 't Hull et al. (2026). The N_2O emission data were log-transformed and fitted to a separate generalized linear model for each individual measurement year (2023-2024 and 2024-2025) using the R 'mgcv' package (Wood, 2004). Treatment factors (drainage and fertilizer) were included as discrete variables, environmental parameters (temperature, precipitation, GWL), day of experiment, and the number of days since the most recent fertilizer application were considered as smoother variables and experimental treatment parameters were included as random effects. The smoother variables were checked for reciprocal collinearity and the Akaike Information Criterion was used as an indicator to select useful covariates for each model (Table 5.3). For both years, a model including drainage, fertilizer, day of experiment, summed precipitation over the last 3 days and GWL was found to perform best (Table 5.3). The model was subsequently used to predict daily N_2O emission values for each treatment level, using the model variables as input data. Cumulative emissions were calculated for each treatment combination using the *agg.fluxes* function in the R 'gasfluxes' package (Fuss, 2023). Where available, the mean (n = 4) measured values where used and on days without measurements the predicted values were used.

***Table 5.3**: Structures and R^2 values of the generalized linear models used to predict the N_2O emissions in each measurement year. The model includes fixed treatment variables (denoted in italics), smoother covariables (s), and a random factor to account for repeated measurements (r).*

Year	Model structure	R^2
2023-2024	Log(N_2O) = *drainage* + *fertilizer* + s(day) + s(precipitation 3 days) + s(GWL) + r(drainage_fertilizer)	0.51
2024-2025	Log(N_2O) = *drainage* + *fertilizer* + s(day) + s(precipitation 3 days) + s(GWL) + r(drainage_fertilizer)	0.79

Emission factors (EF) were calculated as the percentage of applied N that was released as N_2O, following:

$$EF = (N_2O\text{-}N_{treatment} - N_2O\text{-}N_{control})/N_{applied} * 100 \quad (2)$$

Where $N_2O\text{-}N_{treatment}$ and $N_2O\text{-}N_{control}$ are the cumulative emissions observed in the treated and the control plot within the same block (kg N ha^{-1}) and $N_{applied}$ is the amount of fertilizer N applied (kg N ha^{-1}). Yield-scaled N_2O emissions were calculated as the amount of cumulative N_2O emitted per unit of above-ground N uptake within a year (Van Groenigen et al., 2010):

$$\text{Yield-scaled } N_2O = N_2O\text{-}N/N \text{ uptake} \quad (3)$$

5.2.5 Data analysis

All data analyses were performed with the statistical software R (v4.3.1;R Core Team, 2023). Effect sizes of the fertilizers and drainage treatments, as well as their interaction, on cumulative N_2O emissions were tested using analysis of variance (ANOVA). The distributions of datapoints and residuals were checked visually for the conditions of normality and homogeneity. When these conditions were not met, the distributions were reevaluated after a transformation of the response variable. Pair-wise differences of the estimated marginal means between treatment factor levels were tested using Tukey adjustment in the 'emmeans' package (Van Lenth & Piakowski, 2026). The same procedure was followed for the analysis of treatment effects on emission factors.

The effects of fertilizer type, drainage and their interaction on the dry matter yield, N uptake and ANR were tested with a linear mixed effects model using restricted maximum likelihood in the 'nlme' package (Pinheiro et al., 2023). Normality and homogeneity of the datapoints and residual distribution was confirmed for each dataset. The random variance

structure was written as block nested within main plot, nested within year (Response ~ fertilizer * drainage + (1| year/main plot/block)), where main plot is the experimental area on a drainage field (the whole area of 28 plots).

5.3. Results

5.3.1 GWL depth

The mean seasonal GWL depths showed limited differences between the three drainage treatments (Table 5.4, Fig. 5.2). Most pronounced effects of WIS were observed during periods associated with high evaporation and transpiration, i.e. the summer months. Mean GWL depths in the summer of 2023 were -63.0, -47.6 and -34.0 cm, in the CDD, WIS40 and WIS20 fields, respectively. The difference was less strong in the summer of 2024 (-45.1, -42.5 and -32.6, respectively). Minimum GWL values (deepest GWL) in the spring, summer and autumn were generally less negative in the WIS fields than the CDD field, with the exception of spring 2024, which was relatively wet.

5.3.2 N_2O emissions

Cumulative N_2O emissions ranged between -0.6 and 23.9 kg N ha^{-1} (Fig. 5.3). Drainage type had a significant effect on cumulative N_2O (F = 5.3, p = 0.01). Emissions (mean ± SEM) were highest under WIS20 (11.3 ± 1.8 kg N ha^{-1}), followed by CDD (7.9 ± 1.7 kg N ha^{-1}) and WIS40 (6.4 ± 1.6 kg N ha^{-1}). The pair-wise difference between WIS20 and WIS40 drainage was significant (t = 3.2, p = 0.009).

The fertilizer type also significantly affected cumulative N_2O emissions (F = 9.7, p < 0.001) with mean emissions highest under AS (16.7 ± 2.7 kg N ha^{-1}), followed by CAN (14.8 ± 2.8 kg N ha^{-1}). Emissions under the manure fertilizers, CS_liq (8.3 ± 1.5 kg N ha^{-1}), CS (6.2 ± 1.3 kg N ha^{-1}), FYM (6.3 ± 1.7 kg N ha^{-1}) and CS_sol (3.5 ± 1.1 kg N ha^{-1}) were comparatively low and did not differ significantly from the control plots (Fig. 5.3). There was no significant interaction effect between drainage and fertilizer type on cumulative N_2O emissions. Emissions from AS and CAN were consistently highest, irrespective of the drainage type. Simultaneously, all fertilizer types showed highest emissions under the WIS20 drainage treatment. Nitrous oxide emissions often peaked shortly after fertilizer application or precipitation events, with a highest individual peak of 741 mg N m^{-2} day^{-1} under CAN and WIS20 on 11-07-2024 (Fig. S5.3.c).

***Table 5.4**: Summary statistics (mean, median, minimum value, maximum value and standard deviation (sd)) of the daily GWL depths measured in summer (June 1st till September 1st), autumn (September 1st till December 1st), winter (December 1st till March 1st) and spring (March 1st till June 1st) under each drainage treatment.*

		Winter '22'23	Spring '23	Summer '23	Autumn '23	Winter '23'24	Spring '24	Summer '24	Autumn '24	Winter '24'25[c]
CDD[a]	mean	-18.5	-24.0	-63.0	-26.6	-6.2	-21.4	-45.1	-37.6	-7.7
	sd	4.2	14.9	13.8	22.0	4.3	11.1	14.8	15.8	9.3
	min	-26.3	-55.0	-83.8	-64.7	-18.9	-44.5	-68.1	-63.9	-27.2
	max	-10.6	-4.5	-29.8	-2.4	2.9	-2.0	-8.4	0.0	10.6
	median	-17.3	-19.0	-64.8	-13.0	-5.2	-20.5	-44.5	-42.0	-7.8
WIS40	mean	-17.2	-23.6	-47.6	-21.0	-4.3	-19.9	-42.5	-36.7	-14.0
	sd	6.4	11.2	10.9	18.7	4.9	11.4	14.6	13.6	3.1
	min	-29.3	-44.5	-64.2	-53.2	-23.3	-46.8	-64.4	-55.6	-22.0
	max	-8.0	-3.3	-14.2	0.2	6.4	-2.9	-10.5	-6.5	-7.8
	median	-15.9	-21.6	-48.7	-10.2	-2.8	-17.2	-43.6	-41.4	-13.6
WIS20	mean	-[b]	-23.9[b]	-34.0	-16.7	-3.7	-24.0	-32.6	-28.8	-7.5
	sd	-	10.7	10.6	14.3	5.0	9.7	10.1	14.1	8.3
	min	-	-37.0	-54.8	-40.1	-26.9	-51.9	-47.5	-47.9	-26.5
	max	-	-11.3	-8.8	-1.2	7.1	-12.5	-9.9	0.0	0.0
	median	-	-27.7	-33.5	-9.2	-2.2	-20.0	-34.4	-30.5	-5.5

[a]CDD, conventional ditch drainage; WIS40, water infiltration system at -40 cm; WIS20, water infiltration system at -20 cm.
[b]Sensor observations on the WIS20 field started on 04-04-2023. Winter '22'23 measurements were therefore missing and the spring '23 statistics are based on 58 measuring days, instead of 92.
[c]The winter '24'25 statistics in this table are based on the duration of the experiment, i.e. until 30-01-2025.

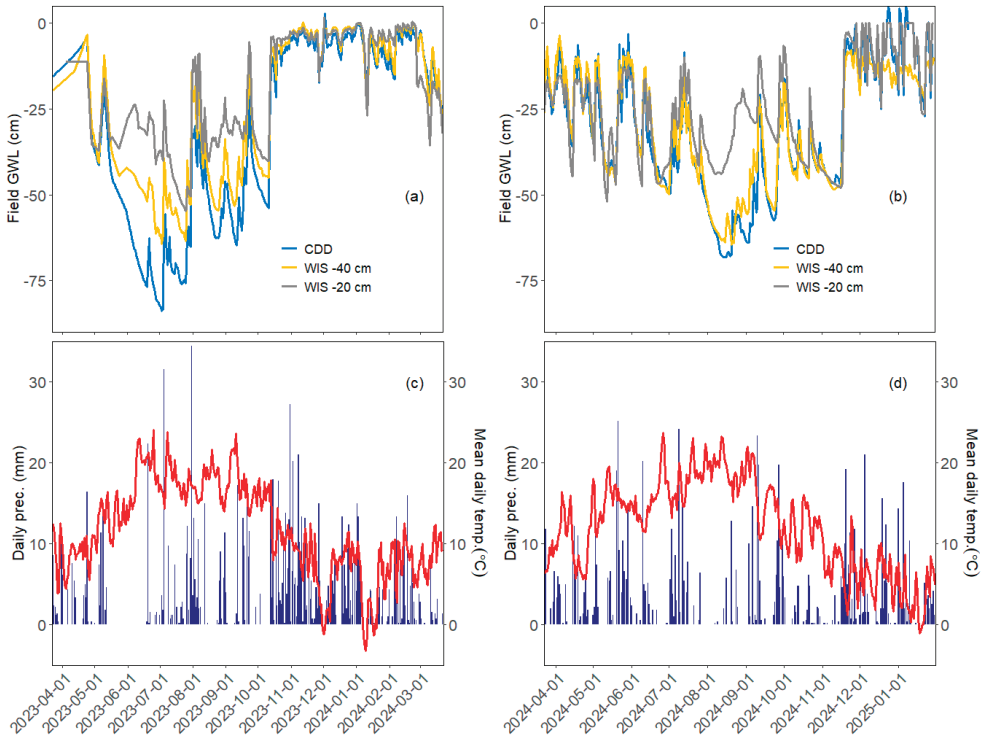


***Figure 5.2**: Groundwater levels in the three fields in the 2023-2024 (a) and 2024-2025 (b), total daily precipitation and daily mean temperature in 2023-2024 (c) and 2024-2025 (d). CDD, conventional ditch drainage; WIS40, water infiltration system at -40 cm; WIS20, water infiltration system at -20 cm.*

5.3.3 Yield

Dry matter yield, grass N uptake, and ANR were all highest under the AS and lowest under FYM fertilization (Table 5.5). Mean total yearly DM yield (n = 8, ± SEM) ranged between 7.5 ± 0.2 and 11.3 ± 0.5 ton ha^{-1} (Table 5.5). The DM yield was significantly affected by fertilizer treatment (F = 37, p = < 0.0001), but not by drainage type (p > 0.05) or the treatment interaction. All fertilizer treatments showed significantly higher DM yield than the unfertilized control (mean 7.8 ± 0.1 ton ha^{-1}, n = 24), and highest yield was observed under AS (10.2 ± 0.2 ton ha^{-1}) fertilizer application, followed by CS, CS_liq, CAN and CS_sol and FYM (Table 5.5). Mean N uptake (n = 8, ± SEM) over the two years ranged between 182 ± 3 and 335 ± 28 kg N ha^{-1} (Table 5.5). Similar to DM yield, the N uptake was significantly affected by fertilizer type (F = 47, p < 0.0001), with highest mean (n = 24) values under AS (314 ± 14 kg ha^{-1}), not by drainage or the fertilizer-drainage interaction.

Mean ANR (n = 8, ± SEM) ranged between 5.2 ± 6.1 and 58.7 ± 8.0 % (Table 5.5). The ANR was significantly affected by fertilizer type (F = 34, p < 0.0001). Mean ANR under WIS20 drainage (37.0 ± 2.6 %, n = 48) exceeded those under CDD (32.3 ± 2.9 %) and WIS40 drainage (29.3 ± 3.5 %), but not significantly.

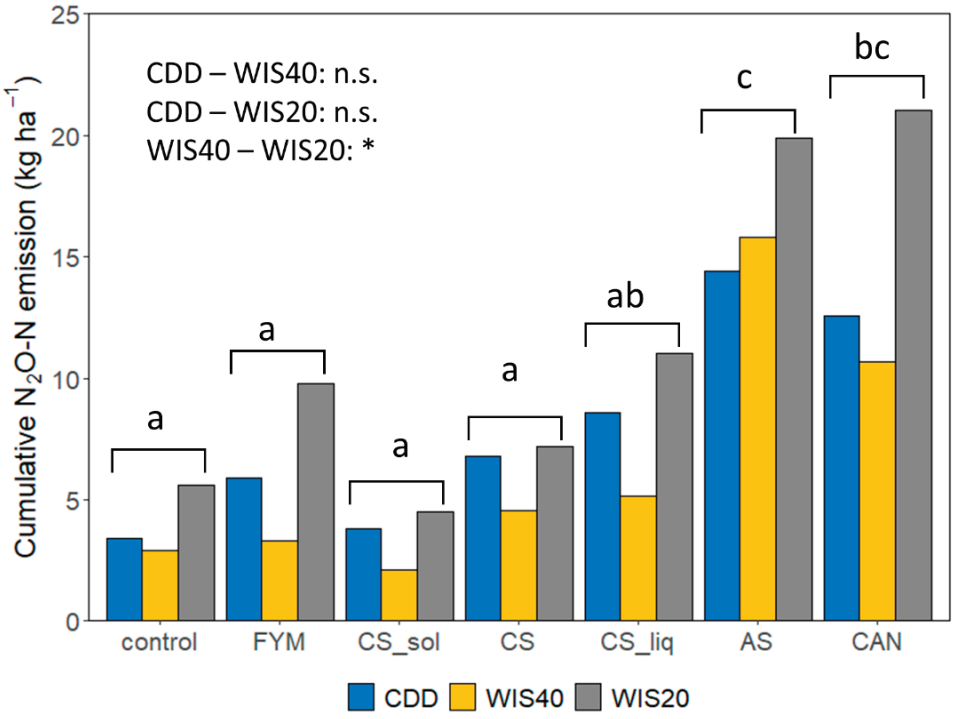


***Figure 5.3**: Mean yearly cumulative N_2O emission (n = 2) calculated from predicted N_2O emissions after non-linear gap filling for two measurement years. Letters above the bars indicate significant differences (t-test, p < 0.05) between fertilizer treatment levels, '*' indicates a significant pair-wise difference (p < 0.05) between drainage levels and 'n.s.' indicates no significance. CDD, conventional ditch drainage; WIS40, water infiltration system at -40 cm; WIS20, water infiltration system at -20 cm; FYM, farmyard manure; CS_sol, solid fraction of cattle slurry; CS, cattle slurry; CS_liq, liquid fraction of cattle slurry; AS, ammonium sulphate; CAN, calcium ammonium nitrate.*

***Table 5.5**: Mean values ± SEM (taken over 4 replicates and two years, n = 8) of the total dry matter yield (ton ha^{-1}), total N uptake (kg ha^{-1}) and apparent nitrogen recovery (%). Total dry matter and N uptakes are the sum of all grass cuts in a year. Letters indicate results of Tukey pair-wise comparisons of the fertilizer treatment levels, where values sharing the same letter were not shown to differ significantly ($p < 0.05$).*

Drainage	Fertilizer	Dry matter yield (ton ha^{-1})	N uptake (kg ha^{-1})	Apparent nitrogen recovery (%)
CDD[a]	Control	8.0 ± 0.2^{a}	217 ± 10^{a}	-
	FYM	9.1 ± 0.3^{b}	246 ± 10^{b}	14.7 ± 2.9^{a}
	CS_sol	9.2 ± 0.2^{bc}	253 ± 11^{bc}	18.9 ± 2.4^{ab}
	CS	10.0 ± 0.2^{d}	264 ± 13^{bc}	24.8 ± 2.7^{bc}
	CS_liq	9.8 ± 0.4^{cd}	274 ± 10^{cd}	31.2 ± 4.7^{cd}
	AS	10.2 ± 0.1^{d}	335 ± 28^{e}	58.7 ± 8.0^{e}
	CAN	10.0 ± 0.2^{d}	307 ± 16^{d}	45.6 ± 4.4^{d}
WIS40	Control	7.9 ± 0.3^{a}	197 ± 14^{a}	-
	FYM	8.4 ± 0.2^{b}	209 ± 12^{b}	5.2 ± 6.1^{a}
	CS_sol	9.1 ± 0.2^{bc}	225 ± 11^{bc}	15.4 ± 3.9^{ab}
	CS	9.7 ± 0.3^{d}	238 ± 13^{bc}	21.7 ± 3.7^{bc}
	CS_liq	10.1 ± 0.3^{cd}	263 ± 23^{cd}	34.6 ± 9.7^{cd}
	AS	10.2 ± 0.4^{d}	314 ± 27^{e}	58.7 ± 7.0^{e}
	CAN	9.8 ± 0.3^{d}	276 ± 18^{d}	40.1 ± 3.8^{d}
WIS20	Control	7.5 ± 0.2^{a}	182 ± 3^{a}	-
	FYM	9.0 ± 0.1^{b}	225 ± 4^{b}	22.9 ± 4.3^{a}
	CS_sol	9.5 ± 0.1^{bc}	244 ± 8^{bc}	31.5 ± 3.3^{ab}
	CS	10.2 ± 0.3^{d}	248 ± 7^{bc}	33.8 ± 3.3^{bc}
	CS_liq	9.7 ± 0.2^{cd}	250 ± 4^{cd}	35.4 ± 2.6^{cd}
	AS	10.3 ± 0.5^{d}	294 ± 20^{e}	54.9 ± 8.7^{e}
	CAN	9.8 ± 0.4^{d}	272 ± 18^{d}	43.5 ± 8.5^{d}

[a]CDD, conventional ditch drainage; WIS40, water infiltration system at -40 cm; WIS20, water infiltration system at -20 cm; FYM, farmyard manure; CS_sol, solid fraction of cattle slurry; CS, cattle slurry; CS_liq, liquid fraction of cattle slurry; AS, ammonium sulphate; CAN, calcium ammonium nitrate.

5.3.4 Emission factors and yield scaled emissions

Emission factors ranged between -0.5 and 8.6% (Table 5.6). Fertilizer type significantly affected the EF ($F = 18.0$, $p < 0.001$), but not drainage type or the drainage-fertilizer interaction. The highest mean EF was found for AS (5.8 ± 0.9 %, $n = 6$), followed by CAN (4.9 ± 0.8 %).

The manure fertilizers (CS_liq, FYM, CS, CS_sol) all showed significantly lower mean EFs than the mineral fertilizers: 2.0, 1.5, 1.0 and -0.2, respectively. Mean emission factors under WIS20 (3.2 ± 0.9 %, n = 12) exceeded those under CDD (2.5 ± 0.6 %) and WIS40 (1.8 ± 0.7 %).

Mean N yield scaled N_2O emissions (± SEM, over two years) ranged between 8 ± 11 and 80 ± 14 g N_2O-N kg^{-1} N uptake, measured for CS_sol under WIS40 and CAN under WIS20, respectively (Fig. 5.4). Similar to the cumulative N_2O emissions, fertilization with AS and CAN produced higher (37 – 80 g N_2O-N kg^{-1} N) yield-scaled N_2O emissions than CS, CS_liq, CS_sol or FYM (8 – 44 g N_2O-N kg^{-1} N). Additionally, yield scaled N_2O was significantly higher under WIS20 than WIS40 (t = 4.6, p < 0.001) and CDD (t = 3.8, p = 0.002).

***Table 5.6**: Emission factors (%) based on gap-filled N_2O emission rates in 2023-2024, 2024-2025 and the mean over both years (n = 2). Superscript letters indicate significant differences (p < 0.05) between treatment levels of the drainage – fertilizer interaction.*

		2023-2024	2024-2025	Mean
CDD[a]	FYM	1.5	1.6	1.5^{abcd}
	CS_sol	0.2	0.2	0.2^{ab}
	CS	2.0	1.1	1.6^{abcde}
	CS_liq	2.0	2.8	2.4^{abcde}
	AS	7.4	2.6	5.0^{bcde}
	CAN	5.7	2.7	4.2^{abcde}
WIS40	FYM	0.4	0.0	0.2^{ab}
	CS_sol	-0.2	-0.5	-0.4^{ab}
	CS	1.0	0.5	0.8^{abc}
	CS_liq	1.3	0.8	1.1^{abcd}
	AS	6.5	5.2	5.9^{cde}
	CAN	4.5	2.6	3.5^{abcde}
WIS20	FYM	1.4	3.9	2.6^{abcde}
	CS_sol	-0.5	-0.6	-0.5^{a}
	CS	1.3	0.2	0.8^{abc}
	CS_liq	1.8	3.3	2.6^{abcde}
	AS	8.6	4.4	6.5^{de}
	CAN	7.1	6.9	7.0^{e}

[a]CDD, conventional ditch drainage; WIS40, water infiltration system at -40 cm; WIS20, water infiltration system at -20 cm; FYM, farmyard manure; CS_sol, solid fraction of cattle slurry; CS, cattle slurry; CS_liq, liquid fraction of cattle slurry; AS, ammonium sulphate; CAN, calcium ammonium nitrate.

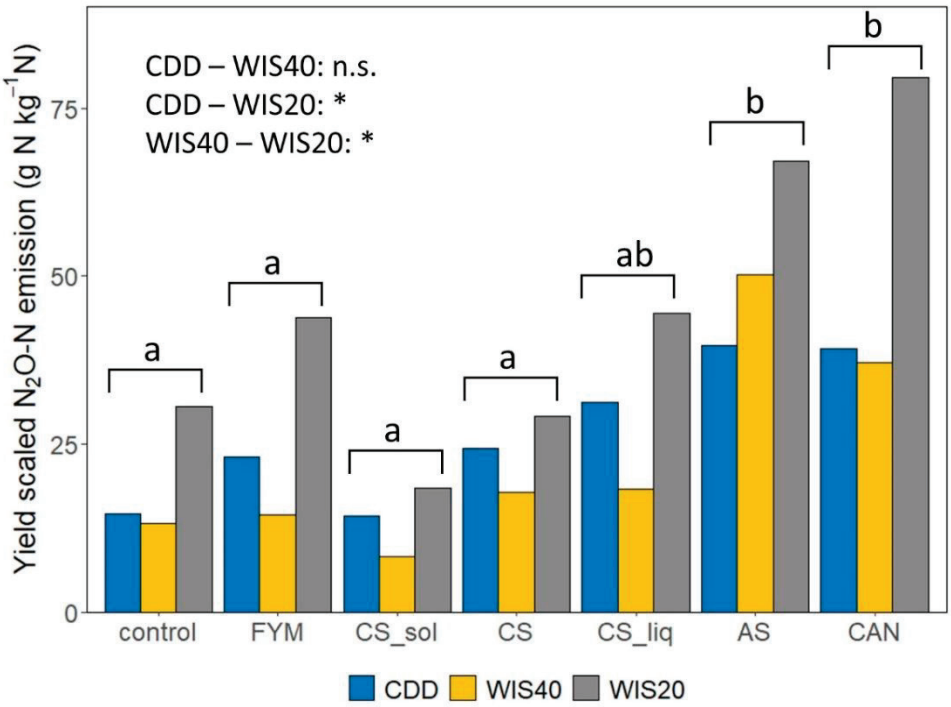


***Figure 5.4**: Mean yield scaled N_2O emissions (n = 2): g cumulative N_2O-N emission per kg above ground N uptake. Letters above the bars indicate significant differences (t-test, p < 0.05) between fertilizer treatment levels, '*' indicates a significant pair-wise difference (p < 0.05) between drainage levels and 'n.s.' indicates no significance. CDD, conventional ditch drainage; WIS40, water infiltration system at -40 cm; WIS20, water infiltration system at -20 cm; FYM, farmyard manure; CS_sol, solid fraction of cattle slurry; CS, cattle slurry; CS_liq, liquid fraction of cattle slurry; AS, ammonium sulphate; CAN, calcium ammonium nitrate.*

5.4 Discussion

5.4.1 Drainage treatment effects

5.4.1.1 N_2O emissions under different drainage treatments

We hypothesized that N_2O emissions resulting from peat mineralization would be lower under WIS40 drainage than under conventional ditch drainage, and to find highest emissions under WIS20 due to favourable conditions for denitrification. Indeed, WIS40 was associated with lower mean (n = 14) N_2O emissions than CDD (6.4 versus 7.9 kg N_2O-N ha^{-1}), and highest emissions were observed under WIS20 (11.9 kg N_2O-N ha^{-1}, Fig. 5.3). The unfertilized control plots followed the

same pattern, with 2.9, 3.4 and 5.6 kg N_2O-N ha^{-1} under WIS40, CDD and WIS20, respectively (n = 2).

Contrary to our results, shallow or no peat drainage is generally associated with a decrease in N_2O emissions compared to deep drainage, due to a reduction in N mineralization (Lin et al., 2022; Liu et al., 2020; Martikainen et al., 1993; Van Beek et al., 2010). Accordingly, the 2013 Wetlands Supplement to the IPCC inventory guidelines provides separate default emission factors for N_2O emissions associated with deep- or shallow drainage of organic temperate nutrient-rich grassland soils of 8.2 and 1.6 kg N_2O-N ha^{-1} yr^{-1}, respectively (Hiraishi et al., 2014). However, a limited number of studies reported increased N_2O emissions from peat grasslands under a shallow groundwater level compared to deeper drainage (Berglund & Berglund, 2011; Norberg et al., 2021). This may be explained by dynamic soil moisture conditions in the topsoil, which accommodate mineralization and nitrification, as well as denitrification (Pärn et al., 2018). Nitrous oxide produced close to the soil surface may leave the soil as N_2O, rather than being further reduced to N_2, due to a low residence time, as well as high availability of the preferred electron acceptor NO_3^- (Clough et al., 2005; Senbayram et al., 2019; Weier et al., 1993; Zhang et al., 2023). In addition, the nitrous oxide reductase enzyme shows a slower response than nitrate or nitrite reductase to the removal of oxygen (Knowles, 1982; Saggar et al., 2013). These mechanisms may enhance incomplete denitrification under sudden moisture increases, while prolonged flooding decreases the N_2O/N_2 product ratio of denitrification (Senbayram et al., 2022).

The importance of drying and wetting for N_2O emissions has been identified in several incubation or mesocosm studies on peat soils. In an outdoor mesocosm study Taft et al. (2018) measured strong N_2O fluxes under a shallow (-15 cm) groundwater level, while a water table at soil surface (0 cm) resulted in low emissions due to low NO_3^- availability. Berendt et al. (2023) discovered in an incubation of disturbed peat samples that the effects of short-term drying and wetting during the (pre-)incubation, as well as the moisture content at the time of sampling, had a larger effect on N_2O emissions than the long-term drainage conditions of the different sites from which the soils were sampled. Similarly, short-term events like irrigation or precipitation can drive high N_2O emissions (Anthony & Silver, 2021). Raising the groundwater level to -20 or 0 cm below the surface induced N_2O emission from drained peat mesocosms in a study by Blondeau et al. (2024). A relatively moist soil (a water filled pore space of around 60% in mineral soils) is often found

to be optimal for N_2O emissions, enabling mineralization and nitrification, as well as incomplete denitrification (Davidson et al., 2000; Van Groenigen et al., 2005b). In peat soils this optimum lies around 80% (Saurich et al., 2019a). Under such conditions, both moderate wetting and drying is likely to stimulate N_2O emissions (Pärn et al., 2018). In agreement with this, the N_2O peaks in this study usually coincided with a rise in the groundwater level, following precipitation (Fig. S5.2, Fig. S5.3).

Water infiltration systems are specifically intended to reduce fluctuations in the groundwater level, in particular by preventing deep drainage in periods of drought (Boonman et al., 2024; Boonman et al., 2022; Harpenslager et al., 2024; Van Asselen et al., 2023). This should not only reduce N mineralization and NO_3^- production, but thereby also NO_3^- reduction (Van 't Hull et al., 2026). Pronounced GWL differences between the three drainage systems were observed during periods of high temperature and low precipitation, i.e. May to October 2023 and July to September 2024 (Fig. 5.2). In periods of frequent rainfall, groundwater levels in the three systems were generally close to each other. In our earlier study on the same peat grassland fields, the combined effects of drainage and grazing on N_2O emissions were studied (Blondeau et al., 2026). While that study did not include a WIS20 treatment, it reported similarly higher emissions under CDD than WIS40. This is the first study that looked at the effect WIS20 on N_2O emissions. In accordance with our second hypothesis, WIS20 had a different effect on N_2O emissions than WIS40. Even in the absence of fertilizer-N application, the shallow groundwater under WIS20 level led to consistently higher emissions than the CDD or WIS40 treatments (Fig. 5.3), suggesting substantial losses originating from mineralized nitrogen (Hiraishi et al., 2014). Van 't Hull et al. (2026), on the other hand, observed lower N_2O emissions under shallow (-20 cm) ditch water levels compared to deep (-55 cm) ditch levels. In their study, peak N_2O fluxes were observed in the autumn months (September and October), during which hardly any effect of WIS on groundwater level was observed. Whereas we measured peak fluxes both in summer and in the autumn, shortly after precipitation or fertilization events (Fig. 5.2, Fig. S5.2, Fig. S5.3). These may therefore have been the result of the application of mineral and organic nitrogen. Highest cumulative N_2O emissions consistently occurred under WIS20, however, even in the absence of a fertilizer treatment and differences between our results and those of Van 't Hull et al. (2026) therefore cannot be explained by an interaction between fertilization and drainage management.

5.4.1.2 Yield, yield scaled emissions and apparent nitrogen recovery

While not significant, mean yearly N uptake was higher under CDD (271 kg ha^{-1}) than WIS40 (246 kg ha^{-1}) or WIS20 (245 kg ha^{-1}). The relationship between drainage depth and grass yield is well understood (De Vos et al., 2010; Van 't Hull et al., 2026; Van Dijk et al., 2026). Improved infiltration by WIS combined with a high ditch level may reduce the soil nitrogen supply, and consequently improve the utilization of fertilizer N (Hoving et al., 2023). Indeed, mean ANR was highest under WIS20, although the effect of drainage type was not significant (Table 5.5). Compared to other studies, mean dry matter yields and N uptake were generally relatively low across our treatments (Deru et al., 2019; Sonneveld & Lantinga, 2011; Van Dijk et al., 2026). This may be due to the high cumulative precipitation, compared to the 1991-2020 average, during parts of the growing seasons of 2023 and 2024 (KNMI, 2026). Additionally, the absence of a fourth grass cut in the summer of 2024 caused particularly low N yields in that year. Several studies suggest that the grass N uptake loss due to reduced N mineralization after raising the soil groundwater level (either through ditch water regulation or WIS) can be compensated by improved nitrogen use efficiency and raising fertilization levels (De Vos et al., 2010; Hoving et al., 2023; Van Dijk et al., 2009). From a perspective of reducing N_2O emissions, our results rather suggest to avoid the combination of a shallow GWL with mineral fertilizers, as denitrification is an important loss pathway in peat soils (Van Beek et al., 2009). As a result of the reduced or similar N uptakes under WIS20 compared to the other drainage treatments, combined with high N_2O emissions, the yield scaled emissions under WIS20 significantly exceeded those under CDD or WIS40 (Fig. 5.4).

5.4.2 Fertilizer effects on N_2O emissions and yield parameters

5.4.2.1 N_2O emissions from different fertilizers

We hypothesized (third hypothesis) to find highest emissions under the application of mineral, particularly nitrate containing, fertilizers. While the two mineral fertilizers, the nitrate-containing CAN and ammonium-based AS, resulted in higher cumulative N_2O emissions than manure fertilizers, CAN was surpassed by AS (14.8 and 16.7 kg N ha^{-1}, respectively). Mean emissions from the cattle manure fertilizers (FYM, CS, CS_sol, CS_liq) ranged between 3.5 and 8.3 kg N ha^{-1}, and did not differ significantly from the unfertilized control treatment. The cattle manures

were all associated with significantly lower N_2O emissions than AS, and all manures except CS_liq showed significantly lower emissions than CAN (Fig. 5.3). Nitrous oxide emissions under AS and CAN application were particularly high in combination with WIS20. This agrees with the third hypothesis that the frequently anaerobic conditions caused by WIS results in strong N_2O releases from mineral fertilizer applications. This additive effect agrees with hypothesis four, that a shallow GWL enhances the increased N_2O emissions caused by mineral fertilizers further, due to the stimulation of denitrification. Denitrification is commonly identified as a main N_2O producing process, particularly in peat soils (Butterbach-Bahl et al., 2013). Correspondingly, nitrate-holding fertilizers are generally associated with higher emissions than ammonium-based fertilizers (McTaggart et al., 1997; Velthof et al., 1997). The fact that emissions from AS and CAN were not significantly different in our experiment, may indicate that the soil is aerated frequently enough to oxidize the available NH_4^+ to NO_3^-, which can be followed by denitrification. Mean yearly emission factors for CAN and AS showed a wide range between 2.6 and 8.6% (Table 5.6), but mostly these exceeded the EF of 3% used in the Dutch national inventory report for mineral fertilizer applied to organic soils (RIVM, 2025; Van der Zee et al., 2025), or the IPCC default EF of 1.6 % for synthetic fertilizers in wet climates (IPCC, 2019). The application of ammonium sulphate obtained from NH_3 scrubbing systems as an alternative to manure fertilizers has clear advantages, including reduced nitrate leaching after land application and improved nutrient recycling (Bittman et al., 2014; Huygens et al., 2020). An adverse effect of using mineral fertilizers on grasslands on organic soils is a relatively high N_2O production due to easily available NH_4^+ and/or NO_3^-. This study suggests that a RENURE fertilizer like ammonium sulphate is no exception to this effect.

The mean manure emission factor of 1.1 % ± 0.2 (mean over the four manure fertilizers, three fields and two years) was similar to the currently used EF of 1% for shallow injection of cattle slurry to organic soils and over two times higher than the current 0.5% EF for surface spreading (Van der Zee et al., 2025; Velthof & Mosquera, 2011a). Slurry injection decreases the risk of NH_3 volatilization compared to surface spreading (Bittman et al., 2014; Van Der Weerden et al., 2021; Webb et al., 2010). This results in a higher N input into the soil, and potentially increases N_2O emissions (Van Der Weerden et al., 2021; Webb et al., 2010). The CS and CS_liq treatments in this study were applied via band spreading with a trailing hose (simulated by using a watering can), which

performs intermediary between surface spreading and injection in terms of NH_3 losses (Webb et al., 2010). Yearly N_2O emission factors for the manure fertilizers showed a wide range between -0.6 and 3.9%, however, with negative to low values for CS_sol and relatively high values for CS_liq and FYM under CDD and WIS20 (Table 5.6). Emission factors from fields fertilized with CS varied strongly between CDD (1.6 %) and WIS40 and WIS20 (both 0.8%). The strikingly high FYM emission factors may be due to the application scheme. This treatment was split over two applications of 60-80 kg N ha^{-1} each, instead of one high application followed by two or three smaller ones, as was practice for the slurry and mineral fertilizers (Table 5.2). Due to unexpectedly high N contents of the FYM, an amount of 176 instead of 60 kg N ha^{-1} was applied in August 2024. High N application in the late summer (from September onwards) may be accompanied by higher soil moisture content and lower N uptake by the grass than earlier in the summer, resulting in relatively high losses as N_2O (Chadwick et al., 2011). This risk is intensified by the typically low content of readily available N and slow release of organic N in FYM (Bell et al., 2016). Unlike the FYM, CS_sol and CS fertilizers, the liquid fraction of cattle slurry did not result in significantly lower (yield-scaled) cumulative emissions than the mineral fertilizers (Fig. 5.3, Fig. 5.4). This may be due to the high moisture content of the fractionation product, which accelerates entry into the soil and can stimulate denitrification losses (Wang et al., 2024). There are indications that liquid slurry fractions can be useful for precise fertilizer application and are associated with lower NH_3 losses than untreated slurry (Wang et al., 2024). Both emissions and yields were higher under the separated CS_liq than the untreated CS, but the differences were not significant (Fig. 5.3, Table 5.5). Mechanical screw press separation alone may not significantly alter nutrient losses or uptake following land application (Holly et al., 2017; Hunt et al., 2019); however, several studies indicate that the addition of flocculants enhances the removal of organic particles from the liquid slurry fraction, thereby substantially modifying its properties and environmental effects (Gao & Wang, 2025; Wang et al., 2024a).

Emissions resulting from fertilizer application, particularly of mineral fertilizers, appeared to contribute more to cumulative N_2O than the background emissions, as measured in the control plots (Fig. 5.3). In a model study by Wang et al. (2024b), background emissions originating from peat oxidation (and to a small extent from atmospheric N deposition) were found to contribute more to total cumulative N_2O than fertilization. Likewise, many studies highlight the potential of rewetting to reduce N_2O

emissions (e.g. Leppelt et al., 2014; Liu et al., 2020). In particular for grassland soils, Wang et al. (2024b) concluded that the largest emission mitigation can be achieved by reducing peat oxidation, rather than by changing the fertilization strategy (i.e. implementing a 20% reduction by 2030). Average fertilizer inputs to temperate grasslands included in their study were only 67 kg N ha^{-1} yr^{-1}, which is 2.5-3.8 times lower than the yearly N application in our experiment (Table 5.2). Under intensive fertilization, the potential emission reduction by lowering application rates is therefore still high, even compared to reducing peat oxidation (Wang et al., 2024b).

5.4.2.2 Yield

In our study, mineral fertilizer treatments (AS and CAN), while producing the highest emissions, showed the highest above-ground dry matter yields and N uptake (Fig. 5.4, Table 5.5), confirming our third hypothesis. Significant pair-wise differences were observed between the fertilizer types, despite similar N application rates. All fertilizer treatments increased ($p < 0.05$) yields compared to the unfertilized control plots. Still, the background N supply by the soil following organic matter oxidation was the main contributor to N uptake: on average, the yearly control N uptakes comprised 64 to 95% of the fertilizer N uptakes (Table 5.5). In the control plots, mean N uptakes (over the three drainage types) of 215 kg N ha^{-1} and 182 kg N ha^{-1} were measured in 2023 and 2024, respectively, approaching or even exceeding the total fertilizer N application in those respective years (excluding the FYM applications, Table 5.2). These unfertilized N uptake rates, which can be attributed to the soil nitrogen supply (SNS), fall towards the lower end of previous observations on temperate peat grasslands (Deru et al., 2019; Sonneveld & Lantinga, 2011; Vellinga & André, 1999). The default SNS value provided in the current fertilization guideline for grasslands on peat soils in the Netherlands is 250 kg N ha^{-1} yr^{-1} (CBGV, 2026).

The aboveground N uptake by crops typically shows an asymptotic relationship with N availability, with diminishing returns on increasing availability. The growth and thereby the N uptake become limited by other requirements, once the N demand is met (De Wit, 1992). In drained peat soils, the soil N supply is typically high as a result of organic matter decomposition, sometimes complemented by application of fertilizers, cattle excreta or other amendments in previous years (Sonneveld & Lantinga, 2011; Van Beek et al., 2009). The importance of organic matter decomposition for the herbage growth becomes apparent from the

significantly higher N uptake under CDD than WIS40 or WIS20 (Table 5.5). The efficiency of additional (fertilizer) N supply, however, is limited compared to mineral soils. This may create a negative relationship between apparent nitrogen recovery and SNS and a risk of gaseous and leaching N losses (De Visser et al., 2001; Deru et al., 2019; Van Beek et al., 2009; Vellinga & André, 1999).

5.4.2.3 Apparent nitrogen recovery

High SNS due to organic matter mineralization may decrease the ANR of fertilizer application in peat soils (Vellinga & André, 1999). The ANR values observed in this study (Fig. 5.5) were relatively low compared to previous observations on peat soils (Deru et al., 2019). Still, the ANR differed strongly between fertilizer types and suggested more efficient use of N applied in mineral fertilizers (AS and CAN) than in manure fertilizers (particularly FYM, CS_sol and CS). The high ANR values in the mineral fertilizer plots - with mean values up to 59% - coincided with highest cumulative N_2O losses under these treatments (Table 5.5, Fig. 5.3). Mean ANR of the manure fertilizers, on the other hand, ranged between 2.3 and 39.8%, indicating 101 to 235 kg N from total the applied N may have been lost either through gaseous emissions (N_2O, N_2 and NH_3) or leaching (NO_3^- or dissolved N). Based on the cumulative N_2O, ANR and N application data in this study, non-N_2O losses from manure fertilizers are estimated to range between 94 and 234 kg N ha^{-1}. Following the same reasoning, non-N_2O N losses from AS and CAN application were lower, 29 - 93, respectively 61 - 112 kg N per hectare. This may indicate a trade-off between the different environmental impacts of fertilizer applications and how they are affected by management measures (Amon et al., 2006; Velthof et al., 2024). Alternatively, the release of organic N from the manure fertilizers was still ongoing as it usually takes several years for all N to be mineralized.

5.5 Conclusion

Grasslands on peat soils form an important source of N_2O emissions due to intensive peat drainage and fertilization. The results of this experiment highlight the importance of drainage intensity and fertilizer type. Highest N_2O emissions were observed under the WIS20 treatment, confirming our hypothesis that a shallow drainage level creates a risk of high N_2O emissions from peat grasslands. The implementation of a WIS aimed at a moderate GWL around -40 cm, on the other hand, can help to reduce N_2O emissions from peat mineralization and fertilization.

For the choice of fertilizer, a trade-off must be considered. Mineral fertilizers (CAN and AS) resulted in high N_2O emissions compared to the manure fertilizers on the one hand, while also producing the highest grass (N) yield. Additionally, the low ANR of the manure fertilizers (cattle slurry products and FYM), suggest N losses in other forms than N_2O, thereby creating a trade-off between different environmental impacts. In accordance with the final hypothesis, the overall highest (yield-scaled) cumulative emissions were found under a water infiltration system aimed at a shallow groundwater level (-20 cm) in combination with CAN or AS fertilization.

Acknowledgements
This project is funded by the Dutch Ministry of Agriculture, Fisheries, Food Security and Nature. The research presented in this paper is part of the project Living on soft soils: subsidence and society (grantnr.: NWA.1160.18.259). This project is funded by the Dutch Research Council (NWO-NWA-ORC), Utrecht University, Wageningen University, Delft University of Technology, Ministry of Infrastructure & Water Management, Ministry of the Interior & Kingdom Relations, Deltares, Wageningen Environmental Research, TNO-Geological Survey of The Netherlands, STOWA, Water Authority: Hoogheemraadschap de Stichtse Rijnlanden, Water Authority: Drents Overijsselse Delta, Province of Utrecht, Province of Zuid-Holland, Municipality of Gouda, Platform Soft Soil, Sweco, Tauw BV, NAM. We would like to thank all researchers, technicians, laboratory staff and field staff who have facilitated or contributed to this project. In particular, we are grateful to Karel van Houwelingen for his contribution to the realization of the experiment.

Chapter 5 Supplementary material

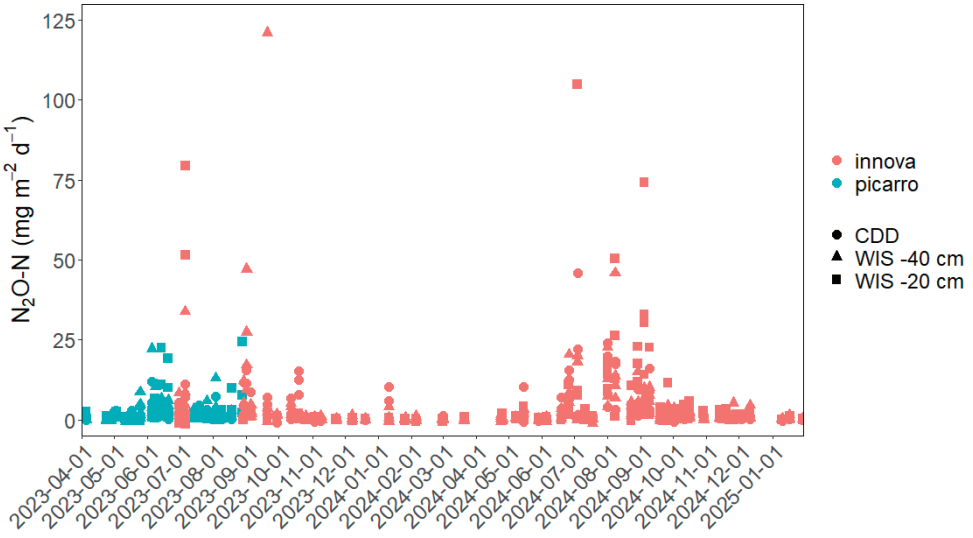


***Figure S5.1**: Time series of the observed N_2O emissions (mg N m^{-2} d^{-1}), measured using the Picarro G2508 cavity ring down spectroscopy analyzer (05-04-2023 to 28-08-2023) or the Innova 1512 photoacoustic infrared spectroscopy analyzer (28-08-2023 to 29-01-2025). CDD, conventional ditch drainage; WIS40, water infiltration system at -40 cm; WIS20, water infiltration system at -20 cm.*

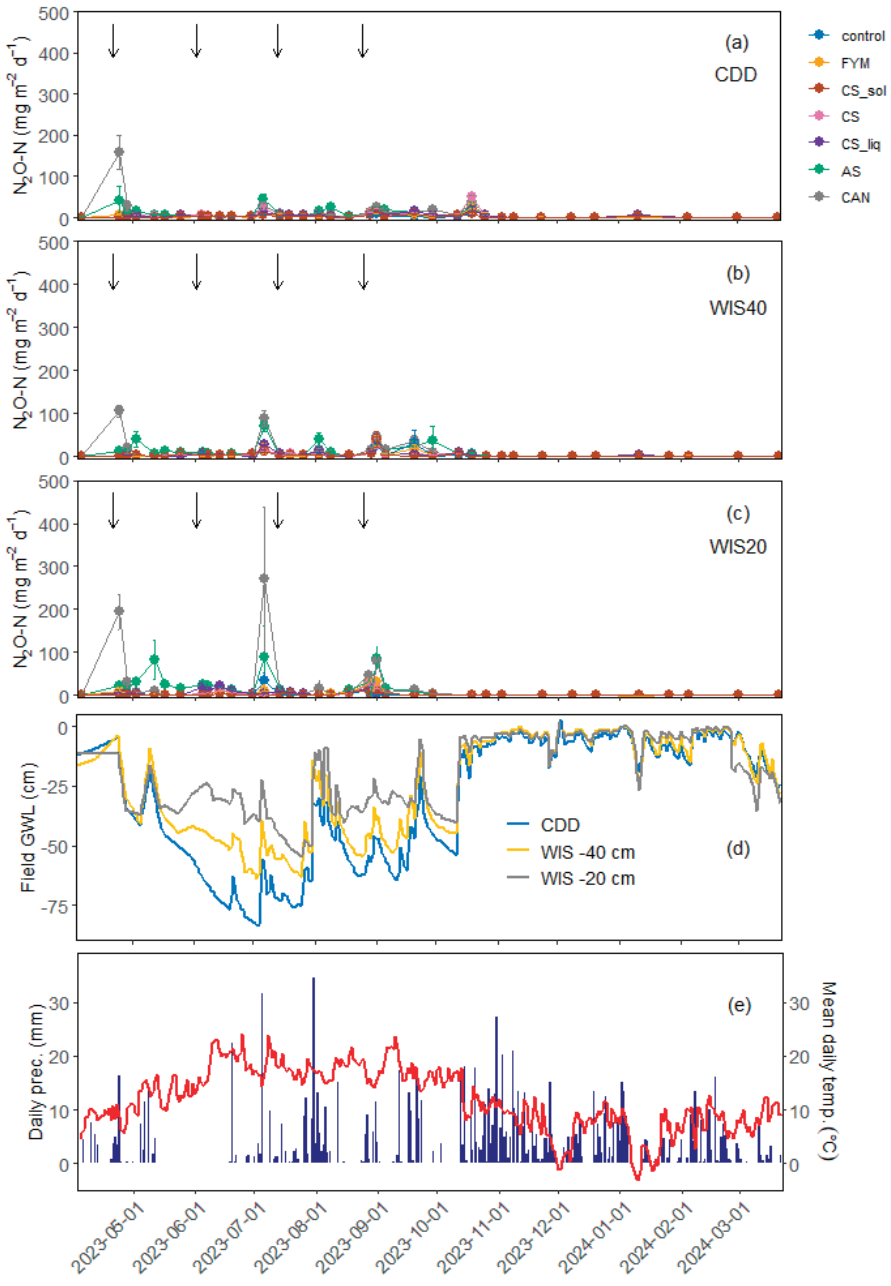


***Figure S5.2**: Mean N_2O emissions (n = 4) over the first year of the experiment on the CDD field (a), WIS -40 cm (b) and WIS -20 (c), the groundwater levels in the three fields (d), and the total daily precipitation and mean daily temperature (e). FYM, farmyard manure; CS_sol, solid fraction of cattle slurry; CS, cattle slurry; CS_liq, liquid fraction of cattle slurry; AS, ammonium sulphate; CAN, calcium ammonium nitrate.*

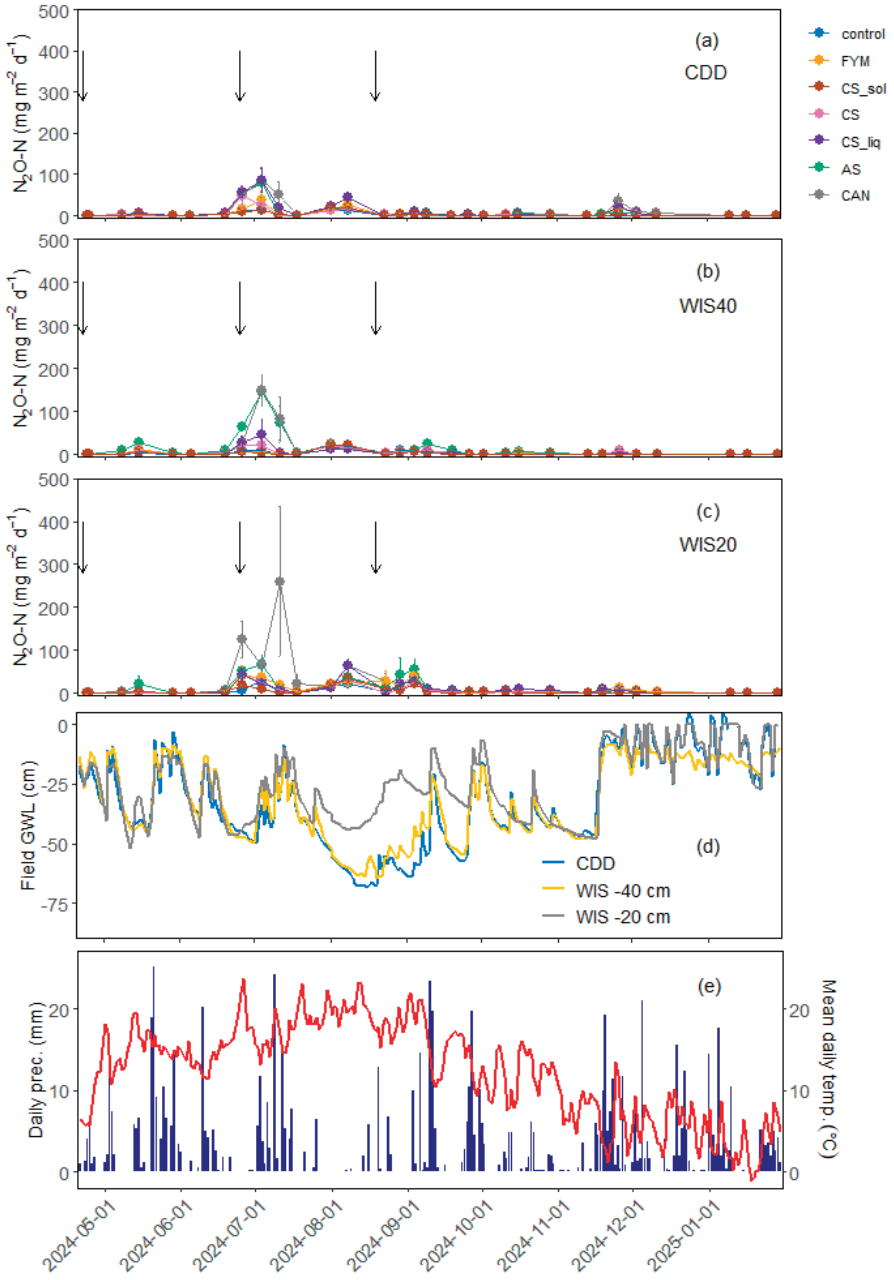


***Figure S5.3**: Mean N_2O emissions (n = 4) over the second year of the experiment on the CDD field (a), WIS -40 cm (b) and WIS -20 (c) and the total daily precipitation and mean daily temperature (d). FYM, farmyard manure; CS_sol, solid fraction of cattle slurry; CS, cattle slurry; CS_liq, liquid fraction of cattle slurry; AS, ammonium sulphate; CAN, calcium ammonium nitrate.*

***Table S5.1**: Monthly and yearly summaries of the mean daily temperature and total precipitation measured at the field site during the experiment.*

	2023		2024		2025	
	mean daily temp. (°C)	total prec. (mm)	mean daily temp. (°C)	total prec. (mm)	mean daily temp. (°C)	total prec. (mm)
January	5.6	125.4	3.8	73.8	3.5	93.0
February	5.6	23.4	8.0	111.4		
March	6.7	89.2	8.6	45.2		
April	8.5	57.0	10.4	80.8		
May	13.1	42.2	15.3	143.4		
June	18.8	27.4	15.6	45.8		
July	17.8	132.4	17.8	101.4		
August	17.4	91.2	19.1	30.6		
September	17.5	84.8	15.7	132.8		
October	13.1	208.4	12.0	43.6		
November	7.8	174.2	6.9	92.6		
December	6.7	105.8	6.1	90.8		
Full year	11.6	1161.4	11.6	992.2		

***Table S5.2**: Compositions of the undiluted ammonium sulphate and manure treatments, before each application. All concentrations are expressed as g kg^{-1} fresh material. The notation "nm" indicates that a property was not measured. FYM, farmyard manure; CS_sol, solid fraction of cattle slurry; CS, cattle slurry; CS_liq, liquid fraction of cattle slurry; AS, ammonium sulphate; CAN, calcium ammonium nitrate.*

Date	Fertili-zer	Dry weight (g kg^{-1})	Ash content (g kg^{-1})	SOM (g kg^{-1})	N-tot. (g kg^{-1})	C/N	N-NH_3 (g kg^{-1})	N-organic (g kg^{-1})	P_2O_5 (g kg^{-1})	K_2O (g kg^{-1})	MgO (g kg^{-1})	Na_2O (g kg^{-1})
21-4-2023	AS	nm	nm	nm	44.4	nm	40.9	3.5	0.16	0.2	0.7	2.6
	CS_liq	61	19	42	3.92	5	1.8	2.1	1.26	6.5	1.5	1.1
	CS	70	19	51	4.11	6	1.8	2.3	1.28	6	1.5	0.9
	CS_sol	302	39	263	5.78	20	1.3	4.5	3.18	4.5	3	0.8
	FYM	173	26	147	4.3	15	0.5	3.8	1.67	5.9	1.3	0.5
2-6-2023	AS	nm	nm	nm	44.4	nm	40.9	3.5	0.16	0.2	0.7	2.6
	CS_liq	56	18	38	3.24	5	1.7	1.5	1.12	6.1	1.3	0.9
	CS	63	19	44	3.29	6	1.7	1.6	1.17	6.1	1.3	0.9
	CS_sol	295	44	251	6.29	18	1.2	5.1	3.23	5.1	2.7	0.8
13-7-2023	AS	nm	nm	nm	44.4	nm	40.9	3.5	0.16	0.2	0.7	2.6
	CS_liq	52	15	37	3.17	5	1.4	1.8	1.12	6	1.5	0.9
	CS	68	16	52	3.31	7	1.4	1.9	1.19	5.9	1.5	0.9
	CS_sol	369	51	318	6.97	21	0.8	6.2	3.39	4.6	3.5	0.8
25-8-2023	AS	nm	nm	nm	44.4	nm	40.9	3.5	0.16	0.2	0.7	2.6
	CS_liq	43	13	30	2.58	5	1.2	1.4	0.82	4.8	1.2	0.8
	CS	58	14	44	2.71	7	1.2	1.5	0.94	4.8	1.2	0.8

Date	Fertili-zer	Dry weight (g kg^{-1})	Ash content (g kg^{-1})	SOM (g kg^{-1})	N-tot. (g kg^{-1})	C/N	N-NH_3 (g kg^{-1})	N-organic (g kg^{-1})	P_2O_5 (g kg^{-1})	K_2O (g kg^{-1})	MgO (g kg^{-1})	Na_2O (g kg^{-1})
	CS_sol	314	56	258	5.74	20	1.1	4.6	3.53	4.1	3.3	0.7
	FYM	216	84	132	6.6	9	0.8	5.8	4.53	9.5	2.8	0.8
22-4-2024	AS	190	20	170	41	2	nm	nm	0.27	0.2	0.7	2.7
	CS_liq	61	24	37	3.34	5	1.4	1.9	1.15	5.7	1.8	0.9
	CS	78	23	55	3.5	7	1.5	2	1.26	5.7	1.8	0.9
	CS_sol	377	61	316	6.41	22	1.2	5.2	3.5	4.8	3.2	0.8
	FYM	248	66	182	7.89	10	0.8	7.1	4.85	9.4	2.7	1.2
25-6-2024	AS	190	20	170	41	2	nm	nm	0.27	0.2	0.7	2.7
	CS_liq	57	19	38	3.46	5	1.4	2.1	1.12	6	1.5	0.9
	CS	71	20	51	3.54	6	1.3	2.2	1.26	6	1.7	0.9
	CS_sol	314	51	263	5.71	21	1.4	4.3	3.53	4.5	3.3	0.8
19-8-2024	AS	190	20	170	41	2	nm	nm	0.27	0.2	0.7	2.7
	CS_liq	53	15	38	3.15	5	1.3	1.9	1.08	5.3	1.5	0.8
	CS	76	20	56	3.34	8	1.4	1.9	1.24	5.3	1.5	0.8
	CS_sol	362	56	306	6.87	20	1.3	5.6	3.41	5.9	3.3	0.8
	FYM	469	85	384	14.8	12	0.5	14.3	4.95	23.4	5.1	5.3


6

Chapter 6

General discussion

Erne Blondeau

6.1 Introduction

Peat soils provide important ecosystem services such as climate regulation, water regulation, biodiversity conservation and crop production and contribute to several sustainable development goals (Batjes, 1996; Deru et al., 2018). In particular the carbon (C) storage capacity in peat soils is impressive: on only 3-4% of the terrestrial land surface, peat soils currently store globally about 25% of the soil C pool (Jobbagy & Jackson, 2000; Loisel et al., 2014; UNEP, 2022). Drainage activities for agriculture and forestry, as well as peat excavation cause worldwide degradation and disappearance of peatlands. In Europe around 10% of the original peat area has been lost as a result of this (UNEP, 2022). In the Netherlands, an estimated volume of 19.8 km^3 of the initial peat has been lost (Erkens et al., 2016). Currently, peat soils cover 11% of the Dutch land area and are mainly in use as grasslands for dairy farming (RIVM, 2026). Drainage of peat grasslands results in high emissions of CO_2 and N_2O, and soil subsidence (Erkens et al., 2016; Hiraishi et al., 2014; Massop et al., 2024; Wang et al., 2024b).

In this PhD thesis I explored the effects of soil conditions, groundwater level management and fertilization and grazing on peat oxidation and the emissions of carbon dioxide (CO_2) and nitrous oxide (N_2O). I specifically aimed to:

1. Explore the controls of soil moisture, soil temperature and peat properties on peat oxidation;
2. Study the potential of water table change to reduce CO_2, N_2O and methane (CH_4) emissions associated with peat oxidation and the possibility of a trade-off between these gases;
3. Study the effect of water infiltration systems (WIS), via submerged drains on N_2O emissions in both fertilized and grazed peat grasslands;
4. Quantify N_2O emissions and emission factors for different mineral fertilizers, processed manures and grazing.

I addressed objective 1 in **Chapter 2**, by measuring the heterotrophic respiration rates, as an indicator of peat oxidation, under controlled conditions in small soil samples. In accordance with kinetic theory, the respiration rate showed a positive relation with soil temperature, which in turn decreased in strength with increasing temperature. Respiration was expected to show a unimodal response to soil moisture under the studied treatment interval of 50 - 95% water-filled pore space (WFPS). Instead,

respiration increased with WFPS under the studied treatments of 50, 60 and 80%, and maintained the highest rate under 95% WFPS. This indicates that moisture availability was a limiting factor for peat soil respiration under a WFPS of 60% and lower (and possibly already at intermediate WFPS values between 60 and 80%). Increased respiration may also be explained by the contribution of anaerobic respiration mediated by alternative electron acceptors. I observed a trend of decreasing temperature sensitivity with increasing WFPS, suggesting that peat oxidation is most susceptible to warming under dry and cold conditions.

In **Chapter 3** I scaled up from small samples to 1 m tall, undisturbed peat cores, in order to study the effect of groundwater level (GWL) on peat oxidation and associated greenhouse gas (GHG) emissions (objective 2). During the step-wise water table changes, I observed highest average CO_2 emissions at a GWL of -80 cm (although there was no significant difference between the GWL treatments), while continued drainage down to -160 cm did not further increase emissions. In agreement with the findings in chapter 2, these results suggest that a moisture limitation, particularly in the upper 20 cm of the soil cores, determined the stabilizing rate of CO_2 emissions during prolonged drainage. I observed that CO_2 emissions dominated the total (CO_2-equivalent) GHG emissions under all groundwater levels between -20 and - 160 cm, but not at saturation (0 cm). This was due to strong N_2O peaks, particularly after a GWL rise from -20 to 0 cm. Methane emissions added low or even negative contributions to the total CO_2-equivalent emissions. I related the GHG emission rates to the mineral N and C concentrations measured in pore water and concluded from this experiment that frequent GWL variations in the top soil generate a risk of high peat oxidation associated with CO_2 emissions and strong N_2O peaks after rewetting events such as precipitation. It is likely that, due to permanent anaerobic conditions, N_2O emissions would decrease again under permanent flooding. Therefore, the best strategy to reduce GHG emissions might be to maintain permanent anaerobic conditions, by keeping the GWL at the soil surface or above.

In **Chapters 4 and 5**, I expanded my analysis to the field scale, examining how a water management measure, which aims for oxidation mitigation, affects N_2O emissions.

In **Chapter 4**, I studied the impact of WIS in combination with grazing effects (urine, dung and trampling applications). A WIS which targeted a relatively stable level around -40 cm reduced GWL fluctuations compared to conventional ditch drainage. Cumulative N_2O emissions resulting from peat oxidation, while not significant, were lower under the WIS treatment than conventional ditch drainage. This was accompanied by increased NH_4^+ concentrations in the soil porewater. Application of cattle urine, however, diminished this effect, indicating that urine excretion on a field with WIS has more impact on N_2O emissions than under conventional drainage. Mean emission factors for urine and/or dung application with or without trampling ranged between -1.0 and 5.0% and were similarly higher under WIS than conventional drainage, although not significant. The emission factors determined in this experiment are lower than those currently used in the Dutch greenhouse gas inventory. These results seem to suggest that conventional drainage produced higher NH_4^+ and NO_3^- availability through peat mineralization, but that a WIS provides the anaerobic conditions which promote denitrification of external mineral N input from grazing. The latter is exacerbated by compaction due to trampling.

In **Chapter 5** I discussed the impact of WIS in combination with different types of fertilizer. The experiment included three drainage treatments: conventional ditch drainage, and a WIS targeting a GWL of -40 cm and -20 cm, respectively. On each field, I compared four cattle manure products (slurry, the liquid and solid fraction of slurry and farmyard manure) and two mineral fertilizers (ammonium sulphate and calcium ammonium nitrate). Analogous to the findings in Chapter 4, I observed lower N_2O emissions under WIS targeting a GWL of -40 cm than under conventional drainage. Conversely, the shallower WIS drainage targeting a GWL of -20, caused emissions almost two times higher than under the other two treatments. Despite higher grass yield and N uptake, and therefore higher N use efficiency, mineral fertilizers (including one recovered from manure) resulted in substantially higher N_2O emissions than the manure fertilizers. The results from this experiment agree with my earlier observation in Chapter 3 that a shallow GWL creates a risk for high N_2O emissions and emphasize the intensification of that risk under application of mineral fertilizers.

In the remainder of this chapter, I discuss the key insights from this study. I discuss recommendations for future research and end with some concluding remarks.

6.2 Oxygen and moisture limitations to peat oxidation

Out of the many negative consequences of peatland management, subsidence and CO_2 emissions are currently the most pressing and apparent (Oleszczuk et al., 2008; Wils et al., 2025). Therefore, the effects of field drainage on CO_2 emissions, as well as the underlying mechanisms have been widely studied (e.g., Aben et al., 2024; Boonman et al., 2022; Byun et al., 2021; Evans et al., 2021; Nielsen et al., 2023; Saurich et al., 2019a). This may help to improve the understanding and implementation of the boundary conditions for peat oxidation in soil modelling (Boonman et al., 2022). As illustrated in Chapter 2 (Fig. 2.1), these boundaries entail a limitation by O_2, as well as soil moisture for oxidation to take place (Berglund & Berglund, 2011; Byun et al., 2021). Contrary to my expectations, oxidation rates did not decrease under the 95% WFPS treatment, but maintained the optimum levels reached under 80% WFPS (Fig. 2.4). These results suggest a significant contribution of anaerobic respiration (Fairbairn et al., 2023), or that a substantial reduction in respiration requires (near) saturated conditions (Berglund & Berglund, 2011). The actual O_2 concentrations or consumption were not measured however, preventing strong conclusions about the WFPS optimum for heterotrophic respiration and the underlying mechanisms. Considering the small size of the samples, O_2 availability may have been relatively high, even at 95% WFPS, as a high surface to volume ratio can enhance the normally slow diffusion of O_2 into pore water (Schjønning et al., 2003). This underlines the limitations of soil respiration measurements on disturbed, repacked samples. This is particularly the case for peat soils, which are characterized by a high pore space, fibrous structure and ability to shrink and swell with changing moisture content (Moyano et al., 2013; Rezanezhad et al., 2016).

While the results of Chapter 2 stress the importance of moisture availability (for the transport capacity of solutes, such as dissolved C and enzymes), the net emissions measured across a one-meter peat profile in Chapter 3 suggested that O_2 availability is the main determinant of oxidation. Initial water table draw-down to 40 cm below the soil surface immediately stimulated CO_2 emissions (Figures 3.2, 3.3 and 3.4). Both observations likely occurred under conditions which amply enable the transport of enzymes and dissolved organic carbon (DOC) while still

providing O_2 for aerobic oxidation. Initial O_2 entry into the top soil of the peat cores in Chapter 3 rapidly stimulated oxidation, but continued drainage did not result in a (substantial) further rise in CO_2 rates. This suggests that, while deeper drainage aerated a new soil layer, simultaneous drought stress may have inhibited oxidation higher up in the profile. Drainage to -80 cm did not, or only slightly, affect the volumetric water content (VWC) in soil layers below 30 cm, but strongly reduced VWC in the upper 20 cm (Fig. S.3.4). The response of the top soil VWC to the subsequent GWL rise was hysteretic - following a different path than during drying - as was the response of CO_2 emissions. The concentrations of DOC, NO_3^- and NH_4^+ and the pH in pore water samples were measured near the water level of the cores during drying and rewetting. The pH and DOC content of the soil solution throughout the soil profile, both indicators of aerobic decomposition (where protons are produced and DOC consumed) had decreased during rewetting relative to the values during drying (Fig. S.3.8). From this I concluded that desiccation strongly inhibited the magnitude of CO_2 emissions during rewetting, in particular in the top soil.

The results from these two lab studies are not fully in line with observations in the field. Most field studies emphasize the impact of drainage on peat oxidation, sometimes even accompanied by estimated global warming impacts per 10 cm drainage (Evans et al., 2021). The drought stress exhibited in the samples and soil cores in my experiments will likely not occur often in the field, where top soil is frequently wetted by precipitation and brought closer to optimum conditions for heterotrophic respiration. The decision to focus on CO_2 emissions from bare peat soil was a practical one, which enabled us to determine losses associated with peat oxidation (heterotrophic respiration). On the other hand, it restricts the potential to extrapolate these results to realistic field situations. Within the C balance of peat grasslands two cycles can be distinguished. First there is the short cycle of photosynthetic C uptake into biomass, and the subsequent decomposition of root exudates and plant litter. Secondly, C is released from the decomposition of "fossil" peat, a pool which can theoretically receive a C input under conditions that hamper the decomposition of plant litter. The net output from the first cycle is subject to diurnal and seasonal variation. Understanding of the net turnover of the short and long cycles together, usually requires measurements (preferably during the day as well as the night) with automated dark and transparent flux chambers to quantify the ecosystem respiration, net ecosystem exchange and gross primary productivity

(Aben et al., 2024; Boonman et al., 2022; Tiemeyer et al., 2024). Calculation of the yearly C budget subsequently entails a gap-filling method to predict the net ecosystem exchange between measurements, using temperature and photosynthetic active radiation (Liu et al., 2022; Nijman et al., 2024). Since Chapters 2 and 3 focused on the mechanisms behind peat soil oxidation, the above methodology did not fit in the scope and budget of this study. Instead, by removing the grass and roots from the top soil, CO_2 fluxes were an expression of heterotrophic respiration, and thereby long cycle peat oxidation, alone.

6.3 Management effects on N_2O emissions from peat grasslands

6.3.1 N_2O emissions from peat oxidation

The scientific consensus about GWL effects on soil subsidence and CO_2 emissions from drained peat soils forms the reasoning behind rewetting or reduced drainage mitigation strategies (Fig. 6.1). In the Netherlands, the objective was formulated to achieve a reduction in yearly emissions from drained peatlands of 1 Tg CO_2-equivalent (Ministry of Agriculture Nature and Food Quality, 2019). This is to be achieved in part, by implementing groundwater levels of -40 to -20 cm in the coastal peat grasslands (Harbers & Heijnen, 2022). Currently, drainage of peat soils is still the largest GHG emission source in the land use, land use change and forestry (LULUCF) sector, with an estimated release of 4.4 Tg CO_2 in 2024 (RIVM, 2026). Additionally, cultivation of organic soils was estimated to release and 0.6 Tg CO_2-equivalent N_2O emissions in 2024, 14% of the total direct and indirect N_2O emissions from Dutch agricultural soils (RIVM, 2026). The estimation is based on an N_2O emission factor for cultivation of organic soils of 0.02 kg N_2O-N per kg mineralized N, or 4.67 kg N_2O-N per ha of peat soil yr^{-1} (Van der Zee et al., 2026). The large variation between years and drainage treatments in Chapter 4 and Chapter 5 demonstrate the difficulty of estimating N_2O emissions based on peat mineralization rates. Control plots in the three grazing treatment campaigns showed emissions ranging from 1.9 – 18.1 and 1.2 – 5.7 kg N_2O-N ha^{-1} over 125 days, on the CDD and WIS40 fields, respectively (Fig. 4.4). The fertilizer experiment showed smaller variation over a longer time span with 0.88 - 6.41 kg N_2O-N ha^{-1} yr^{-1} (CDD), 0.70 – 5.49 kg N_2O-N ha^{-1} yr^{-1} (WIS40) and 5.25 – 7.93 kg N_2O-N ha^{-1} yr^{-1} (WIS20) in the control plots. In Chapter 3, absolute mineralization rates without the uptake of mineral N strongly exceeded the values from the field experiments. In the bare peat cores from three locations in the Netherlands, mean cumulative emissions (over two drying wetting cycles

spanning 370 days) ranged between 15.4 and 29.7 kg N_2O-N ha^{-1} yr^{-1} (Table 3.2).

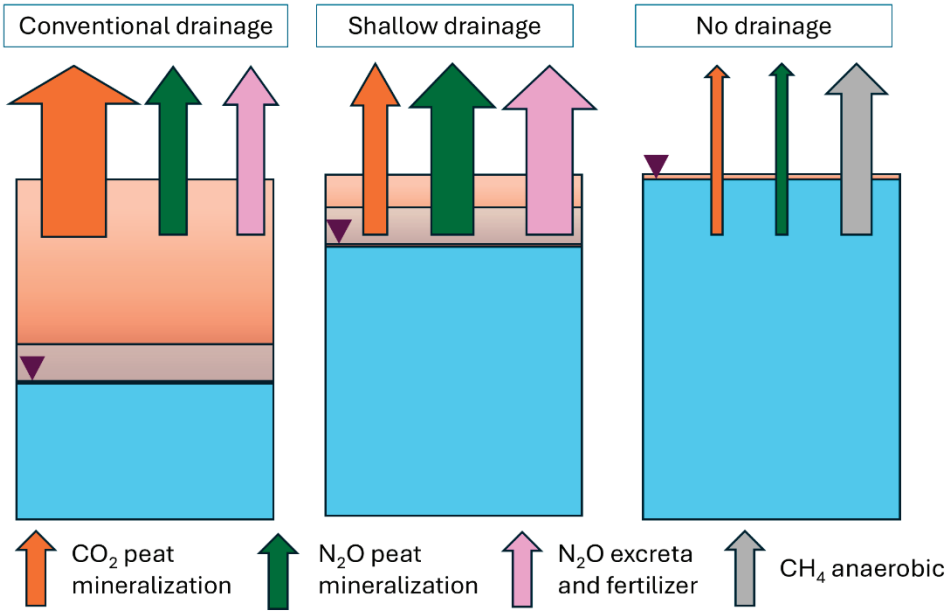


***Figure 6.1**: Expected relative contributions of greenhouse gas emissions under conventional drainage, shallow drainage and no drainage (without excreta and fertilizer application), where carbon dioxide (CO_2) emission decreases with higher GWL, nitrous oxide (N_2O) emissions from peat mineralization, excreta and fertilizer are highest under shallow drainage and methane (CH_4) is only emitted under no drainage.*

Remarkably high N_2O emissions in the grazing experiment were due to the warm and dry conditions of 2022 (summer and autumn campaign), which particularly had an effect on the CDD field. Interannual and seasonal meteorological variations can thus strongly impact the N_2O-N losses from mineralized peat, indicating the necessity for experiments with a time span of at least five years (Berendt et al., 2023; Van 't Hull et al., 2026; Velthof et al., 1996).

While raised groundwater levels will reduce organic-N mineralization (Van Beek et al., 2010; Wang et al., 2024b), the effects on N_2O production are inconsistent and strongly affected by fluctuations in local moisture content (Berendt & Wrage-Mönnig, 2023; Hu et al., 2020). Under high NO_3^- availability, soil anaerobicity may stimulate denitrification. Whether this will result in N_2O emissions, i.e. in a high

N_2O:N_2 ratio of denitrification end products, depends on local soil moisture conditions and O_2 content, NO_3^- content (Clough et al., 2005; Senbayram et al., 2019; Weier et al., 1993; Zhang et al., 2023), pH (Weslien et al., 2009) and residence time in the soil (Clough et al., 2005). An explanation for the N_2O peaks after groundwater level rise in Chapter 3, is the rapid denitrification of available NO_3^- close to the surface. During the last step of rewetting from -20 to 0 cm, high porewater NO_3^- concentrations were measured in the upper 10 cm of the soil, with values up to 220 mg NO_3-N l^{-1} (Fig. S.3.7). Due to the short distance from the surface, N_2O produced at this depth may exit the soil before it is reduced further to N_2. Similar observations were reported in incubation studies (Dinsmore et al., 2009; Taft et al., 2018) and in the field (Velthof et al., 1996).

Although nitrification is an essential step in the transformation of organic N, necessary for denitrification (Regina et al., 1996), N_2O emissions from peat soils are predominantly allocated to other processes than the decomposition of hydroxylamine during nitrification. However, under dry conditions, nitrification can be the dominant N_2O producing pathway (Pihlatie et al., 2004). In Chapter 3, relatively high N_2O emissions were observed during GWL *lowering* in the soil cores from Aldeboarn, at drainage levels of -40 to -80 cm (Fig. 3.2), which could reflect nitrification as the production pathway. Alternatively, this can be explained by downwards leaching of NO_3^- from the aerobic layers into the anaerobic zone (Regina et al., 1996).

In general, the results from Chapter 3 demonstrate the risk that the introduction of moisture in previously dry peat soil, particularly in the top soil, can cause strong N_2O flux events (Fig. 6.1). In a field situation, precipitation can prompt such a result. The results in Chapter 5 suggest that a more frequent shallow GWL may have a similar effect. This was demonstrated by the effect of a water infiltration system targeting a GWL of -20 cm (WIS20). While it did not achieve a constant level of -20 cm, this system elevated the GWL during the summers of 2023 and 2024, compared to conventional ditch drainage or WIS40, which targeted a GWL of -40 cm (Fig. 5.2, Table 5.4). Over the two years, mean N_2O emissions from unfertilized experimental plots under this shallow drainage exceeded those under the other two drainage treatments (Fig. 5.3). However, this was solely attributed to the results of the second year (2024-2025), while little difference was observed between drainage treatments in the first year (2023-2024). Similarly, large differences in emissions between 2022 and 2023 were observed in Chapter 4 (Fig. 4.4). Nitrous oxide emissions are subject to seasonal changes and sometimes high interannual

variability (Velthof et al., 1996). The results from this thesis suggest a risk for N_2O peaks under shallow (summer) groundwater levels, but were subject to interannual variation. The efficacy of WIS to reduce N_2O emissions is therefore not straight-forward and requires further research (Offermanns et al., 2023; Weideveld et al., 2021). The correct implementation and management of WIS are critical for the desired outcome, and local site conditions need to be taken into account (van de Craats et al., 2025). Future research should include multiyear observations on several field sites, with different hydrological characteristics and soil conditions (e.g. the occurrence of upwards seepage).

6.3.2 Effects of N management

While organic carbon mineralization is an important source of N_2O emissions from managed peat lands, fertilizer applications and grazing constitute the major other part (Fig. 6.1). The results in Chapters 4 and 5 suggest that a more frequent shallow GWL may exacerbate the N_2O production from these sources.

Grassland is the predominant land use of peat soils in Europe, particularly in the Netherlands (UNEP, 2022). This is generally combined with cattle farming, grazing and N amendments using manure and/or mineral fertilizers. The application of animal manure is restricted in the Netherlands and some other EU member states to prevent water pollution, which is one of the measures of the Nitrates Directive (Councel of the European Communities, 1991). Manure is frequently processed to help improve nutrient utilization, by creating fractions of different composition, in particular with regards to the organic matter and NH_4^+ contents. Products are eligible for the label RENURE when mineral N ≥90% of the total N content and the total organic carbon to total N ratio does not exceed 3 kg kg^{-1} (Huygens et al., 2020). Manure fertilizers adhering to these criteria are expected to enable relatively fast infiltration in the soil and subsequent plant uptake, therein resembling mineral fertilizers (Saju et al., 2023).

The default emission factor for fertilizer application provided by the IPCC predicts a 1% loss of applied N for all fertilizers, or disaggregated factors of 1.6% and 0.6% for synthetic fertilizers and other N inputs, respectively (IPCC, 2019). The Netherlands has formulated country specific N_2O emission factors that disaggregate (amongst others) for fertilizer type (inorganic or animal manure), soil type (mineral or organic soils) and for the application method of animal manures (surface

spreading or incorporation into the soil), as well as grazing. For grasslands on organic soils, N_2O EFs are 3%, 0.5%, 1% and 6% for inorganic fertilizers, manure spreading, manure injection, and grazing, respectively (Van der Zee et al., 2026). The EFs for manure spreading and injection are based on observations in an incubation study, which were multiplied with a conversion factor to make them applicable to field conditions (Velthof & Mosquera, 2010, 2011a). While these factors provide crucial differentiation of N_2O emissions from peat soils, that is lacking in the IPCC default equations, the underlying methodology does not meet the preferred standard for EF estimation (De Klein et al., 2020). Similarly, the EFs for inorganic fertilizer and grazing were determined in a relatively old study (Velthof et al., 1996). Chapters 4 and 5 provide data to improve the national emission estimates in the future, and to expand the EF disaggregation to the solid and liquid fraction of cattle slurry, farmyard manure and ammonium sulphate.

In both the grazing (Chapter 4) and fertilizer experiment (Chapter 5), EF variation between the two measurement years was too high to detect significant differences between WIS treatments. The grazing treatments did show consistently higher EFs under WIS40 than CDD (Table 4.3). Mean EFs from mineral and organic fertilizer followed the order WIS20 > CDD > WIS40 (Table 5.6). It is therefore still difficult to conclude a general interaction effect between raising the GWL through WIS and fertilizer or grazing N inputs on N_2O emission factors. This means more observations are necessary for a disaggregation of the factor drainage intensity in organic soils. The same conclusion applies to differentiation between manure processing products. Emissions and emission factors increased in the expected order, with decreasing C/N ratio, CS_sol < CS < CS_liq, yet without significant pair-wise differences (Fig. 5.3, Table 5.6, Table S5.2). The mean EF for all manures (including FYM) agrees with the currently used EF for manure incorporation in organic soils in the Netherlands (1.1% versus 1%).

Our observations for mineral fertilizers, on the other hand, consistently exceeded the currently used 3% EF. Repetition of these treatments is necessary for robust disaggregated EFs for mineral fertilizers, yet these results already provide some important considerations for peat grassland management options. The cumulative N_2O observations in chapter 5 suggest that implementation of WIS aiming for a shallow GWL can best be combined with a manure fertilizer that is relatively high in organic carbon content (Fig. 5.3). Inorganic fertilizers

(including RENURE) on the other hand, should be avoided in combination with raised GWLs.

6.4 A broader view on grassland cultivation on peat soils

One important limitation to my research project was the limited focus on CH_4 emissions, which were only included in the measurements of Chapter 3. While CH_4 emissions from the peat cores were erratic and generally absent, this may not rule out CH_4 formation in field conditions. Because the experiment studied the relatively short-term effects of drying and rewetting on GHG emissions, flooded conditions were not maintained for longer than five weeks. Absence of CH_4 emissions may be due to the oxidation of other electron acceptors present in the soil profile, during the preceding period of drainage, which inhibited methanogenesis during the flooded period (Bridgham et al., 2013; Knorr et al., 2009). However, the methanogenic potential of peat grasslands may be small in general, due to low presence of monomers and fermentation products in the subsoil (despite suitable anaerobic conditions) and aerobic conditions in the topsoil which prevent methane fermentation of the abundant labile C fractions (Schlesinger & Bernhardt, 2013; Van den Pol-van Dasselaar et al., 1997). Abundance of NO_3^- after fertilizer application can inhibit methanogenesis by providing an energetically more favorable anaerobic oxidation pathway. Nevertheless, CH_4 emissions from the soil remain challenging to measure. Methane has the ability to rapidly leave the soil in the shape of gas bells, thereby circumventing contact with O_2 in aerobic soil layers (Abdalla et al., 2016). These events are difficult to capture with low frequency measurements. Another bypass mechanism for CH_4 emissions in wetlands is transportation through the vessels of aerenchymatous plants (Abdalla et al., 2016; Bridgham et al., 2013). Additionally, drainage ditches on agricultural soils were estimated to emit 12.0 Mg CH_4 in 2024, equal to 0.3 Tg CO_2 (RIVM, 2026) and can contribute up to 70% of total CH_4 emissions from the farm land and ditches (not including enteric fermentation) (Schrier-Uijl et al., 2010). The observations from the unvegetated soil cores in Chapter 3 therefore by no means give a complete picture of the potential CH_4 formation, consumption and transport mechanisms in a field situation.

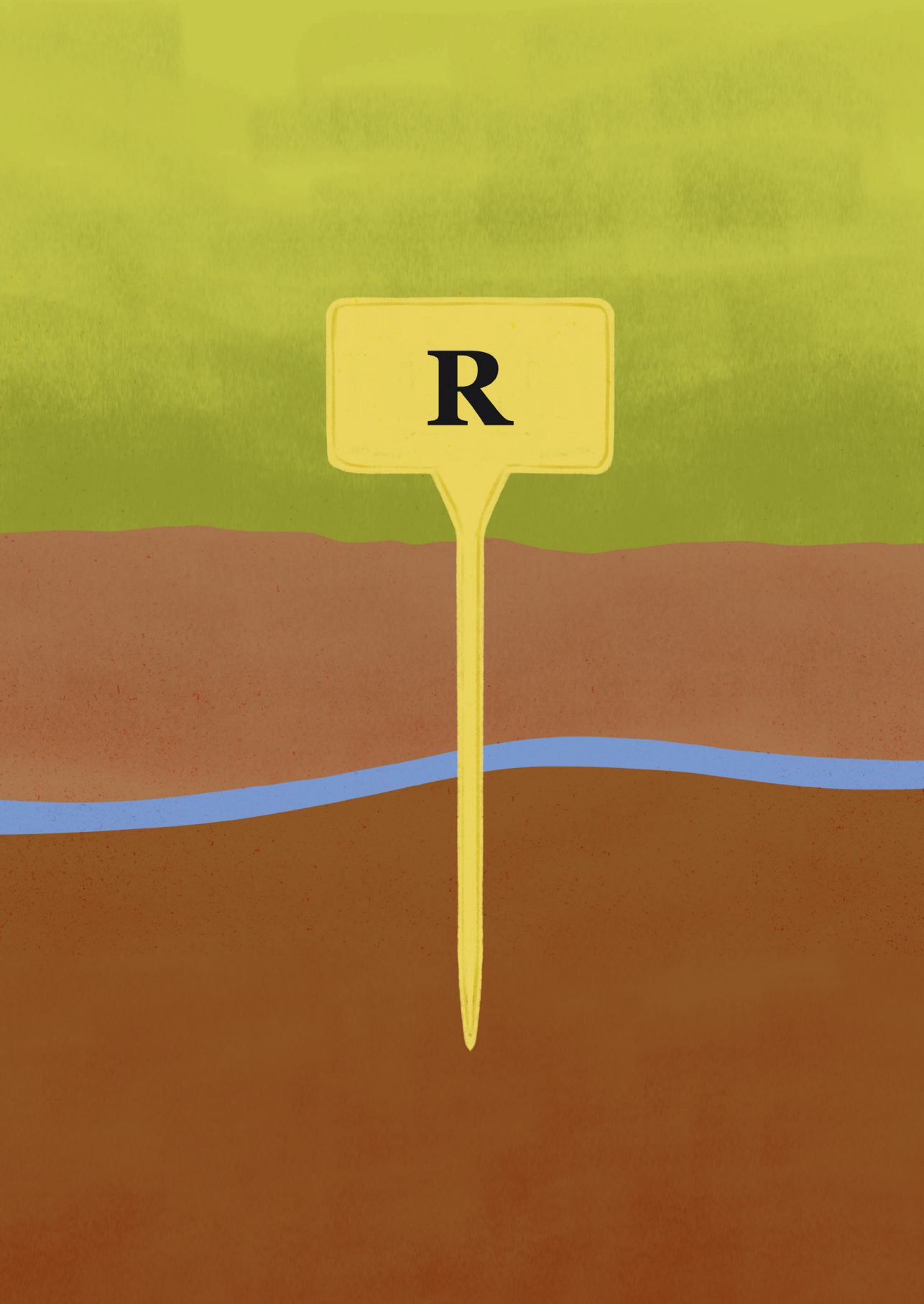
Methane is commonly the main GHG emitted from natural peatlands (Abdalla et al., 2016). Some studies have attributed a rise in CH_4 emissions after peatland restoration to the high availability of labile C present in the soil as a legacy from the years of drainage. Conversely, CH_4 emissions were low or absent in long term natural peatlands (Abdalla

et al., 2016). A transition period of relatively high CH_4 emissions may therefore be inevitable. While this can have large impact on the short-term – the 20-year warming potential of CH_4 is estimated to be 80 times as high as CO_2 (Forster et al., 2021) – there is general confidence that the avoidance of CO_2 losses in the long term compensates for the CH_4 emissions that come in their place (Evans et al., 2021; Gunther et al., 2020).

There seems to be, in short, strong indication that the trade-off between avoided CO_2 emissions and created CH_4 emissions does not overturn the positive climate effects of peatland rewetting. The dilemma rather concerns the stakeholders involved, who are experiencing the costs and benefits of the current land use (Wils et al., 2025). In recent years, research on wet agriculture and peatland restoration has increased. In some cases the call for a more radical transformation of the current land use of European peatlands has become more present, while emphasizing the complexity of the natural and social mechanisms involved, which ultimately determine the success rate of a transition (Freeman et al., 2022; Jurasinski et al., 2020; Stouthamer et al., 2020; Zak & McInnes, 2022). Current use of the Dutch coastal peat soils requires periodic lowering of the regional groundwater levels, to catch up with soil subsidence (Van den Born et al., 2016). The results of soil subsidence are costly for the regional water authorities, regional and national governments, as well as the people living and working in the peat areas, as infrastructure damage and flood risk continues to increase (Van den Born et al., 2016). Simultaneously, emission reduction goals demand (partial) rewetting of the soils (Ministry of Agriculture Nature and Food Quality, 2019). Yet cultural factors, questions of responsibility and lack of a collective sense of urgency complicate decision-making (Van den Ende et al., 2023; Wils et al., 2025).

As this thesis shows, the biological processes underlying the climate impact from drained peat grasslands are complex as well. There may not be one method to control this agricultural system with the least climate and environmental impact. The management of cattle excreta and manure and application to grassland systems has multiple facets, where measures to reduce NH_3-N losses increase the risk for N_2O emissions, especially on organic soils (Velthof et al., 2024). Additionally, CH_4 emissions from enteric fermentation and manure management in livestock production systems are the largest GHG source in the agriculture sector in the Netherlands (RIVM, 2026). While I have focused on exclusively on soil GHG emissions, the mitigation potential of transforming

the land use of peat grasslands in the Netherlands is not limited to the soil emissions alone. Understanding the effects of grassland management measures is useful in the short term, yet alternative land uses may be more viable for this region in the long term.


R

References

Abalos, D., De Deyn, G., Kuyper, T., & van Groenigen, J. (2014). Plant species identity surpasses species richness as a key driver of N2O emissions from grassland. *Global Change Biology, 20*, 265-275. doi:10.1111/gcb.12350

Abbasi, M. K., & Adams, W. A. (2000). Gaseous N emission during simultaneous nitrification-denitrification associated with mineral N fertilization to a grassland soil under field conditions. *Soil Biology & Biochemistry, 32*(8-9), 1251-1259. doi:10.1016/s0038-0717(00)00042-0

Abdalla, M., Hastings, A., Truu, J., Espenberg, M., Mander, Ü., & Smith, P. (2016). Emissions of methane from northern peatlands: a review of management impacts and implications for future management options. *Ecology and Evolution, 6*(19), 7080-7102. doi:10.1002/ece3.2469

Aben, R., van de Craats, D., Boonman, J., Peeters, S., Vriend, B., Boonman, C., . . . van den Berg, M. (2024). CO2 emissions of drained coastal peatlands in the Netherlands and potential emission reduction by water infiltration systems. *Biogeosciences, 21*, 4099-4118. doi:10.5194/bg-21-4099-2024

Amon, B., Kryvoruchko, V., Amon, T., & Zechmeister-Boltenstern, S. (2006). *Methane, nitrous oxide and ammonia emissions during storage and after application of dairy cattle slurry and influence of slurry treatment.* Paper presented at the Agriculture, Ecosystems and Environment.

Anthony, T. L., & Silver, W. L. (2021). Hot moments drive extreme nitrous oxide and methane emissions from agricultural peatlands. *Global Change Biology, 27*(20), 5141-5153. doi:10.1111/gcb.15802

Anthony, T. L., & Silver, W. L. (2024). Hot spots and hot moments of greenhouse gas emissions in agricultural peatlands. *Biogeochemistry, 167*, 461-477. doi:10.1007/s10533-023-01095-y

Arets, E. J. M. M., van Baren, S. A., Kramer, H., Lesschen, J. P., & Schelhaas, M. J. (2022). *Greenhouse gas reporting of the LULUCF sector in the Netherlands; Methodological background, update 2022*. Wettelijke Onderzoekstaken Natuur & Milieu, WOt-technical report 217.

Arnold, C., Ghezzehei, T. A., & Berhe, A. A. (2015). Decomposition of distinct organic matter pools is regulated by moisture status in structured wetland soils. *Soil Biology & Biochemistry, 81*, 28-37. doi:10.1016/j.soilbio.2014.10.029

Bader, C., Muller, M., Schulin, R., & Leifeld, J. (2018). Peat decomposability in managed organic soils in relation to land use, organic matter composition and temperature. *Biogeosciences, 15*(3), 703-719. doi:10.5194/bg-15-703-2018

Baggs, E. M. (2011). Soil microbial sources of nitrous oxide: recent advances in knowledge, emerging challenges and future direction. *Current Opinion in Environmental Sustainability, 3*(5), 321-327. doi:10.1016/j.cosust.2011.08.011

Baggs, E. M., & Philippot, L. (2010). Microbial terrestrial pathways to nitrous oxide. In K. A. Smith (Ed.), *Nitrous Oxide and Climate Change*. London, UK: Earthscan.

Bakema, G., Bloem, J., Heinen, M., Knotters, M., & Van Rooijen, N. (2022). *De invloed van klimaatverandering op de bodemtemperatuur; Inventarisatie van de ontwikkeling van de bodemtemperatuur en de invloed op de biotische en abiotische processen in natuurgebieden.* Retrieved from Wageningen:

Bakema, G., Hessel, R., van den Akker, J., & Massop, H. (2025). *50 jaar maaivelddaling van veengrasland: ruim vijf decennia (1968-2024) meten op 29 locaties*. Retrieved from Wageningen:

Batjes, N. H. (1996). Total carbon and nitrogen in the soils of the world. *European Journal of Soil Science, 65*(1), 10-21. doi:10.1111/ejss.12114_2

Beare, M., Gregorich, E., & St-Georges, P. (2009). Compaction effects on CO2 and N2O production during drying and rewetting of soil. *Soil Biology & Biochemistry, 41*(3), 611-621. doi:10.1016/j.soilbio.2008.12.024

Bell, M. J., Hinton, N. J., Cloy, J. M., Topp, C. F. E., Rees, R. M., Williams, J. R., . . . Chadwick, D. R. (2016). How do emission rates and emission factors for nitrous oxide and ammonia vary with manure type and time of application in a Scottish farmland? *Geoderma, 264*, 81-93. doi:10.1016/j.geoderma.2015.10.007

Berendt, J., Jurasinski, G., & Wrage-Mönnig, N. (2023). Influence of rewetting on N2O emissions in three different fen types. *Nutrient Cycling in Agroecosystems, 125*(2), 277-293. doi:10.1007/s10705-022-10244-y

Berendt, J., & Wrage-Mönnig, N. (2023). Denitrification is not necessarily the main source of N2O from rewetted fens. *Journal of Soil Science and Plant Nutrition, 23*(3), 3705-3713.

Berglund, O., & Berglund, K. (2011). Influence of water table level and soil properties on emissions of greenhouse gases from cultivated peat soil. *Soil Biology & Biochemistry, 43*(5), 923-931. doi:10.1016/j.soilbio.2011.01.002

Bergman, I., Lundberg, P., & Nilsson, M. (1999). Microbial carbon mineralisation in an acid surface peat: effects of environmental factors in laboratory incubations. *Soil Biology & Biochemistry, 31*(13), 1867-1877. doi:10.1016/s0038-0717(99)00117-0

Bethke, C. M., Sanford, R. A., Kirk, M. F., Jin, Q. S., & Flynn, T. M. (2011). The Thermodynamic Ladder in Geomicrobiology. *American Journal of Science, 311*(3), 183-210. doi:10.2475/03.2011.01

Bhandral, R., Saggar, S., Bolan, N., & Hedley, M. (2007). Transformation of nitrogen and nitrous oxide emission from grassland soils as affected by compaction. *Soil & Tillage Research, 94*(2), 482-492. doi:10.1016/j.still.2006.10.006

Bittman, S., Dedina, H. C., Oenema, O., & Sutton, M. A. (2014). *Options for Ammonia Mitigation: Guidance from the UNECE Task Force on Reactive Nitrogen*. Edinburgh, UK: Centre for Ecology and Hydrology

Bittman, S., Hunt, D. E., Kowalenko, C. G., Chantigny, M., Buckley, K., & Bounaix, F. (2011). Removing solids improves response of grass to surface-banded dairy manure slurry: a multiyear study. *Journal of Environmental Quality, 40*(2), 393-401.

Blondeau, E., Velthof, G. L., Heinen, M., Hendriks, R. F. A., Stam, A., van den Akker, J. J. H., . . . van Groenigen, J. W. (2024). Groundwater level effects on greenhouse gas emissions from undisturbed peat cores. *Geoderma, 450*. doi:10.1016/j.geoderma.2024.117043

Blondeau, E., Westerik, D., Gremmen, T., Harpenslager, S. F., Heinen, M., Van Dijk, G., . . . Velthof, G. (2026). Drainage, cattle excreta and trampling effects on nitrous oxide emissions from a peat grassland. *Agriculture, Ecosystems and Environment, 397*. doi:10.1016/j.agee.2025.110093

Boelter, D. H. (1969). Physical properties of peats as related to degree of decomposition. *Soil Science Society of America Journal, 33*(4), 606-609.

Bolan, N. S., Saggar, S., Luo, J. F., Bhandral, R., & Singh, J. (2004). Gaseous emissions of nitrogen from grazed pastures: Processes, measurements and modelling, environmental implications, and mitigation. *Advances in Agronomy, Vol 84, 84*, 37-120. doi:10.1016/s0065-2113(04)84002-1

Boon, A., Robinson, J., Chadwick, D., & Cardenas, L. (2014). Effect of cattle urine addition on the surface emissions and subsurface concentrations of greenhouse gases in a UK peat grassland. *Agriculture Ecosystems & Environment, 186*, 23-32. doi:10.1016/j.agee.2014.01.008

Boonman, J., Harpenslager, S. F., van Dijk, G., Smolders, A. J. P., Hefting, M. M., van de Riet, B. P., & van der Velde, Y. (2024). Redox potential is a robust indicator for decomposition processes in drained agricultural peat soils: A valuable tool in monitoring peatland wetting efforts. *Geoderma, 441*. doi:10.1016/j.geoderma.2023.116728

Boonman, J., Hefting, M. M., van Huissteden, C. J. A., van den Berg, M., van Huissteden, J., Erkens, G., . . . van der Velde, Y. (2022). Cutting peatland CO2 emissions with water management practices. *Biogeosciences, 19*(24), 5707-5727. doi:10.5194/bg-19-5707-2022

Bremner, J. M., Blackmer, A. M., & Waring, S. A. (1980). Formation of nitrous oxide and dinitrogen by chemical decomposition of hydroxylamine in soils. *Soil Biology and Biochemistry, 12*(3), 263-269. doi:10.1016/0038-0717(80)90072-3

Bridgham, S. D., Cadillo-Quiroz, H., Keller, J. K., & Zhuang, Q. L. (2013). Methane emissions from wetlands: biogeochemical, microbial, and modeling perspectives from local to global scales. *Global Change Biology, 19*(5), 1325-1346. doi:10.1111/gcb.12131

Bucx, T., Van Ruiten, C., Erkens, G., & De Lange, G. (2015). An integrated assessment framework for land subsidence in delta cities. *Proceedings of the International Association of Hydrological Sciences, 372*(372), 485-491.

Bunemann, E. K., Bongiorno, G., Bai, Z. G., Creamer, R. E., De Deyn, G., de Goede, R., . . . Brussaard, L. (2018). Soil quality - A critical review. *Soil Biology & Biochemistry, 120*, 105-125. doi:10.1016/j.soilbio.2018.01.030

Burgin, A. J., Yang, W. H., Hamilton, S. K., & Silver, W. L. (2011). Beyond carbon and nitrogen: how the microbial energy economy couples elemental cycles in diverse ecosystems. *Frontiers in Ecology and the Environment, 9*(1), 44-52. doi:10.1890/090227

Butterbach-Bahl, K., Baggs, E. M., Dannenmann, M., Kiese, R., & Zechmeister-Boltenstern, S. (2013). Nitrous oxide emissions from soils: how well do we understand the processes and their controls? *Philosophical Transactions of the Royal Society B-Biological Sciences, 368*(1621). doi:10.1098/rstb.2013.0122

Byun, E., Rezanezhad, F., Fairbairn, L., Slowinski, S., Basiliko, N., Price, J., . . . Van Cappellen, P. (2021). Temperature, moisture and freeze-thaw controls on CO2 production in soil incubations from northern peatlands. *Scientific Reports, 11*(1). doi:10.1038/s41598-021-02606-3

Cai, Y., & Akiyama, H. (2016). Nitrogen loss factors of nitrogen trace gas emissions and leaching from excreta patches in grassland ecosystems: A summary of available data. *Science of the Total Environment, 572*, 185-195. doi:10.1016/j.scitotenv.2016.07.222

Cai, Y., Chang, S., & Cheng, Y. (2017). Greenhouse gas emissions from excreta patches of grazing animals and their mitigation strategies. *Earth-Science Reviews, 171*, 44-57. doi:10.1016/j.earscirev.2017.05.013

Canadell, J. G., Monteiro, P. M. S., Costa, M. H., Cotrim da Cunha, L., Cox, P. M., Eliseev, A. V., . . . Zickfeld, K. (2021). *Global Carbon and other Biogeochemical Cycles and Feedbacks.* Cambridge University Press, Cambridge, United Kingdom and New York, NY, USA, pp. 673–816, doi:10.1017/9781009157896.007.: In Climate Change 2021: The Physical Science Basis. Contribution of Working Group I to the Sixth Assessment Report of the Intergovernmental Panel on Climate Change [Masson-Delmotte, V., P. Zhai, A. Pirani, S.L. Connors, C. Péan, S. Berger, N. Caud, Y. Chen, L. Goldfarb, M.I. Gomis, M. Huang, K. Leitzell, E. Lonnoy, J.B.R. Matthews, T.K. Maycock, T. Waterfield, O. Yelekçi, R. Yu, and B. Zhou (eds.)].

Carter, M. (2007). Contribution of nitrification and denitrification to N2O emissions from urine patches. *Soil Biology & Biochemistry, 39*, 2091-2102. doi:10.1016/j.soilbio.2007.03.013

Carter, M. R., Gregorich, E., Anderson, D., Doran, J., Janzen, H., & Pierce, F. (1997). Concepts of soil quality and their significance. In (Vol. 25, pp. 1-19): Elsevier.

CBGV. (2026). *Bemestingsadvies*. Commissie Bemesting Grasland en Voedergewassen. Wageningen, The Netherlands

Chadwick, D., Cardenas, L., Dhanoa, M., Donovan, N., Misselbrook, T., Williams, J., . . . Rees, R. (2018). The contribution of cattle urine and dung to nitrous oxide emissions: Quantification of country specific emission factors and

implications for national inventories. *Science of the Total Environment, 635*, 607-617. doi:10.1016/j.scitotenv.2018.04.152

Chadwick, D., Sommer, S., Thorman, R., Fangueiro, D., Cardenas, L., Amon, B., & Misselbrook, T. (2011). Manure management: Implications for greenhouse gas emissions. *Animal Feed Science and Technology, 166-167*, 514-531. doi:10.1016/j.anifeedsci.2011.04.036

Chapin, F. S., Matson, P. A., & Mooney, H. A. (2002a). Terrestrial decomposition. In *Principles of Terrestrial Ecosystem Ecology*.

Chapin, F. S., Matson, P. A., & Mooney, H. A. (2002b). Terrestrial nutrient cycling. In *Principles of Terrestrial Ecosystem Ecology*.

Chapuis-Lardy, L., Wrage, N., Metay, A., Chotte, J. L., & Bernoux, M. (2007). Soils, a sink for N2O? A review. *Global Change Biology, 13*(1), 1-17. doi:10.1111/j.1365-2486.2006.01280.x

Charteris, A. F., Chadwick, D. R., Thorman, R. E., Vallejo, A., de Klein, C. A. M., Rochette, P., & Cárdenas, L. M. (2020). Global Research Alliance N2O chamber methodology guidelines: Recommendations for deployment and accounting for sources of variability. *Journal of Environmental Quality, 49*(5), 1092-1109. doi:10.1002/jeq2.20126

Chen, H., Zou, J., Cui, J., Nie, M., & Fang, C. (2018). Wetland drying increases the temperature sensitivity of soil respiration. *Soil Biology & Biochemistry, 120*, 24-27. doi:10.1016/j.soilbio.2018.01.035

Clark, M. D., & Gilmour, J. T. (1983). The effect of temperature on decomposition at optimum and saturated soil-water contents. *Soil Science Society of America Journal, 47*(5), 927-929. doi:10.2136/sssaj1983.03615995004700050017x

Clough, T., Sherlock, R., & Rolston, D. (2005). A review of the movement and fate of N2O in the subsoil. *Nutrient Cycling in Agroecosystems, 72*(1), 3-11. doi:10.1007/s10705-004-7349-z

Clymo, R. S. (1984). THE LIMITS TO PEAT BOG GROWTH. *Philosophical Transactions of the Royal Society of London Series B-Biological Sciences, 303*(1117), 605-654. doi:10.1098/rstb.1984.0002

Councel of the European Communities. (1991). *Council Directive 91/676/EEC of 12 December 1991*

concerning the protection of waters against pollution caused by nitrates from agricultural

sources (OJ L 375, 31.12.1991, ELI: http://data.europa.eu/eli/dir/1991/676/oj).

Cuhel, J., Simek, M., Laughlin, R., Bru, D., Chèneby, D., Watson, C., & Philippot, L. (2010). Insights into the Effect of Soil pH on N2O and N2 Emissions and Denitrifier Community Size and Activity. *Applied and Environmental Microbiology, 76*(6), 1870-1878. doi:10.1128/AEM.02484-09

Dasilva, F. F., Wallach, R., & Chen, Y. (1993). Hydraulic properties of sphagnum peat moss and tuff (scoria) and their potential effects on water availability. *Plant and Soil, 154*(1), 119-126. doi:10.1007/bf00011080

Davidson, E., Keller, M., Erickson, H., Verchot, L., & Veldkamp, E. (2000). Testing a conceptual model of soil emissions of nitrous and nitric oxides.

Bioscience, 50(8), 667-680. doi:10.1641/0006-3568(2000)050[0667:TACMOS]2.0.CO;2

Davidson, E. A., & Janssens, I. A. (2006). Temperature sensitivity of soil carbon decomposition and feedbacks to climate change. *Nature, 440*(7081), 165-173. doi:10.1038/nature04514

Davidson, E. A., Janssens, I. A., & Luo, Y. Q. (2006). On the variability of respiration in terrestrial ecosystems: moving beyond Q(10). *Global Change Biology, 12*(2), 154-164. doi:10.1111/j.1365-2486.2005.01065.x

De Bakker, H., & Schelling, J. (1989). *Systeem van bodemclassificatie voor Nederland, de hogere niveaus* (D. J. Brus & C. Van Wallenburg Eds. 2nd ed.). Wageningen: Centrum voor Landbouwpublikaties en Landbouwdocumentatie.

De Klein, C., Smith, L., & Monaghan, R. (2006). Restricted autumn grazing to reduce nitrous oxide emissions from dairy pastures in Southland, New Zealand. *Agriculture Ecosystems & Environment, 112*, 192-199. doi:10.1016/j.agee.2005.08.019

De Klein, C. A. M., Alfaro, M. A., Giltrap, D., Topp, C. F. E., Simon, P. L., Noble, A. D. L., & van der Weerden, T. J. (2020). Global Research Alliance N2O chamber methodology guidelines: Statistical considerations, emission factor calculation, and data reporting. *Journal of Environmental Quality, 49*(5), 1156-1167. doi:10.1002/jeq2.20127

De Klein, C. A. M., & Vanlogtestijn, R. S. P. (1994). Denitrification in the top-soil of managed grasslands in the Netherlands in relation to soil type and fertilizer level. *Plant and Soil, 163*(1), 33-44. doi:10.1007/bf00033938

De Visser, P. H. B., Van Keulen, H., Lantinga, E. A., & Udo, H. M. J. (2001). Efficient resource management in dairy farming on peat and heavy clay soils. *Netherlands Journal of Agricultural Science, 49*(2-3), 255-276. doi:10.1016/S1573-5214(01)80010-5

De Vos, J. A., Van Bakel, P. J. T., Hoving, I. E., & Smidt, R. A. (2010). Raising surface water levels in peat areas with dairy farming. Upscaling hydrological, agronomical and economic effects from farm-scale to local scale. *Agricultural Water Management, 97*(11), 1887-1897. doi:10.1016/j.agwat.2010.06.017

De Wit, C. T. (1992). Resource use efficiency in agriculture. *Agricultural Systems, 40*(1-3), 125-151. doi:10.1016/0308-521X(92)90018-J

Deru, J., Bloem, J., de Goede, R., Hoekstra, N., Keidel, H., Kloen, H., . . . van Eekeren, N. (2019). Predicting soil N supply and yield parameters in peat grasslands. *Applied Soil Ecology, 134*, 77-84. doi:10.1016/j.apsoil.2018.10.018

Deru, J., Bloem, J., de Goede, R., Keidel, H., Kloen, H., Rutgers, M., . . . van Eekeren, N. (2018). Soil ecology and ecosystem services of dairy and semi-natural grasslands on peat. *Applied Soil Ecology, 125*, 26-34. doi:10.1016/j.apsoil.2017.12.011

Dinsmore, K. J., Skiba, U. M., Billett, M. F., & Rees, R. M. (2009). Effect of water table on greenhouse gas emissions from peatland mesocosms. *Plant and Soil, 318*(1-2), 229-242. doi:10.1007/s11104-008-9832-9

Doran, J. W., & Parkin, T. B. (1994). Defining and assessing soil quality. *Defining soil quality for a sustainable environment, 35*, 1-21.

Eickenscheidt, T., Heinichen, J., Augustin, J., Freibauer, A., & Drösler, M. (2014). Nitrogen mineralization and gaseous nitrogen losses from waterlogged and drained organic soils in a black alder (Alnus glutinosa (L.) Gaertn.) forest. *Biogeosciences, 11*, 2961-2976. doi:10.5194/bg-11-2961-2014

Erkens, G., van der Meulen, M. J., & Middelkoop, H. (2016). Double trouble: subsidence and CO2 respiration due to 1,000 years of Dutch coastal peatlands cultivation. *Hydrogeology Journal, 24*(3), 551-568. doi:10.1007/s10040-016-1380-4

European Commission. (2026). *Commission Directive (EU) 2026/288 of 9 February 2026 amending Council Directive 91/676/EEC as regards the use of certain fertilising materials from livestock manure (OJ L, 2026/288, 10.2.2026, ELI: http://data.europa.eu/eli/dir/2026/288/oj)*.

European Environment Agency. (2024). *Annual European Union greenhouse gas inventory 1990–2022 and inventory document 2024*.

Evans, C. D., Peacock, M., Baird, A. J., Artz, R. R. E., Burden, A., Callaghan, N., . . . Morrison, R. (2021). Overriding water table control on managed peatland greenhouse gas emissions. *Nature, 593*, 548-552. doi:10.1038/s41586-021-03523-1

Evans, C. D., Renou-Wilson, F., & Strack, M. (2016). The role of waterborne carbon in the greenhouse gas balance of drained and re-wetted peatlands. *Aquatic Sciences, 78*(3), 573-590.

Fairbairn, L., Rezanezhad, F., Gharasoo, M., Parsons, C., Macrae, M., Slowinski, S., & Van Cappellen, P. (2023). Relationship between soil CO2 fluxes and soil moisture: Anaerobic sources explain fluxes at high water content. *Geoderma, 434*. doi:10.1016/j.geoderma.2023.116493

Fangueiro, D., Senbayran, M., Trindade, H., & Chadwick, D. (2008). Cattle slurry treatment by screw press separation and chemically enhanced settling: effect on greenhouse gas emissions after land spreading and grass yield. *Bioresource Technology, 99*(15), 7132-7142.

Fierer, N., Craine, J. M., McLauchlan, K., & Schimel, J. P. (2005). Litter quality and the temperature sensitivity of decomposition. *Ecology, 86*(2), 320-326. doi:10.1890/04-1254

Firestone, M. K., & Davidson, E. A. (1989). Microbiological basis of NO and N2O production and consumption in soil. In M. O. Andreae & D. S. Schimel (Eds.), *Exchange of Trace Gases between Terrestrial Ecosystems and the Atmosphere* (pp. 7-21). New York: John Wiley & Sons Ltd.

Forster, P., Storelvmo, T., Armour, K., Collins, W., Dufresne, J.-L., Frame, D., . . . Zhang, H. (2021). *The Earth's Energy Budget, Climate Feedbacks, and Climate Sensitivity.* Cambridge University Press, Cambridge, United Kingdom and New York, NY, USA, pp. 923–1054,

doi:10.1017/9781009157896.009: In Climate Change 2021: The Physical Science Basis. Contribution of Working Group I to the Sixth Assessment Report of the Intergovernmental Panel on Climate Change [Masson-Delmotte, V., P. Zhai, A. Pirani, S.L. Connors, C. Péan, S. Berger, N. Caud, Y. Chen, L. Goldfarb, M.I. Gomis, M. Huang, K. Leitzell, E. Lonnoy, J.B.R. Matthews, T.K. Maycock, T. Waterfield, O. Yelekçi, R. Yu, and B. Zhou (eds.)].

Freeman, B. W. J., Evans, C. D., Musarika, S., Morrison, R., Newman, T. R., Page, S. E., . . . Jones, D. L. (2022). Responsible agriculture must adapt to the wetland character of mid-latitude peatlands. *Global Change Biology, 28*, 3795-3811. doi:10.1111/gcb.16152

Freeman, C., Ostle, N., & Kang, H. (2001). An enzymic 'latch' on a global carbon store - A shortage of oxygen locks up carbon in peatlands by restraining a single enzyme. *Nature, 409*(6817), 149-149. doi:10.1038/35051650

Freeman, C., Ostle, N. J., Fenner, N., & Kang, H. (2004). A regulatory role for phenol oxidase during decomposition in peatlands. *Soil Biology & Biochemistry, 36*(10), 1663-1667. doi:10.1016/j.soilbio.2004.07.012

Fuss, R. (2023). gasfluxes: Greenhouse Gas Flux Calculation from Chamber Measurements. https://CRAN.R-project.org/package=gasfluxes: R package version 0.5.

Gao, Z., & Wang, S. (2025). Mitigating Gas Emissions from the Dairy Slurry Management Chain: An Enhanced Solid–Liquid Separation Technology with Tannic Acid. *Agronomy, 15*(5), 1202.

Goldberg, S. D., Knorr, K. H., Blodau, C., Lischeid, G., & Gebauer, G. (2010). Impact of altering the water table height of an acidic fen on N2O and NO fluxes and soil concentrations. *Global Change Biology, 16*(1), 220-233. doi:10.1111/j.1365-2486.2009.02015.x

Gunther, A., Barthelmes, A., Huth, V., Joosten, H., Jurasinski, G., Koebsch, F., & Couwenberg, J. (2020). Prompt rewetting of drained peatlands reduces climate warming despite methane emissions. *Nature Communications, 11*(1). doi:10.1038/s41467-020-15499-z

Harbers, M., & Heijnen, V. L. W. A. (2022). *Kamerbrief Water en Bodem sturend*. The Hague

Hardie, S. M. L., Garnett, M. H., Fallick, A. E., Rowland, A. P., Ostle, N. J., & Flowers, T. H. (2011). Abiotic drivers and their interactive effect on the flux and carbon isotope (C-14 and delta C-13) composition of peat-respired CO2. *Soil Biology & Biochemistry, 43*(12), 2432-2440. doi:10.1016/j.soilbio.2011.08.010

Harpenslager, S. F., van Dijk, G., Boonman, J., Weideveld, S. T. J., van de Riet, B. P., Hefting, M. M., & Smolders, A. J. P. (2024). Rewetting drained peatlands through subsoil infiltration stabilises redox-dependent soil carbon and nutrient dynamics. *Geoderma, 442*. doi:10.1016/j.geoderma.2024.116787

Haynes, R. J., & Williams, P. H. (1992). Changes in soil solution composition and pH in urine-affected areas of pasture. *Journal of Soil Science, 43*, 323-334.

Heil, J., Vereecken, H., & Brüggemann, N. (2016). A review of chemical reactions of nitrification intermediates and their role in nitrogen cycling and nitrogen trace gas formation in soil. *European Journal of Soil Science, 67*(1), 23-39. doi:10.1111/ejss.12306

Heinen, M. (2006). Simplified denitrification models: Overview and properties. *Geoderma, 133*(3-4), 444-463. doi:10.1016/j.geoderma.2005.06.010

Hendriks, D. M. D., van Huissteden, J., Dolman, A. J., & van der Molen, M. K. (2007). The full greenhouse gas balance of an abandoned peat meadow. *Biogeosciences, 4*(3), 411-424. doi:10.5194/bg-4-411-2007

Hergoualc'h, K., Akiyama, H., Bernoux, M., Chirinda, N., Del Prado, A., Kasimir, Å., . . . Van der Weerden, T. J. (2019). N2O emissions from managed soils, and CO2 emissions from lime and urea application. In IPCC (Ed.), *2019 Refinement to the 2006 IPCC Guidelines for National Greenhouse Gas Inventories* Switzerland.

Herrera-García, G., Ezquerro, P., Tomás, R., Béjar-Pizarro, M., López-Vinielles, J., Rossi, M., . . . Teatini, P. (2021). Mapping the global threat of land subsidence. *Science, 371*(6524), 34-36.

Hiraishi, T., Krug, T., Tanabe, K., Srivastava, N., Baasansuren, J., Fukuda, M., & Troxler, T. G. (2014). *2013 Supplement to the 2006 IPCC Guidelines for National Greenhouse Gas Inventories: Wetlands*. IPCC, Switzerland.

Holly, M. A., Larson, R. A., Powell, J. M., Ruark, M. D., & Aguirre-Villegas, H. (2017). Greenhouse gas and ammonia emissions from digested and separated dairy manure during storage and after land application. *Agriculture, Ecosystems & Environment, 239*, 410-419.

Hoogland, T., van den Akker, J. J. H., & Brus, D. J. (2012). Modeling the subsidence of peat soils in the Dutch coastal area. *Geoderma, 171*, 92-97. doi:10.1016/j.geoderma.2011.02.013

Hooijer, A., Page, S., Jauhiainen, J., Lee, W. A., Lu, X. X., Idris, A., & Anshari, G. (2012). Subsidence and carbon loss in drained tropical peatlands. *Biogeosciences, 9*(3), 1053-1071. doi:10.5194/bg-9-1053-2012

Hoving, I. E., Van Riel, J. W., Massop, H. T. L., Van den Akker, J. J. H., & Van Houwelingen, K. (2023). *Statistische analyse veldexperimenten waterinfiltratiesystemen in het westelijke veenweidegebied van Nederland. Rapportage van veldonderzoeken die hebben plaatsgevonden in de periode 2004-2021.* Retrieved from Wageningen:

Hoving, I. E., van Riel, J. W., Massop, H. T. L., van Houwelingen, K., & Bijman, M. (2022). *Waterinfiltratie met drukdrains en greppels voor veenbehoud en emissiereductie; Deelonderzoek 'natte veeteelt' in het Innovatie Programma Veen (2018-2021).* Wageningen Livestock Research, Openbaar Rapport 1345.

Hu, J., Liao, X., Vardanyan, L., Huang, Y., Inglett, K., Wright, A., & Reddy, K. (2020). Duration and frequency of drainage and flooding events

interactively affect soil biogeochemistry and N flux in subtropical peat soils. *Science of the Total Environment, 727*. doi:10.1016/j.scitotenv.2020.138740

Hunt, D., Bittman, S., Chantigny, M., & Lemke, R. (2019). Year-round N2O emissions from long-term applications of whole and separated liquid dairy slurry on a perennial grass sward and strategies for mitigation. *Frontiers in Sustainable Food Systems, 3*, 86.

Huygens, D., Orveillon, G., Lugato, E., Tavazzi, S., Comero, S., Jones, A., . . . Saveyn, H. G. M. (2020). *Technical proposals for the safe use of processed manure above the threshold established for Nitrate Vulnerable Zones by the Nitrates Directive (91/676/EEC)*. Retrieved from Publications Office of the European Union, Luxembourg:

IPCC. (2019). *2019 Refinement to the 2006 IPCC Guidelines for National Greenhouse Gas Inventories*. Switzerland: IPCC.

Ishikura, K., Hirano, T., Okimoto, Y., Hirata, R., Kiew, F., Melling, L., . . . Ishii, Y. (2018). Soil carbon dioxide emissions due to oxidative peat decomposition in an oil palm plantation on tropical peat. *Agriculture Ecosystems & Environment, 254*, 202-212. doi:10.1016/j.agee.2017.11.025

IUSS Working Group WRB. (2015). *World Reference Base for Soil Resources 2014, update 2015. International soil classification system for naming soils and creating legends for soil maps.* Retrieved from Rome:

Janssen, P. W. L., Hoekstra, N. J., & van Eekeren, N. (2023). Higher density swards have a higher load bearing capacity. *Grass and Forage Science, 78*, 204-213. doi:10.1111/gfs.12603

Jellema, A., Gosselink, I., & Ramaekers, P. (2025). *Staat van landbouw, visserij, voedsel en natuur 2025*. Retrieved from Wageningen:

Jobbagy, E. G., & Jackson, R. B. (2000). The vertical distribution of soil organic carbon and its relation to climate and vegetation. *Ecological Applications, 10*(2), 423-436. doi:10.2307/2641104

Jongbloed, M., Hoekstra, N. J., Groot, J. C. J., van den Hout, M., Hoving, I. E., Janssen, P. W. L., & van Eekeren, N. (2026). The effect of raised groundwater tables on load-bearing capacity of peat grassland on a dairy farm. *Soil and Tillage Research, 261*, 107186.

Jurasinski, G., Ahmad, S., Anadon-Rosell, A., Berendt, J., Beyer, F., Bill, R., . . . Wrage-Monnig, N. (2020). From Understanding to Sustainable Use of Peatlands: The WETSCAPES Approach. *Soil Systems, 4*(1). doi:10.3390/soilsystems4010014

Kandel, T. P., Karki, S., Elsgaard, L., & Laerke, P. E. (2019). Fertilizer-induced fluxes dominate annual N2O emissions from a nitrogen-rich temperate fen rewetted for paludiculture. *Nutrient Cycling in Agroecosystems, 115*(1), 57-67. doi:10.1007/s10705-019-10012-5

Karki, S., Elsgaard, L., Kandel, T. P., & Laerke, P. E. (2016). Carbon balance of rewetted and drained peat soils used for biomass production: a mesocosm study. *Global Change Biology Bioenergy, 8*(5), 969-980. doi:10.1111/gcbb.12334

Kayranli, B., Scholz, M., Mustafa, A., & Hedmark, Å. (2010). Carbon storage and fluxes within freshwater wetlands: a critical review. *Wetlands, 30*(1), 111-124.

Kechavarzi, C., Dawson, Q., Bartlett, M., & Leeds-Harrison, P. B. (2010a). The role of soil moisture, temperature and nutrient amendment on CO2 efflux from agricultural peat soil microcosms. *Geoderma, 154*(3-4), 203-210. doi:10.1016/j.geoderma.2009.02.018

Kechavarzi, C., Dawson, Q., & Leeds-Harrison, P. B. (2010b). Physical properties of low-lying agricultural peat soils in England. *Geoderma, 154*(3-4), 196-202. doi:10.1016/j.geoderma.2009.08.018

Kechavarzi, C., Dawson, Q., Leeds-Harrison, P. B., SzatyLowicz, J., & Gnatowski, T. (2007). Water-table management in lowland UK peat soils and its potential impact on CO2 emission. *Soil Use and Management, 23*, 359-367. doi:10.1111/j.1475-2743.2007.00125.x

Keiluweit, M., Wanzek, T., Kleber, M., Nico, P., & Fendorf, S. (2017). Anaerobic microsites have an unaccounted role in soil carbon stabilization. *Nature Communications, 8*. doi:10.1038/s41467-017-01406-6

Klemedtsson, L., von Arnold, K., Weslien, P., & Gundersen, P. (2005). Soil CN ratio as a scalar parameter to predict nitrous oxide emissions. *Global Change Biology, 11*(7), 1142-1147. doi:10.1111/j.1365-2486.2005.00973.x

Klingenfuß, C., Roßkopf, N., Walter, J., Heller, C., & Zeitz, J. (2014). Soil organic matter to soil organic carbon ratios of peatland soil substrates. *Geoderma, 235*, 410-417.

KNMI. (2026). *Jaaroverzicht van het weer in Nederland*. Koninklijk Nederlands Meteorologisch Instituut. De Bilt, The Netherlands. Obtained from www.knmi.nl/nederland-nu/klimatologie/gegevens/mow

Knorr, K. H., Lischeid, G., & Blodau, C. (2009). Dynamics of redox processes in a minerotrophic fen exposed to a water table manipulation. *Geoderma, 153*(3-4), 379-392. doi:10.1016/j.geoderma.2009.08.023

Knowles, R. (1982). Denitrification. *Microbiological Reviews, 46*(1), 43-70. doi:10.1128/mmbr.46.1.43-70.1982

Kool, D. M., Hoffland, E., Abrahamse, S. P. A., & van Groenigen, J. (2006). What artificial urine composition is adequate for simulating soil N2O fluxes and mineral N dynamics? *Soil Biology & Biochemistry, 38*, 1757-1763. doi:10.1016/j.soilbio.2005.11.030

Koops, J., vanBeusichem, M., & Oenema, O. (1997a). Nitrous oxide production, its source and distribution in urine patches on grassland on peat soil. *Plant and Soil, 191*(1), 57-65. doi:10.1023/A:1004285221368

Koops, J. G., Oenema, O., & Van Beusichem, M. L. (1996). Denitrification in the top and sub soil of grassland on peat soils. *Plant and Soil, 184*(1), 1-10. doi:10.1007/bf00029269

Koops, J. G., Van Beusichem, M. L., & Oenema, O. (1997b). Nitrogen loss from grassland on peat soils through nitrous oxide production. *Plant and Soil, 188*(1), 119-130. doi:10.1023/a:1004252012290

Koster, K., Stafleu, J., & Stouthamer, E. (2018). Differential subsidence in the urbanised coastal-deltaic plain of the Netherlands. *Netherlands Journal of Geosciences-Geologie En Mijnbouw, 97*(4), 215-227. doi:10.1017/njg.2018.11

Koven, C. D., Hugelius, G., Lawrence, D. M., & Wieder, W. R. (2017). Higher climatological temperature sensitivity of soil carbon in cold than warm climates. *Nature Climate Change, 7*(11), 817-822.

Kreyling, J., Tanneberger, F., Jansen, F., van der Linden, S., Aggenbach, C., Bluml, V., . . . Jurasinski, G. (2021). Rewetting does not return drained fen peatlands to their old selves. *Nature Communications, 12*. doi:10.1038/s41467-021-25619-y

Krol, D. J., Carolan, R., Minet, E., McGeough, K. L., Watson, C. J., Forrestal, P. J., . . . Richards, K. G. (2016). Improving and disaggregating N2O emission factors for ruminant excreta on temperate pasture soils. *Science of the Total Environment, 568*, 327-338. doi:10.1016/j.scitotenv.2016.06.016

Kupper, T., Häni, C., Neftel, A., Kincaid, C., Bühler, M., Amon, B., & VanderZaag, A. (2020). Ammonia and greenhouse gas emissions from slurry storage - A review. *Agriculture, Ecosystems and Environment, 300*. doi:10.1016/j.agee.2020.106963

Laiho, R. (2006). Decomposition in peatlands: Reconciling seemingly contrasting results on the impacts of lowered water levels. *Soil Biology & Biochemistry, 38*(8), 2011-2024. doi:10.1016/j.soilbio.2006.02.017

Lal, R., Bouma, J., Brevik, E., Dawson, L., Field, D. J., Glaser, B., . . . Lascelles, B. (2021). Soils and sustainable development goals of the United Nations: An International Union of Soil Sciences perspective. *Geoderma Regional, 25*, e00398.

Lambie, S., Schipper, L., Balks, M., & Baisden, W. (2013). Priming of soil decomposition leads to losses of carbon in soil treated with cow urine. *Soil Research, 51*(6), 513-520. doi:10.1071/SR13148

Lan, X., Thoning, K. W., & Dlugokencky, E. J. (2025). Trends in globally-averaged CH4, N2O, and SF6 determined from NOAA Global Monitoring Laboratory measurements. *Version 2025-12. Retrieved December 28, 2025.*

Le Mer, J., & Roger, P. (2001). Production, oxidation, emission and consumption of methane by soils: A review. *European Journal of Soil Biology, 37*(1), 25-50. doi:10.1016/s1164-5563(01)01067-6

Leifeld, J., Klein, K., & Wust-Galley, C. (2020). Soil organic matter stoichiometry as indicator for peatland degradation. *Scientific Reports, 10*(1). doi:10.1038/s41598-020-64275-y

Leifeld, J., Müller, M., & Fuhrer, J. (2011). Peatland subsidence and carbon loss from drained temperate fens. *Soil Use and Management, 27*(2), 170-176. doi:10.1111/j.1475-2743.2011.00327.x

Leifeld, J., Wüst-Galley, C., & Page, S. (2019). Intact and managed peatland soils as a source and sink of GHGs from 1850 to 2100. *Nature Climate Change, 9*(12), 945-947.

Leip, A., Billen, G., Garnier, J., Grizzetti, B., Lassaletta, L., Reis, S., . . . Weiss, F. (2015). Impacts of European livestock production: nitrogen, sulphur, phosphorus and greenhouse gas emissions, land-use, water eutrophication and biodiversity. *Environmental Research Letters, 10*(11), 115004.

Leppelt, T., Dechow, R., Gebbert, S., Freibauer, A., Lohila, A., Augustin, J., . . . Stromgren, M. (2014). Nitrous oxide emission budgets and land-use-driven hotspots for organic soils in Europe. *Biogeosciences, 11*, 6595-6612. doi:10.5194/bg-11-6595-2014

Li, Q., Leroy, F., Zocatelli, R., Gogo, S., Jacotot, A., Guimbaud, C., & Laggoun-Defarge, F. (2021). Abiotic and biotic drivers of microbial respiration in peat and its sensitivity to temperature change. *Soil Biology & Biochemistry, 153*. doi:10.1016/j.soilbio.2020.108077

Lin, F., Zuo, H., Ma, X., & Ma, L. (2022). Comprehensive assessment of nitrous oxide emissions and mitigation potentials across European peatlands. *Environmental Pollution, 301*. doi:10.1016/j.envpol.2022.119041

Linn, D. M., & Doran, J. W. (1984). Effect of water-filled pore space on carbon dioxide and nitrous oxide production in tilled and nontilled soils. *Soil Science Society of America Journal, 48*(6), 1267-1272. doi:10.2136/sssaj1984.03615995004800060013x

Liu, H., Janssen, M., & Lennartz, B. (2016). Changes in flow and transport patterns in fen peat following soil degradation. *European Journal of Soil Science, 67*, 763-772.

Liu, H., Rezanezhad, F., Zhao, Y., He, H., Van Cappellen, P., & Lennartz, B. (2024). The apparent temperature sensitivity (Q10) of peat soil respiration: A synthesis study. *Geoderma, 443*. doi:10.1016/j.geoderma.2024.116844

Liu, H. J., Wrage-Mönnig, N., & Lennartz, B. (2020). Rewetting strategies to reduce nitrous oxide emissions from European peatlands. *Communications Earth & Environment, 1*. doi:10.1038/s43247-020-00017-2

Liu, W. E., Fritz, C., Weideveld, S. T. J., Aben, R. C. H., van den Berg, M., & Velthuis, M. (2022). Annual CO2 Budget Estimation From Chamber-Based Flux Measurements on Intensively Drained Peat Meadows: Effect of Gap-Filling Strategies. *Frontiers in Environmental Science, 10*. doi:10.3389/fenvs.2022.803746

Lloyd, J., & Taylor, J. A. (1994). On the temperature-dependence of soil respiration. *Functional Ecology, 8*(3), 315-323. doi:10.2307/2389824

Lockyer, D. R., & Whitehead, D. C. (1990). Volatilization of ammonia from cattle urine applied to grassland. *Soil Biology & Biochemistry, 22*(8), 1137-1142.

Loisel, J., van Bellen, S., Pelletier, L., Talbot, J., Hugelius, G., Karran, D., . . . Holmquist, J. (2017). Insights and issues with estimating northern peatland carbon stocks and fluxes since the Last Glacial Maximum. *Earth-Science Reviews, 165*, 59-80. doi:10.1016/j.earscirev.2016.12.001

Loisel, J., Yu, Z. C., Beilman, D. W., Camill, P., Alm, J., Amesbury, M. J., . . . Zhou, W. J. (2014). A database and synthesis of northern peatland soil

properties and Holocene carbon and nitrogen accumulation. *Holocene, 24*(9), 1028-1042. doi:10.1177/0959683614538073

Ma, L., Zhu, G., Chen, B., Zhang, K., Niu, S., Wang, J., . . . Zuo, H. (2022). A globally robust relationship between water table decline, subsidence rate, and carbon release from peatlands. *Communications Earth & Environment, 3*(1), 254.

Mäkiranta, P., Laiho, R., Fritze, H., Hytonen, J., Laine, J., & Minkkinen, K. (2009). Indirect regulation of heterotrophic peat soil respiration by water level via microbial community structure and temperature sensitivity. *Soil Biology & Biochemistry, 41*(4), 695-703. doi:10.1016/j.soilbio.2009.01.004

Malmer, N., & Holm, E. (1984). Variation in the C/N-quotient of peat in relation to decomposition rate and age-determination with Pb-210. *Oikos, 43*(2), 171-182. doi:10.2307/3544766

Martikainen, P. J., Nykanen, H., Crill, P., & Silvola, J. (1993). Effect of a lowered water table on nitrous oxide fluxes from northern peatlands. *Nature, 366*(6450), 51-53. doi:10.1038/366051a0

Massop, H. T. L., Hessel, R., van den Akker, J. J. H., van Asselen, S., Erkens, G., Gerritsen, P., & Gerritsen, F. (2024). Monitoring long-term peat subsidence with subsidence platens in Zegveld, The Netherlands. *Geoderma, 450*, 117039.

McLatchey, G. P., & Reddy, K. R. (1998). Regulation of organic matter decomposition and nutrient release in a wetland soil. *Wetlands and Aquatic Processes*.

McTaggart, I. P., Parker, J., Swan, L., Clayton, H., & Smith, K. A. (1997). Nitrous oxide emissions from grassland and spring barley, following N fertiliser application with and without nitrification inhibitors. *Biology and Fertility of Soils, 25*(3), 261-268. doi:10.1007/s003740050312

Megonigal, J. P., Hines, M. E., & Visscher, P. T. (2004). Aaerobic Metabolism: Linkages to Trace Gases and Aerobic Processes. In W. H. Schlesinger (Ed.), *Biogeochemistry* (Vol. 8, pp. 317-424).

Ministerie van Landbouw Natuur en Voedselkwaliteit. (2019). *Klimaatakkoord- C4 Landbouw en Landgebruik*. The Hague

Ministry of Agriculture Nature and Food Quality. (2019). *Klimaatakkoord- C4 Landbouw en Landgebruik*. The Hague

Minkkinen, K., Ojanen, P., Koskinen, M., & Penttilä, T. (2020). Nitrous oxide emissions of undrained, forestry-drained, and rewetted boreal peatlands. *Forest Ecology and Management, 478*. doi:10.1016/j.foreco.2020.118494

Moinet, G., Morán-Rivera, K., Moinet, A., & Wadoux, A. (2025). Large underestimations of warming-induced soil carbon emissions from oversimplistic Q10 indicator. *Soil Biology & Biochemistry, 207*. doi:10.1016/j.soilbio.2025.109839

Monaghan, R. M., & Barraclough, D. (1992). Some chemical and physical factors affecting the rate and dynamics of nitrification in urine-affected soil. *Plant and Soil, 143*(1), 11-18. doi:10.1007/BF00009124

Monaghan, R. M., & Barraclough, D. (1993). Nitrous oxide and dinitrogen emissions from urine-affected soil under controlled conditions. *Plant and Soil, 151*(1), 127-138. doi:10.1007/BF00010793

Moore, T. R., & Dalva, M. (1993). The influence of temperature and water table position on carbon dioxide and methane emissions from laboratory columns of peatland soils. *Journal of Soil Science, 44*(4), 651-664. doi:10.1111/j.1365-2389.1993.tb02330.x

Morán-Rivera, K., Hagens, M., Creamer, R. E., Comans, R. N. J., Murray, S., Hendriksen, R., . . . Moinet, G. Y. K. (2026). Temperature Response of Soil Organic Matter Decomposition Rates: Construction and Applications of a Temperature Gradient Block. *JoVE (Journal of Visualized Experiments)*(227), e69785.

Moyano, F. E., Manzoni, S., & Chenu, C. (2013). Responses of soil heterotrophic respiration to moisture availability: An exploration of processes and models. *Soil Biology & Biochemistry, 59*, 72-85. doi:10.1016/j.soilbio.2013.01.002

Moyano, F. E., Vasilyeva, N., Bouckaert, L., Cook, F., Craine, J., Yuste, J. C., . . . Chenu, C. (2012). The moisture response of soil heterotrophic respiration: interaction with soil properties. *Biogeosciences, 9*(3), 1173-1182. doi:10.5194/bg-9-1173-2012

Moyano, F. E., Vasilyeva, N., & Menichetti, L. (2018). Diffusion limitations and Michaelis-Menten kinetics as drivers of combined temperature and moisture effects on carbon fluxes of mineral soils. *Biogeosciences, 15*(16), 5031-5045. doi:10.5194/bg-15-5031-2018

Nielsen, C. K., Elsgaard, L., Jorgensen, U., & Lærke, P. E. (2023). Soil greenhouse gas emissions from drained and rewetted agricultural bare peat mesocosms are linked to geochemistry. *Science of the Total Environment, 896*. doi:10.1016/j.scitotenv.2023.165083

Nijman, T. P., van Giersbergen, Q., Heuts, T. S., Nouta, R., Boonman, C. C., Velthuis, M., . . . Fritz, C. (2024). Drainage effects on carbon budgets of degraded peatlands in the north of the Netherlands. *Science of the Total Environment, 935*, 172882.

NOBV. (2021). *Nationaal onderzoeksprogramma Broeikasgassen Veenweiden (NOBV) Operationele jaarrapportage 2020-2021.*

Norberg, L., Hellman, M., Berglund, K., Hallin, S., & Berglund, Ö. (2021). Methane and nitrous oxide production from agricultural peat soils in relation to drainage level and abiotic and biotic factors. *Frontiers in Environmental Science, 9*. doi:10.3389/fenvs.2021.631112

Oenema, O., Velthof, G. L., Yamulki, S., & Jarvis, S. C. (1997). Nitrous oxide emissions from grazed grassland. *Soil Use and Management, 13*(4), 288-295. doi:10.1111/j.1475-2743.1997.tb00600.x

Offermanns, L., Tiemeyer, B., Dettmann, U., Rüffer, J., Düvel, D., Vogel, I., & Brümmer, C. (2023). High greenhouse gas emissions after grassland renewal on bog peat soil. *Agricultural and Forest Meteorology, 331*. doi:10.1016/j.agrformet.2023.109309

Ojanen, P., & Minkkinen, K. (2020). Rewetting Offers Rapid Climate Benefits for Tropical and Agricultural Peatlands But Not for Forestry-Drained Peatlands. *Global Biogeochemical Cycles, 34*(7). doi:10.1029/2019gb006503

Oleszczuk, R., Regina, K., Szajdak, L., Höper, H., & Maryganova, V. (2008). Impacts of agricultural utilization of peat soils on the greenhouse gas balance. In *Peatlands and climate change* (pp. 70-97).

Olsen, S. R., Cole, C. V., Watanabe, F. S., & Dean, L. A. (1954). *Estimation of available phosphorus in soils by extraction with sodium bicarbonate*. Gov. Printing Office, Washington D.C.

Oram, N., van Groenigen, J., Bodelier, P., Brenzinger, K., Cornelissen, J., De Deyn, G., & Abalos, D. (2020). Can flooding-induced greenhouse gas emissions be mitigated by trait-based plant species choice? *Science of the Total Environment, 727*. doi:10.1016/j.scitotenv.2020.138476

Panis, F., & Rompel, A. (2022). The novel role of tyrosinase enzymes in the storage of globally significant amounts of carbon in wetland ecosystems. *Environmental Science & Technology, 56*(17), 11952-11968.

Parish, F., Sirin, A., Charman, D., Joosten, H., Minayeva, T., Silvius, M., & Stringer, L. (2008). *Assessment on Peatlands, Biodiversity and Climate Change: Main Report*. Global Environment Centre, Kuala Lumpur and Wetlands International, Wageningen.

Pärn, J., Verhoeven, J. T. A., Butterbach-Bahl, K., Dise, N. B., Ullah, S., Aasa, A., . . . Mander, U. (2018). Nitrogen-rich organic soils under warm well-drained conditions are global nitrous oxide emission hotspots. *Nature Communications, 9*. doi:10.1038/s41467-018-03540-1

Pihlatie, M., Syväsalo, E., Simojoki, A., Esala, M., & Lång, K. (2004). *Contribution of nitrification and denitrification to N2O production in peat, clay and loamy sand soils under different soil moisture conditions.* Paper presented at the Nutrient Cycling in Agroecosystems.

Pijlman, J., Holshof, G., van den Berg, W., Ros, G., Erisman, J., & van Eekeren, N. (2020). Soil nitrogen supply of peat grasslands estimated by degree days and soil organic matter content. *Nutrient Cycling in Agroecosystems, 117*(3), 351-365. doi:10.1007/s10705-020-10071-z

Pinheiro, J., Bates, D., & Team, R. C. (2023). nlme: Linear and Nonlinear Mixed Effects Models. https://CRAN.R-project.org/package=nlme: R package version 3.1-162.

Portmann, R. W., Daniel, J. S., & Ravishankara, A. R. (2012). Stratospheric ozone depletion due to nitrous oxide: Influences of other gases. *Philosophical Transactions of the Royal Society B: Biological Sciences, 367*(1593), 1256-1264. doi:10.1098/rstb.2011.0377

R Core Team. (2023). R: A Language and Environment for Statistical Computing. Vienna, Austria. https://www.R-project.org/: R Foundation for Statistical Computing.

Ravishankara, A. R., Daniel, J. S., & Portmann, R. W. (2009). Nitrous oxide (N2O): The dominant ozone-depleting substance emitted in the 21st century. *Science, 326*(5949), 123-125. doi:10.1126/science.1176985

Reay, D. S., Davidson, E. A., Smith, K. A., Smith, P., Melillo, J. M., Dentener, F., & Crutzen, P. J. (2012). Global agriculture and nitrous oxide emissions. *Nature Climate Change, 2*(6), 410-416. doi:10.1038/nclimate1458

Regina, K., Nykanen, H., Silvola, J., & Martikainen, P. J. (1996). Fluxes of nitrous oxide from boreal peatlands as affected by peatland type, water table level and nitrification capacity. *Biogeochemistry, 35*(3), 401-418. doi:10.1007/bf02183033

Regina, K., Sheehy, J., & Myllys, M. (2015). Mitigating greenhouse gas fluxes from cultivated organic soils with raised water table. *Mitigation and Adaptation Strategies for Global Change, 20*(8), 1529-1544. doi:10.1007/s11027-014-9559-2

Reiche, M., Hädrich, A., Lischeid, G., & Küsel, K. (2009). Impact of manipulated drought and heavy rainfall events on peat mineralization processes and source-sink functions of an acidic fen. *Journal of Geophysical Research-Biogeosciences, 114*. doi:10.1029/2008JG000853

Rezanezhad, F., Price, J. S., Quinton, W. L., Lennartz, B., Milojevic, T., & Van Cappellen, P. (2016). Structure of peat soils and implications for water storage, flow and solute transport: A review update for geochemists. *Chemical Geology, 429*, 75-84. doi:10.1016/j.chemgeo.2016.03.010

Rivera, J. E., & Chara, J. (2021). CH4 and N2O Emissions From Cattle Excreta: A Review of Main Drivers and Mitigation Strategies in Grazing Systems. *Frontiers in Sustainable Food Systems, 5*. doi:10.3389/fsufs.2021.657936

RIVM. (2022). *Greenhouse gas emissions in the Netherlands 1990–2020, National Inventory Report 2022*. Bilthoven, the Netherlands.

RIVM. (2024). *Greenhouse gas emissions in the Netherlands 1990-2022, National Inventory Report 2024*. Bilthoven, the Netherlands.

RIVM. (2025). *Greenhouse gas emissions in the Netherlands 1990-2023, National Inventory Document 2025*. National Institute for Public Health and the Environment. Bilthoven, the Netherlands.

RIVM. (2026). *National Inventory Document 2026, Greenhouse gas emissions in the Netherlands 1990–2024*. National Institute for Public Health and the Environment, RIVM. Bilthoven, the Netherlands.

Saggar, S., Jha, N., Deslippe, J., Bolan, N., Luo, J., Giltrap, D., . . . Tillman, R. (2013). Denitrification and N2O:N2 production in temperate grasslands: Processes, measurements, modelling and mitigating negative impacts. *Science of the Total Environment, 465*, 173-195. doi:10.1016/j.scitotenv.2012.11.050

Saju, A., Van De Sande, T., Ryan, D., Karpinska, A., Sigurnjak, I., Dowling, D. N., . . . Meers, E. (2023). Exploring the short-term in-field performance of recovered nitrogen from manure (RENURE) materials to substitute synthetic nitrogen fertilisers. *Cleaner and Circular Bioeconomy, 5*, 100043.

Saurich, A., Tiemeyer, B., Dettmann, U., & Don, A. (2019a). How do sand addition, soil moisture and nutrient status influence greenhouse gas fluxes from

drained organic soils? *Soil Biology & Biochemistry, 135*, 71-84. doi:10.1016/j.soilbio.2019.04.013

Saurich, A., Tiemeyer, B., Don, A., Fiedler, S., Bechtold, M., Arnelung, W., & Freibauer, A. (2019b). Drained organic soils under agriculture - The more degraded the soil the higher the specific basal respiration. *Geoderma, 355*. doi:10.1016/j.geoderma.2019.113911

Schimel, J. P., & Bennett, J. (2004). Nitrogen mineralization: Challenges of a changing paradigm. *Ecology, 85*(3), 591-602. doi:10.1890/03-8002

Schimel, J. P., & Weintraub, M. N. (2003). The implications of exoenzyme activity on microbial carbon and nitrogen limitation in soil: a theoretical model. *Soil Biology & Biochemistry, 35*(4), 549-563. doi:10.1016/s0038-0717(03)00015-4

Schjønning, P., Thomsen, I., Moldrup, P., & Christensen, B. (2003). Linking soil microbial activity to water- and air-phase contents and diffusivities. *Soil Science Society of America Journal, 67*(1), 156-165.

Schlesinger, W. H. H., & Bernhardt, E. S. S. (2013). *Biogeochemistry*: Elsevier.

Schothorst, C. J. (1977). Subsidence of low moor peat soils in western Netherlands. *Geoderma, 17*(4), 265-291. doi:10.1016/0016-7061(77)90089-1

Schrier-Uijl, A. P., Kroon, P. S., Leffelaar, P. A., Van Huissteden, J. C., Berendse, F., & Veenendaal, E. M. (2010). Methane emissions in two drained peat agro-ecosystems with high and low agricultural intensity. *Plant and Soil, 329*(1), 509-520.

Schwärzel, K., Renger, M., Sauerbrey, R., & Wessolek, G. (2002). Soil physical characteristics of peat soils. *Journal of Plant Nutrition and Soil Science, 165*(4), 479-486. doi:10.1002/1522-2624(200208)165:4<479::aid-jpln479>3.0.co;2-8

Scott, J., Lambie, S., Stevenson, B., Schipper, L., Parfitt, R., & McGill, A. (2015). Carbon and nitrogen leaching under high and low phosphate fertility pasture with increasing nitrogen inputs. *Agriculture Ecosystems & Environment, 202*, 139-147. doi:10.1016/j.agee.2014.12.021

Selbie, D. R., Buckthought, L. E., & Shepherd, M. A. (2015) The Challenge of the Urine Patch for Managing Nitrogen in Grazed Pasture Systems. In, *Advances in Agronomy: Vol. 129. Advances in agronomy* (pp. 229-292).

Senbayram, M., Budai, A., Bol, R., Chadwick, D., Márton, L., Gündoğan, R., & Wu, D. (2019). Soil NO3 level and O2 availability are key factors in controlling N2O reduction to N2 following long-term liming of an acidic sandy soil. *Soil Biology and Biochemistry, 132*, 165-173. doi:10.1016/j.soilbio.2019.02.009

Senbayram, M., Wei, Z. J., Wu, D., Shan, J., Yan, X. Y., & Well, R. (2022). Inhibitory effect of high nitrate on N2O reduction is offset by long moist spells in heavily N loaded arable soils. *Biology and Fertility of Soils, 58*(1), 77-90. doi:10.1007/s00374-021-01612-x

Sinsabaugh, R. L., Antibus, R. K., & Linkins, A. E. (1991). An enzymic approach to the analysis of microbial activity during plant litter decomposition. *Agriculture, Ecosystems & Environment, 34*(1-4), 43-54.

Skopp, J., Jawson, M. D., & Doran, J. W. (1990). Steady-state aerobic microbial activity as a function of soil-water content. *Soil Science Society of America Journal, 54*(6), 1619-1625. doi:10.2136/sssaj1990.03615995005400060018x

Smith, P., Adams, J., Beerling, D. J., Beringer, T., Calvin, K. V., Fuss, S., . . . Kraxner, F. (2019). Land-management options for greenhouse gas removal and their impacts on ecosystem services and the sustainable development goals. *Annual Review of Environment and Resources, 44*(1), 255-286.

Sonneveld, M. P. W., & Lantinga, E. A. (2011). The contribution of mineralization to grassland N uptake on peatland soils with anthropogenic A horizons. *Plant and Soil, 340*(1-2), 357-368. doi:10.1007/s11104-010-0608-7

Stouthamer, E., Erkens, G., Cohen, K., Hegger, D., Driessen, P., Weikard, H. P., . . . Van Rijswick, M. (2020). *Dutch national scientific research program on land subsidence: Living on soft soils – subsidence and society.* Paper presented at the IAHS: TISOLS: the Tenth International Symposium On Land Subsidence – living with subsidence.

Swails, E. E., Ardón, M., Krauss, K. W., Peralta, A. L., Emanuel, R. E., Helton, A. M., . . . Ward, S. (2022). Response of soil respiration to changes in soil temperature and water table level in drained and restored peatlands of the southeastern United States. *Carbon Balance and Management, 17*(1). doi:10.1186/s13021-022-00219-5

Syakila, A., & Kroeze, C. (2011). The global nitrous oxide budget revisited. *Greenhouse Gas Measurement and Management, 1*, 17-26.

Taft, H. E., Cross, P. A., & Jones, D. L. (2018). Efficacy of mitigation measures for reducing greenhouse gas emissions from intensively cultivated peatlands. *Soil Biology & Biochemistry, 127*, 10-21. doi:10.1016/j.soilbio.2018.08.020

Taggart, M., Heitman, J. L., Shi, W., & Vepraskas, M. (2012). Temperature and water content effects on carbon mineralization for sapric soil material. *Wetlands, 32*(5), 939-944.

Taghizadeh-Toosi, A., Elsgaard, L., Clough, T. J., Labouriau, R., Ernstsen, V., & Petersen, S. O. (2019). Regulation of N2O emissions from acid organic soil drained for agriculture. *Biogeosciences, 16*(23), 4555-4575. doi:10.5194/bg-16-4555-2019

Tanneberger, F., Birr, F., Couwenberg, J., Kaiser, M., Luthardt, V., Nerger, M., . . . Närmann, F. (2022). Saving soil carbon, greenhouse gas emissions, biodiversity and the economy: paludiculture as sustainable land use option in German fen peatlands. *Regional Environmental Change, 22*. doi:10.1007/s10113-022-01900-8

Temmink, R. J. M., Lång, K., Vroom, R. J. E., Leifeld, J., Fritz, C., Zeug, W., . . . Tanneberger, F. (2026). Agriculture on wet peatlands: the sustainability

potential of paludiculture. *Agricultural Systems, 231*. doi:10.1016/j.agsy.2025.104561

Temmink, R. J. M., Robroek, B. J. M., van Dijk, G., Koks, A. H. W., Kaeaermelahti, S. A., Barthelmes, A., . . . Smolders, A. J. P. (2023). Wetscapes: Restoring and maintaining peatland landscapes for sustainable futures. *Ambio, 52*(9), 1519-1528. doi:10.1007/s13280-023-01875-8

Temmink, R. J. M., Vroom, R. J. E., van Dijk, G., Käärmelahti, S., Koks, A. H. W., Joosten, H., . . . Fritz, C. (2024). Restoring organic matter, carbon and nutrient accumulation in degraded peatlands: 10 years Sphagnum paludiculture. *Biogeochemistry, 167*, 347-361. doi:10.1007/s10533-023-01065-4

Thomas, S., Beare, M., Francis, G., Barlow, H., & Hedderley, D. (2008). Effects of tillage, simulated cattle grazing and soil moisture on N2O emissions from a winter forage crop. *Plant and Soil, 309*(1), 131-145.

Tian, H., Xu, R., Canadell, J. G., Thompson, R. L., Winiwarter, W., Suntharalingam, P., . . . Yao, Y. (2020). A comprehensive quantification of global nitrous oxide sources and sinks. *Nature, 586*(7828), 248-256. doi:10.1038/s41586-020-2780-0

Tian, L., Cai, Y., & Akiyama, H. (2019). A review of indirect N2O emission factors from agricultural nitrogen leaching and runoff to update of the default IPCC values. *Environmental Pollution, 245*, 300-306. doi:10.1016/j.envpol.2018.11.016

Tiemeyer, B., Borraz, E. A., Augustin, J., Bechtold, M., Beetz, S., Beyer, C., . . . Zeitz, J. (2016). High emissions of greenhouse gases from grasslands on peat and other organic soils. *Global Change Biology, 22*(12), 4134-4149. doi:10.1111/gcb.13303

Tiemeyer, B., Heller, S., Oehmke, W., Gatersleben, P., Bräuer, M., & Dettmann, U. (2024). Effects of water management and grassland renewal on the greenhouse gas emissions from intensively used grassland on bog peat. *Agicultural and Forest Meteorology, 345*. doi:10.1016/j.agrformet.2023.109858

Tolunay, D., Kowalchuk, G., Erkens, G., & Hefting, M. (2024). Aerobic and anaerobic decomposition rates in drained peatlands: Impact of botanical composition. *Science of the Total Environment, 930*. doi:10.1016/j.scitotenv.2024.172639

UNEP. (2022). *Global Peatlands Assessment – The State of the World's Peatlands: Evidence for action toward the conservation, restoration, and sustainable management of peatlands*. United Nations Environment Programme, Nairobi.

Van 't Hoff, J. (1898). *Lectures on Theoretical and Physical Chemistry. Part 1. Chemical Dynamics* London: Edward Arnold.

Van 't Hull, J., Ros, M., Van Groenigen, J. W., & Velthof, G. L. (2026). *Effect of water management on nitrous oxide and carbon dioxide emissions from mineralization in drained grassland on peat soil* [Submitted, under

review]. Team sustainable soil management, Wageningen University & Research.

Van 't Hull, J., Van Middelkoop, J., Van Schooten, H., Ros, M., Van Groenigen, J. W., & Velthof, G. L. (2025). Potential measures to reduce nitrate and nitrous oxide losses from renovated grasslands. *Agriculture Ecosystems & Environment, 384*. doi:doi.org/10.1016/j.agee.2025.109549

Van Asselen, S. v., Erkens, G., Jansen, S., Aben, R., Hessel, R., Akker, J. J. H. v. d., . . . Gerritsen, P. (2023). *Effects of subsurface water infiltration systems on phreatic groundwater levels in peat meadows.* NOBV.

Van Baren, S. A., Arets, E. J. M. M., Hendriks, C. M. J., Kramer, H., Lesschen, J. P., & Schelhaas, M. J. (2024). *Greenhouse gas reporting of the LULUCF sector in the Netherlands; Methodological background, update 2024*. Wettelijke Onderzoekstaken Natuur & Milieu, WOt-technical report 255.

Van Beek, C. L., Hummelink, E. W. J., Velthof, G. L., & Oenema, O. (2004). Denitrification rates in relation to groundwater level in a peat soil under grassland. *Biology and Fertility of Soils, 39*(5), 329-336. doi:10.1007/s00374-003-0685-3

Van Beek, C. L., Pleijter, M., Jacobs, C. M. J., Velthof, G. L., van Groenigen, J. W., & Kuikman, P. J. (2010). Emissions of N2O from fertilized and grazed grassland on organic soil in relation to groundwater level. *Nutrient Cycling in Agroecosystems, 86*(3), 331-340. doi:10.1007/s10705-009-9295-2

Van Beek, C. L., Van der Salm, C., Plette, A., & Van de Weerd, H. (2009). Nutrient loss pathways from grazed grasslands and the effects of decreasing inputs: experimental results for three soil types. *Nutrient Cycling in Agroecosystems, 83*(2), 99-110. doi:10.1007/s10705-008-9205-z

van de Craats, D., van Riel, J. W., van Asselen, S., Jansen, S., Aben, R. C. H., & Hessel, R. (2025). Effects of Subsurface Water Infiltration Systems on Groundwater Table Dynamics in Drained Peat Soils. *Hydrological Processes, 39*(12). doi:10.1002/hyp.70347

Van de Riet, B. P., Hefting, M. M., & Verhoeven, J. T. A. (2013). Rewetting drained peat meadows: risks and benefits in terms of nutrient release and greenhouse gas exchange. *Water Air and Soil Pollution, 224*(4). doi:10.1007/s11270-013-1440-5

Van den Akker, J. J. H., Kuikman, P. J., de Vries, F., Hoving, I., Pleijter, M., Hendriks, R. F. A., . . . Kwakernaak, C. (2008). *Emission of CO2 from agricultural peat soils in the Netherlands and ways to limit this emission.* Paper presented at the the 13th International Peat Congress After Wise Use – The Future of Peatlands, Vol. 1 Oral Presentations, Tullamore, Ireland.

Van den Born, G. J., Kragt, F., Henkens, D., Rijken, B., Van Bemmel, B., & Van der Sluis, S. (2016). *Dalende bodem, stijgende kosten.* PBL, The Hague.

Van den Ende, M. A., Hegger, D. L. T., Mees, H. L. P., & Driessen, P. (2023). Wicked problems and creeping crises: A framework for analyzing governance challenges to addressing environmental land-use problems. *Environmental Science & Policy, 141*, 168-177.

Van den Pol-van Dasselaar, A., van Beusichem, M. L., & Oenema, O. (1997). Effects of grassland management on the emission of methane from intensively managed grasslands on peat soil. *Plant and Soil, 189*(1), 1-9. doi:10.1023/a:1004219522404

Van der Meulen, M. J., van der Spek, A. J. F., de Lange, G., Gruijters, S., van Gessel, S. F., Nguyen, B. L., . . . Krogt, R. (2007). Regional sediment deficits in the Dutch lowlands: Implications for long-term land-use options. *Journal of Soils and Sediments, 7*(1), 9-16. doi:10.1065/jss2006.12.199

Van Der Weerden, T. J., Noble, A., de Klein, C. A. M., Hutchings, N., Thorman, R. E., Alfaro, M. A., . . . Velthof, G. L. (2021). Ammonia and nitrous oxide emission factors for excreta deposited by livestock and land-applied manure. *Journal of Environmental Quality, 50*(5), 1005-1023. doi:10.1002/jeq2.20259

Van der Zee, T. C., Bleeker, A., Bussink, W., Van Dooren, H. J. C., Mosquera, J., Huijsmans, J. F. M., . . . Weijers, S. (2026). *Methodology for the calculation of emissions from agriculture. Calculations for methane, ammonia, nitrous oxide, nitrogen oxides, non-methane volatile organic compounds, fine particles and carbon dioxide emissions using the National Emission Model for Agriculture (NEMA).* RIVM report 2026-0020. RIVM, Bilthoven.

Van der Zee, T. C., Bleeker, A., van Bruggen, C., Bussink, W., van Dooren, H. J. C., Groenestein, C. M., . . . Velthof, G. L. (2024). *Methodology for the calculation of emissions from agriculture. Calculations for methane, ammonia, nitrous oxide, nitrogen oxides, non-methane volatile organic compounds, fine particles and carbon dioxide emissions using the National Emission Model for Agriculture (NEMA).* RIVM report 2024-0015. RIVM, Bilthoven.

Van der Zee, T. C., Bleeker, A., Van Bruggen, C., Bussink, W., Van Dooren, H. J. C., Groenestein, C. M., . . . Velthof, G. L. (2025). *Methodology for the calculation of emissions from agriculture. Calculations for methane, ammonia, nitrous oxide, nitrogen oxides, non-methane volatile organic compounds, fine particles and carbon dioxide emissions using the National Emission Model for Agriculture (NEMA).* RIVM report 2025-0003. RIVM, Bilthoven.

Van Dijk, H. M., Hoekstra, N. J., Ripoll-Bosch, R., Hoving, I., Pijlman, J., & Van Eekeren, N. (2026). Evaluating peat pasture performance under elevated groundwater conditions. *European Journal of Agronomy, 174*. doi:10.1016/j.eja.2025.127961

Van Dijk, J., Didden, W. A. M., Kuenen, F., Van Bodegom, P. M., Verhoef, H. A., & Aerts, R. (2009). Can differences in soil community composition after peat meadow restoration lead to different decomposition and mineralization rates? *Soil Biology & Biochemistry, 41*(8), 1717-1725. doi:10.1016/j.soilbio.2009.05.016

Van Grinsven, H. J. M., Erisman, J. W., De Vries, W., & Westhoek, H. (2015). Potential of extensification of European agriculture for a more sustainable

food system, focusing on nitrogen. *Environmental Research Letters, 10*(2), 025002.

Van Groenigen, J. W., Kuikman, P. J., de Groot, W. J. M., & Velthof, G. L. (2005a). Nitrous oxide emission from urine-treated soil as influenced by urine composition and soil physical conditions. *Soil Biology & Biochemistry, 37*(3), 463-473. doi:10.1016/j.soilbio.2004.08.009

Van Groenigen, J. W., Velthof, G. L., Oenema, O., Van Groenigen, K. J., & Van Kessel, C. (2010). Towards an agronomic assessment of N2O emissions: a case study for arable crops. *European Journal of Soil Science, 61*(6), 903-913. doi:10.1111/j.1365-2389.2009.01217.x

Van Groenigen, J. W., Velthof, G. L., van der Bolt, F. J. E., Vos, A., & Kuikman, P. J. (2005b). Seasonal variation in N2O emissions from urine patches: Effects of urine concentration, soil compaction and dung. *Plant and Soil, 273*(1-2), 15-27. doi:10.1007/s11104-004-6261-2

Van Lent, J., Hergoualc'h, K., Verchot, L., Oenema, O., & van Groenigen, J. W. (2019). Greenhouse gas emissions along a peat swamp forest degradation gradient in the Peruvian Amazon: soil moisture and palm roots effects. *Mitigation and Adaptation Strategies for Global Change, 24*(4), 625-643. doi:10.1007/s11027-018-9796-x

Van Lenth, R., & Piakowski, J. (2026). emmeans: Estimated Marginal Means, aka Least-Squares Means. https://rvlenth.github.io/emmeans/: R package version 2.0.3.

Vellinga, T. V., & André, G. (1999). Sixty years of Dutch nitrogen fertiliser experiments, an overview of the effects of soil type, fertiliser input, management and of developments in time. *Netherlands Journal of Agricultural Science, 47*(3-4), 215-241.

Velthof, G. L., Brader, A. B., & Oenema, O. (1996). Seasonal variations in nitrous oxide losses from managed grasslands in The Netherlands. *Plant and Soil, 181*(2), 263-274. doi:10.1007/bf00012061

Velthof, G. L., Cals, T. C. A., van 't Hull, J. P., Lesschen, J. P., Lessmann, M., Porre, R. J., . . . Westerik, D. (2024). Managing organic resources in agriculture: future challenges from a scientific perspective. *Frontiers in Sustainable Food Systems, 8*. doi:10.3389/fsufs.2024.1393190

Velthof, G. L., Kuikman, P. J., & Oenema, O. (2003). Nitrous oxide emission from animal manures applied to soil under controlled conditions. *Biology and Fertility of Soils, 37*(4), 221-230. doi:10.1007/s00374-003-0589-2

Velthof, G. L., & Mosquera, J. (2010). *Effect of manure application technique on nitrous oxide emission from agricultural soils*. Retrieved from Wageningen:

Velthof, G. L., & Mosquera, J. (2011a). *Calculation of nitrous oxide emission from agriculture in the Netherlands. Update of emission factors and leaching fraction*. Retrieved from Wageningen:

Velthof, G. L., & Mosquera, J. (2011b). The impact of slurry application technique on nitrous oxide emission from agricultural soils. *Agriculture Ecosystems & Environment, 140*(1-2), 298-308. doi:10.1016/j.agee.2010.12.017

Velthof, G. L., & Oenema, O. (1995). Nitrous oxide fluxes from grassland in the Netherlands: 2. Effects of soil type, nitrogen fertilizer application and grazing. *European Journal of Soil Science, 46*(4), 541-549. doi:10.1111/j.1365-2389.1995.tb01350.x

Velthof, G. L., Oenema, O., Postma, R., & Van Beusichem, M. L. (1997). Effects of type and amount of applied nitrogen fertilizer on nitrous oxide fluxes from intensively managed grassland. *Nutrient Cycling in Agroecosystems, 46*(3), 257-267. doi:10.1007/bf00420561

Velthof, G. L., & Rietra, R. P. J. J. (2018). *Nitrous oxide emissions from agricultural soils*. Retrieved from Wageningen:

Venables, W. N., & Ripley, B. D. (2002). *Modern Applied Statistics with S*. New York: Springer.

Verhoeven, J. T. A., & Toth, E. (1995). Decomposition of Carex and Sphagnum litter in fens - effect of litter quality and inhibition by living tissue homogenates. *Soil Biology & Biochemistry, 27*(3), 271-275. doi:10.1016/0038-0717(94)00183-2

Wagner-Riddle, C., Baggs, E. M., Clough, T. J., Fuchs, K., & Petersen, S. O. (2020). Mitigation of nitrous oxide emissions in the context of nitrogen loss reduction from agroecosystems: managing hot spots and hot moments. *Current Opinion in Environmental Sustainability, 47*, 46-53. doi:10.1016/j.cosust.2020.08.002

Wang, S., Wang, W., Cui, Y., Bai, Y., Liu, C., Liao, W., & Gao, Z. (2024a). Impacts of liquid fractions from two solid–liquid separation technologies on the soil porosity, ammonia, and greenhouse gas emissions. *Agronomy, 14*(1), 186.

Wang, Y. Q., Calanca, P., & Leifeld, J. (2024b). Sources of nitrous oxide emissions from agriculturally managed peatlands. *Global Change Biology, 30*. doi:10.1111/gcb.17144

Webb, J., Pain, B., Bittman, S., & Morgan, J. (2010). The impacts of manure application methods on emissions of ammonia, nitrous oxide and on crop response-A review. *Agriculture, Ecosystems and Environment, 137*(1-2), 39-46. doi:10.1016/j.agee.2010.01.001

Weideveld, S., Liu, W., van den Berg, M., Lamers, L., & Fritz, C. (2021). Conventional subsoil irrigation techniques do not lower carbon emissions from drained peat meadows. *Biogeosciences, 18*(12), 3881-3902. doi:10.5194/bg-18-3881-2021

Weier, K. L., Doran, J. W., Power, J. F., & Walters, D. T. (1993). Denitrification and the dinitrogen/nitrous oxide ratio as affected by soil water, available carbon, and nitrate. *Soil Science Society of America Journal, 57*(1), 66-72. doi:10.2136/sssaj1993.03615995005700010013x

Weslien, P., Klemedtsson, A. K., Borjesson, G., & Klemedtsson, L. (2009). Strong pH influence on N2O and CH4 fluxes from forested organic soils. *European Journal of Soil Science, 60*(3), 311-320. doi:10.1111/j.1365-2389.2009.01123.x

Wickland, K., & Neff, J. (2008). Decomposition of soil organic matter from boreal black spruce forest: environmental and chemical controls. *Biogeochemistry, 87*(1), 29-47. doi:10.1007/s10533-007-9166-3

Wils, T. H. G., van den Akker, J. J. H., Korff, M., Bakema, G., Hegger, D. L. T., Hessel, R., . . . Verstand, D. (2025). Measures to reduce land subsidence and greenhouse gas emissions in peatlands: A Dutch case study. *Land Use Policy, 152*, 107500.

Wilson, D., Blain, D., Couwenberg, J., Evans, C. D., Murdiyarso, D., Page, S. E., . . . Tuittila, E. S. (2016a). Greenhouse gas emission factors associated with rewetting of organic soils. *Mires and Peat, 17*. doi:10.19189/MaP.2016.OMB.222

Wilson, D., Farrell, C. A., Fallon, D., Moser, G., Muller, C., & Renou-Wilson, F. (2016b). Multiyear greenhouse gas balances at a rewetted temperate peatland. *Global Change Biology, 22*(12), 4080-4095. doi:10.1111/gcb.13325

Winiwarter, W., Höglund-Isaksson, L., Klimont, Z., Schoepp, W., & Amann, M. (2018). Technical opportunities to reduce global anthropogenic emissions of nitrous oxide. *Environmental Research Letters, 13*(1). doi:10.1088/1748-9326/aa9ec9

Wood, S. N. (2004). Stable and efficient multiple smoothing parameter estimation for generalized additive models. *Journal of the American Statistical Association, 99*(467), 673-686. doi:10.1198/016214504000000980

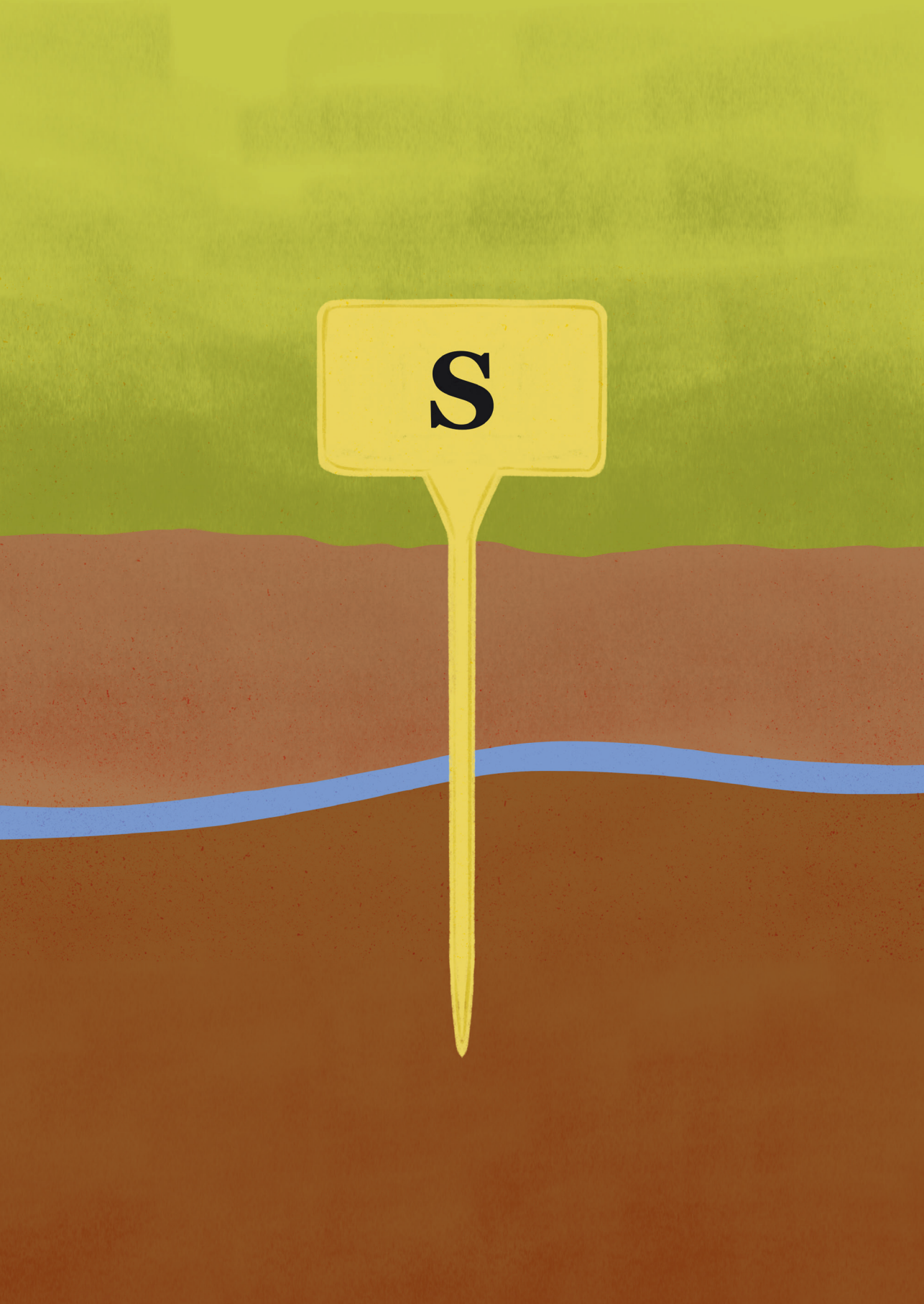
Wösten, J. H. M., Ismail, A. B., & vanWijk, A. L. M. (1997). Peat subsidence and its practical implications: A case study in Malaysia. *Geoderma, 78*(1-2), 25-36. doi:10.1016/s0016-7061(97)00013-x

Yeo, I., & Johnson, R. (2000). A new family of power transformations to improve normality or symmetry. *Biometrika, 87*, 954-959.

Yu, Z. C., Loisel, J., Brosseau, D. P., Beilman, D. W., & Hunt, S. J. (2010). Global peatland dynamics since the Last Glacial Maximum. *Geophysical Research Letters, 37*. doi:10.1029/2010gl043584

Zak, D., & McInnes, R. J. (2022). A call for refining the peatland restoration strategy in Europe. *Journal of Applied Ecology, 59*(11), 2698-2704.

Zhang, B., Zhou, M., Zhu, B., Pfülb, L., Burkart, S., Liu, H., . . . Well, R. (2023). Threshold-like effect of soil NO3- concentrations on denitrification product N2O/(N2O+N2) ratio is mediated by soil pH. *Soil Biology & Biochemistry, 187*. doi:10.1016/j.soilbio.2023.109213


S

Summary

Peat soils store a large part of the global soil carbon stock, which can potentially be lost when they are drained for agricultural use, to improve the load-bearing capacity for cattle and machinery. This results in emissions of the greenhouse gases (GHG) carbon dioxide (CO_2) and nitrous oxide (N_2O), as well as land subsidence. In the Netherlands, CO_2 and N_2O emissions resulting from peat drainage account for 3% of the total national GHG emissions. These gases are formed during the oxidation of the soil organic matter mediated by microbes, a process that is enhanced when oxygen enters the soil.

The oxidation of peat during microbial oxidation is strongly affected by moisture and temperature conditions, yet the interaction between these effects is not fully clear. Improving the understanding of these mechanisms and the variation across different peat types will benefit modelling of mitigation measure effects. Raising the groundwater level (GWL) has been proposed to mitigate peat oxidation, but may lead to increased emissions of N_2O and methane (CH_4), creating a potential trade-off between different greenhouse gases. Installation of a water infiltration system (WIS) may reduce peat oxidation while enabling grass production and cattle grazing. However, their effects on N_2O emissions and interaction with cattle excreta and fertilizer applications have not been studied yet.

In this PhD I aimed to:

1) Explore the effects of soil moisture, temperature and peat properties on peat oxidation;
2) Study the potential of water management to reduce CO_2, N_2O and CH_4 emissions associated with peat oxidation and the possibility of a trade-off between these gases;
3) Study the effect of raised water levels, achieved by water infiltration systems on N_2O emissions in fertilized or grazed peat grasslands;
4) Quantify N_2O emissions and emission factors for different mineral fertilizers, manure and grazing.

I addressed objective 1 in Chapter 2, where I incubated soil samples (3 g) from three contrasting Dutch grassland peat sites and three depths (within the upper 50 cm of the soil). Temperature treatments of 4.6, 13.9, 23.2 or 34 °C (±1.5 °C) and water filled pore spaces (WFPS)

of 50, 60, 80 or 95%, were applied in a full factorial design. Heterotrophic respiration rates (the oxidation of soil organic matter as energy source for microbial organisms) were measured and the Q_{10} (the relative respiration increase for a 10 °C temperature increase) was calculated for each treatment combination (WFPS, location and depth) over the whole studied temperature interval. Additionally, an Arrhenius function was fitted for each combination of WFPS and sampling depth and location for the calculation of temperature-specific Q_{10} values. Respiration ranged between 0 and 79 μg CO_2-C g^{-1} C h^{-1} and increased both with temperature and with WFPS (up to 80% WFPS, after which respiration remained constant). Temperature and WFPS did not have a significant interaction effect on respiration rates. However, an interaction between temperature and moisture became apparent from the significant negative WFPS effect on Q_{10}, which indicates a potential oxygen limitation on the temperature impact. The temperature-specific Q_{10} strongly decreased with temperature. These results suggested that heterotrophic respiration of peat soil is most susceptible to warming under both dry and cold conditions.

The second objective was studied in an incubation study (Chapter 3) on incubated soil cores of 1 m length and, 24 cm diameter. These undisturbed soil cores were sampled after removal of the grass layer, from the same sites as those described in Chapter 2, and incubated in a climate controlled room for 370 days at 16°C. The cores were subjected to two drying-wetting cycles, with the GWL varying between near the soil surface to 160 cm below the surface. I measured gas fluxes of CO_2, N_2O and CH_4 from the soil surface, extracted pore water for DOC and mineral nitrogen analysis, and measured soil hydraulic and shrinkage characteristics. Emissions of CO_2 increased after lowering the GWL, but showed different GWL-response curves during rewetting of the soil. On average, highest CO_2 emissions of 1.5 g C m^{-2} day^{-1} were found at a GWL of 80 cm below the surface. However, the 0 cm GWL was the only treatment with significantly lower CO_2 emissions than other GWLs. Cumulative CO_2 emissions differed significantly between sampling sites. Emissions of N_2O showed a different response, peaking at GWL heights above -20 cm, particularly after a recent GWL rise. Though not significantly different, the highest N_2O emissions were measured at the 0 cm GWL treatment. I confirmed this pattern for N_2O in un-replicated soil cores with grass sward, although emission values were lower in these cores due to the root uptake of mineral nitrogen. CH_4 emissions or -uptake remained low under any GWL. From this experiment, I concluded that raising the GWL is a

successful strategy to reduce CO_2 emissions from peat oxidation. However, raising the GWL close to the soil surface could lead to N_2O emissions that negate any gains in terms of global warming potential. These results suggest that raising the GWL in peat grasslands to -20 cm creates such a risk.

The mechanisms behind peat N_2O emissions were further explored in two field experiments that addressed objectives 3 and 4.

In chapter 4, I studied the combined effects of a water infiltration system and simulated grazing on N_2O emissions from a peat grassland. The experiment included two drainage intensities: conventional ditch drainage (CDD) and WIS aiming for a GWL of -40 cm. Additionally, grazing effects (urine application, dung application and trampling) were simulated in a full factorial design on each field in three measurement campaigns, during the summer of 2022, autumn 2022 and autumn 2023. Nitrous oxide emissions were measured weekly and the autumn campaigns included measurements of biochemical parameters in soil (pore water). Without nitrogen inputs, cumulative N_2O emissions from peat oxidation were lower, but not significantly, under a water infiltration system compared to conventional drainage (1.2 ± 0.25 kg N ha^{-1} vs 8.8 ± 3.7 kg N ha^{-1}). Urine, dung and trampling application all significantly increased cumulative N_2O emissions in both drainage systems. There was a significant interaction effect between drainage type and urine application, indicating different effects of water infiltration systems in the absence or presence of urine application. Urine and dung emission factors were higher under a water infiltration system than conventional ditch drainage. The results from this experiment suggested that water infiltration system effects on N_2O emissions from peat grasslands are not consistent, and interact with external nitrogen inputs through cattle grazing.

A second field experiment was conducted from early 2023 to early 2025. It included three drainage treatments: conventional ditch drainage (CDD) and water infiltration systems aimed for water levels of 20 cm (WIS20) and 40 cm (WIS40) below the surface. On each field, plots were fertilized with mineral (calcium ammonium nitrate and ammonium sulphate) or organic (cattle slurry, the liquid and solid fractions of cattle slurry, and farmyard manure) fertilizers, differing in nitrogen and carbon content. Nitrous oxide emissions were measured weekly, and the grass yield and N uptake were measured over multiple cuts per year. Cumulative N_2O emissions were lower under WIS40 than under CDD, while highest emissions were observed for the most shallow drainage treatment

(WIS20). Application of mineral fertilizers resulted in significantly higher emissions (14.8 to 16.7 kg N ha^{-1}) than organic fertilizers (3.5 to 8.3 kg N ha^{-1}), particularly under WIS20. These differences remained when expressed as yield-scaled emissions, despite a greater apparent nitrogen recovery for mineral than for organic fertilizers. These results suggest that maintaining a shallow groundwater level increases the risk for N_2O emissions from peat grasslands, potentially due to increased denitrification rates in the topsoil. This is exacerbated when combined with mineral fertilizer application.

The findings in this thesis demonstrate that soil moisture as well as oxygen are limiting factors for peat soil respiration, and that reducing drainage may help to mitigate CO_2 emissions from peat soils. The effect of a raised GWL on N_2O emissions originating from peat oxidation is less clear, as a shallow GWL may actually exacerbate N_2O emissions resulting from denitrification. This may particularly be the case in combination with urine excretion from grazing cattle and application of mineral fertilizers.

Samenvatting

Veengronden bevatten een groot deel van de wereldwijde koolstofopslag in de bodem. Dit kan verloren gaan als gevolg van drainage, wat wordt toegepast in de landbouw om de draagkracht van de grond te verbeteren voor grazend vee en landbouwmachines. Dit resulteert in emissie van de broeikasgassen koolstofdioxide (CO_2) en lachgas (N_2O), en een dalende bodem. In Nederland dragen CO_2 en N_2O emissie door veendrainage bij aan 3% van de totale nationale broeikasgasemissies. Deze gassen worden gevormd tijdens de oxidatie van het organisch materiaal onder invloed van microbiële organismen, een proces dat versterkt wordt wanneer zuurstof de bodem in treedt. De oxidatie van veen tijdens microbiële respiratie wordt sterk beïnvloed door de vocht- en temperatuuromstandigheden, maar er zijn kennishiaten over de interactie tussen deze effecten. Verbeterd begrip van deze mechanismen en de variatie daarvan tussen verschillende veensoorten zal het modelleren van de effecten van mitigatieopties bevorderen. Het verhogen van het grondwaterniveau is een veel voorgestelde maatregel om veenoxidatie tegen te gaan, maar kan emissies van methaan (CH_4) en zelfs N_2O doen toenemen, waardoor er mogelijk een afwenteling bestaat tussen de verschillende broeikasgassen. De installatie van een waterinfiltratiesysteem kan veenoxidatie reduceren en tegelijkertijd grasproductie en begrazing mogelijk maken. De effecten hiervan op N_2O emissies en interactie met begrazing en bemesting zijn echter nog niet onderzocht.

Mijn doel in deze PhD was het onderzoeken van:

1) De effecten van vocht, temperatuur en bodemeigenschappen op veenoxidatie;
2) Het potentieel van waterbeheer om CO_2, N_2O en CH_4 emissies als gevolg van veenoxidatie te reduceren en het onderzoeken van de eventuele aanwezigheid van een afwenteling tussen deze gassen;
3) Het effect van een verhoogd grondwaterniveau, bereikt met een waterinfiltratiesysteem, op N_2O emissies in bemeste of begraasde veenweiden;
4) De N_2O emissies en emissiefactoren horend bij verschillende minerale en dierlijke meststoffen en de effecten van begrazing.

Doelstelling 1 heb ik geadresseerd in Hoofdstuk 2, in een incubatieproef met kleine bodemmonsters (3 gram) van drie verschillende Nederlandse veenweidelocaties en drie bemonsteringsdiepten (in de bovenste 50 cm van de bodem). Het experiment was opgezet als een *full*

factorial design, met temperatuurbehandelingen van ongeveer 5, 14, 23 en 34 °C (±1,5 °C) en vochtbehandelingen van 50, 60, 80 en 95% watergevuld poriënvolume (*water filled pore space*, WFPS). Heterotrofe respiratiesnelheden (de oxidatie van organisch materiaal als onderdeel van de energievoorziening van microbiële organismen) werden gemeten en de Q_{10} (de relatieve toename in respiratiesnelheid bij een temperatuurstijging van 10 °C) werden berekend voor elke behandelingscombinatie (WFPS, locatie en diepte) met een exponentiële functie over het hele temperatuurinterval. Daarnaast werd een Arrheniusfunctie gebruikt voor elke combinatie van WFPS, bemonsteringslocatie en -diepte voor de berekening van temperatuur-specifieke Q_{10} waarden. Respiratiesnelheden varieerden tussen 0 en 79 μg CO_2-C g^{-1} C u^{-1} en namen zowel toe met temperatuur als WFPS (tot aan 80% WFPS, waarna de respiratie constant bleef). Er was geen significant interactie-effect tussen en WFPS op respiratiesnelheden. De WFPS had echter wel een significant negatief effect op de Q_{10}, wat mogelijk duidt op een zuurstofvereiste voor de impact van temperatuur. Deze resultaten suggereren dat heterotrofe respiratie van veenbodem het meest gevoelig is voor opwarming onder zowel droge als koude condities.

Het tweede onderzoeksdoel is onderzocht in een incubatie van grote bodemkolommen (Hoofdstuk 3) van 1 meter lengte en 24 cm in diameter. Deze onverstoorde bodemkolommen werden bemonsterd na verwijdering van de zode, van dezelfde onderzoeklocaties als die in Hoofdstuk 2, en gedurende 370 dagen onderzocht in een klimaatkamer bij 16 °C. De kolommen werden blootgesteld aan twee cycli van verdrogen en vernatten, waarbij het grondwaterniveau werd gevarieerd tussen het bodemoppervlak en 160 cm onder het oppervlak. Ik heb gasfluxen uit het bodemoppervlak gemeten van CO_2, N_2O en CH_4, porievocht onttrokken uit verschillende dieptes voor analyse van opgeloste organische koolstof en minerale stikstof, en bodemvocht en -krimp karakteristieken gemeten. Emissies van CO_2 namen toe na het verlagen van het grondwaterniveau maar vertoonden een ander responsverloop gedurende het verhogen van het grondwaterniveau. De gemiddeld hoogste CO_2 emissie van 1,5 g m^{-2} dag^{-1} werd gemeten onder een grondwaterniveau 80 cm onder het oppervlak. Een significant onderscheid in CO_2 emissies werd echter alleen gemeten tussen de lage emissiewaarden onder een grondwaterniveau van 0 cm en de hogere waarden bij diepere grondwaterniveaus. Cumulatieve CO_2 emissies verschilden significant tussen de bemonsteringslocaties. Emissies van N_2O lieten een andere respons zien, met pieken bij een grondwaterniveau in de bovenste 20 cm van de bodem, met name na een

stijging van het grondwaterpeil. De hoogste emissies werden gemeten onder een grondwaterniveau van 0 cm onder het oppervlak, hoewel het verschil met andere niveaus niet significant was. Dit patroon zag ik terug in (niet gerepliceerde) bodemkolommen met een graszode, hoewel N_2O emissies hier lager waren vanwege stikstofopname door wortels. Emissies en opname van CH_4 waren laag onder alle grondwaterniveaus. Uit dit experiment concludeerde ik dat verhoging van het grondwaterniveau een succesvolle strategie is om CO_2 emissies door veenoxidatie te reduceren. Verhoging van het grondwaterpeil tot dicht onder het oppervlak zou echter kunnen leiden tot hoge N_2O emissies die het positieve effect van CO_2 reductie afzwakken. Deze resultaten suggereren dat een dergelijk risico ontstaat bij grondwaterniveau rond 20 cm onder het bodemoppervlak.

De mechanismen achter N_2O emissies zijn verder verkend in twee veldexperimenten die doelstellingen 3 en 4 adresseerden.

In hoofdstuk 4 bestudeerde ik de gecombineerde effecten van een waterinfiltratiesysteem en een simulatie van begrazing op N_2O emissies uit veenweidebodem. Het experiment bevatte twee drainagebehandelingen: conventionele slootdrainage en een waterinfiltratiesysteem met een grondwaterniveau van 40 cm onder het bodemoppervlak als streefpeil. Daarnaast werden begrazingseffecten gesimuleerd (urineplek, mestflat en vertrapping) in een *full factorial design* op beide velden gedurende drie meetcampagnes: tijdens de zomer van 2022, herfst 2022 en herfst 2023. Wekelijks werden N_2O emissies gemeten en tijdens de twee herfstcampagnes daarnaast ook biochemische parameters in bodem(vocht)monsters. In de afwezigheid van een stikstofinput (via urine of mest) waren cumulatieve N_2O emissies door veenoxidatie lager, hoewel niet significant, onder een waterinfiltratiesysteem dan conventionele slootdrainage (1,2 ± 0,25 kg N ha^{-1} t.o.v. 8,8 ± 3,7 kg N ha^{-1}). Behandeling met urine, mest en vertrapping leidden allen tot een significante toename in cumulatieve N_2O emissies, onder beide drainagebehandelingen. Er was een significant interactie-effect tussen drainagebehandeling en urinebehandeling, wat duidt op een ander effect van het waterinfiltratiesysteem in een situatie met urinebehandeling, dan zonder. Emissiefactoren voor urineplekken en mestflatten waren hoger bij een waterinfiltratiesysteem dan bij conventionele slootdrainage. De resultaten uit dit experiment suggereren dat het effect van een waterinfiltratiesysteem op N_2O emissies uit veenweide niet consistent is en dat er een interactie bestaat met invoer van stikstof als gevolg van begrazing.

Een tweede veldexperiment werd uitgevoerd tussen het begin van 2023 en het begin van 2025. Dit experiment omvatte drie drainagebehandelingen: conventionele slootdrainage (CDD), en waterinfiltratiesystemen met een grondwaterniveau van respectievelijk 40 cm (WIS40) en 20 cm (WIS20) onder het oppervlak als streefpeil. Op ieder veld werden experimentele plots bemest met een minerale (kalkammonsalpeter en ammoniumsulfaat) of dierlijke mestsoort (drijfmest, de dunne en dikke fractie van drijfmest en stalmest), welke van elkaar verschillen in stikstof- en koolstofgehalte. Lachgasemissies werden wekelijks gemeten en de grasopbrengst en stikstofopname werden gemeten in meerdere grassnedes per jaar. Cumulatieve N_2O emissies waren lager bij WIS40 dan CDD, maar de hoogste emissies vonden plaats bij de minst diepe drainage, WIS20. De applicatie van minerale meststoffen resulteerde in significant hogere emissies (14,8 tot 16,7 kg N ha^{-1}) dan dierlijke mestsoorten (3,5 tot 8,3 kg N ha^{-1}), met name bij WIS20. Deze verschillen waren ook aanwezig bij de opbrengst-gecorrigeerde emissies, ondanks een hogere stikstofbenutting voor de minerale dan de dierlijke meststoffen. Deze resultaten suggereren dat een ondiep grondwaterniveau door drainage met een waterinfiltratiesysteem het risico op N_2O emissies uit veenweidebodem vergroot, mogelijk door verhoogde denitrificatie in de toplaag van de bodem. Het risico op hoge emissies is met name aanwezig in combinatie met minerale meststoffen.

De bevindingen in dit proefschrift laten zien dat zowel beschikbaarheid van bodemvocht als zuurstof limiterende factoren zijn voor veenoxidatie en dat het beperken van drainagediepte kan helpen om CO_2 emissies uit veenbodem te reduceren. Het effect van een verhoogd grondwaterniveau op N_2O emissies door veenoxidatie is minder duidelijk, omdat N_2O emissies als gevolg van denitrificatie kunnen toenemen bij een ondiep grondwaterniveau. Dit risico kan met name bestaan in combinatie met urine excretie door grazend vee en het gebruik van minerale meststoffen.

Acknowledgements

This PhD thesis would not have been completed without the help and support of countless people.

In the first place, I want to thank my supervisors, Jan Willem, Gerard and Marius for your continuous guidance, expertise and patience. Despite your full calendars, I could always count on elaborate feedback to my texts and interesting discussions in our meetings. Jan Willem, thank you for giving me the opportunity to start this PhD and the confidence to finish it. I've always admired your efficient and disciplined way of planning your many tasks. It was very useful for me too, as it was clear what you expected from me, and when. Gerard, with your long-standing experience on greenhouse gas emissions from peat grasslands, your supervision was indispensable. Even more so when I could join your project on N_2O field experiments, which encompass two chapters of this thesis. I'm happy we now continue to be colleagues in the team Duurzaam Bodemgebruik. Marius, you joined the supervision team a little later on, bringing expertise on soil physics and hydrology. Your involved and empathetic guidance has been very important since then.

Thank you to the members of the promotion committee for taking the time to read and asses my thesis.

I am grateful to Esther Stouthamer that I could be part of the exciting research program Living on Soft Soils and to the leader of my work package Mariet Hefting. It was a pleasure to work closely together with my fellow work package PhDs and postdoc, Bente, Duygu, Pepijn and Tom. And I have happy memories of all the nice conversations, presentations and guidance of all the other researcher within LOSS.

Thank you to my advisors Jan van den Akker and Rob Hendriks, who provided decades of experience and knowledge in peat research. Jan initiated the link between Wageningen and LOSS and the insights and efforts of Rob were essential in the design of the peat core experiment.

Being part of the Soil Biology group has been truly a treat. When I joined the group in September 2020, despite covid measures being in place, I immediately felt welcome thanks to the personal attentions of Marnella. I am grateful for all the support that I received from Marnella,

Susy, Selene and Asma throughout the years. Thank you for all the good times to my fellow PhDs that were there during my time at SBL: Zhongchen, Laura, Omotola, Zhibiao, Hannah, Wietse, Makrina, Tullia, Anna-Reetta, Enno, Luuk, Angel, Doina, Chindi, Karen, Yizan, Mubonda, Jiyu, Leila, Bobby, Felix, Shevani, Robin, Frank, Jonas, Gidena, Dorien, Jurrian, Gonso, Roelof, Mumba, Karin, Matthew, Julia, Maria-Franca, and others who I may have forgotten to mention. And thank you to all the other SBL colleagues for the great work environment during and after work hours: Mirjam, Giulia, Carmen, Arlete, Ali, Nikos, Paolo, Ellis, Maria, Gerlinde, Willeke, Marie, Gabriel, Alix, Ron, Michiel, Rachel, Luciana, Marente, Florien, Tamas, Henk, Evandro, Danielle, Thom.

A special thank you to my paranymphs, Zhongchen and Tullia. Zhongchen, we started only two weeks apart in September 2020 and shared our office during the entire course of our PhDs. Your universal knowledge and discipline were a bit intimidating at first, but I quickly learned how considerate and easy-going you are. Tullia, as soon as you joined SBL as a new PhD, we became friends. Your warmth and cheerfulness make being with you and talking to you the easiest thing ever. Anna-Reetta, thank you for always looking out for me and others around you with your generosity and humor, even on top of your own busy brain and schedule. Shevani, your fun and compassionate personality has given me loads of joy and inspiration since I know you and I'm so happy we became friends. Karen, thank you for your relaxed presence and the amazing dinner parties. Hopefully we will still go camping some weekend! Luuk, it was great fun sharing the office with you. Although in practice we were walking in and out to our respective experiments or lab work half of the time, there was always an opportunity to catch up or exchange ideas.

The chapters in this thesis are the result of many pleasant collaborations with people within and outside of WUR. In the first place, the work done by Monne, Anneke and Eva for their MSc theses has been indispensable. Being your supervisor was a pleasure and very educative. Two of these projects were supervised in happy collaboration with Jos van Dam. Additionally, I received a lot of help over the years from Wonnie Sheik Abdulla, Frank Gerritsen, Paul Gerritsen, Harm Gooren, and Rudi Hessel. I have spent many, many days preparing, measuring and cleaning up the peat core experiment in Nergena, during which I could always count on the help from Rinie Verwoert, Rohan van Genderen, Marcel Otten, Wilfred Krijnen and Matthijs Dellink even with the most

difficult/annoying questions. The field experiments would have been impossible without all the people from KTC Zegveld, in particular Karel van Houwelingen and Jasper Beek. I am thankful to NOBV and the owners of the farms in Vlist and Aldeboarn, for the opportunity to take soil samples on those locations. Thank you to our colleagues from B-WARE, Gijs van Dijk, Sarah-Faye Harpenslager and Thomas Gremmen for the experiment we carried out together.

Nearly two years ago I was lucky enough to become part of the team Duurzaam Bodemgebruik. Thank you Gert Jan, for your flexibility and support during this time. I really couldn't have wished for a better situation to finish writing my thesis. Dorien, we have been working closely together for a long time already on the field experiments in Zegveld, even before I joined this team. Your calm and analytical way of working have always been inspiring to me. I want to thank all my other colleagues at DB, especially those who I work(ed) with directly, Rima, Mart, Gerard, Mieke, René, Jurrian, Gert, Jordy, Laura, Kimo, Lotte, Karin, Rachel and Wieneke.

Mijn vrienden uit Utrecht en Leiden zijn een enorme steun geweest door de jaren heen. Jullie zullen je wel hebben afgevraagd wanneer dit eindelijk voorbij zou zijn! Gelukkig viel er samen genoeg te ontspannen, met etentjes, tuinieren, concerten… Bedankt lieve Natascha, Maaike, Sofie, Yvana, Arvid, Steye en anderen. Bedankt Annika voor het mooie ontwerp van de omslag en het binnenwerk van dit boekje.

Ik zou nergens zijn geweest zonder mijn familie en vraag me af of ik een PhD had kunnen volbrengen zonder zo'n stevige basis. In de eerste plaats Max en Nelly: wat een geluk om jullie dochter te zijn. Jullie hebben me nooit een bepaalde richting op willen sturen, maar toch hebben jullie interesses ongetwijfeld bijgedragen aan die van mij. Dankzij jullie hecht ik waarde aan de juiste dingen in het leven en ik kan altijd bij jullie terecht.

Thomas en Eva, het brengt me veel plezier dat we tegenwoordig in dezelfde stad wonen en elkaar zo vaak kunnen zien. Thomas, ik heb van jongs af aan veel aan je gehad als grote broer, en zo ook gedurende de afgelopen jaren. En kleine Leon niet te vergeten, ik had mijn proefschrift net een paar dagen ingeleverd toen je werd geboren, maar het vooruitzicht van je komst heeft me vast geholpen!

Karin, Mark, Thijs en Cecile, het kerngezin is altijd een warm bad, een tweede familie! Sorry Karin, dat ik zo weinig vertelde over mijn onderzoek. Misschien kwam dat doordat ik de helft van de tijd ook niet wist wat ik aan het doen was.

En tot slot Gosse. Woorden schieten natuurlijk te kort om uit te drukken wat jij voor me hebt betekend, de afgelopen jaren en de jaren daarvoor. Het thuis dat we voor elkaar zijn heeft ervoor gezorgd dat ik de uitdagingen van een PhD aankon. Wanneer ik mezelf de grond in praatte kwam je kalm met tegenargumenten zodat ik weer normaal kon nadenken. Jij vindt het zelf vanzelfsprekend, maar het was nooit een probleem om onze plannen aan te passen aan experimenten of ander werk. De belangrijkste steun heb je me gegeven door er gewoon te zijn, maar ook daarvoor bedankt!

About the author

Erne Blondeau was born on 10 July 1995 in Leiden. As a little girl, someone told her that civilization might end in December 2012 due to climate change events as predicted in the Mayan calendar. While not very accurate, this first raised her attention to the large impacts of greenhouse gas emissions and environmental pollutants. As it turned out, civilization was spared in 2012. But by then the concern for climate and environment had become present in her life. This eventually resulted in the decision to start a BSc in Milieu-Natuurwetenschappen at Utrecht University, which was followed by an MSc in Environmental Sciences at Gothenburg University. In Gothenburg, her interest in soil sciences was stirred, with a particular fascination for soil-atmosphere interactions. Her MSc thesis project on the effects of increased atmospheric temperature and CO_2 concentration on soil greenhouse gas production, was performed at the research facilities of the Department of Plant Ecology at the Justus-Liebig-University in Giessen, Germany.

During her MSc in Gothenburg, she learned of the costs of peat soil drainage and the difficulty of mitigating these effects, while taking into account trade-off effects and the stakes of different parties. This motivated her to start a PhD study on greenhouse gas emissions from the peat grasslands in home country the Netherlands, at the Soil Biology group of Wageningen University. This PhD is part of the NWA program Living on Soft Soils – Subsidence and Society.
Currently, Erne works as a researcher in the Sustainable Soil Management team at Wageningen Environmental Research.



Affiliations of co-authors

Listed below are the affiliations of the co-authors of the various chapters of this thesis at the time of their contribution.

T. Gremmen
B-WARE Research Centre, Nijmegen, The Netherlands
Department of Ecology, Radboud Institute for Biological and Environmental Sciences, Radboud University, Nijmegen, The Netherlands

S. F. Harpenslager
B-WARE Research Centre, Nijmegen, The Netherlands
Department of Ecology, Radboud Institute for Biological and Environmental Sciences, Radboud University, Nijmegen, The Netherlands

M. Heinen
Team Soil, Water and Land Use, Wageningen Environmental Research, Wageningen University and Research, The Netherlands

R. F. A. Hendriks
Team Sustainable Soil Management, Wageningen Environmental Research, Wageningen University and Research, The Netherlands

E. Lammerts
Soil Biology Group, Wageningen University and Research, The Netherlands

R. Porre
Team Sustainable Soil Management, Wageningen Environmental Research, Wageningen University and Research, The Netherlands

M. Ros
Team Sustainable Soil Management, Wageningen Environmental Research, Wageningen University and Research, The Netherlands

A. Stam
Soil Biology Group, Wageningen University and Research, The Netherlands

J. J. H. van den Akker
Team Soil, Water and Land Use, Wageningen Environmental Research, Wageningen University and Research

G. van Dijk
B-WARE Research Centre, Nijmegen, The Netherlands
Department of Ecology, Radboud Institute for Biological and Environmental Sciences, Radboud University, Nijmegen, The Netherlands

J. W. van Groenigen
Soil Biology Group, Wageningen University and Research, The Netherlands

G. L. Velthof
Soil Biology Group, Wageningen University and Research, The Netherlands
Team Sustainable Soil Management, Wageningen Environmental Research, Wageningen University and Research, The Netherlands

M. Weghorst
Soil Physics and Land Management Group, Wageningen University and Research , The Netherlands

D. Westerik
Soil Biology Group, Wageningen University and Research, The Netherlands
Team Sustainable Soil Management, Wageningen Environmental Research, Wageningen University and Research, The Netherlands

PE&RC Training and Education Statement

With the training and education activities listed below the PhD candidate has complied with the requirements set by the Graduate School for Production Ecology and Resource Conservation (PE&RC) which comprises of a minimum total of 30 ECTS (= 22 weeks of activities)

Review/project proposal

- Groundwater level effects on peat oxidation in Dutch pastures on peat soils | 4.5 ECTS

In-depth / Topical / On-site Postgraduate Courses

- SBL soil biology lab skills course for assessing soil functions | Soil biology group, WUR | 2021 | 1.5 ECTS
- Redesign agriculture to improve resource use efficiency | PE&RC | 2024 | 1.5 ECTS

Methodological / Statistical Postgraduate Courses

- Tidy data transformation and visualization with R (online) | PE&RC | 2020 | 1.2 ECTS
- Linear models | PE&RC | 2022 | 0.9 ECTS
- Mixed linear models | PE&RC | 2022 | 0.6 ECTS

Competence, skills and career-oriented activities

- Competence assessment | WGS | 2020 | 0.3 ECTS
- Efficient writing strategies (online) | WGS | 2021 | 1.3 ECTS
- Scientific publishing (online) | WGS | 2021 | 0.3 ECTS
- Workshop carousel: Designing an attractive and effective poster (online) | PE&RC | 2021 | 0.075 ECTS
- Workshop carousel: Supervising MSc students (online) | PE&RC | 2021 | 0.075 ECTS
- Supervising BSc & MSc thesis students | WGS | 2023 | 0.6 ECTS

Scientific Integrity/Ethics in science activities

- Ethics in plant and environmental sciences | WGS | 2024 | 0.3 ECTS

PE&RC Retreat, PE&RC Day, and other PE&RC events
- PE&RC first year's weekend | 2021 | 0.9 ECTS
- PE&RC last year's weekend | 2024 | 0.6 ECTS
- PE&RC day | 2022 | 0.3 ECTS

National/local scientific meetings, seminars, and discussion groups
- PE&RC discussion group: Plant- soil interactions | 2021 | 0.2 ECTS
- PE&RC discussion group: Emissions and nutrient management | 2022-2024 | 0.4 ECTS
- NERN symposium: Current Themes 2021 - Nitrogen: Past, Present and Future | 2021 | 0.3 ECTS
- NERN Netherlands Annual Ecology Meeting (poster) | 2024 | 0.6 ECTS
- STOWA deelexpedities | 2021 | 0.2 ECTS
- LOSS programme consortium days and symposia | 2020-2024 | 2.4 ECTS
- LOSS research programme scientific meetings | 2020-2024 | 6.0 ECTS

International symposia, workshops and conferences
- Tenth International Symposium on Land Subsidence (oral presentation) | Delft | 2023 | 2.2 ECTS
- International Symposium on Non-CO2 Greenhouse Gases (oral presentation) | Amsterdam | 2023 | 1.9 ECTS
- European Geosciences Union (EGU) General Assembly (oral presentation) | Vienna | 2024 | 2.5 ECTS

Lecturing/Supervision of practicals/tutorials
- Soil plant relations (help with practical) | 2024 | 2 days | 0.5 ECTS

BSc/MSc thesis supervision
- Research topic 1: Simulation of a column experiment on greenhouse gas emissions from peat and peat subsidence, using SWAP and DNDC | 3.0 ECTS
- Research topic 2: Greenhouse gas emissions from Dutch peat soils during drying and rewetting track: a column experiment | 2.0 ECTS
- Research topic 3: Combined moisture and temperature effects on peat soil respiration | 1.0 ECTS

List of publications

Blondeau, E., Velthof, G. L., Heinen, M., Hendriks, R. F. A., Stam, A., van den Akker, J. J. H., Weghorst, M., van Groenigen, J. W. (2024). Groundwater level effects on greenhouse gas emissions from undisturbed peat cores. *Geoderma, 450*. https://doi.org/10.1016/j.geoderma.2024.117043

Blondeau, E., Westerik, D., Gremmen, T., Harpenslager, S. F., Heinen, M., van Dijk, G., van Groenigen, J. W., Velthof, G. (2026). Drainage, cattle excreta and trampling effects on nitrous oxide emissions from a peat grassland. *Agriculture, Ecosystems and Environment, 397*. https://doi.org/10.1016/j.agee.2025.110093

Blondeau, E., Westerik, D., Heinen, M., Porre, R., Ros, M., van Groenigen, J. W., Velthof, G. (2026). Drainage and fertilizer effects on nitrous oxide emissions from peat grasslands. *Under review for publication.*

The research described in this thesis is part of the project Living on Soft Soils - Subsidence and Society (grantnr.: NWA.1160.18.259). This project is funded by the Dutch Research Council (NWO-NWA-ORC), Utrecht University, Wageningen University, Delft University of Technology, Ministry of Infrastructure & Water Management, Ministry of the Interior & Kingdom Relations, Deltares, Wageningen Environmental Research, TNO-Geological Survey of The Netherlands, STOWA, Water Authority: Hoogheemraadschap de Stichtse Rijnlanden, Water Authority: Drents Overijsselse Delta, Province of Utrecht, Province of Zuid-Holland, Municipality of Gouda, Platform Soft Soil, Sweco, Tauw BV, NAM.

Financial support from Wageningen University and the Dutch Research Council for printing this
thesis is gratefully acknowledged.

Cover design by Annika Provily
Printed by ProefschriftMaken

